Novel *Drosophila* Models for Unravelling the Mechanisms of Frontotemporal Dementia and Amyotrophic Lateral Sclerosis

A thesis submitted to the University of Manchester for the degree of

Doctor of Philosophy

in the Faculty of Biology, Medicine and Health

2021

Joanne L. Sharpe

School of Biological Sciences

Department of Neuroscience and Experimental Psychology

Table of Contents

Word Count: 53,163

List of Figures

List of Tables

List of Abbreviations

AD	Alzheimer's disease
ALS	Amyotrophic lateral sclerosis
AP	Alanine-proline
BAC	Bacterial artificial chromosome
BDSC	Bloomington Stock Centre
BS	Bang sensitive
bvFTD	behavioural variant FTD
C9orf72	Chromosome 9 open reading frame 72
CBD	Corticobasal degneration
CHMP2B	Charged multivesicular body protein 2B
DCTN1	Dynactin
DENN	Differentially expressed in normal and neoplastic cells
DIG	Digoxigenin
DMEM	Dulbecco's Modified Medium
DPRs	Dipeptide repeat proteins
EEG	Electroencephalogram
EGFP	Enhanced green fluorescent protein
EJP	Excitatory junction potential
ER	Endoplasmic reticulum
ESCRT	Endosomal sorting complexes required for transport
FTD	Frontotemporal dementia
FTD-3	FTD associated with chromosome 3
FTDP-17	FTD with Parkinson’s linked to chromosome 17
FUS	Fused in sarcoma
GA	Glycine-alanine
GEF	Guanine exchange factor
GP	Glycine-proline
GR	Glycine-arginine
GWAS	Genome-wide association studies
HD	Huntington's disease
hnRNPA1	Heterogeneous nuclear riboprotein 1
iACT	Inner antennocerebral tract
IBM	Inclusion body myopathy
iPSC	Induced pluripotent stem cells
LCD	Low complexity domain
LLPS	Liquid-liquid phase separation
lncRNA	Long non-coding RNA
LPR	Lateral protocerebrum
MAPT	Microtubule associated protein tau
mEJP	mini-EJP
mEPSP	mini excitatory post-synaptic potential
NEB	New England Biolabs
NMJ	Neuromuscular junction
PD	Parkinson's Disease

PD	Pedunculus
PE	Post-eclosion
PFN1	Profilin 1
PNFA	Progressive non-fluent aphasia
PR	Proline-arginine
PSP	Progressive supranuclear palsy
PTX	Picrotoxin
PVDF	Polyvinylidene
RAN	Repeat-associated non-AUG translation
RBP	RNA binding protein
rDNA	Ribosomal DNA
RFP	Red fluorescent protein
Ri	Input resistance
RI	Relay interneurons
RO	RNA only
ROS	Reactive oxygen species
SD	Semantic dementia
SDHAF 4	Succinate dehydrogenase assembly factor 4
SDS	Sodium dodecyl sulfate
SEM	Standard error of the mean
SING	Startle-induced negative geotaxis
SMCR8	Smith-Magenis chromosome region 8
SNP	Single nucleotide polymorphism
SOD1	Cu/Zn superoxide dismutase 1
SOD2	Mn superoxide dismutase 2
TBE	Tris-borate-EDTA
TDP-43	Trans-activation response DNA-binding protein 43
TMS	Transcranial magnetic stimulation
UAS	Upstream activating sequence
UBQLN2	Ubiquilin-2
UPS	Ubiquitin proteasome system
VAPB	Vesicle-associated membrane protein B
VCP	Valosin containing protein
WDR14	WD-repeat containing protein 4

Abstract

A hexanucleotide repeat expansion in a non-coding region of the *C9orf72* gene is the most common genetic cause of frontotemporal dementia (FTD) and amyotrophic lateral sclerosis (ALS), neurodegenerative diseases with considerable clinical and pathological overlap. FTD and ALS are invariably fatal and there is no cure. An understanding of the mechanisms through which the *C9orf72* mutation leads to FTD/ALS will be crucial for development of effective therapeutics.

There is evidence to support three possible pathogenic mechanisms underlying *C9orf72* toxicity: (1) haploinsufficiency of C9orf72; (2) repetitive RNA transcripts arising from the repeat are toxic; (3) repeat-associated non-AUG (RAN) translation produces five different toxic dipeptide repeat proteins (DPRs) – AP, GP, GA, PR, and GR – from repeat RNA. The majority of evidence points to a gain of function mechanism and DPRs as the main toxic species, but does not rule out possible contributions from RNA toxicity and haploinsufficiency via synergistic mechanisms. Despite many studies into DPR-mediated toxicity *in vitro* and *in vivo*, the precise mechanisms through which DPR expression leads to neurodegeneration are still poorly understood.

Drosophila models of DPR toxicity have been instrumental in the discovery that DPRs are the main drivers of toxicity. However, there remains a lack of consistent and physiologically relevant DPR models. Most express up to only 100 repeat units, whereas in patients, the expansion is several hundreds to thousands of repeats in length. Furthermore, despite the average age of onset of *C9orf72*-related FTD/ALS being 57 years of age, there are few studies investigating the effect of increasing age on DPR toxicity. The aims of this study were to address the lack of *Drosophila* models expressing DPRs of a physiological repeat length, fully characterise the effect of DPR expression on age-related neurodegenerative phenotypes, and subsequently use these models to unravel the mechanisms underpinning DPR toxicity.

Firstly, we showed that 1000 repeat DPRs are stable in the *Drosophila* genome for over 3 years (~100 generations), and flies pan-neuronally expressing DPRs are viable with a reasonable lifespan. Each DPR was associated with a distinct age-related phenotypic profile. In support of previous studies, GR1000 showed the greatest age-related toxicity. However, AP1000, generally considered the least toxic of the DPRs, showed neurodegeneration, reduced climbing speed, and electrophysiological defects. Given that all DPRs have the capacity to be present in the same cell in patients, we next looked to see if co-expressing DPRs can alter their phenotypic profiles. Co-expression revealed a novel bang-sensitive seizure susceptibility not previously observed in DPR fly models. Subsequently, a dominant modifier screen was designed to identify mutations that could exacerbate seizure susceptibility in DPR flies. The screen implicated genes involved in mitochondrial function, oxidative stress, microtubule dynamics, and synaptic inhibition in DPR-mediated neurotoxicity.

In summary, novel *Drosophila* models expressing physiologically relevant repeat length DPRs have been generated. Characterisation revealed age- and DPR- specific phenotypic profile, and highlights the importance of co-expression. We anticipate that this model will be useful for future studies elucidating the mechanisms underpinning DPR toxicity in *C9orf72*-related FTD/ALS.

Declaration

Data from this thesis (chapters 3 and 4) has been published in Acta Neuropathologica Communications (West et al., 2020), and a review article focused on *Drosophila* models of *C9orf72* (Sharpe et al., 2021) is published in Frontiers of Cellular Neuroscience.

No portion of the work referred to in the thesis has been submitted in support of an application for another degree or qualification of this or any other university or other institute of learning.

Copyright statement

Acknowledgements

I would like to take this opportunity to thank everyone who have supported me throughout the course of my PhD.

Firstly, I would like to thank my supervisors Ryan West, Andreas Prokop and Stuart Pickering-Brown. In particular I have to thank Ryan for his continued patience and support in all aspects of my PhD. I would also like to thank him for his guidance and encouragement, without which I would never have had the confidence to try anything because I am an eternal pessimist.

I would also like to thank Sara Rollinson, without whom I would still be crying over Southern blots, and Peter Walker, who gave up many hours of his time to help work out how to embed and section *Drosophila* heads. For his help in every aspect of fly work, thank you to Sanjai Patel, who was always willing to talk about flies and offer his expert advice. I also extend my gratitude to members of the SPB and Prokop labs past and present, in particular, Bea, André, and Ines, who made me feel so welcome.

I also owe huge thanks to my friends and family for indulging my anecdotes about flies, and providing endless support. Special thanks go to my colleagues: Nikki for making doing Southern blots immeasurably less painful, and keeping me sane in my last months of writing through regular squash games, and Sarah, who has always been on hand to offer advice and distractions from aforementioned Southern blots.

Lastly, I have to thank James, mainly for buying me soft and squishy octopuses, but also for always being there and taking the bins out.

1 Introduction

1.1 Rationale

Neurodegenerative diseases affect millions of people worldwide and are invariably incurable. Age is the biggest risk factor for most neurodegenerative diseases. Therefore, as the average life expectancy rises, the number affected will increase and exacerbate the financial and emotional burdens on society. In 2019, there were estimated to be 850,000 people living with dementia in the UK, and this is forecast to increase to 1,000,000 by 2025[2]. Worldwide, around 50 million people live with dementia, costing an estimated US$1 trillion annually[3]. Frontotemporal dementia (FTD), the second most common cause of dementia in under 65s[4], and amyotrophic lateral sclerosis (ALS), a neurodegenerative disease that results in muscle wasting and weakness, are closely related, often simultaneously occurring in one individual[5]. They have a strong genetic link, and the most common genetic cause of both FTD and ALS is a hexanucleotide expansion in the *C9orf72* gene. Currently, there is a lack of coherence between researchers as to what underpins the toxicity caused by this mutation. Poor understanding of the underlying mechanism hinders progress towards therapeutic interventions. Therefore, the aim of this research is to address a gap in current available tools for studying *C9orf72*-related FTD/ALS by generating and characterising novel *Drosophila* models, with the goal of aiding future investigations into mechanisms, as well as providing useful tools for drug screening.

1.2 Frontotemporal dementia and amyotrophic lateral sclerosis

1.2.1 Overview

FTD and ALS are heterogeneous and progressive diseases of the nervous system which overlap genetically, pathologically, and clinically. Whilst ALS is primarily characterised as a motor disorder and FTD by cognitive impairment, it is estimated that 50% of ALS patients develop some cognitive dysfunction with 15% meeting the criteria for an FTD diagnosis, and 15% of FTD patients also meet ALS criteria[5].

1.2.2 Clinical characteristics

1.2.2.1 FTD

FTD is the second most common early-onset dementia in the under 65s, accounting for up to 20% presenile dementia cases[6]. It most commonly occurs between the ages of 45-65 years, but can present before the age of 30 and in the elderly[6,7]. The defining clinical characteristic of FTD is an alteration to behaviour and character, with relative preservation of memory in the early phases of disease.

FTD is a highly heterogeneous disorder but can be defined by three main subtypes: behavioural variant FTD (bvFTD), semantic dementia (SD), and progressive non-fluent aphasia (PNFA). bvFTD accounts for 70% FTD cases and is characterised by behavioural changes, whereas SD and PNFA account for 15% and 10% respectively and are primarily language disorders[6,8]. There is also some overlap with other neurodegenerative disorders, most commonly ALS, corticobasal degeneration (CBD), progressive supranuclear palsy (PSP) and inclusion body myopathy (IBM)[9,10]. In addition, rarely FTD patients exhibit extrapyramidal motor symptoms more similar to those seen in Parkinson's Disease (PD), such as altered posture, tremor and hypophonia[6]. This is commonly observed in FTD with Parkinson's linked to chromosome 17 (FTDP-17). The age at onset is generally consistent between subtypes of FTD but the rate of progression varies, with bvFTD and FTD with motor deficits associated with more rapid progression[11,12]. For example, the average time between diagnosis and death for PSP is just 2.9 years compared to 9.1 years for SD[13].

The behavioural changes associated with bvFTD result in an alarming and fundamental change in character, including emotional blunting, apathy, tactlessness, and social disinhibition[6,14]. Patients tend not to notice these alterations and lack of insight is also a key feature of early bvFTD[8]. Changes in food preferences and eating behaviours are also relatively common, usually cravings for sweet and fatty foods and a tendency to display ritualistic eating habits. As the disease progresses, patients become more disinhibited and may grab food off other's plates[15]. It is these characteristics that drive diagnosis towards FTD rather than other dementias, particularly Alzheimer's Disease[16]. Psychosis and other repetitive stereotyped behaviours are also observed in FTD patients, in particular those with the *C9orf72* mutation[14].

Patients with SD or PNFA have progressive loss of different language functions; in SD, patients have fluent and spontaneous speech, but lose word meaning, whereas PNFA patients struggle with the production of words (anomia) and grammar but retain word

meaning and comprehension[8]. Impairments in language will also occur more frequently in the later stages of bvFTD[8]. Interestingly, some patients with SD may develop new and often impressive artistic abilities such as painting or music, progressive neurodegeneration in one area seemingly releasing new functions elsewhere[17].

1.2.2.2 ALS

ALS is a motor disorder whereby denervation of motor neurons in the brain and spinal cord leads to progressive motor deficits and muscle atrophy that eventually results in death due to respiratory failure. Symptoms usually present between the ages of 55-75 years old, and the median survival time from onset to death ranges from three to five years, although up to 20% of patients are reported living beyond 10 years with the disease[18]. Patients with older age of onset tend to progress more rapidly[19,20].

The most common initial symptom of ALS is extremity weakness, resulting in difficulty writing, general stiffness, weakness, and twitching[21]. These are manifestations of spinal-onset disease, which accounts for approximately two thirds of cases[22].The other third of patients have the more aggressive bulbar-onset ALS which presents as dysphagia and dysarthria (speech and swallowing difficulties) as well as an inability to control facial expressions. The two subtypes are defined by the location in which motor neuron degeneration begins: spinal onset ALS begins with degeneration of the lower motor neurons in the ventral horn of the spinal cord, whereas bulbar onset initially affects the upper motor neurons in the corticobulbar tract[22,23]. Patients with bulbar-onset ALS have an increased susceptibility to lung infections and pneumonia due to the inability to clear the airway[18]. Consequently, prognosis is consistently worse in patients with bulbar onset. Patients have a shorter survival (< 2 years post diagnosis), and an increased burden of cognitive and language impairments compared with spinal-onset ALS[24].

1.2.3 Neuropathology

FTD is pathologically characterised by bilateral atrophy of frontal and temporal lobes as well as degeneration of the striatum[8]. The topological pattern of atrophy in FTD brains is variable, reflecting the heterogeneity of symptoms. Each variant is associated with a distinct topographical pattern of cerebral pathology which determines the clinical subtype[6,8]: bvFTD has predominantly symmetrical atrophy of the frontal and anterior temporal lobes, PNFA has predominantly left frontotemporal hemisphere degeneration, and SD is marked by anterior temporal cortex atrophy[6,25]. In later stages of disease, posterior brain regions may also atrophy[8].

ALS, in contrast, is characterised by the degeneration of motor neurons, predominantly in the spinal cord, brainstem, motor cortex and corticospinal tract[26]. This is in addition to skeletal muscle atrophy. A depletion of over 50% of spinal motor neurons is usually observed in post-mortem ALS brains, and there is evidence of infiltration of grey and white matter in the spinal cord by microglia[27]. Both FTD and ALS brains show widespread severe astrocytic gliosis, a common feature of neurodegenerative disease, in affected and adjacent brain regions[6,26].

Proteinopathy, a common feature of neurodegenerative disease, refers to the formation, aggregation and accumulation of misfolded proteins within neurons. FTD and ALS are heterogeneous proteinopathies that are categorised by the predominant protein component of these inclusions (Figure 1.1). Most cases of FTD show one of three different proteinopathies, and are categorised as such: Tau-Positive inclusions in FTD-Tau, Trans-activation response (TAR) DNA-binding protein 43 (TDP-43) in FTD-TDP, and fused in sarcoma (FUS) in FTD-FUS[28]. Most cases of FTD are accounted for by these subtypes, but rare cases have ubiquitin/p62 positive inclusions that are not labelled by one of the above three antibodies. These are known as FTD-UPS (ubiquitin proteasome system) and are found in FTD associated with chromosome 3 (FTD-3) caused by the *CHMP2B* (charged multivesicular body protein 2B) mutation, and, to date, there is no single major pathological protein identified[28-30].

Neuronal pathology is generally consistent between bulbar-onset and spinal-onset ALS[24] and is similarly sub-categorised, with the majority of cases having TDP-43 positive inclusions. The other two predominant pathological proteins found in ALS are aggregations of mutant Cu/Zn superoxide dismutase 1 (SOD1) and FUS[22]. In addition, ALS brains display bunina bodies, small eosinophilic intraneuronal inclusions.

Aggregates of ubiquitinated and hyperphosphorylated tau are found in neuronal filamentous inclusions in many neurodegenerative diseases, but the characteristics of such lesions varies[31]. FTD-Tau represents around 40% of all FTD cases including those with familial *MAPT* mutations and some sporadic cases. The nature of tau pathology varies between clinical subtypes of FTD is determined by the ratio of different tau isoforms, 3R and 4R. Historically, bvFTD with Tau pathology was referred to as Pick's Disease due to the presence characteristic rounded lesions known as Pick Bodies[32], composed of mainly 3R tau. FTDP-17 is associated with both 3R and 4R tau and forms straight filamentous structures, depending on the mutation[33].

Misfolded SOD1 aggregates accumulate in the cytoplasm in ALS cases with *SOD1* mutation and occasionally sporadic cases[34,35]. Mutated SOD1 has an increased

propensity to aggregate because it is unstable and consequently has a tendency to misfold[36].

The discovery of TDP-43 as a component of tau- negative, ubiquitin- positive protein inclusions in both FTD and ALS in 2006 provided the first pathological link between the two diseases[37]. FUS and TDP-43 are DNA and RNA binding proteins involved in the

regulation of different aspects of RNA processing. They are found in the nucleus of most tissues, but continuously shuttle to and from the cytoplasm[38]. Hyperphosphorylated and ubiquitinated aggregations of both TDP-43 and FUS are found in both FTD and ALS[37,39].

FUS aggregations are present in a small percentage of FTD and ALS cases, including all cases with *FUS* mutations, in which the nuclear import of FUS is disrupted leading to aggregation of mutant FUS in the cytoplasm[39]. TDP-43 is the major pathological protein in both FTD and ALS, occurring in 50-60% and 95-97% familial cases respectively. Inclusions are predominantly cytoplasmic but can also be interneuronal and are rarely found in glia and dystrophic neurites. The appearance of inclusions varies, and in FTD this has led to further subcategorization based on four distinct pathological phenotypes as described in Table 1.1[40]. Each subtype is associated with different clinical phenotypes and mutations which lead to that particular pathology. For example, around 50% of FTD-TDP type A are familial associated with progranulin (*GRN*) mutations and *GRN* mutations always cause FTD-TDP type A pathology[41]. Type D pathology is incredibly rare, accounting for only 1% of familial FTD, always with valosin containing protein (*VCP*) mutations. This is summarised in Table 1.1.

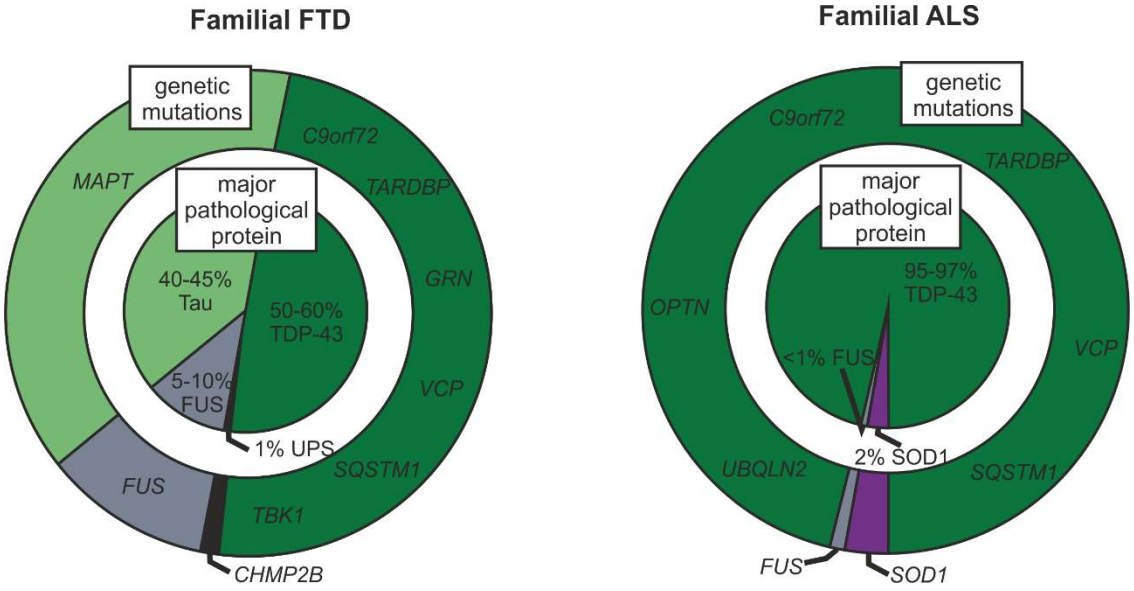

Figure 1.1 Genetic mutations and associated pathological proteins of familial FTD and ALS.

1.2.4 Epidemiology and aetiology

Table 1.1 Summary of FTD TDP-43 pathological subtypes as described by Mackenzie et al. (2009).

FTD-TDP subtype	Cortical pathology	Associated Clinical Syndrome	Associated Genetic Mutations
FTD-TDP Type A	Many neuronal cortical inclusions and short dystrophic neurites Predominantly cortical layer 2	bvFTD PNFA	*GRN* Rarely *C9orf72*
FTD-TDP Type B	Moderately abundant neuronal cortical inclusions and few dystrophic neurites All layers	bvFTD FTD/ALS	*C9orf72* Rarely *GRN*
FTD-TDP Type C	Few neuronal cortical inclusions and many long dystrophic neurites Predominantly layer 2	bvFTD SD	None known
FTD-TDP Type D	Few neuronal cortical inclusions, lentiform neuronal intranuclear inclusions, many short dystrophic neurites All layers	Inclusion body myopathy with FTD	*VCP*

The incidence of ALS is approximately 2 in 100,000[42] and the majority of cases are sporadic, with only 5-10% cases familial[22]. In contrast, 40-50% of FTD cases have a family history[43,44], and 20% of cases show an autosomal dominant inheritance pattern[45]. Of all the subtypes, bvFTD shows the strongest familial link, and SD the weakest[46,47].

The estimated incidence of FTD is reported between 2.7 and 15.1 per 100,000 adults, and accounts for up to ~20% of presenile dementia cases[6,48]. The average age of onset of FTD is between 45 and 65, but it is estimated that 20-25% of all FTD cases are in individuals over the age of 65 years, and is likely an underdiagnosed cause of dementia

in this age group[12,49]. Individuals much younger have also been reported with FTD including both familial and sporadic cases as young as 21[50].

1.2.5 Genetic causes

The genetics of FTD and ALS are highly heterogeneous, reflecting the range of both clinical and pathological features. The mutations identified in familial FTD and ALS do, however, follow common themes that point to mechanisms underlying cellular dysfunction, neurodegeneration and ultimately disease progression. 40-50% of FTD cases are familial, usually autosomal dominant[43]. ALS has a weaker genetic influence (5-10% cases are familial), but crucially the same range of pathological features are observed in both sporadic and familial cases[22]. This means that research aimed at dissecting the molecular basis of familial FTD and ALS can be translated to sporadic cases and importantly, allow targeted therapeutic intervention. Different mutations are associated with different pathology (explored in 1.2.3), variable age of onset, and different clinical syndromes. Investigating the genetic architecture underpinning each variant and the link between genotype and phenotype will be vital in order to tailor therapeutic action.

Although there are over 50 genes which have been implicated in FTD, the majority of heritability is accounted for by mutations in three genes: microtubule associated protein tau (*MAPT*)[51,52], progranulin (*GRN*)[53,54], and chromosome 9 open reading frame 72 (*C9orf72*)[55,56] (Figure 1.2). There is geographical variability in the prevalence of each mutation within populations (for example, *GRN* mutations are the most common in FTD cases in Northern Italy[57]) but generally *C9orf72* mutations account for the majority of familial cases, followed by *GRN* and *MAPT.* Rarer mutations each accounting for fewer than 5% of familial FTD are found in other genes, as detailed in Table 1. Some mutations that cause FTD are also known to cause ALS, most notably *C9orf72*.

In addition to *C9orf72* mutations, familial ALS has been linked to mutations in more than 20 different genes, most commonly *SOD1*[35], *TARDBP* (encoding TDP-43)[58,59], and *FUS*[60] (Figure 1.2). Although most familial cases are inherited in an autosomal dominant manner, rare instances of X-linked or recessive transmission have been reported[61,62]. In addition to the main genes detailed in Table 1.2, there are more than 1000 mutations that have been reported as risk factor, increasing susceptibility or modifying the phenotype[62].

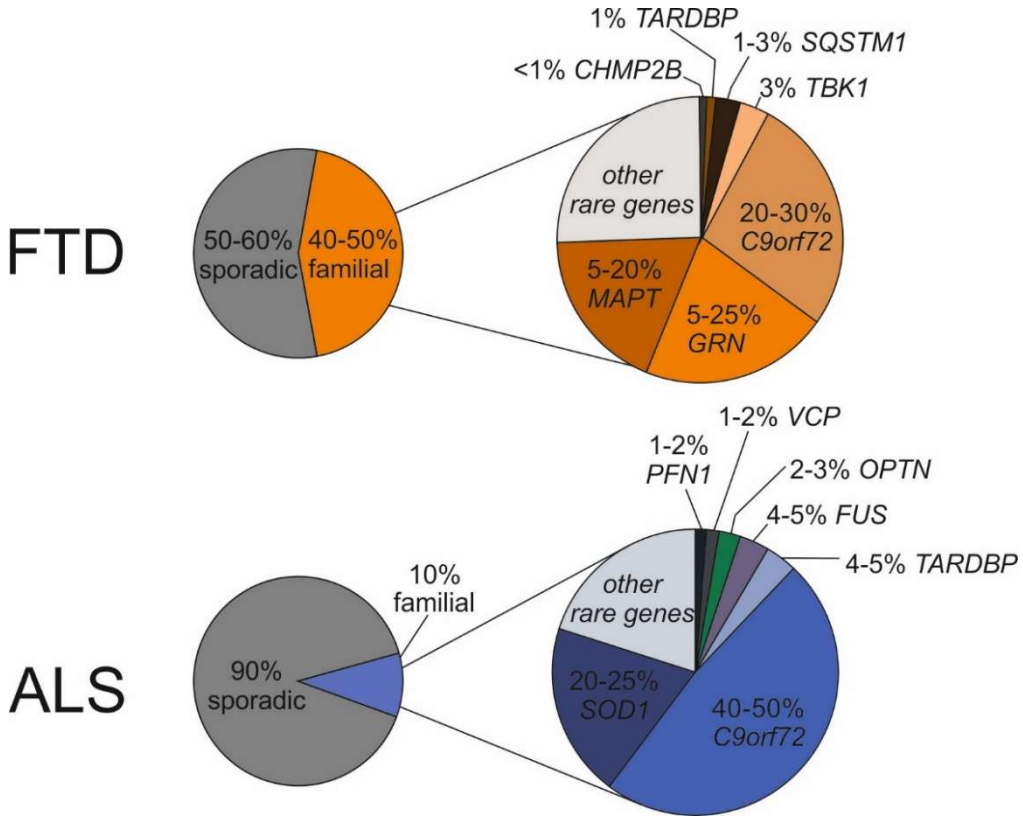

Figure 1.2 Summary of the genetic mutations implicated in familial FTD and ALS and their relative prevalence.

Despite the large number of genes implicated in FTD and ALS, common themes have emerged. A key feature of neurodegenerative disease in general, it is not surprising that motor neuron death in ALS has been linked to misfolding, aggregation and deposition of ubiquitinated proteins. It is thought that mutations in wild-type proteins increase the propensity of proteins to misfold and develop prion-like properties, as is the case with *SOD1* mutations[63]. SOD1 is a ubiquitously expressed metalloenzyme that catalyses the conversion of superoxide radicals into hydrogen peroxide and oxygen. Misfolded forms of mutant SOD1 are toxic through different mechanisms, including mitochondrial damage, implicating mitochondrial dysfunction and oxidative stress in ALS pathogenesis[64].

RNA processing has been implicated in both FTD and ALS since the discovery that mutations in RNA binding proteins *TARDBP* and *FUS* are causative in both diseases. Additional rare mutations in other RNA-binding proteins such as hnRNPA1 and A2/B1[65] and matrin 3[66] provide further evidence that RNA processing is likely a key process underlying pathology in these disorders.

Defects in the endosomal/lysosomal pathway are implicated in a number of neurodegenerative disorders, and mutations found in familial FTD and ALS provide

evidence that defects in this pathway are indeed a key pathogenic mechanism here. Splice-site mutations in *CHMP2B* leading to inclusion of an intronic sequence between exons 5 and 6 (*CHMP2B*^{Intron5}) cause FTD in a Danish family[67]. *CHMP2B* is a component of the endosomal sorting complexes required for transport (ESCRT) III complex, important in the multivesicular bodies (MVBs) sorting pathway. This pathway is critical for protein trafficking between the plasma membrane, trans-Golgi network, and lysosomes[68]. Additionally, mutations in *VCP*[69] and ubiquilin-2 (*UBQLN2*)[61], a multi-ubiquitin cain targeting factor involved in proteasomal degradation and a regulator of protein degradation respectively, are identified causes of FTD/ALS, pointing towards protein degradation as a common dysregulated pathway between diseases.

A defining characteristic of motor neurons is the length of their axons, and it stands to reason that this would render them particularly vulnerable to defects in intracellular transport[70]. Causative mutations in vesicle-associated membrane protein B (*VAPB*)[71] and dynactin (*DCTN1*)[72] support the involvement of microtubule transport defects in ALS pathogenesis: VAPB is important for Golgi and ER vesicle transport, whilst dynactin is required for tethering cargos to the retrograde transport motor dynein. A dynamic cytoskeleton is critical for maintaining normal transport mechanisms. Profilin 1 (*PFN1*), an essential factor for converting monomeric (G)-actin to filamentous (F)- actin, has been found to be a rare cause of ALS[73]. Taken together, these mutations along with *MAPT* mutations strongly implicate defects in intracellular transport in neuronal death, and likely contributes to the burden caused by defective protein degradation.

PFN1 is also linked to altered stress granule dynamics[74]. *PFN1* mutations and the identification of *TIA1* mutations in ALS/FTD, as well as other potent modifiers of disease such as *Ataxin-2* mutations, suggest aberrant formation and dissolution of stress granules could be contributing to pathogenesis in some cases[75].

Table 1.2 Summary of main genes implicated in familial FTD, ALS, FTD/ALS and related syndromes.

IBM: inclusion body myopathy; multisystem proteinopathy: rare complex phenotype associated with FTD.

Mutated gene	Protein	References	Gene function	FTD/ALS
C9orf72	C9orf72	DeJesus-Hernandez et al. 2011; Renton et al. 2011	Endocytosis; autophagy	ALS, FTD, FTD/ALS
CCNF	Cyclin F	Williams et al. 2016	Proteostasis	Rare in ALS
CHCHD10	Coiled-coil-helix coiled-coil-helix domain containing 10	Chaussenot et al. 2014; Bannwarth et al. 2014	Mitochondrial function	Rare in FTD/ALS
CHMP2B	Charged multivesicular body protein 2b	Skibinski et al. 2005	Autophagy, multivesicular body biogenesis	Rare in FTD
DCTN1	Dynactin	Munch et al. 2004	Vesicular transport	Rare in ALS
FUS	FUS RNA Binding Protein	Kwiatkowski et al. 2009; Vance et al. 2009	RNA processing	ALS, FTD/ALS, rarely FTD
GRN	Progranulin	Baker et al. 2006; Cruts et al. 2006	Lysosome function	FTD
hnRNPA1	Heterogeneous ribonucleoprotein A1	Kim et al. 2013	RNA processing	Rare in ALS and multisystem proteinopathy
hnRNPA2B1	Heterogeneous ribonucleoprotein A2/B1	Kim et al. 2013	RNA processing	Rare in ALS and multisystem proteinopathy

Table 1.2 Summary of main genes implicated in familial FTD, ALS, FTD/ALS and related syndromes.

IBM: inclusion body myopathy; multisystem proteinopathy: rare complex phenotype associated with FTD.

Mutated gene	Protein	References	Gene function	FTD/ALS
MAPT	Tau	Hutton et al. 1998; Poorkaj et al. 1998	Microtubule stabilisation	FTD
MATR3	Matrin3	Johnson et al. 2014; Millecamps et al. 2014	RNA processing	Rare in ALS
OPTN	Optineurin	Maruyama et al. 2010; Pottier et al. 2015	Vesicular transport, NF-kB signalling	Rare in FTD, ALS, FTD/ALS
PFN1	Profilin 1	Wu et al. 2012	Cytoskeletal regulation	
SOD1	SOD1	Rosen et al. 1993	Oxidative stress; mitochondrial function	ALS
SQSTM1	p62	Fecto et al. 2011; Le Ber et al. 2013	NFkB signalling; apoptosis; autophagy	Rare in ALS, Paget's disease of bone, FTD/ALS, FTD
TARDBP	TDP-43	Sreedharan et al. 2008; Rutherford et al. 2008	RNA processing	FTD/ALS
TIA1	T-cell restricted intracellular antigen 1	Mackenzie et al. 2017	Stress granules	Rare in ALS, FTD/ALS
TREM2	Triggering receptor expressed on myeloid cells 2	Guerreiro et al. 2013; Borroni et al. 2014	Inflammation	Rare in FTD

Table 1.2 Summary of main genes implicated in familial FTD, ALS, FTD/ALS and related syndromes.

IBM: inclusion body myopathy; multisystem proteinopathy: rare complex phenotype associated with FTD.

Mutated gene	Protein	References	Gene function	FTD/ALS
TUBA4A	Tubulin, Alpha 4A protein	Smith et al. 2014	Microtubules	Rare in ALS, FTD/ALS
UBQLN2	Ubiquilin 2	Daoud et al. 2012; Deng et al. 2011	Protein degradation	ALS, FTD/ALS, rarely FTD
VAPB	Vesicle-associated membrane protein B	Nishimura et al. 2004; Sanhueza et al. 2014	Vesicle trafficking	Rare in ALS
VCP	Valosin-containing protein	Watts et al. 2004; Forman et al. 2006	Protein degradation via UPS, autophagy, ER	FTD with IBM, ALS, FTD/ALS

1.3 *C9orf72* mutation

1.3.1 Discovery

Genetic linkage analyses of large FTD/ALS families, along with several genome-wide association studies (GWAS) first narrowed the risk haplotype to the 9p21 locus[76-78]. Further GWAS detected a single nucleotide polymorphism (SNP) within a 232 kb block of linkage disequilibrium in this region associated with ALS risk that also overlapped with a region known to be a risk factor for FTD[79]. This indicated a causative mutation for both diseases at this locus. In 2011 two groups independently identified an intronic GGGGCC repeat expansion as the mutation responsible[55,56]. Its discovery was hampered by the GC rich nature of the expansion preventing traditional sequencing techniques; high-throughput next-generation sequencing was eventually successful in uncovering the expansion within the first intron of the *C9orf72* gene[55,56].

1.3.2 Epidemiology

The *C9orf72* mutation explains approximately 4-29% of FTD patients[80,81]. There is a much stronger familial link with FTD than ALS, but of the 10% inherited cases of ALS, the *C9orf72* mutation is observed on average in 30%-50% of individuals. In individuals with no family history of ALS the prevalence is 4-10%[81,82]. In familial patients with both FTD and ALS, the expansion accounts for up to 88% of cases[81].

The frequency of the expansion varies by geography and ethnicity. The highest rates of the mutation are observed in those of northern European heritage, in particular in Scandinavian countries[81,83,84]. The expansion has been observed in the USA[81], Australia[85], and Africa, although it is relatively understudied in African populations[86]. Much lower rates are observed in Asian countries[81,87,88]. The relative absence of the mutation in India, Asia and the Pacific Islands could be explained by their physical distance from Europe, and therefore a lack of mixing between populations[81].

It has been posited that the *C9orf72* expansion arose from a single founder. Comparisons of haplotype data identified a SNP that is highly associated with the *C9orf72* mutation[81]. In a study of a large Italian cohort of familial and sporadic ALS patients, 95% of repeat expansion carriers also carried this SNP which was only present in 28% of the control group[89]. A high frequency of the mutation throughout Europe, along with the high prevalence of the expansion in Finnish populations, led to the hypothesis that the mutation arose from a common Finnish founder. Detailed genetic analysis of the

SNP in European populations predicted that the origin of the mutation was approximately 6300 years ago[84]. The selection pressure to remove the allele is expected to be relatively low as disease age of onset is generally after child-bearing age, so it is unlikely that the frequency of the expansion would decrease due to selective purification, although there is an argument that grandparents with the disease will be a burden on their children and thus reduce the likelihood that they will have children themselves. The SNP haplotype previously identified in European cohorts was found in FTD/ALS patients in China, pointing to a single founder, but casting some uncertainty as to the founder's origin. It has been speculated that the expansion spread from Finland, disseminated by the Vikings[90].

1.3.3 Pathology

There are a number of pathological features which set apart expansion carriers from non *C9orf72*-related FTD/ALS cases. MRI of FTD patients with and without the expansion has shown substantial atrophy of the thalamus and cerebellum in *C9orf72* carriers compared to non-carriers[91,92], areas which are known to have high *C9orf72* expression[93]. All cases of *C9orf72*-related ALS exhibit the classical molecular pathology of ALS including loss of motor neurons in the motor cortex and spinal cord, ubiquitinated, TDP-43- and OPTN-positive neuronal and glial cytoplasmic inclusions, Bunina bodies and pyramidal tract degeneration. The most striking difference between *C9orf72* -related ALS cases and those without the expansion is the degree of p62-positive neuronal cytoplasmic inclusions outside of motor areas, most markedly in the CA4 and CA3 regions of the hippocampus, a feature rarely observed in non-expansion carriers[94]. These inclusions presented in all cortical layers with few dystrophic neurites, consistent with Type B FTD-TDP pathology[40,94].

In addition to TDP-43 pathology, abundant p62-positive, TDP-43-negative inclusions were detected in the cerebellum and hippocampus of *C9orf72* patients[92,94-97]. Globular and star shaped cytoplasmic inclusions were identified in pyramidal cells of the hippocampus and cerebellar granular and molecular layers, as well as neuronal intranuclear inclusions in the majority of cases in the hippocampus, with fewer in the cerebellum. These unusual inclusions were later shown to contain dipeptide-repeat proteins (DPRs) produced by non-canonical translation of the GGGGCC repeat, as discussed later and shown in Figure 1.3[1]. These inclusions have since been observed in the basal ganglia, frontal and motor corteces[92,94-97] and shown to contain ubiquillin, a

ubiquitin-like protein involved in proteasomal degradation and autophagy[98]. DPRs also appear to be present in glial cells at a low frequency[99], as well as in skeletal muscle[100].

As well as protein inclusions, *C9orf72* RNA foci have been detected in the neurons of the frontal cortex, hippocampus and cerebellum in *C9orf72* -related FTD/ALS cases, as well as a small fraction of microglia and astroctytes[101,102]. They contain both sense and antisense RNA transcripts[103], but these are not equally distributed; sense transcripts have been detected at higher frequency in cerebellar Purkinje neurons and motor neurons compared to antisense transcripts which are present more often in cerebellar granule neurons in *C9orf72* ALS patients[104]. Moreover, despite having similar interactions with cellular proteins, mislocalisation of TDP-43 in motor neurons correlated with the presence of antisense foci only, suggesting that different RNA transcripts may have differential toxicity and roles in neurodegeneration. However, there is still much debate concerning the involvement of RNA foci in *C9orf72*-related FTD/ALS pathogenesis.

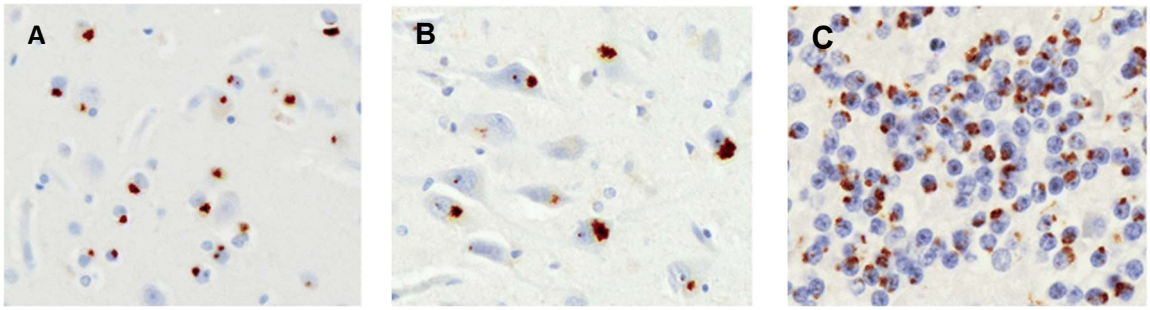

Figure 1.3 Dipeptide-repeat protein pathology in *C9orf72* expansion cases.
Neuronal cytoplasmic inclusions of GA seen in the frontal cortex **A**,CA3/4 pyramidal cells of the hippocampus **B**, and cerebellum **C**. Image from Mackenzie et al., 2014[1].

1.3.4 Clinical features

The most common variant of *C9orf72* FTD is bvFTD, accounting for 73-100% of all cases[55,105-108]. Bulbar onset is more common amongst *C9orf72* -related ALS than in those without the expansion, and psychosis is more common in FTD with the *C9orf72* mutation than in those without[109,110]. In a study of a Manchester cohort, patients reported disturbing delusions such as seeing the devil, hearing the voice of God or being infested with mites which congregated in the earlobe[14]. Another psychotic aspect of FTD in the misuse of objects that cannot be explained in cognitive terms. For example, one patient repeatedly used a toilet brush as a toothbrush, whilst another wrapped her faeces in newspaper and baked it in the oven[14].

In general, the symptomatic presentation of patients carrying the *C9orf72* repeat expansion are remarkably heterogeneous; most often they present with symptoms covered by the FTD and/or ALS umbrella, but other neurological disorders such as Alzheimer's Disease (AD)[111], Huntington's Disease (HD) phenocopies[112], CBD[113], intellectual disability[114], sporadic spinocerebellar ataxia [115] and parkinsonism[116,117] have also been reported. The diversity of clinical syndromes associated with the *C9orf72* mutation can delay diagnosis, as was evidenced in a case of bvFTD in a 64 year old woman who presented initially with atypical manifestations similar to those observed in anorexia nervosa, including restriction of oral intake, disordered eating and anxiety, leading to very low weight[118]. In addition to the vast range of symptoms, the age at onset varies widely, with cases reported from as young as 29 to as old as 82 at first symptoms. Not only does it vary between families, but within, up to 22 years of difference[95].

Taken together, the incredible variation of clinical presentation within expansion carriers suggests a substantial contribution by genetic modifiers to *C9orf72* mutation-related toxicity.

1.3.5 Repeat Length

The length of the *C9orf72* expansion in patients and its role as a potential genetic modifier has proved a contentious issue. There is no precise threshold of the number of repeat units at which the individual will definitely present symptoms. Dissecting the role of repeat length out from the tangled web of other genetic risk factors, clinical heterogeneity, and variable age of onset, is difficult. The general consensus of what constitutes a pathogenic expansion is one between several hundred and several thousand repeat units[56,119-122]. This is in contrast to most healthy control cohorts in which repeat lengths of up to 24 units are observed[55,56,108,120]. Larger repeat sizes have been reported in unaffected individuals, including some over 400 repeats in length[119], likely reflecting variability in onset age and reduced disease penetrance due to other factors.

There is substantial evidence to suggest that the very longest repeat expansions are only found in the CNS, and the expansions in non-CNS tissues are much smaller[123]. Furthermore, the intra-individual variation in expansion size between tissues is greater than the size variations within tissues of different individuals[124]. It is postulated those certain properties of each tissue, or their embryonic origin may influence the size of the expansion.

1.3.6 Mechanisms of disease

There are three main hypotheses of how the *C9orf72* repeat mutation results in neurodegeneration (summarised in Figure 1.4) and they are (1) haploinsufficiency caused by reduced transcription, (2) RNA-mediated toxicity, whereby the repeat is transcribed and the resulting RNA forms toxic foci that sequester important proteins, (3) DPR-mediated toxicity caused by non-canonical translation of the repeat RNA producing five different repeat proteins that disrupt cellular processes. It is generally accepted that the predominant driver of toxicity is the DPRs, but it is unclear to what degree each different DPR is responsible and how they may interact with the other mechanisms.

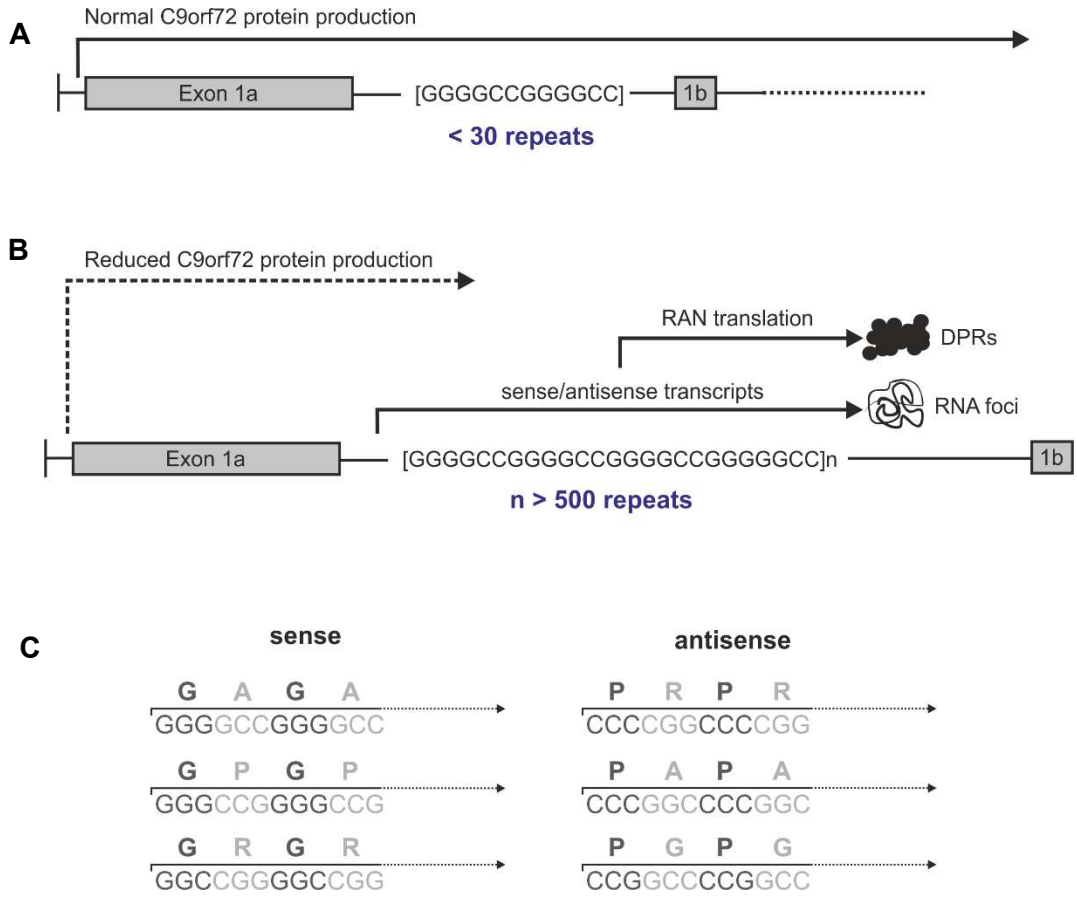

Figure 1.4 Mechanisms of GGGGCC repeat toxicity.

A Wild type *C9orf72* gene. **B** Large hexanucleotide repeat expansion disrupts C9orf72 protein production; the repeat itself is transcribed to produce both sense and antisense RNA, prone to forming RNA foci; repeat is translated to produce DPRs. **C** Repeat-associated non-ATG translation (RAN translation) of sense and antisense RNA produces 5 different dipeptide repeat proteins (DPRs).

1.3.7.1 Protein function and haploinsufficency

The C9orf72 protein itself is homologous to DENN (differentially expressed in normal and neoplastic cells) proteins, suggesting that it acts as a GEF (guanine exchange factor) for Rab GTPases, which are involved in the control of membrane trafficking events such as autophagy and endocytosis. It is most abundant in the brain and spinal cord, and is highly soluble, detectable in both the cytoplasm and the nucleus. In neurons it is localised to the presynaptic region where it forms a stable complex with WDR14 (WD-repeat containing protein 4) and SMCR8 (Smith-Magenis chromosome region 8), which recruits Rab proteins and thus controls autophagy from the initial recruitment of ubiquitinated substrates through to autophagosome-lysosome fusion.

The GGGGCC (G4C2) repeat sequence is situated in the first intron of the *C9orf72* gene and is thought to reduce gene expression via early transcription abortion, methylation of adjacent CpG islands and histones, as well as by causing persistent DNA hypermethylation[125,126]. Loss of function *C9orf72* mice develop inflammatory and autoimmune phenotypes, suggesting that C9orf72 may play a role in immune homeostasis in microglia[127]. However, the lack of neurodegenerative phenotypes and absence of TDP-43 accumulation in *C9orf72* knock-out mice strongly suggests that loss of function is not the primary cause of neurotoxicity in FTD and ALS[128]. It is possible that haploinsufficiency may potentiate toxic RNA and DPR gain-of-function in a non-cell autonomous manner, but it is unlikely to precipitate the disease in its own right[129].

1.3.7.2 Transcription and RNA toxicity

Bidirectional transcription of the G4C2 repeat produces repeat RNA prone to forming atypical secondary structures. Sense RNA is more abundant and tends to form hairpins and G-quadruplexes[130], whereas antisense RNA forms i-motifs and protonated hairpins[131]. Accumulations of sense and antisense RNA structures are known as RNA foci. RNA foci are a hallmark of FTD/ALS pathology, predominantly nuclear, and abundant in the frontal cortex. They are also observed to a lesser extent in astrocytes, microglia and oligodendrocytes[101]. Examination of RNA foci in *C9orf72* ALS cases revealed that RNA foci colocalise and directly interact with hnRNPA1 (heterogeneous nuclear riboprotein) and Pur-α, but not other RNA binding proteins including, significantly, TDP-43 and FUS[132,133]. However, hnRNPA1 is a binding partner for TDP-43, so this does not rule out RNA foci indirectly contributing to TDP-43 pathology[134]. They interact with RNA-binding proteins and disrupt gene regulation, translation and splicing[132,133,135]. RNA foci have been demonstrated to be involved in pathogenesis in

other repeat diseases; for example, in myotonic dystrophy type 1, they cause alterations in gene expression and splicing by binding and disrupting the function of RNA binding proteins[136].

However, evidence from RNA-only animal and cell models suggests that their contribution to toxicity is minimal[137,138]. In order to model the effect of RNA without DPRs, GGGGCC repeats can be regularly interspersed with stop codons to prevent translation in every frame. *Drosophila* models expressing RNA-only repeats of 36, 103 and 288 repeat units was not toxic[137,139]. However, a study in mice refutes this, as expression of 43 GGGGCC repeats from an intron is toxic to primary cortical and motor neurons without the production of DPRs[140]. Another *Drosophila* model expressed sense repeat RNA within an intron and although this was sufficient to form RNA foci, the efficient splicing of intronic RNA prevented nuclear export and therefore translation and was not toxic[138]. Taken together, the results suggest that expanded RNA may be toxic but only in certain systems, and therefore it is unlikely to be the main driver of neurodegeneration in *C9orf72*-related FTD/ALS. However, more research into in the role of repeat RNA, in particular antisense RNA, is needed to fully assess the contribution of RNA to toxicity.

1.3.7.3 RAN translation and DPR toxicity

The phenomenon of repeat associated non-AUG (RAN) translation was first observed in the microsatellite expansion disease spinocerebellar ataxia type 8[141]. Subsequently, interrogation of the potential for translation of *C9orf72* -related repeat RNA confirmed the production of DPRs. RAN translation of sense and anti-sense RNA produces five different dipeptide repeats: from the sense strand, glycine-alanine (GA) and glycine-arginine (GR); from the antisense strand, alanine-proline (AP) and proline-arginine (PR); from both strands, glycine-proline (GP)[142,143]. RAN translation of the *C9orf72* repeat is impervious to inhibition by the integrated stress response; in fact it is selectively enhanced[144], thus creating a potential positive-feedback loop that contributes to neurodegeneration.

The unique pathological hallmark of *C9orf72* -mediated disease is TDP-43 negative, p62 and ubiquitin-positive star-shaped cytoplasmic inclusions within neurons, glia and skeletal muscle[100,142,145,146], as discussed in 1.2.3. Clinico-pathological studies investigating the distribution and quantifying GA in a *C9orf72* mutation cohort found DPR pathology to be consistent across the cohort regardless of clinical phenotype[147,148]. There is some evidence to suggest a lack of correlation between DPR load and the extent of

neurodegeneration[149] but these studies are based on post-mortem tissue, where only surviving cells can be analysed. Therefore, the absence of DPR pathology in end-stage disease does not preclude their toxicity in cells already lost. Additionally, the observations were made using immunohistochemistry techniques which do not take into account any pathological burden of soluble DPR oligomers, an emerging theme in other neurodegenerative diseases such as Alzheimer's and Parkinson's Disease[150].

Not all DPRs are equal, in terms of abundance, physical properties, and likely toxicity. GA inclusions appear most visible in *C9orf72* patient brains, followed by GP, GR, PR and AP[148], although it must be considered that this is based on immunohistochemistry where antibody affinity may vary. The reported relative abundance of soluble and insoluble DPRs varies throughout the brain and there is a large degree of variability in DPR protein levels between individuals[151]. Whilst human studies have proved inconclusive in terms of the role of DPRs in disease progression, overexpression cell and animal models provide strong evidence that DPRs are the toxic species. GA, PR and in particular GR have all been widely reported to have toxic effects in various model systems[137,152,153], and there is a plethora of pathways thought to be dysregulated by their expression. This is further complicated with the expectation that they could interact with each other and act synergistically with loss of function mechanisms.

The secondary structures formed by each DPR have been investigated *in vitro* but the link between their distinct structural properties and cellular toxicity have yet to be fully elucidated. GA has been the most extensively researched in this regard due to its amyloid-beta like structure; it forms flat, densely packed, ribbon-type fibrils that have been shown to have the potential to transmit between cells[154], disrupt nucleocytoplasmic transport[155] and recruit and inhibit the proteasome[154-159]. It is this ability to form beta sheets that sets it apart from the other DPRs and could explain why it is more toxic than AP and GP, the other two uncharged DPRs. GR has been shown to form a similar structure, and therefore it has been suggested that glycine contributes most to this characteristic[160].

The unique biochemical configuration of proline precludes the formation of beta sheets in AP, GP, and PR due to the central ring restricting possible confirmations of the backbone[161]. The structure of AP and GP is flexible coils and they are unable to aggregate by themselves in the same way[74,162]. Indeed, as predicted based on their structural properties, GP and AP interact with fewer intracellular proteins[74], which is consistent with their lack of toxicity in model systems[74,137,140,163].

PR also contains proline but unlike AP, GA, and GP, it is charged and highly polar due to the presence of arginine. This is likely why it behaves more similarly to GR in terms of toxicity. Indeed, collectively these two DPRs are often referred to as “arginine-rich” DPRs, due to the predicted importance of this residue to their toxicity. It confers a high hydrophilicity and is likely responsible for their highly interactive nature. We know that both GR and PR accumulate in the nucleus of transfected cells[152,153], and post-mortem patient brain tissues[99,147] and disrupt ribosomal RNA biogenesis when overexpressed[152]. Nuclear localisation signal domains tend to be rich in in arginine, and it is possible these DPRs are able to mimic this and gain access to the nucleus through transportation[152]. Additionally, multiple studies have focused on perturbed liquid-liquid phase separation (LLPS) dynamics, important in the formation and dissolution of membraneless organelles such as the nucleolus[74,140]. This theory is based on the concept that arginine containing proteins are capable of interacting with low complexity sequence domains (LCDs) of RNA binding proteins (RBPs) and thus alter LLPS dynamics[74,164]. Perturbation of physiological LLPS by GR and PR in both cytoplasmic (e.g. stress granules, Cajal bodies) as well as within the nucleus[74,165-167] provides another mechanism by which arginine-rich DPRs could act to cause neurodegeneration. However, there has been limited *in vivo* work to confirm this.

PR and GR are also capable of interacting with different cytoplasmic targets, such as translation initiation factor eIF3η and ribosomal subunits, causing translational inhibition and disrupting ribosome biogenesis and rRNA processing respectively[74,167-169]. GR has also been shown to induce oxidative stress by interacting with mitochondrial ribosomes[74,170]. Dysregulation of nucleocytoplasmic transport genes has also been implicated in PR and GR toxicity in *Drosophila* and yeast[171,172].

1.4 Modelling *C9orf72*-related gain of function toxicity *in vivo*

Broadly, there are 3 types of gain of function *C9orf72* model: pure repeat, RNA-only, and DPR-only. Pure repeat models contain the G4C2 sequence and therefore produce both repetitive RNA and all five DPRs, as in patients. The disadvantage of these models is the inability to distinguish between the effect of RNA and DPRs. Therefore, transgenes that produce only repetitive RNA without DPRs, and transgenes encoding each of the DPRs individually using alternative codons have been developed and used to generate *in vivo* RNA-only and DPR-only models.

1.4.1 Gain of function mouse models

There are several mouse models of gain of function toxicity, including both pure repeat and DPR models. Transgenic overexpression of GGGGCC repeats in mice, either on their own via somatic brain transgenesis mediated by adeno-associated virus[173] or as part of a patient derived bacterial artificial chromosome (BAC)[174-176], produces RNA foci and at least some DPR expression. However, the presence of TDP-43 pathology, motor and cognitive impairment, and survival deficits are inconsistent. This is likely due to differences in the genetic background of the mice, known to have a significant impact on neurodegenerative phenotypes in mice rather than the nature of the repeat itself[177]. Additionally, expression levels between models are different; Chew et al.[173] and Liu et al.[174] showed that high levels of overexpression of shorter repeats was toxic, suggesting that a threshold level of DPR and/or RNA was not reached in non-toxic models.

Models expressing individual DPRs without repeat RNA allow the contribution of each DPR to be examined. To date, there are few mouse models of DPR toxicity. Schludi et al (2017) generated a mouse expressing GA149 in neurons which exhibited motor deficits without apparent neuronal loss[178]. Abundant GA inclusions were observed in the spinal cord and in lower motor neurons and this was shown to increase over time. Additionally, GA co-aggregated with p62, which is consistent with data from patient tissue, but did not sequester Unc119 which contradicts other studies suggesting that GA is toxic via Unc119 sequestration[158]. Moderately elevated levels of phosphorylated TDP-43 were observed, but no mislocalisation, suggesting that GA was contributing to, but not capable of causing TDP-43 pathology alone. In 2019 a PR28 mouse model was developed, which showed motor imbalance, neuronal loss, and inflammation in the cerebellum and spinal cord[179]. Transcriptional analysis indicated that PR28 caused differential expression of genes relating to synaptic transmission. Furthermore, it was shown that in the cerebellum, heterozygous mice show differential expression of genes related to synaptic transmission[179]. However, a repeat length of 28 is well below the threshold thought to be pathogenic in patients, and other equivalent length DPRs were not modelled in this study. In 2020, GA175 and PR175 expressing mice were generated[180]. 40% of poly-PR mice showed ataxia and seizures, requiring euthanasia by 6 weeks of age, but the remaining mice were asymptomatic and this was attributed to decreases in transgenic mRNA. All GA175 mice displayed neuronal loss, inflammation, and muscle denervation and wasting, and they had to be euthanised before 7 weeks of age[180]. As yet, there has been little further investigation into mechanistic pathways using these models. Whilst mice provide a mammalian system which is anatomically and genetically more similar to humans, the current understanding of DPR-mediated toxicity

is limited, and thus a higher throughput model system is required. In future, when there is a deeper understanding and greater consensus as to the mechanisms underpinning *C9orf72*-related FTD/ALS, mouse models will be invaluable to validate and further examine hypotheses in a mammalian model. For now, *Drosophila* models provide a tractable and high-throughput system to investigate the role of DPRs in *C9orf72* -related FTD/ALS.

1.4.2 *Drosophila* as a model to study neurodegeneration and human neurodegenerative disorders

In order to probe the mechanisms underpinning neurodegenerative diseases, we must develop robust and reliable models. Human genetic studies can implicate genetic loci, and post-mortem studies can provide limited insight into molecular mechanisms, but focus only on end-stage disease. Not to mention the ethical and technical considerations required for human studies. The fruit fly, *Drosophila melanogaster*, is an ideal model organism for the study of human neurodegenerative diseases for a number of reasons.

Drosophila has been a popular choice for studying the genetic basis of human diseases over the past century due to its genetic tractability, short generation time, and relatively low cost. The fly genome was sequenced in 2000 and there are a number of well-established and highly sophisticated tools that are readily available for virtually every disease-related fly gene, of which 75% have homology in humans. Furthermore, *Drosophila* has a relatively low genetic redundancy, which is incredibly useful when dissecting the role of a particular gene. The fruit fly is particularly suited to neurodegenerative disease research, as demonstrated by the number of successful studies using *Drosophila* models of, for example, AD[181,182], PD[183,184], and Lysosomal Storage Disorders[185]. Furthermore, despite having a mere ~200,000–300,000 neurons compared to the human brain's 86 billion, the underlying neuronal architecture and function of the fly central nervous system are similar, comprising a brain and thoracic ganglion, the equivalent of the human spinal cord (Figure 1.5). The fly CNS has the advantage of being less complex, whilst still retaining important similarities such as the blood-brain barrier, support from glia, as well as similarities at the molecular level[186]. *Drosophila* display complex behaviours such as learning and memory, reflecting their complex nervous system and making them attractive for studies looking into neuronal dysfunction[187]. As most neurodegenerative diseases are late-onset, the short lifespan of *Drosophila* is a key advantage for such studies. A healthy *Drosophila* population will have a median lifespan of approximately 70 days at 25 ˚C, so ageing a fly to the equivalent of

an older person (>65 years), takes only approximately four weeks. Crucially, flies show signs of physiological ageing equivalent to those seen in humans, such as impaired memory and negative geotaxis[188,189].

Drosophila do not have a *C9orf72* orthologue and whilst this precludes investigating the contribution of loss of function, it provides the ideal model for looking exclusively at gain of function toxicity. There are many examples of pure repeat, RNA-only and DPR fly models, summarised in Figure 1.6. There is a lesser focus on the sense and antisense repeat RNA produced by transcription in isolation because the DPRs are considered the major toxic species. Nevertheless, there are RNA-only fly models that have been used to determine what contribution repeat RNA makes to disease progression. These models usually carry G4C2 repeat under the control of a *UAS* promoter but interspersed with stop codons to prevent translation. More recently, the RNA sequence was introduced into an intron and there is evidence that the genomic location of RNA-only repeats alters the formation and location of RNA foci in adult neurons[190]. Most RNA-only models produce only sense RNA and there is limited data on antisense RNA, but there is no evidence to suggest that antisense RNA is more toxic[190]. In almost all RNA-only models, regardless of size or the nature of the transgene, RNA expression was not strongly toxic. It did not cause toxicity up to 288 repeats, in contrast to pure repeats which caused severe degeneration at 103 repeats, and there are no survival defects[137]. When extended to a physiologically relevant length of over 1000 repeat units, the only difference of note was the increase in the number of RNA foci observed in adult neurons[190]. However, this does not rule out a contribution for RNA in disease progression; in *C9orf72*-related FTD patient brains RNA foci are abundant in the frontal cortex where there is greatest neuronal loss, and there are studies which point to specific mechanisms by which RNA can be toxic[101,191].

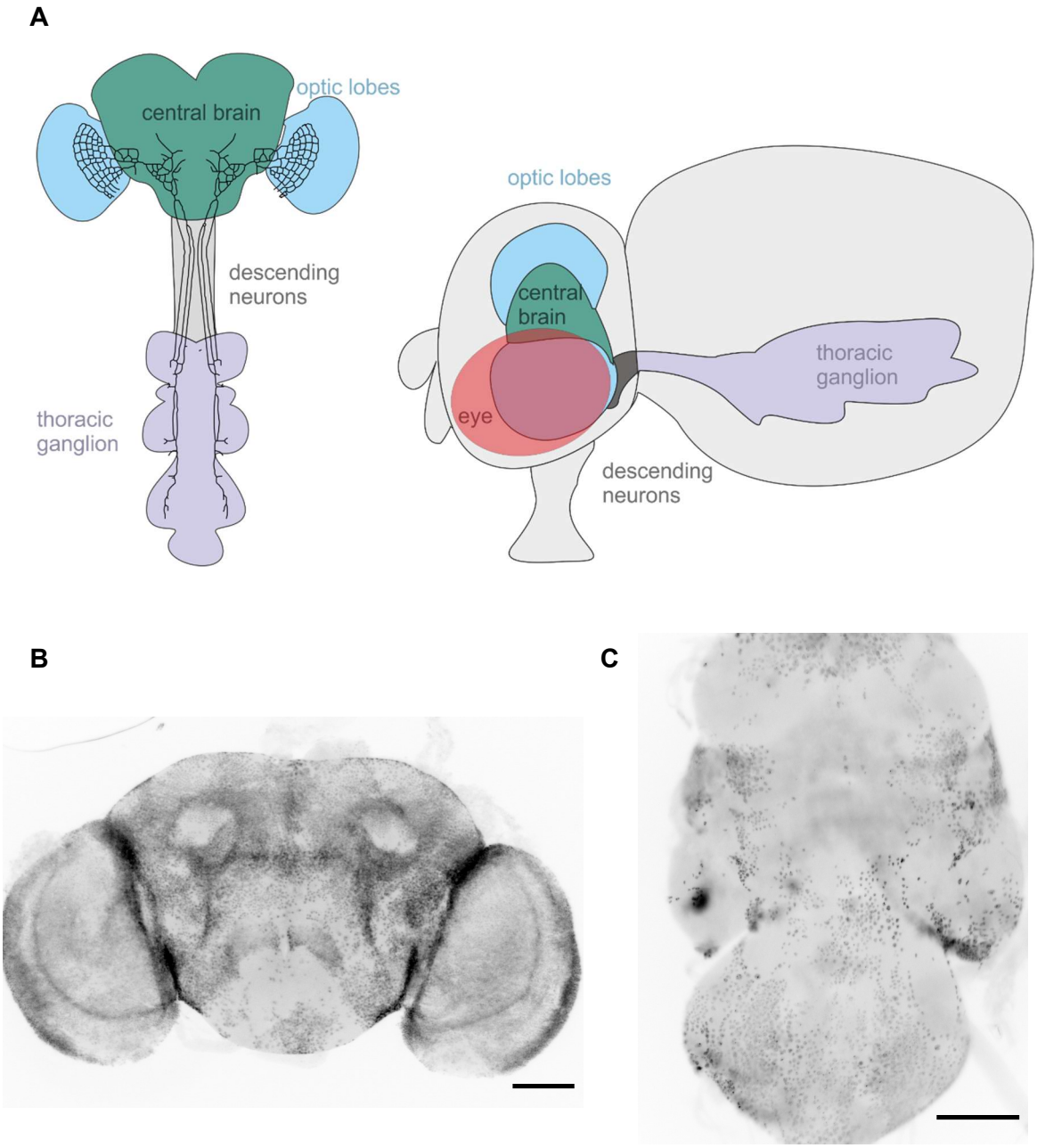

Figure 1.5 The *Drosophila* central nervous system.

A Diagram showing the brain and thoracic ganglion (ventral nerve cord) in the adult fly. The thoracic ganglion is the insect analogue of the vertebrate spinal cord and is the site of reception and integration of sensory information, generating locomotion actions in the legs and wings. Visual information from the eye is relayed to the central brain via the optic lobes. **B**,**C** Images of **A** the adult fly brain and **B** the adult thoracic ganglion stained with anti-elav (neuronal nuclei). Scale bars 100 µm.

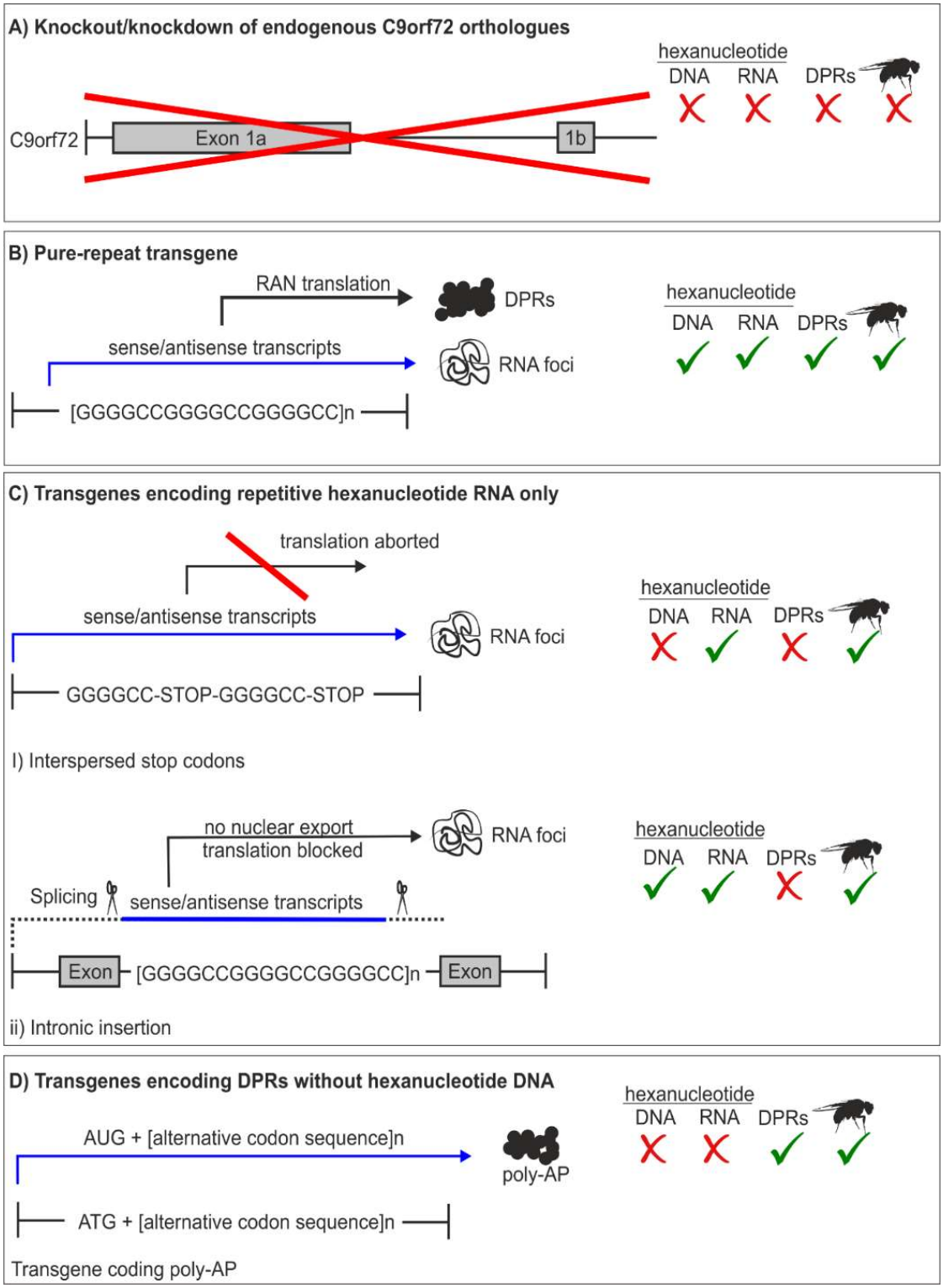

Figure 1.6 Different fly models of *C9orf72*-FTD/ALS.

A Due to the absence of a *Drosophila* orthologue of *C9orf72*, only gain of function mechanisms can be studied: **B** insertion of a pure repeat transgene that produces both RNA and all 5 DPRs, **C** RNA constructs either containing interspersed stop codons or inserted into an intron to prevent translation, **D** transgenes encoding DPRs only, using an alternative codon sequence to produce each DPR individually.

There are a plethora of fly DPR models, as detailed in Table 1.3. In these models, each DPR is produced independently of repeat RNA and the other DPRs by using an alternative coding sequence. Generally, consistent with other approaches, arginine-rich GR and PR, and to a lesser extent GA, appear most toxic in fly models[137]. However, most DPRs expressed in these models are shorter than the repeat length observed in patients.

Furthermore, studies using these models tend to focus on the already established toxic species PR and GR. Therefore, any mechanistic contributions from the other DPRs remain relatively unexplored. The most popular method to gauge the relative toxicity of each DPR is often via expression in the eye using *GMR-Gal4*. However, although the *Drosophila* eye is a robust screening tool, it is not necessarily the most relevant expression system to investigate DPR toxicity in the nervous system. Short repeat PR and GR, up to 100 repeats, appear overtly toxic even when expressed solely in the eye, or when expression is induced in adulthood[137,192,193]. Lifespan, and viability are severely reduced in pan-neuronally expressing PR and GR flies[137], which precludes further exploration of age-related phenotypes. Moreover, there is limited research testing motor function in DPR-expressing flies despite motor problems being a defining characteristic of ALS. There is no doubt that existing DPR fly models have made huge contributions to our understanding of DPR toxicity, but there is the possibility that by using apparently acutely toxic short DPRs, we are missing subtle age- and length- dependent phenotypes that may help us to understand more about the intricacies of *C9orf72*-related FTD/ALS.

Table 1.3 Summary of *C9orf72 Drosophila* models to date.

Model	Repeat length	Reference
Pure repeat		
UAS-GGGGCC	3, 36, 103	Mizielinska et al. 2014
	8, 28, 58	Freibaum et al. 2015
	29, 49	Goodman et al. 2019
UAS-GGGGCC-EGFP	3, 30	Xu and Xu, 2013
UAS-DsRed2-GGGGCC	8, 32, 38, 56, 64, 128	Solomon et al. 2018
UAS-LDS-(G4C2)44.GR-GFP	44	Goodman et al. 2019
RNA only		
UAS-GGGGCC RO	36, 108, 288	Mizielinska et al. 2014
UAS-GGGGCC RO	48	Burguete et al. 2018
UAS-CCCCGG RO	107	Moens et al. 2018
UAS-GGGGCC RO	800, 100, >1000	Moens et al. 2018

Table 1.3 Summary of *C9orf72 Drosophila* models to date.

UAS-CCCCGG RO (intronic)	108	Moens et al. 2018
UAS- GGGGCC RO (intronic)	106, 1152	Moens et al. 2018
GA		
UAS-polyGA	36, 100	Mizielinska et al. 2014
	8, 64	Solomon et al. 2018
UAS-FLAG-EGFP-polyGA	50	Wen et al. 2014
UAS-FLAG-polyGA	25, 50	Boeynaems et al 2016
	80	Yang et al. 2015
UAS-EGFP-polyGA	50	Freibaum et al. 2015
	36	Xu and Xu 2018
UAS-polyGA-mCherry	36, 100, 200	Morón-Oset et al. 2019
UAS-polyGA-EGFP	1020	West et al. 2020
AP		
UAS-polyAP	36, 100	Mizielinska et al. 2014
	8, 64	Solomon et al. 2018
UAS-FLAG-EGFP-polyAP	50	Wen et al. 2014
UAS-FLAG-polyAP	25, 50	Boeynaems et al 2016
UAS-EGFP-polyAP	50	Freibaum et al. 2015
	36	Xu and Xu 2018
UAS-polyAP-EGFP	1024	West et al. 2020
PR		
UAS-polyPR	36, 100	Mizielinska et al. 2014
	8, 64	Solomon et al. 2018
UAS-FLAG-EGFP-polyPR	50	Wen et al. 2014
UAS-FLAG-polyPR	25, 50	Boeynaems et al 2016
	80	Yang et al. 2015
UAS-EGFP-polyPR	50	Freibaum et al. 2015
	36	Xu and Xu 2018
UAS-polyPR-EGFP	1100	West et al. 2020
GR		
UAS-polyGR	36, 100	Mizielinska et al. 2014
	8, 64	Solomon et al. 2018
UAS-FLAG-EGFP-polyGR	50	Wen et al. 2014
UAS-FLAG-polyGR	25, 50	Boeynaems et al 2016
	80	Yang et al. 2015
UAS-EGFP-polyGR	50	Freibaum et al. 2015
	36	Xu and Xu 2018

Table 1.3 Summary of *C9orf72 Drosophila* models to date.

UAS-polyGR-EGFP	1136	West et al. 2020
GP		
UAS-EGFP-polyGP	47	Freibaum et al. 2015

1.4.3 Genetics

1.4.4 Balancer chromosomes

Balancer chromosomes are a fundamental component of *Drosophila* research due to their usefulness in maintaining stable stocks carrying a deleterious heterozygous mutation. Multiple chromosome inversions prevent homologous recombination in females (it does not occur in males) by preventing synapsis between homologous chromosomes whilst allowing normal segregation. In the event of recombination, chromosomal fragment duplication and deletions causes lethality. Balancer chromosomes are also homozygous lethal and therefore the desired heterozygous mutation can be maintained in the population. Additionally, they carry dominant phenotypic markers which allow them, and therefore the opposite allele, to be followed through the mating scheme, as shown in Figure 1.7.

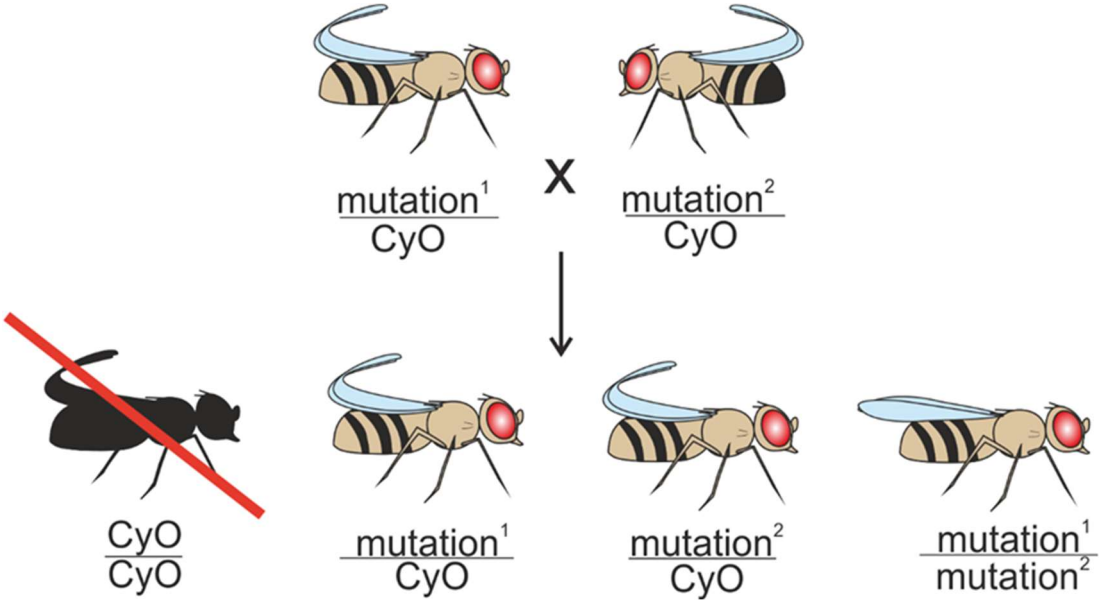

Figure 1.7 *Drosophila* mating scheme design.
Scheme designed to combine two mutations on the same chromosome. The *CyO* balancer carries a phenotypic marker, curly wings. Therefore, the progeny with a copy of each mutation can be identified by straight wings.

1.4.5 The *UAS-Gal4* system

The *UAS-Gal4* system is an incredibly useful and versatile expression system first developed as a tool in *Drosophila* by Andrea Brand and Norbert Perrimon, in 1993[194]. It has become the most widely used system for ectopic spatially restricted transgene expression in the fly, and its use has since been extended to allow temporal as well as spatial regulation[195]. *UAS-GAL4* is a bipartite expression system that utilises the yeast GAL4 protein and its upstream activating sequence (*UAS*). The *Gal4* is under the control of a tissue specific promoter and therefore expressed in a specific pattern. In turn, the *UAS* target gene is expressed in an identical pattern. Crucially, the *Gal4* gene and the *UAS*-transgene are separated into different transgenic fly lines; only when the flies are crossed do the progeny express the gene in the directed pattern (Figure 1.8).

The system has been further developed to allow even more tightly controlled expression, through expression of the GAL4 agonist, GAL80, as well as drug- and heat-inducible *Gal4*s.

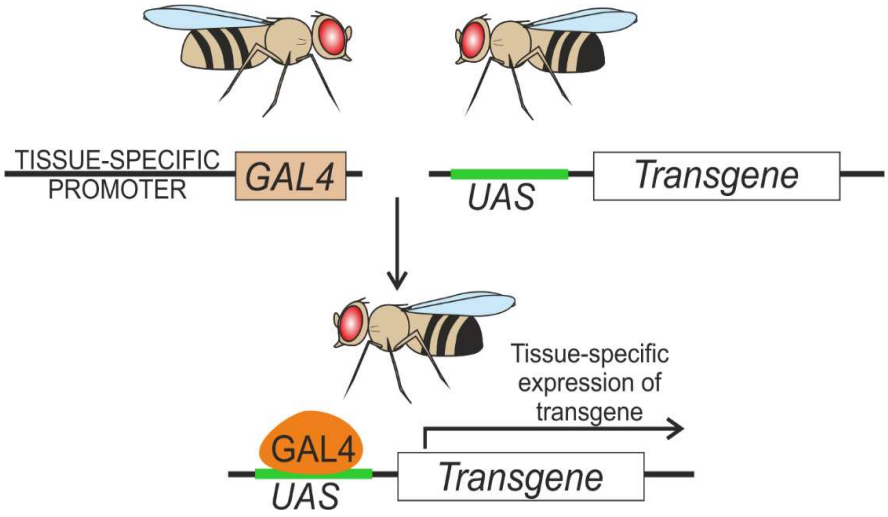

Figure 1.8 The *UAS/Gal4* system.

Allows ectopic gene expression in a controlled tissue specific manner. Two fly lines, each carrying one of the two components (*Gal4*/*UAS*), can be crossed to produce progeny where the *UAS*-transgene is expressed in a specified pattern.

1.5 Research Aims

It has been one decade since the discovery of the *C9orf72* mutation as a major genetic cause of FTD/ALS. Since then, there has been considerable progress in our understanding of how it precipitates disease. *Drosophila* and other models have played a key part in this, in particular in delineating the role of RNA and DPR toxicity. However, there remains a lack of models using physiologically relevant repeat lengths to elucidate

mechanisms. Much of the current research focuses on the arginine-rich DPRs, PR and GR, and ignores the potential contribution of AP, GA and GP. Furthermore, there have been few attempts to assess what happens when two or more DPRs are co-expressed in the same model, as is likely to be the case in patients. Therefore, we may be missing important aspects in DPR pathogenesis by focusing on individually expressed DPRs at shorter repeat lengths.

The main aims of this research project were therefore to:

1. Generate a novel *Drosophila* model expressing over 1000 repeat DPRs
2. Fully characterise each DPR's effect on established neurodegenerative phenotypes
3. Investigate the impact of co-expressing two DPRs on the toxicity of individual DPRs.

2 Materials and Methods

2.1 *Drosophila* husbandry and genetics

Drosophila used in this study were either purchased from Bloomington Stock Centre (BDSC, Indiana University, Bloomington, U.S.A), kind gifts from the *Drosophila* community, or an existing stock of the Manchester Fly Facility (University of Manchester, UK). DPR lines were generated as part of this work, or shortly before by Ryan West, as described in 2.2. A detailed list of stocks is included in Table 2.1. The two *nSyb-Gal4* lines used in this investigation will be referred to as *nSyb-Gal4* (II) and *nSyb-Gal4* (III), referring which chromosome they are situated, throughout.

Fly stocks were maintained at 29 °C, 25 °C or 18 °C on a 12 h light:dark cycle, in constant humidity on standard maize flour–yeast–glucose medium, and transferred to fresh food every 2 and 4 weeks respectively. Fly food was prepared by the University of Manchester Media Service according to a standard recipe (72 g/l maize flour, 50 g/l yeast, 80 g/l glucose, 8 g/l agar). Following mixing with water and autoclaving, the food is allowed to cool before adding nipagin and propionic acid for a final concentration of 2.7% and 0.3% respectively.

In order to determine sex and genotype, flies were anaesthetised on a porous gas pad supplying constant CO_2. Experimental crosses were raised at 25 °C, unless stated otherwise, giving a ~ 10-12 day life cycle (egg to adult). Female *Drosophila* must be collected as virgins for crosses to ensure only sperm from the chosen male genotype will be capable of fertilising the egg. Females remain virgins for ~ 8 h post-eclosion, therefore vials are emptied and any females that eclose in the next 6-8 h are collected. Additionally, young virgins can be identified by pale pigmentation, folded wings, and the presence of meconium visible through the abdominal cuticle[196].

Table 2.1 Stocks used during the course of this investigation.

Only primary stocks are listed; double balanced stocks and stocks combining multiple genetic elements are not listed for brevity.

Stock	Chromosome	Source	Description
Wild Type			
w^{1118}	N/A	Manchester Fly Facility	Wild type (white eye)
Canton S	N/A	Manchester Fly Facility	Wild type (red eye)
UAS lines			
UAS-AP1000^{1}*-EGFP/TM6B, Tb*^{1}*, Hu, e*^{1}	Third	Generated During Study	AP1000 with EGFP tag
UAS-AP1000^{3}*-EGFP/TM6B, Tb*^{1}*, Hu, e*^{1}	Third	Generated During Study	AP1000 with EGFP tag
UAS-GA1000^{2}*-EGFP/TM6B, Tb*^{1}*, Hu, e*^{1}	Third	Generated During Study	GA1000 with EGFP tag
UAS-GA1000^{3}*-EGFP/TM6B, Tb*^{1}*, Hu, e*^{1}	Third	Generated During Study	GA1000 with EGFP tag
UAS-PR1000^{H} *-EGFP/TM6B, Tb*^{1}*, Hu, e*^{1}	Third	Generated During Study	PR1000 with EGFP tag
UAS-PR1000^{B} *-EGFP/ M6B, Tb*^{1}*, Hu, e*^{1}	Third	Generated During Study	PR1000 with EGFP tag
UAS-GR1000^{1}*-EGFP/TM6B, Tb*^{1}*, Hu, e*^{1}	Third	Generated During Study	GR1000 with EGFP tag
UAS-GR1000^{2}*-EGFP/TM6B, Tb*^{1}*, Hu, e*^{1}	Third	Generated During Study	GR1000 with EGFP tag
UAS-mCD8-EGFP/TM6B, Tb^{1}*, Hu, e*^{1}	Third	RRID:BDSC_32184	Membrane-targeted Enhanced Green Fluorescent Protein
Gal4 **lines**			
nSyb-Gal4/TM6B, Tb^{1}*, Hu, e*^{1}	Third	RRID:BDSC_51635	Neuronal Synaptobrevin, pan-neuronal driver
nSyb-Gal4/CyO-GFP	Second	Chris Elliot (University of York, UK)	Neuronal Synaptobrevin, pan-neuronal driver
Tub-Gal4/TM6B, Tb^{1}*, Hu, e*^{1}	Third	RRID:BDSC_5138	Tubulin promoter, global driver

Table 2.1 Stocks used during the course of this investigation.

Only primary stocks are listed; double balanced stocks and stocks combining multiple genetic elements are not listed for brevity.

Stock	Chromosome	Source	Description
GMR-Gal4/*CyO-GFP*	Third	Sean Sweeney (University of York, UK)	Glass multimer reporter, eye-specific driver
Repo-Gal4/*TM6B*	Third	RRID:BDSC_7415	Reversed polarity, glial-specific driver
nSyb-Gal4, *mCD8-GFP*/*TM6B, Tb*^{1}*, Hu, e*^{1}	Third	Sean Sweeney (University of York, UK)	Pan-neuronally driven membrane-localised GFP
nSyb-Gal4, *mCD8-GFP*/*CyO*	Second	Sean Sweeney (University of York, UK)	Pan-neuronally driven membrane-localised GFP
Balancers			
TM3/*TM6B*	Third		Third chromosome balancer
CyO-GFP/*If*	Second		Second chromosome balancer
CyO-GFP/*If*;MKRS/*TM6B, Tb*^{1}*, Hu, e*^{1}	Second, third		Second and third chromosome balancer
Bang-sensitive seizure mutants			
Sod2^{n283}/*CyO*	Second	RRID:BDSC_34060	*Sod2* (superoxide dismutase 2 (Mn)) loss of function (imprecise P-element excision)
Sod2^{KG06854}/*CyO*	Second	RRID:BDSC_14052	Hypomorphic *Sod2* (superoxide dismutase 2 (Mn)) allele (P-element insertion)
kdn^{KG04873}/*FM7c*	X	RRID:BDSC_14436	Hypomorphic *knockdown* (mitochondrial citrate synthase) allele (P-element insertion)

Table 2.1 Stocks used during the course of this investigation.

Only primary stocks are listed; double balanced stocks and stocks combining multiple genetic elements are not listed for brevity.

Stock	Chromosome	Source	Description
β4GalNAcTA$^{4.1}$/CyO	Second	RRID:BDSC_9379	*β1,4-N-acetylgalactosaminyltransferaseA* loss of function allele (imprecise P-element excision)
stai^{B200}/CyO	Second	RRID:BDSC_16165	Hypomorphic *stathmin* allele (piggyBac transposon insertion)
stai^{irdtp}/CyO	Second	RRID:BDSC_32541	Hypomorphic *stathmin* allele (spontaneous P-element insertion)
Sirup^{1}/CyO	Second	RRID:BDSC_76570	TALEN induced *sirup* (succinate dehydrogenase 4) loss of function
Sirup^{2}/CyO	Second	RRID:BDSC_76571	TALEN induced *sirup* (succinate dehydrogenase 4) loss of function
kcc$^{P20-180}$/SM6a	Second	RRID:BDSC_5206	EMS induced hypomorphic *kazachoc* (Solute Carrier Family 12 Member 4) allele
kcc^{Ad-4}/SM6a	Second	RRID:BDSC_5207	EMS induced hypomorphic *kazachoc* (Solute Carrier Family 12 Member 4) allele
Syn^{97}	Third	RRID:BDSC_83706	Null *synapsin* allele (imprecise P-element excision)

2.2 Generation of transgenic DPR flies

2.2.1 Generation of DPR constructs

Subcloning was completed by Ryan West. 1000 repeat DPR constructs[153] were subcloned from the pEGFP-N1 vector (#6085-1, Takara Bio, US) into pUASt-attB using EcoRI and XbaI restriction sites to maintain the EGFP tag. Transformations were performed using 5-alpha Competent *E. coli* (#C2992, New England Biolabs, MA, US) to minimize retraction of repeats, and DNA extracted using QIAprep Spin Miniprep kits (QIAGEN, UK), following the manufacturer's instructions. Constructs were screened by sequencing (GATC, light run) using pUASt (forward: AGCGCAGCTGAACAAGCTA, reverse: TGTCCAATTATGTCACACCACA) and EGFP primers (forward: CATGGTCCTGCTGGAGTTCGTG, reverse: CGTCGCCGTCCAGCTCGACCAG) and restriction digest for the repeat region with both EcoRI and BamHI and for the repeat region and EGFP with EcoRI (#R3101) and XbaI (#R0145) (high fidelity, NEB) and agarose gel electrophoresis. The full DPR construct sequence is shown in Appendix 1.

2.2.2 Microinjection and transformant selection

Transgenic fly lines were generated by site directed phiC31-integrase-mediated insertion into the *attP-9A* locus. Constructs were microinjected into M[vas-int.DM]ZH-2A;PBac[y[+]-attP-9A]VK00005 embryos. Microinjection was carried out by the Department of Genetics Fly Facility, University of Cambridge. Resulting flies were then crossed to w^{1118} flies and potential transformants identified by an orange eye resulting from the pUAST mini-white element. Individual transformants were crossed to flies carrying the third chromosome balancer in a white eye background w^{1118}*;;TM6B/TM3*; offspring carrying *TM6B* were then selected to make a stable stock. The full genotypes of DPR stocks is listed in Table 2.1. Repeat lengths for each DPR are AP:1024 repeat units, GA:1020, PR:1100, GR:1136. Each construct is followed by a C-Terminal EGFP tag, which is established to have no effect on DPR localisation or pathology[153]. Stocks were routinely (every few months) screened for repeat length and stability using Southern blotting, due to the observed instability of DPR constructs in other models[197]. However, as it is not possible to determine the exact number of repeats by Southern blotting and for simplicity, DPR fly lines are referred to as, for example, AP1000.

2.2.3 Screening transgenic *Drosophila* for repeat length

Due to the large, repetitive and GC rich nature of the DPR constructs, PCR-based genotyping cannot be used to screen the DNA for the correct repeat length. Therefore, Southern Blotting was used. A previously established protocol was modified for fly DNA[145]. DNA was extracted from ~50 adult heads using standard genomic extraction. Heads were separated from the abdomen by snap freezing and vortexing in a 15 ml Falcon tube inside a 50 ml Falcon tube containing a piece of dry ice. After homogenising with a pipette tip filled with genomic extraction buffer (25 mM NaCl, 10 mM Tris-HCl pH 8.2, 1 mM EDTA, Proteinase K 200 µg/m, 1 ml per head), and expelling all the liquid, heads were incubated overnight at 57 °C. One volume phenol-chloroform-isoamylalcohol (25:24:1) was added and incubated at room temperature for 1 h with rotation. Following centrifugation for 5 min at 13000 rpm, the aqueous layer was removed to a new tube, and the procedure repeated with pure chloroform. The DNA was recovered by a standard ethanol precipitation and dissolved in 100 µl nuclease free water. DNA was digested with Dde1 (#R0175) and NlaIII (#R0125) enzymes (NEB) in Cutsmart buffer (#B7204 NEB) to leave DPR construct. Restriction enzyme digests were carried out in 50 µl total volume and incubated at 37 °C overnight to ensure complete digestion of genomic DNA. Following ethanol precipitation, DNA was dissolved at 4 °C for ~ 2 days in nuclease free water before running the Southern Blot.

The negative control for Southern Blotting was DNA extracted from Canton S flies and digested as above. The positive controls were wild-type (Canton S) DNA spiked with 154.7 ng of pUAST-AttB containing DPR construct per 1 µg of genomic DNA. This was calculated based on the amount of plasmid required to give the equivalent of haploid DPR DNA. 5 ng of this DNA was loaded for the blot. Samples were mixed with 5 X loading buffer (NEB) containing bromophenol blue and electrophoresed at 100 V on a 1 % agarose gel containing 0.5 µg/ml ethidium bromide in tris-borate-EDTA (TBE) buffer for ~ 3 h. DIG-labelled DNA marker II (Roche, UK) and 1kb plus DNA ladder (NEB) was loaded to alongside the samples. The visible ladder is used as a reference for the size of the DNA fragments when the gel is trimmed after electrophoresis.

After trimming, the gel was incubated with depurination solution (0.25 M HCl) with shaking for 10min or until the bromophenol blue turns yellow. After briefly rinsing in distilled water, the gel was incubated with denaturing solution (0.6 M NaCl, 0.2 M NaOH) for 30 min, followed by 30 min in neutralising solution (1.5 M NaCl, 0.5 M Tris-HCl pH8.0). The gel was equilibrated for 20 min in 20 X SSC (3M NaCl, 300mM Sodium citrate pH 7.4) before the blot was assembled. The Southern Blot was assembled as shown in Figure 2.1. Briefly, three strips of Whatman™ (#WHA30306185, GE Healthcare, UK) 3MM paper were cut to slightly wider than the gel and long enough to allow buffer from

the buffer reservoir to wick up into the gel. A nylon membrane was placed on top of the gel using clean forceps, followed by 3 pieces of 3MM paper and 15 of thick blotting paper of the same size. A light, even weight was placed on top of the blotting paper, and the gel left to transfer overnight at room temperature.

The blot was then disassembled and the membrane gently washed in 2 X SSC before UV fixation for 3 min. The membrane was pre-hybridised in 30 ml prewarmed DIG easy hyb (Roche, Cat. No. 11 603 558 001) with 3000 µg of freshly denatured salmon sperm DNA (Agilent Technologies, UK, Part No. 201190) (boiled for 10 min and removed to ice to prevent re-annealing) in a hybridisation bottle for 4 h at 42 °C with rotation. After pre-hybridisation, the solution was poured off and replaced by hybridisation solution: 15 ml pre-warmed DIG easy hyb with 1500 µg freshly denatured salmon sperm and 7.5 µl 10 ng/µl oligo probe stock (Eurofins, UK):

GA probe: DIG-GGCAGGAGCTGGAGCTGGCGCAGGAGCTGGTGCTGGG-DIG

GR probe: DIG-AGGCAGAGGTCGTGGGAGAGGCAGGGGTCGCGGACGTGGA-DIG

AP probe: DIG-AGCACCAGCACCGGCGCCAGCTCCAGCACCAGCACCC-DIG;

PR probe: DIG-AGACCCCGTCCTCGTCCTCGTCCAAGACCAAGGCCGAGGC-DIG

The membrane was hybridised overnight at 42 °C. After hybridisation, the solution was poured off and then subject to two successive 15 min washes in prewarmed 2 X SSC, 0.1 % Sodium dodecyl sulfate (SDS) at 65 °C. A further wash in 0.5 X SSC, 0.1 % SDS was added to remove background.

After washing, the hybridisation bottle is briefly rinsed in maleic acid wash buffer (DIG Wash and Block Buffer Set, Roche, #1 585 762 001) and the membrane transferred to a clean plastic dish (90 mm x 9 mm) and incubated with shaking for 2 min in maleic acid buffer (DIG Wash and Block Buffer Set). The membrane was then incubated with 50 ml 10 X DIG block (DIG Wash and Block Buffer Set) diluted in maleic acid buffer for 30 min, followed by incubation in 20 ml antibody solution for 30 min: 20 µl anti-Digoxigenin-AP, Fab fragments (Roche, RRID:AB_2734716) diluted 1:20,000 in DIG block after centrifuging the tube for 15 min at 13,000 rpm to separate antibody complexes. After two 15 min washes in maleic acid wash buffer, the membrane was equilibrated for 5 min in 20 ml detection buffer (DIG Wash and Block Buffer Set) diluted in PCR grade water. Chemiluminescent detection was used to detect DNA fragments; the membrane was covered in 1.5 ml CDP-*Star*® chemiluminescent substrate (Roche, #CAS160081-62-9) and sandwiched between two sheets of clean acetate before imaging. Blots were imaged using a G:box imaging unit (Syngene, UK).

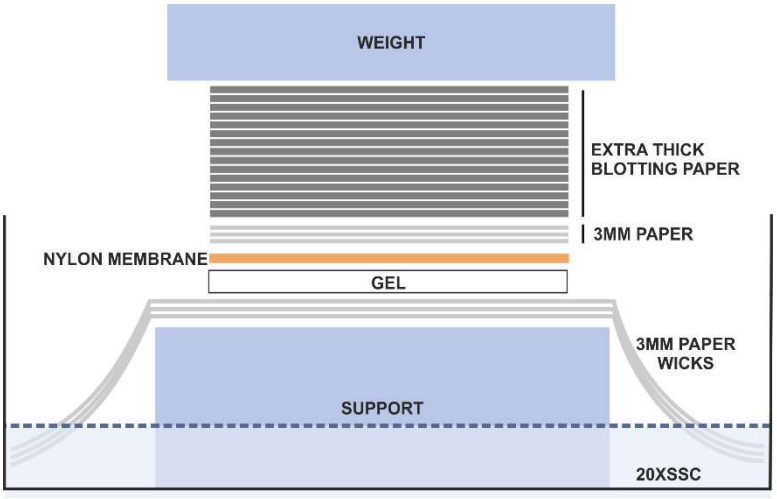

Figure 2.1 Southern blotting assembly.

2.3 Immunoprecipitation and western blotting

Immunoprecipitation and western blotting were performed by Ryan West. Heads were isolated from ~ 1000 *Drosophila*, per genotype, pan-neuronally expressing either UAS-AP1000, UAS-GA1000, UAS-PR1000, UAS-GR1000 or UAS-mCD8-GFP under the control of *nSyb-Gal4* (III). Wild type controls were Canton-S outcrossed to w^{1118}. Heads were lysed in RIPA buffer (10 mM Tris–Cl pH 8.0, 1 mM EDTA, 0.5 mM EGTA, 1 % Triton X-100, 0.1 % Sodium deoxycholate, 0.1 % SDS, 140 mM NaCl), lysate cleared via centrifugation and filtration through 0.45 µm filters and diluted to 4 mg/ml. Lysates were incubated with pre-washed ChromoTek GFP-Trap® magnetic affinity beads (30 µl, overnight 4 °C). Beads were then washed and protein eluted in 4 X laemmli buffer. Samples were diluted and run on 4–15% Mini-PROTEAN ® TGX™ Precast Gels. Transfers were performed overnight at 4 °C (25 V, 0.02 % SDS, 10 % methanol, immobilon-P .45 µm Polyvinylidene fluoride (PVDF)). Primary antibodies were anti-GFP (abcam, preabsorbed against *Drosophila* embryos) and anti-GR repeat (Proteintech) (Table 2.2). Secondary antibodies were HRP conjugated anti-rabbit IgG (Stratech) (Table 2.3). Blots were imaged using a G:box imaging unit (Syngene).

2.4 Survival assays

2.4.1 Viability assays

Homozygous DPR flies were crossed to heterozygous *nSyb* (III), *repo*, or *tubulin- Gal4* flies to give an expected ratio of 50:50 for flies with and without the *TM6B* balancer (Figure 2.2), carrying humeral. Offspring from a minimum of three crosses per genotype were counted.

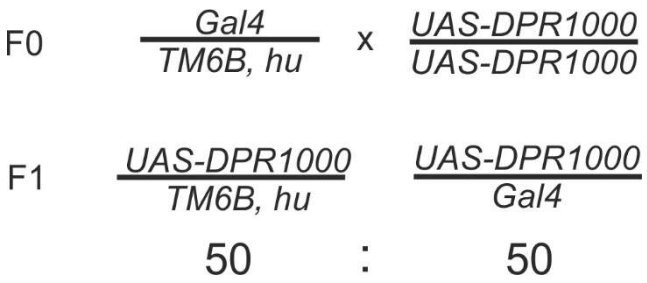

Figure 2.2 Crossing scheme for viability assay.
Designed to give a 50:50 ratio of balanced to non-balanced (experimental) flies.

2.4.2 Longevity assay

Adult male flies expressing the DPRs or GFP under the control of *nSyb-Gal4* (III) in addition to wild type controls were collected within 24 h post-eclosion and maintained in standard culture vials with 10 flies per vial at 25 °C. Flies were counted daily and transferred to fresh food every 3 days. Kaplan-Meier survival curves were plotted using the survival analysis function in GraphPad Prism 7. Significance was determined using a Log-rank (Mantel-Cox) test with Bonferroni correction for multiple comparisons. A minimum of one hundred flies per genotype was analysed.

2.5 Eye screens

2.5.1 Classification of eye score

Eye screens were carried out at 25 °C, apart from in the experiment analysing the effect of dose on phenotype (Figure 3.7) where they were carried out at 29 °C to increase expression. The *GMR-Gal4* driver was used to drive expression of DPRs in the eye. Eyes were examined under a dissecting microscope within 3 days post-eclosion. An 8-point scoring system, modified from Pandey et al. (2007), Ritson et al. (2010)[198,199] to allow differentiation between more subtle phenotypes was used. A fly scored one point for each for: pigmentation defects, melanised patches, ommatidial fusion, ommatidial disorganisation, misarranged/duplication of interommatidial bristles, alterations to eye size, gross morphological disruption (Figure 2.3). Pharate lethality scored 9. Flies from a minimum of 3 crosses per genotype were used.

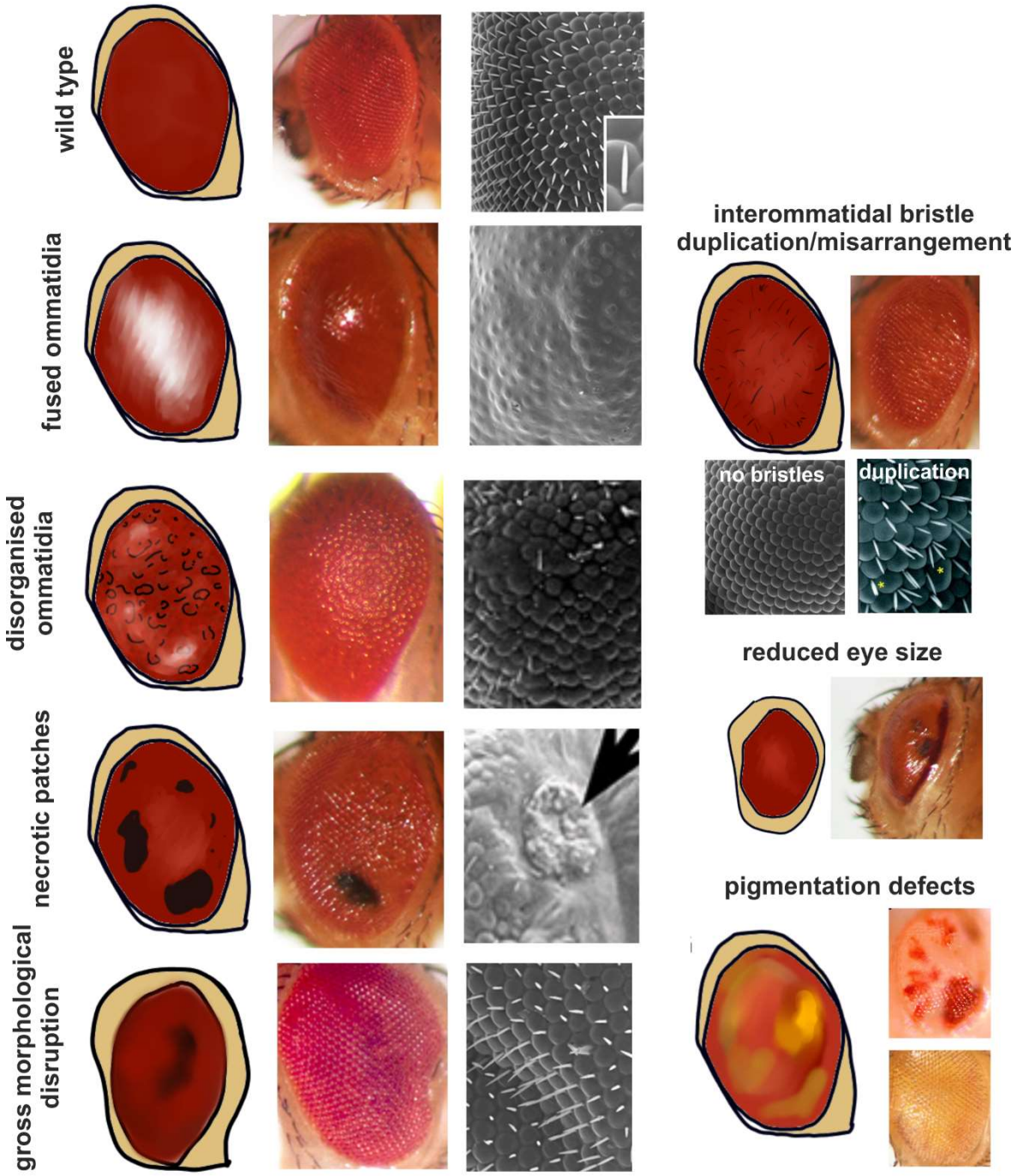

Figure 2.3 Eye screen point scoring system.

Graphical (left), photographic (centre), and scanning electron micrographs (right, where appropriate) of each phenotype which scored one point in the eye screens detailed in 2.5.1. Graphics created for this project, colour photos and micrographs obtained from Son et al. (2020)[200], Oortvel (2013) [201], Tazelaar et al. (2020)[202], M'Angale et al. (2016)[203], Barmchi et al. (2016)[204], Ambegaokar et al. (2010)[205], Bose et al. (2006)[206].

2.5.2 Microscopy and imaging

Eyes were imaged using a Zeiss Z.1 lightsheet confocal using the autofluorescence from the fly cuticle in the 488 nm wavelength. The lightsheet chamber was filled with PBS. Whole flies fixed in 3.7 % formaldehyde in PBS and mounted in 1% low melting point agar were imaged using a 5x objective with 2x zoom, bidirectional scanning. ImageJ (v1.53) was used to generate a maximum intensity projection for an image of the whole surface of the eye.

2.6 Behavioural assays

2.6.1 Larval crawling assay

Individual third-instar wandering larvae were collected and allowed to acclimatise to the stage. Arenas were made by pouring 2 % agarose into the lid of a 96 well plate, cutting channels between four equal sections, and filling the grooves with 5 M NaCl to dissuade larvae from crawling out (Figure 2.4). Larval locomotion was tracked using the DanioVision™ Observation Chamber connected to a computer with EthoVision® XT software (Noldus Information Technology, VA, US). Locomotion was tracked for 3 min and total distance crawled in the tracking period was calculated by the EthoVision® XT software using centroid tracking.

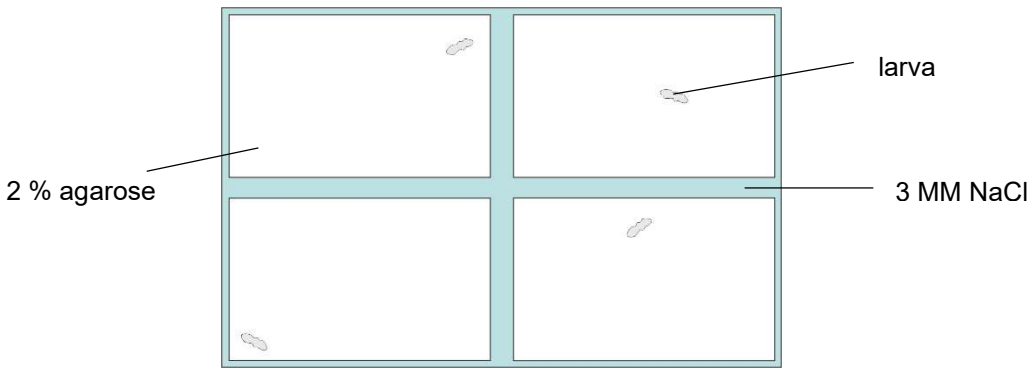

Figure 2.4 Schematic of larval crawling experimental setup.
Crawling arenas. One larva is placed in each arena, and the grooves are filled with 3 MM NaCl to prevent larvae from leaving their arena. Not to scale.

2.6.2 Startle-induced negative geotaxis assay

Male flies were placed, without anaesthetisation, into boiling tubes (one fly per tube) mounted on a white background (Figure 2.5) and allowed to acclimatise for one minute.

To elicit the start-induced negative geotactic (SING) response, flies were banged to the bottom of the tubes in a consistent manner. Flies were filmed for a maximum of 90 s using a Silverlabel Focus Action Camera (1080P, OneCall #PY32209). The assay was performed at 25 °C and at the same time of day within one 30 min window to ensure no circadian differences. The driver used was *nSyb-Gal4* (III) on the third chromosome for the initial climbing assay, and *nSyb-Gal4* (II) on the second chromosome for the co-expression experiment to circumvent the need to recombine DPR constructs with the *nSyb-Gal4* driver. Offspring from three independent crosses per genotype were used for the assay.

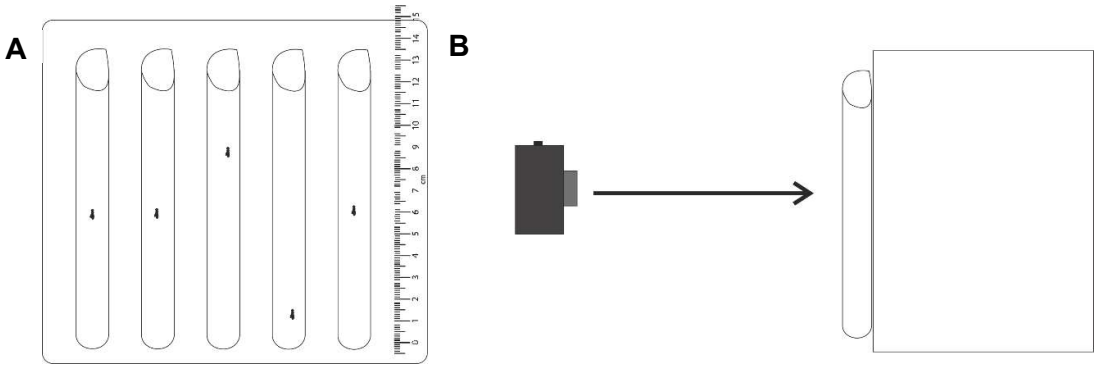

Figure 2.5 Schematic of adult climbing apparatus.

A Front view of flies climbing in glass boiling tubes mounted on white background with scale. **B** Side view showing camera and mounted boiling tubes. Not to scale.

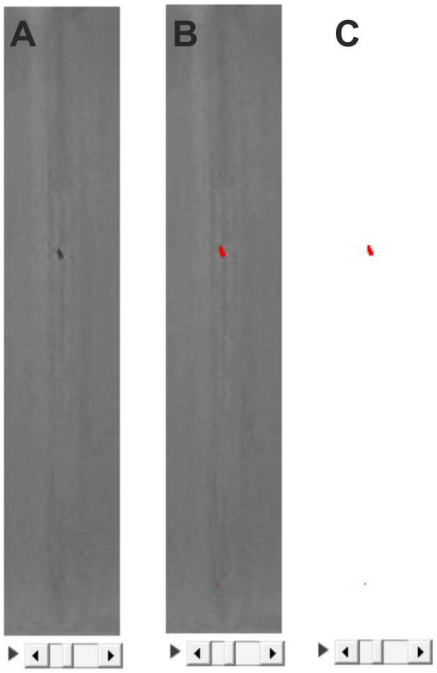

Figure 2.6 Thresholding in ImageJ.

Choosing a pixel value cut-off that distinguished the fly as pixels greater than this cut-off and excludes background. Screenshots of **A** Original video, **B** adjusting the threshold, **C** tube with threshold applied, showing only the fly. This process was automated by a custom macro.

The videos were temporally cropped to remove the banging down phase, and spatially cropped into separate videos for each lane. Videos were analysed in batches using custom macros in ImageJ (v1.53). A threshold was applied to the videos to isolate the fly (Figure 2.6), and the MTrack2 plugin used to track movement and plot the position between frames at a rate of 30 frames per second. The relative positions of the flies were used to calculate the median speed over a 15 s period. Where possible, the 15 s period was selected to cover the time where the fly was moving, as too many 0s, indicating a stationary fly, would skew the median speed.

2.6.3 Bang-sensitive seizure assay

Flies were transferred to empty food vials with a maximum of 5 flies per vial. The vial was vortexed in a VORTEX-GENIE® 2 (Scientific Industries Inc., NY, US) at maximum speed (10) for 10 s and the flies filmed until the last fly had recovered or for a maximum of 3 minutes. Videos were then analysed and the presence of, and the length of a seizures recorded. Data was recorded in Microsoft Excel and analysed in RStudio (R version 3.6.3). Due to the known instability of DPR constructs[197], *nSyb-Gal4*/*CyO*;DPR/*TM6B* flies were made as an intermediate, rather than kept as a stock. A stock where the DPRs are permanently driven would potentially increase the selective pressure to lose repeats or excise the construct completely. Therefore, *nSyb-Gal4*/*CyO*;DPR/*TM6B* flies were immediately crossed to DPR/*TM6B* flies, or bang-sensitive mutants depending on the experimental genotype desired. A minimum of 3 crosses produced each intermediate and experimental genotype.

2.7 Electrophysiology

Electrophysiological recordings and analysis were performed on *nSyb-Gal4* (III) driven DPR larvae by Anna Munro as described[207]. Electrophysiological recordings were carried out at room temperature in third instar wandering larvae. Larval dissection and electrophysiological recordings were performed in HL3 saline (70 mM NaCl, 5 mM KCl, 20 mM $MgCl_2$ hexahydrate, 10 mM $NaHCO_3$, 115 mM Sucrose, 5 mM HEPES, 1.5 mM $CaCl_2$). Borosilicate glass electrodes (Harvard Apparatus #GC100F-10) were pulled to a resistance of 25-35 MΩ (Flaming brown micropipette puller, P-97; Sutter Instruments) and back filled with 3 mM KCl. Intracellular recordings were performed on muscle 6 of segments A3-4 using an AxoClamp-2B amplifier controlled by pClamp (version 10.3) with a Digidata 1322A analogue–digital converter (Molecular Devices, Axon Instruments). Frequency and amplitude of mEJP events was calculated using

MiniAnalysis (v6.0.7, Synaptosoft), with mEJP events selected manually. Input Resistance (R_i) and EJP amplitude calculated using Clampfit (v10.6, Axon Instruments).

2.8 Histology

2.8.1 Sample preparation

Histological analysis was performed on *nSyb-Gal4* (III) driven DPR flies. 28 days post-eclosion, *Drosophila* heads were removed, leaving the proboscis intact so as not to damage the brain, and fixed in 3.7 % formaldehyde in PBS + 0.1 % tween, 4 °C with rotation. Heads were embedded using JB-4 resin (Sigma #EM0100). Heads were dehydrated and infiltrated using a graded series of ethanol:infiltration solution (0:50, 25:75, 10:90, 0:100 × 3, 30 min 4 °C followed by 0:100 for 48 h 4 °C with rotation, Infiltration solution: 2.5% catalyst (benzoyl peroxide, plasticized) in JB-4 Solution A (w/v)). Heads were embedded in 1:25 accelerator (JB-4 Solution B):infiltration solution in polyethylene embedding moulding trays (Polysciences Europe GmbH, Germany #16643A-1) with embedding stubs (agar scientific, UK #AGG3552). They were left to polymerise overnight at 4 °C.

2.8.2 Sectioning and staining

Heads were sectioned at 4 µm intervals using tungsten blades on a Leica RM2255 microtome. When the head was reached, a constant slicing speed of 1 mm/s was attained using the automatic single cut mode. Each section was collected using a paintbrush and placed in a 40 °C water bath. From there it was picked up using a charged microscope slide and left to dry for 1-2 days. Hematoxylin and eosin staining and coverslipping was performed using a Leica ST5010 Autostainer XL. Slides were left to dry for a further 2 days.

2.8.3 Imaging and vacuolisation analysis

Histological sections were imaged using H&E autofluorescence in the 633 nm channel on a Leica DM6000 B Microscope using a Hamamatsu ORCA-R^2 C10600-10B-H camera. Quantification of vacuoles in histological sections was performed by measuring the diameter of all vacuoles within a defined 500 µm region of interest using ImageJ (v1.53). Measurements were taken across multiple sections covering the same region of the brain and from at least 3 animals per genotype. From this, the number of holes > 5

µm and > 10 µm were counted. These sizes were chosen based on previous reports of what constitutes a neurodegenerative vacuole (> 5 µm), and what is described as a "large" vacuole (>10 µm)[208-210].

2.9 *Drosophila* brain and larval immunohistochemistry

2.9.1 *Drosophila* brain and thoracic ganglion dissection

Heads (for brain dissection) or the thorax (for thoracic ganglion dissection) of adult flies were transferred to a sylgard dish (Silicone elastromere kit, DowCorning, MI, USA) and dissected in PBS (137 mM NaCl, 2.7 mM KCl, 10 mM Na_2HPO_4 and 1.8 mM KH_2PO_4 in dH_2O) using forceps and under a dissecting microscope. The dissected brains/thoracic ganglia were fixed in 3.7 % formaldehyde (FA, Sigma #252549) in PBS for 1 h. Brains were then washed three times in 0.5 % PBS-T (0.5 % triton X-100 in PBS (v/v)) and transferred to a 1.5 ml Eppendorf tube.

2.9.2 *Drosophila* larval dissection

Female third instar wandering larvae of the required genotype were transferred onto a sylgard dish and dissected in PBS under a dissecting microscope. Larvae were pinned, dorsal side up at posterior and anterior ends using minuten pins (Austerlitz Insect Pins 0.1 mm diameter, Fine Science Tools, Germany #26002-10). Using Vannas sprung straight bladed dissection scissors (Fine Science Tools, #15610-08), an incision was made along the dorsal midline of the larvae from the posterior to anterior. Forceps were used to remove the internal organs and the muscle walls pinned out (Figure 2.7)[211]. Preps were fixed in 3.7 % FA for 7 min, unpinned and transferred to a 1.5 ml Eppendorf tube and washed 3 times in 0.5 % PBS-T.

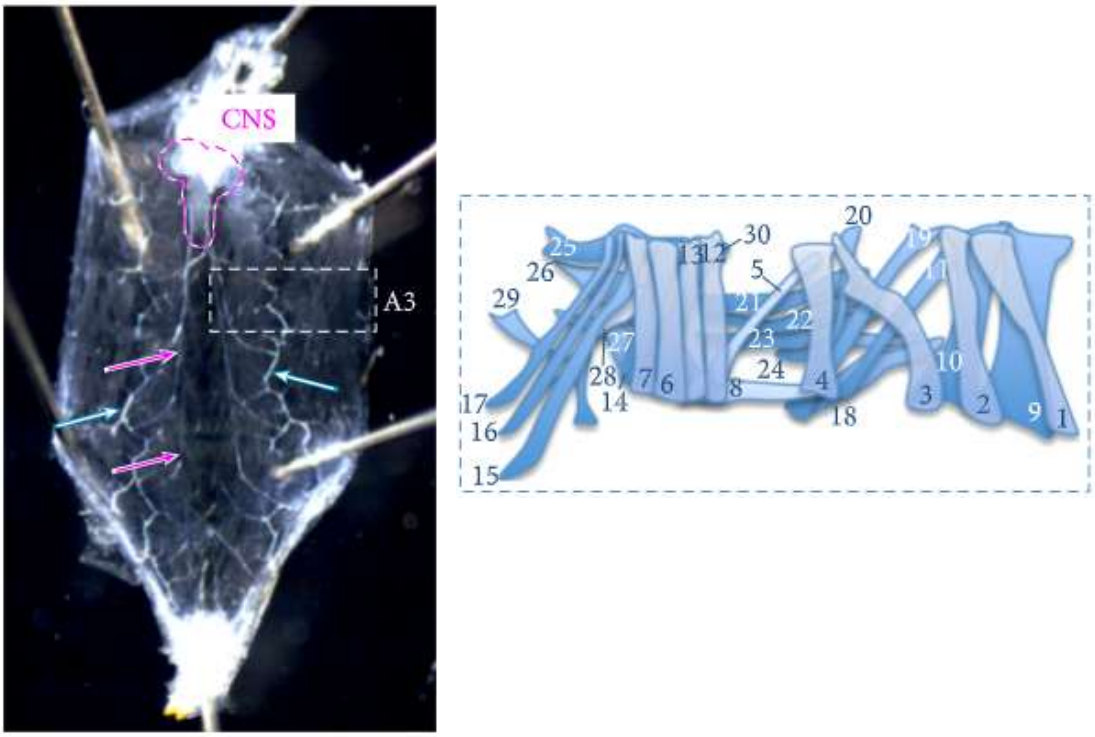

Figure 2.7 Larval NMJ dissection.

Larval NMJ dissection. Dissection of third instar *Drosophila* larvae to reveal 14 segments, 3 of which define the head and mouth region, 3 thoracic segments (T1–T3), and 8 abdominal segments (A1–A8; segment A3 indicated by the white dotted line). The CNS is outlined in magenta, the main nerve trunks indicated by magenta arrows. Abdominal segments A2–A7 are composed of 2 bilaterally symmetrical hemisegments, each of which displays an archetypal structure comprising 30 distinct muscles, as shown in right panel. Image and diagram from West et al. (2015).

2.9.3 Immunohistochemical staining

Brains and larvae were incubated in primary antibodies (Table 2.2) in 0.5 % PBT at 4 °C, overnight, in darkness with rotation. Following primary antibody incubation brains and larvae were washed 3 times in 0.5 % PBS-T, followed by incubation with secondary antibodies (Table 2.3) in 0.5 % PBT for 1 h, in darkness, with rotation at room temperature. Brains and larvae were washed 3 times in 0.5 % PBT before mounting. Prior to mounting, larvae were submerged in 70 % glycerol (70 % v/v in PBS) for 1-2 h to displace air. Brains and larvae were mounted on standard microscope slides with glass coverslips in Vectashield® hard set mounting media (Vector Laboratories LTD, UK #H-1400-10).

2.9.4 Microscopy and imaging

Adult brains and larvae were imaged using a Leica DM6000 B Microscope with different objectives and a Hamamatsu ORCA-R^2 C10600-10B-H camera. For larval neuromuscular junction images, the OptiGrid (Qioptiq Imaging Solutions) was used to improve resolution via structured illumination microscopy in z-stacked images.

2.9.5 Image processing and analysis

Larval neuromuscular junction (NMJ) analysis was performed as described previously[212]. Briefly, anti-HRP-Cy3 was used to mark the nervous system, and anti-bruchpilot to mark active zones. Z-stack projections of muscle 4 NMJ's were analyzed using ImageJ (v1.53). Synaptic bouton numbers at muscles 6/7 and 4, hemisegment A3, were determined by counting each distinct, spherical, anti-bruchpilot–positive varicosity contacting the muscle. NMJ length was measured using the NeuronJ ImageJ (v1.53) plugin.

Due to uneven background autofluorescence in the GFP channel, images of adult brains expressing the DPRs were processed in ImageJ (v1.53) to remove background using a rolling-ball radius of 50 pixels. Adult brains stained with ubiquitin antibody were imaged using identical settings and projected from 15 µm z-stacks (0.5 µm z-interval).

Table 2.2 Primary antibodies used during the course of this investigation.

Antigen	Dilution	Species / Type	Source
Bruchpilot	IF 1:50	Mouse monoclonal	DSHB (RRID AB_2314866)
Elav	IF 1:50	Mouse monoclonal	DSHB (RRID AB_528217)
GFP	WB 1:1000	Rabbit polyclonal	abcam (RRID AB_303395)
GFP	IF 1:1000	Alpaca Alexa Fluor® 488-conjugated	ChromoTek (RRID AB_2827573)
GR repeat	WB 1:1000	Rabbit polyclonal	Proteintech (RRID AB_2879387)
HRP	IF 1:200	Goat polyclonal Cy™3 conjugate	Stratech (RRID AB_2338959)
Ubiquitinylated proteins	IF 1:2000	Mouse monoclonal	Enzo Life Sciences (RRID AB_2051891)

Table 2.3 Secondary antibodies used during the course of this investigation.

Antibody	Dilution	Source
Goat anti-Rabbit Alexa Fluor® 647	IF 1:500	Stratech (RRID AB_2338079)
Goat anti-Mouse Alexa Fluor® 647	IF 1:500	Stratech (RRID AB_2338902)
Goat anti-Mouse Alexa Fluor® 594	IF 1:500	Stratech (RRID AB_2338890)
Goat anti-rabbit HRP	WB 1:5000	Stratech (RRID AB_2337938)

2.10 HeLa cell culture and imaging

2.10.1 Maintenance of HeLa cell culture

HeLa cells (ECACC #93021013) were maintained at 37 °C with 5 % CO_2 in Dulbecco's Modified Medium (DMEM, Sigma, #D5796) supplemented with 10 % v/v fetal calf serum (Gibco #10500064), 2 mM L-glutamine (Sigma #1294808), 100 U/ml penicillin and 100 µg/ml streptomycin (Sigma, #P0781). Cells were passaged when ~70 % confluent; media was removed by aspiration, cells washed in warm phosphate buffered saline (PBS, Sigma #P5493), and then incubated with 2 ml trypsin solution (Sigma, #T3924) at 37 °C for 5 min, after which 8 ml DMEM was added to prevent excessive digestion. Cells were pelleted at 2000RPM for 5min and subsequently resuspended in 7 ml DMEM. 1 ml of cell suspension was transferred to a T75 culture flask (Corning, UK) containing 15 ml fresh DMEM.

2.10.2 Transient transfection of DPR constructs

HeLa cells were seeded to give 110,000 cells per well on 22 mm glass coverslips (pre-treated with 1 M HCl, washed in distilled H_2O, stored in 70 % ethanol, and washed in distilled H2O immediately prior to use) in 6 well plastic plates. After overnight incubation at 37 °C, cells were transiently transfected with DPR constructs or empty pEGP-N1 vector. Appropriate volumes of DNA to give 800 ng plasmid were added to 7.2 µl FuGene (Promega, UK #E2691) transfection reagent, diluted in OptiMEM (Thermofisher Scientific, UK #31985062) to give a total volume of 200 µl. After thorough mixing, the reaction mixture was incubated at room temperature for 15 min, then added to cells and incubated for 48 h at 37 °C before fixing. Coverslips were mounted on glass slides with Invitrogen ProLong™ Diamond Anti-fade mounting media (Invitrogen, UK #P36961) with DAPI and dried.

2.10.3 Microscopy and imaging

HeLa cells were imaged using a Coolsnap HQ2 camera and Zeiss Axioimager.D2 upright microscope with a 63x objective.

2.11 Statistics and Graphics

All data was initially recorded in Excel (Microsoft®, NM, US). Statistical analysis, apart from the seizure assay, was carried out in GraphPad Prism 7.04 for Windows (GraphPad

Software, CA, US). Unless stated otherwise, ANOVA with appropriate post-hoc tests were used, and error bars represent SEM unless. Data processing and chi-squared tests between genotypes in the seizure assay were performed in RStudio (R version 3.6.3). Figures were assembled and diagrams were made using CorelDRAW X7 (CorelDRAW Graphics Suite, ON, Canada).

3 Development and Validation of Novel *C9orf72*-FTD/ALS *Drosophila* Models Expressing DPRs of over 1000 Repeats

3.1 Introduction

Existing fly models have proved crucial in implicating DPRs, and not repeat RNA, as the toxic species in *C9orf72*-FTD/ALS[137], and continue to be used to dissect underlying mechanisms of DPR toxicity[163,170,213,214]. However, these models have relied on expressing DPRs between 36 and 100 repeats. These are considerably shorter than those in patients, where over 1000 repeats are typical[56]. Although there is an argument that intermediate expansions can be toxic, only a small proportion of patients with ALS have been identified as carrying expansions smaller than 30 repeats[215] and western blotting of peptides extracted from patient tissue indicates that long DPRs are produced[142,146]. Therefore, it is important to consider that whilst it remains a significant challenge for the field to determine the importance of repeat length in disease, it is likely that longer repeats are present in patients and therefore we may be missing key aspects of DPR behaviour by only modelling short repeats. Shorter repeats have been used because there are difficulties associated with generating and maintaining long repeats *in vivo.* The sequence needed to produce the DPRs is repetitive, despite not being pure GGGGCC repeats, and they are inherently unstable with a propensity to retract and lose repeats between generations[197]. Despite this, there is strong evidence that length is an important factor in determining pathology and toxicity[137,153,216] and this pointed to a need for a *Drosophila* model expressing DPRs of a physiologically relevant repeat length. To address this, we looked to develop a fly model expressing DPRs of over 1000 repeats using DPR constructs previously characterised in cell models[153].

A theme amongst the existing DPR models is the acute toxicity of arginine-rich DPRs, PR and GR. Expressing PR100 and GR100 in the eye proves acutely toxic and an inducible expression system is required to allow them to be expressed in the nervous system as viable, if short lived, adult flies[137]. This is compared to humans, where the expansion does not cause measurable deficits until around 50 years of age. It is unclear whether short repeats are so toxic because of the nature of the repeat itself, whether it is more easily translated or aggregates in a particular way, or whether it is due to the expression levels associated with the genomic location of the insertion site. It is well established that the genomic location of a transgene can affect expression levels; it has been shown that transgenes can be stochastically repressed if inserted in proximity to

heterochromatin[217] and local regulatory elements can epigenetically regulate expression[218]. As well as being much shorter than seen in patients, the acute toxicity of the current DPR models has precluded the study of the effect of DPR expression over the lifespan. As an adult-onset neurodegenerative condition, this is key aspect that is missing from the current models, and which this project aims to address with the generation of a full-length DPR fly model.

The objectives of this Chapter are to establish novel *Drosophila* models expressing 1000 repeat DPRs, assess their stability over multiple generations, examine viability and longevity, and test their toxicity when expressed in the eye, with a view to evaluating the differences between these and the existing *Drosophila* models.

3.2 Results

3.2.1 DPRs of over 1000 repeats remain stable in the *Drosophila* genome for over 3 years and are translated into full-size proteins

The pUASt-DPR constructs used in this study were adapted from constructs previously used for expression in mammalian cells[153]. The original sequences were produced utilising alternative codon sequences to produce each DPR at over 1000 repeat units (6 base pairs, 2 amino acids, per unit) without the repetitive GGGGCC RNA. GP was the exception, and so far, no research group has reported successful generation of a GP construct beyond 43 repeats[158]. The repeat lengths for each DPR are: AP, 1024 repeat units; GA,1020, PR,1100, GR,1136. These were cloned into pEGFP-N1 vectors for expression in mammalian cell models[153]. We subsequently translated these into fly models by subcloning from pEGFP-N1 into the PUAST-attB vector, maintaining the EGFP tag (Figure 3.1 A). We know from previous studies that the inclusion of a fluorescent tag does not affect localisation or pathology[153]. For simplicity, each DPR will be referred to as, e.g. AP1000, which includes the DPR and the C-terminal EGFP. Length checks and validation of PUASt-DPR-EGFP vectors was done prior to microinjection into the VK00005 embryos by Cambridge Microinjection Facility. This site was chosen due to its relatively good transformation score and moderate expression levels (Figure 3.1 B). It was thought that if the DPRs were landed into a site with high expression, it might prove too toxic. Subcloning and subsequent validation of plasmids was performed by Ryan West prior to the start of this PhD study.

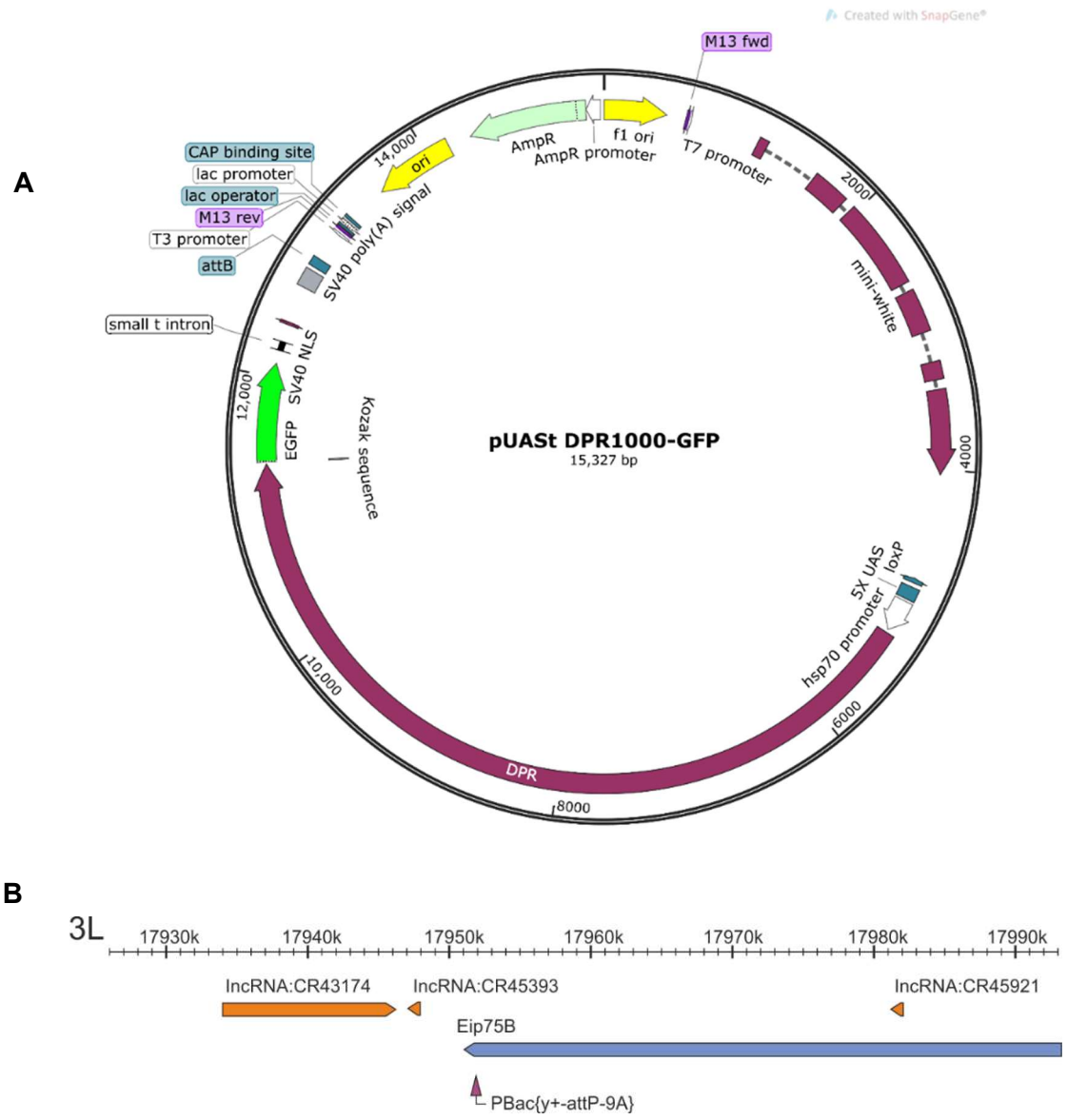

Figure 3.1 Schematic of plasmid and genomic insertion site used in the generation of 1000 repeat DPR *Drosophila.*

A pUASt-DPR1000-GFP plasmid map showing mini-white element, DPR sequence and EGFP tag (made using Snapgene Viewer). DPR construct contains ATG sequence. **B** Genomic region into which the construct was site landed. Chromosome 3L region between 17930k-17990k shown. Insertion site shown in purple (PBac[y+-attP-9A]). Insertion site is flanked by long non-coding RNAs (lncRNA).

Transformants were initially identified by their eye colour. The mini-white element contained within the injected plasmid conferred an orange, rather than red, eye due to moderate expression levels in the chosen insertion site (Figure 3.1 B). Potential transformants were screened using Southern blotting, due to the inability to sequence repetitive sequences. Initial blots of all lines revealed 7 of the 10 AP lines, 3 of the 5 GA lines, and 6 of the 10 PR1000 lines carried the full-length construct (Figure 3.2 A). Of these, two were picked to take forward to further experiments. GR1000 required another round of microinjections as there were no successful transformants in the first instance. There were only two positive transformant lines of GR from the second injection and both of these were found to be positive for the full-length construct (Figure 3.2 A). It is impossible to measure the exact repeat length from Southern Blotting, but an approximation based on equivalence to the positive control and a band at ~6000bp was sufficient to consider the full-length construct present. Studies have reported that repeats are unstable[197,219], and so the DPR fly lines chosen for experiments were routinely screened by Southern Blot. DPRs have maintained ~1000 repeats for over three years which equates to over 100 generations due to the rapid generation time of *Drosophila* (10 days at 25 °C). From the blots in Figure 3.1 A, two lines were taken forward for initial experiments and these were screened 12 months post-injection (Figure 3.1 B). Once it was established there were no major differences in viability (Figure 3.4) between the two lines, one was chosen to be used for further investigations. The blots in Figure 3.1 C show these experimental lines and additional stocks made by double balancing the original DPR lines. Screening of all independent lines in use is crucial because any stock has the potential to retract or lose the transgene completely.

Immunoblotting, performed by Ryan West, confirmed that pan-neuronally driven expression resulted in functional expression of each DPR transgene and the production of proteins of comparable size to those observed previously in mammalian cell models (Fig 3.3)[153].

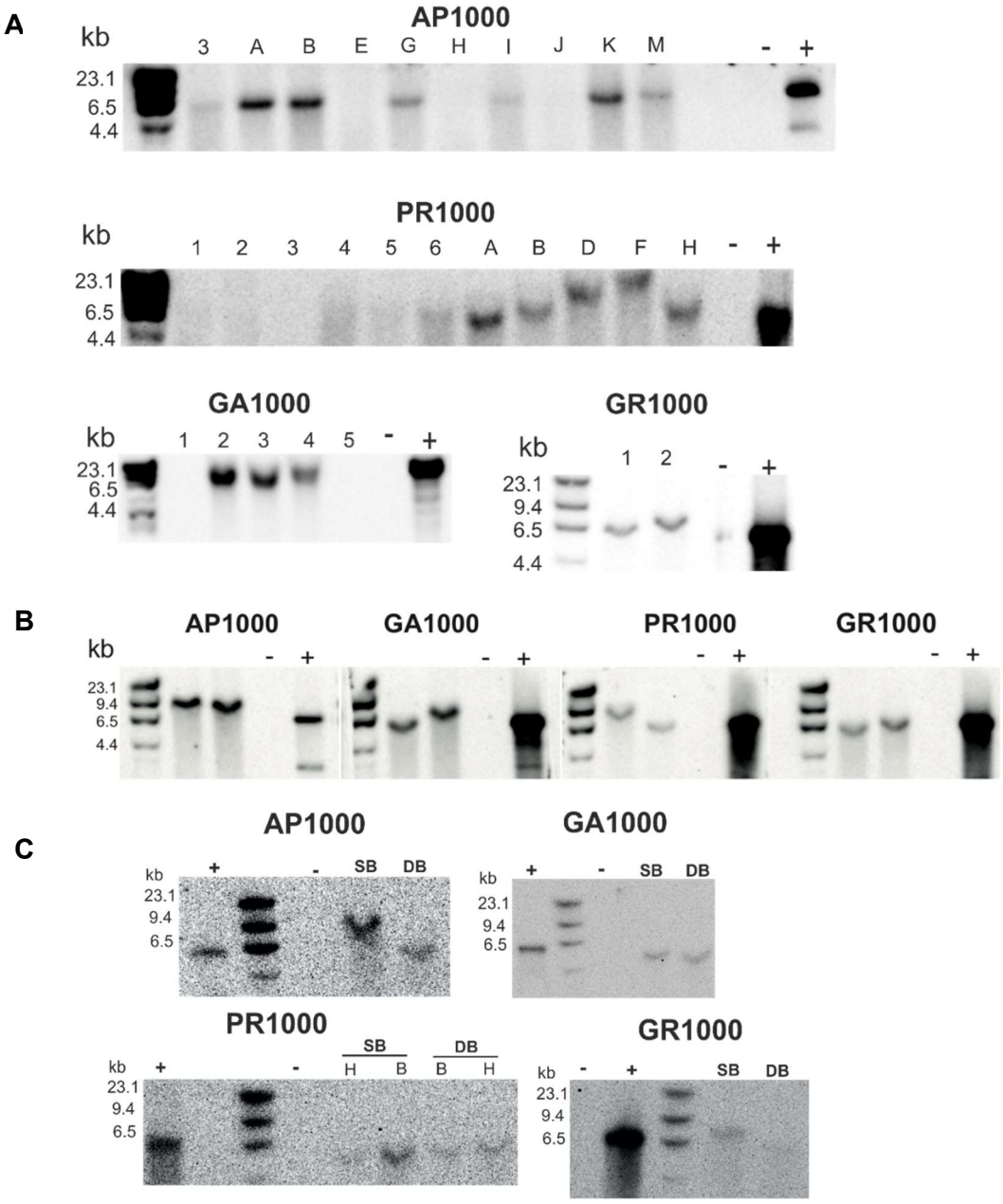

Figure 3.2 1000 repeat DPRs are stable in the Drosophila genome for over 3 years post-injection (~ 100 generations).

Southern Blots showing DPR-EGFP constructs at expected length relative to positive controls (+) and predicted size (~6000bp). Lanes show ladder, positive control (+, DNA from wild type flies spiked with 1000 repeat DNA), negative control (-, DNA from wild type flies). **A** Original Southern blots performed during transformant selection (June-October 2018). Labels are arbitrary naming system to identify DPR fly lines, from which two lines were taken forward. **B** Two independent fly lines tested at 12 months post-injection. **C** Subsequent balancing of DPR lines produced additional DPR fly lines (SB = original, single balanced DPR/TM6b, DB = double balanced *CyO/If ; DPR/TM6B*). For PR, the two independent lines (B and H) were tested as both are used in experiments. Full, uncropped blots can be found in Appendix 2.

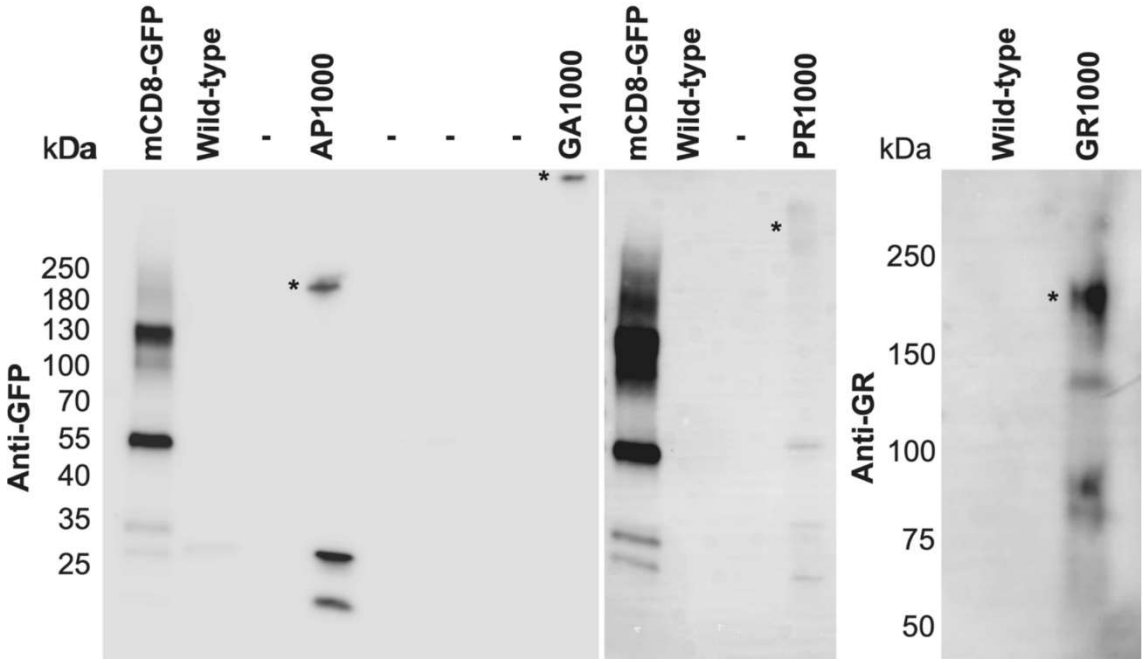

Figure 3.3 DPRs are detected in the *Drosophila* nervous system.
Immunoblots of *Drosophila* heads pan-neuronally expressing (*nSyb-Gal4* III) DPRs. DPRs were detected with either anti-GFP (AP1000, GA1000 and PR1000) or anti-GR antibodies. Asterisks show DPR bands at predicted size. Immunoblots performed by Ryan West**.**

3.2.2 Pan-neuronal DPR expression differentially affects longevity but not viability

Given the acute toxicity of other DPR models, it was important to assess if DPR expression conferred any degree of lethality. From the selection of DPR1000 lines, two were selected per DPR for viability experiments to ensure that there are no differences between supposedly identical transgenes. Viability was assessed using three different drivers (*tubulin-, repo-, nSyb-Gal4)*, to test for lethality in different tissues. Viability was measured against an expected 50:50 ratio of driven/undriven progeny based on a specifically designed mating scheme (Figure 3.4 A). For both pan-neuronal (*nSyb-Gal4*) and glial expression (*repo-Gal4*), viability showed no difference form typical mendelian inheritance and the ratio of driven/undriven progeny observed in controls (Figure 3.4 B, C). This is in stark contrast to previously developed DPR fly models where GR100 and PR100 driven in only the eye (*GMR-Gal4*) caused significantly reduced egg-to-adult viability[137]. *GMR-Gal4* is a commonly used screening tool in *Drosophila* research, as it allows relatively toxic transgenes to be expressed in living flies, with eye degeneration providing non-lethal but measurable readouts. The fact that viability is affected by expression in the eye indicates that the arginine-rich DPRs in these models are extremely toxic. Global expression using a *tubulin-Gal4* caused lethality with AP1000

and PR1000, and partially with GR1000. Global expression is not representative of expression patterns in FTD/ALS patients, where DPRs have been observed in neurons, glia and muscle but not every cell in the body[100,142], but it is interesting to note that whilst GA1000 is not toxic, AP1000 - usually considered the least toxic of the DPRs - is. Furthermore, whilst AP1000 proves toxic in the pharate stage, indicated by blackened pupal cases and death at this stage, GR1000 and PR1000 are lethal at the first instar larval stage (Table 3.1), suggesting different processes in development are affected. Although GR1000 was only partially lethal, no pharate or third instar lethality was observed, which implies that once a larva was able to make it past second instar stage of development, it was not hindered in further development by GR1000 expression. However, it is important to emphasise global expression is not physiologically relevant, and therefore further experiments will concentrate on neuronal expression.

After establishing that pan-neuronal DPR expression is not detrimental to egg-to-adult viability, the effect on adult longevity was investigated. Consistent with previous findings[137,220], GR1000 significantly reduces lifespan ($p < 0.001$) (Figure 3.4 E). However, AP1000 and GA1000 expressing flies had a slight but significant increase in lifespan ($p < 0.001$, $p < 0.01$ respectively). This is in contrast to other studies that looked at lifespan, which show GA100 had a late-onset decrease in survival and AP100 has no effect compared to controls[221]. Furthermore, although GR1000 did have some degree of toxicity, it was less acute, causing the drop off in survival after around 40 days, which equates to mid-late life in humans. This is in contrast to other studies in which an inducible neuronal driver (*elav-GeneSwitch*) was used to express DPRs in adult flies, where the toxicity is much more severe with both PR100 and GR100 flies dying around 10 days post-eclosion[221]. Therefore, the 1000 repeat model arguably provides a more physiologically relevant model to detect subtle age-dependent phenotypes and the mechanisms underlying them.

Table 3.1 Lethal phase of Drosophila expressing DPRs globally (*tubulin-Gal4*).

DPR	Lethal phase
AP1000	Pharate
GA1000	--
GR1000	1st instar larval
PR1000	1st instar larval

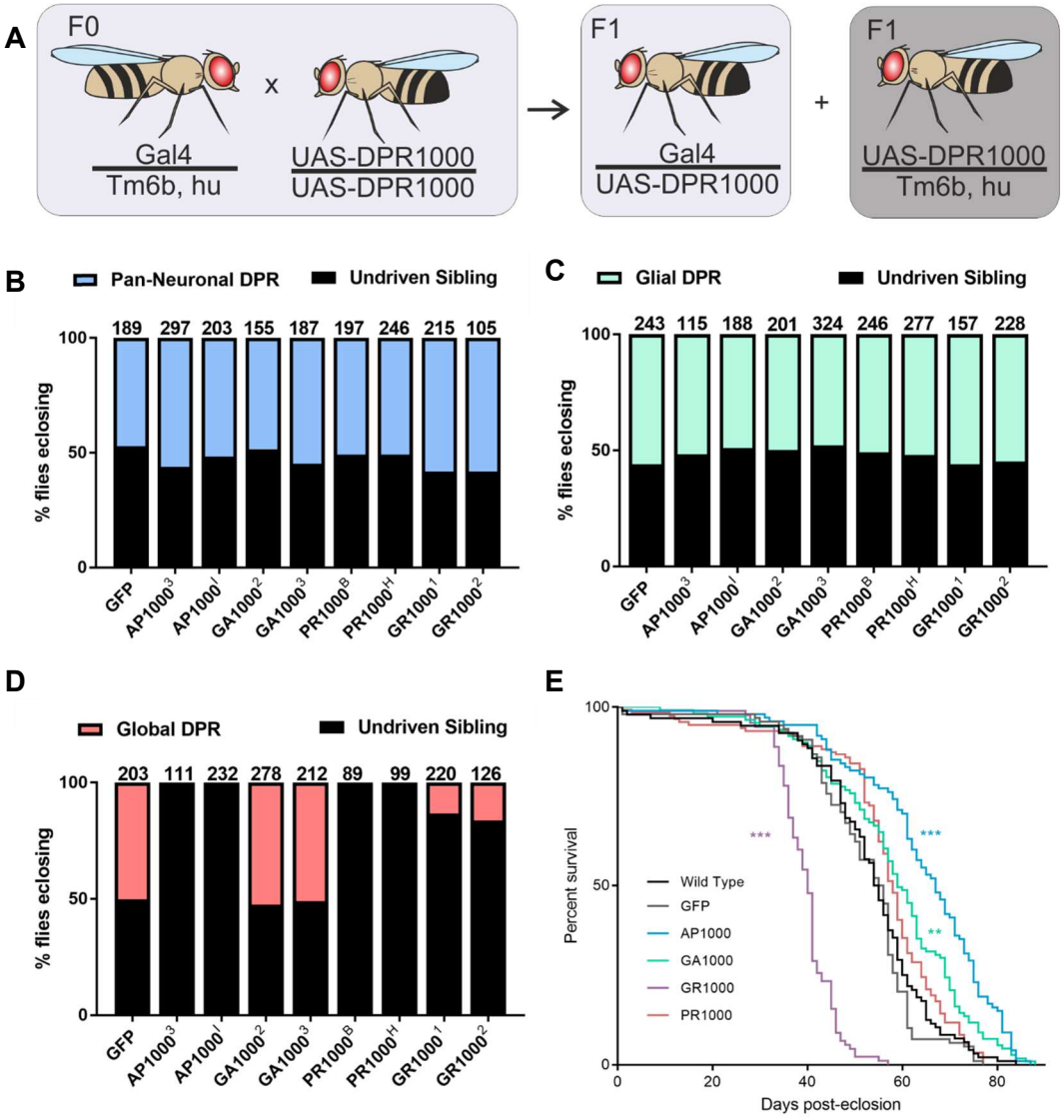

Figure 3.4 Longevity and viability are differentially affected by DPR expression.
Two independent lines of each 1000 repeat DPR were tested. **A** *Drosophila* mating scheme designed to produce a 50:50 ratio of driven and undriven progeny if driven flies are 100% viable. Homozygous DPR flies were crossed to flies heterozygous for the driver in question, and progeny with and without *TM6B* balancer (marked with humeral) counted**. B, C** DPR expression in neurons (*nSyb-Gal4*) and glial cells (*repo-Gal4*) has no effect on viability**. D** Global expression (*tubulin-Gal4*) of AP caused 100% pharate lethality. Global PR expression caused 100% second instar lethality, and GR partial second instar lethality. **E** Flies pan-neuronally expressing GR1000 show a significant reduction in longevity compared to wild type (CantonS outcrossed to w^{1118}) and control flies (Survival Log-Rank (Mantel-Cox) with Bonferroni Correction, *** $p < 0.001$ ** $p < 0.01$ (see Appendix 3). N: wild type = 96, GFP = 98, AP = 100, GA = 111, PR = 119, GR = 90. All flies were collected from at least 3 independent crosses for B, C, D, E.

3.2.3 Pan-neuronal expression reveals DPR-specific localisation and morphology in the nervous system

There is a distinct morphology and localisation associated with each of the DPRs both in *C9orf72* patient tissue and in cell models. Immunohistochemical analysis of patient tissue revealed characteristic inclusion pathology unique to *C9orf72* expansion carriers, in particular p62-positive star-shaped cytoplasmic inclusions[146]. Additionally, diffuse, granular cytoplasmic "pre-inclusions" are observed in cortical neurons and Purkinje cells, as well as smaller spherical cytoplasmic aggregates[147]. Inclusions in *C9orf72* patients have been shown to contain all sense DPRs (GA, GR, and GP), and rarely AP[145]. In contrast, PR has been detected in nuclear inclusions and was notably absent from any cytoplasmic inclusions[145]. GA is consistently found to form cytoplasmic inclusions abundant in areas affected by FTD/ALS such as the cerebellum, hippocampus and frontal, temporal and motor cortices, and these could either be spherical or stellate in shape[145,147,149]. There are caveats to looking at pathology in post-mortem tissue and observing end-stage disease. It is not possible to ascertain what the pathology is throughout the course of disease progression and as neurons die. This is why it is useful to observe the morphological patterns and localisation in cell and animal models. However, there are inconsistencies as to the appearance of DPRs depending on length and on the system in which they are expressed. It has been demonstrated that length is important for the formation of characteristic cytoplasmic fern-like inclusions in GA expressing cells, which are reminiscent of the star-shaped inclusions seen in patient tissue[153]. However, in cell models, PR and GR are frequently observed to localise to the nucleolus, something not generally observed in patients[152,153], raising questions as to the validity of these models.

Therefore, to further evaluate the relevance of our model to disease, the localisation and morphology of DPRs in the adult brain and thoracic ganglion was examined. DPRs expressed pan-neuronally had distinct localisation patterns (Figure 3.5, 3.6) which can be observed by their GFP signal. AP and GA were largely confined to the central brain whereas arginine-positive DPRs PR and GR were seen throughout the brain and the optic lobes. Intracellular localisation resembled that seen in post-mortem brains. AP was localised to the cytoplasm in a diffuse pattern, similar to the "pre-inclusions" seen in patient cortical neurons[147,222]. Both PR and GR had a much weaker signal, and required a GFP booster (anti-GFP-488 conjugate) in order to see them clearly. PR and GR were observed both in the nucleus and the cytoplasm, diffusely and as smaller spherical inclusions, similar to that seen in post-mortem patient tissue[99]. GA formed clearly defined fern-like aggregates in the cytoplasm, often perinuclear or appearing in neurites (Figure 3.5, 3.6).

Transfection of the same length DPRs into HeLa cells using pN1-EGFP DPR constructs described previously[153] revealed distinct differences between fly and HeLa models (Figure 3.6). Although the characteristic fern-like perinuclear GA and diffuse cytoplasmic granular AP were observed in HeLa, PR and GR showed what appears to be nucleolar localisation not comparable to those seen in patients. Results demonstrate distinct differences depending on model, even using DPRs of the same length.

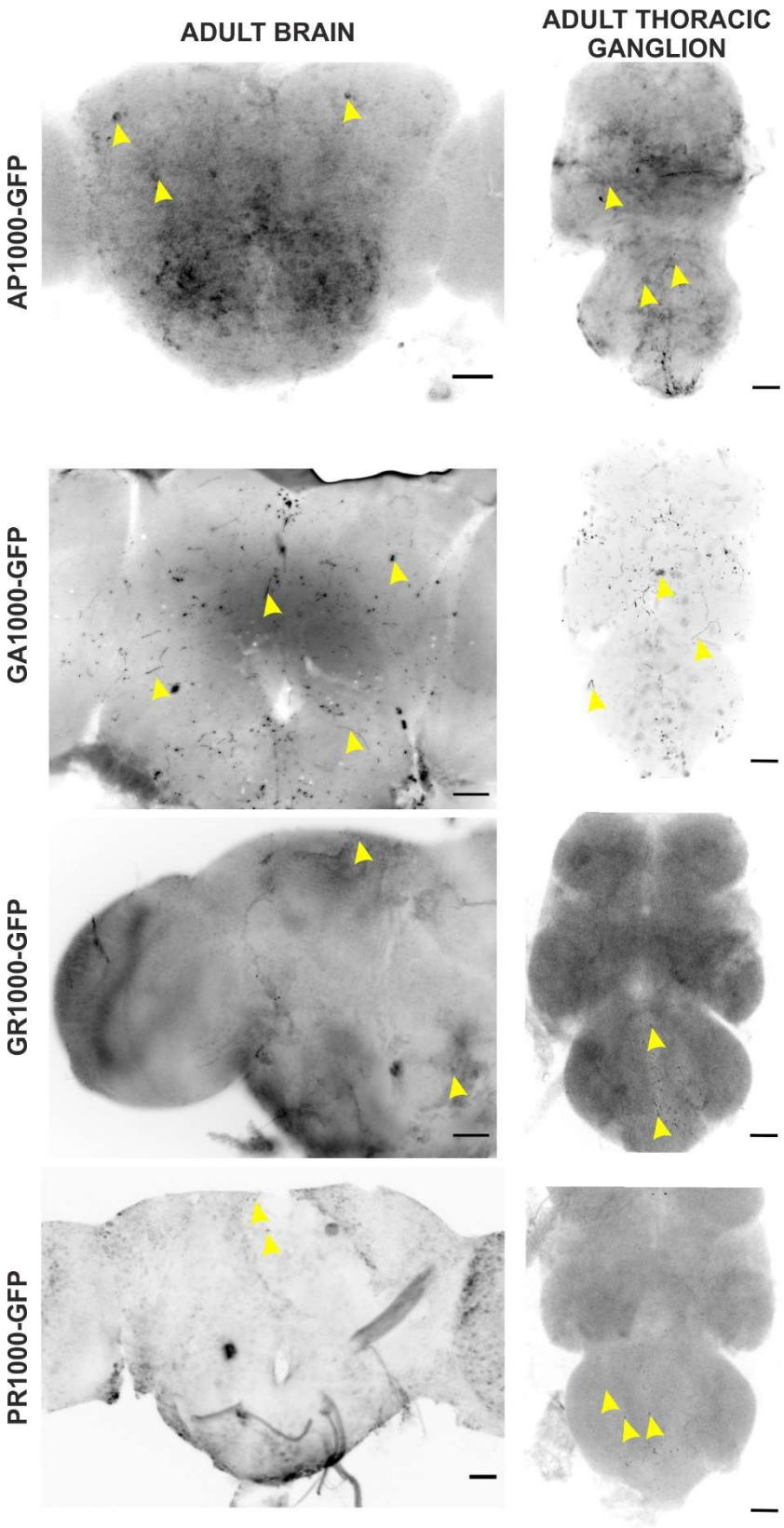

Figure 3.5 Distinct localisation of 1000 repeat DPRs in adult fly brain and thoracic ganglion.

Fluorescence images of adult brains and thoracic ganglia dissected from flies 28 days post-eclosion. GFP-tagged DPRs pan-neuronally (*nSyb-Gal4* III) driven, and visualised using an anti-GFP-488 conjugate. Yellow arrows indicate DPR inclusions. Scale bars 50 µm

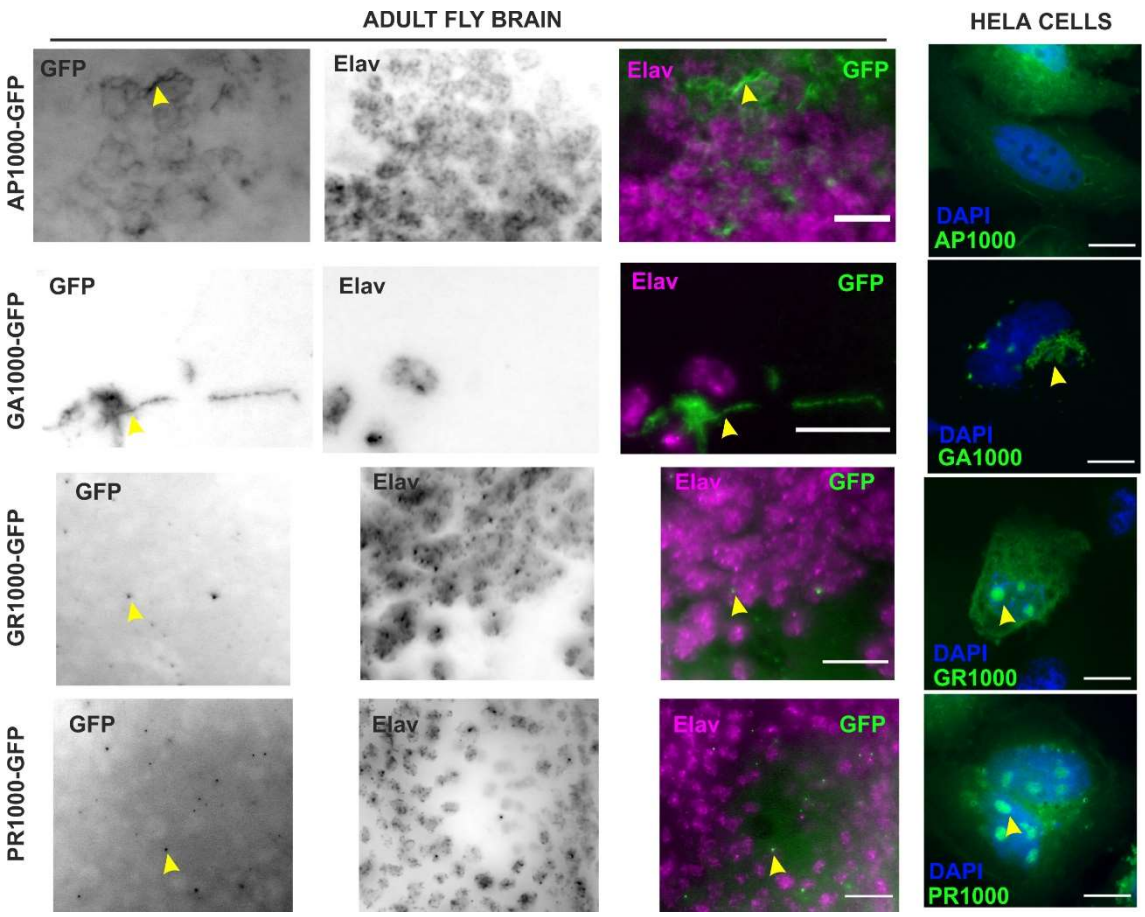

Figure 3.6 Distinct cellular localisation and morphology of 1000 repeat DPRs in adult brains and HeLa cells.

Fluorescence images of adult brains dissected from flies 28 days post-eclosion. GFP-tagged DPRs pan-neuronally (*nSyb-Gal4* III) driven, and visualised using an anti-GFP-488 conjugate. Transiently transfected HeLa cells expressing DPRs and nuclei labelled with DAPI. Yellow arrows indicate DPR inclusions. Scale bars: adult brains 15 µm; HeLa cells 10 µm.

Due to the nature of the models, with each DPR being expressed individually, whether or not DPRs are sequestered by each other when found in the same cell cannot be ascertained. This would explain why, in patients, we see GR present in the stellate structures that more closely resemble GA1000 in our model. It is possible that GR and GA co-aggregate when expressed together, but alone GR does not have the propensity to form such structures.

3.2.4 Pan-neuronally expressed 1000 repeat DPRs do not appear to colocalise with ubiquitin

Ubiquitinated p62-positive and TDP-43-negative cytoplasmic inclusions are a pathological hallmark of *C9orf72*-FTD/ALS[95,96,142]. Therefore, we looked to see if the 1000 repeat DPR inclusions observed in the nervous system (Figure 3.5, 3.6) contained ubiquitin. Immunohistochemistry with an antibody targeting mono- and poly-ubiquitinated proteins showed no colocalization between DPRs and ubiquitin, in at least 5 brains per genotype (Figure 3.7). The characteristic stellate fibrous GA inclusions, nor cytoplasmic AP inclusions, showed any colocalisation with the ubiquitin antibody. Similarly, diffuse and punctate GR and PR signal showed little overlap with ubiquitin signal. Colocalisation of DPRs with TBPH, the *Drosophila* TDP-43 homolog, was assessed elsewhere[207,213] and will be discussed before.

3.2.5 Expression in the *Drosophila* eye produces a DPR- and dose-dependent toxicity

The *Drosophila* eye is a useful system to examine toxicity and is widely used as a screening tool[223]. By expressing a transgene specifically in the fly eye using *GMR-Gal4* and genetically combining this with other mutations, the change in eye morphology can be used as a readout for toxicity. Modifier screens, in which genes are identified by their ability to alter the phenotype of flies that are genetically sensitized for the process of interest, are invaluable for elucidating signal-transduction pathways[224]. The majority of DPR fly models are initially assessed for their toxicity using *GMR-Gal4* expression, and therefore it was useful to compare the 1000 repeat DPRs to the published data on shorter models. Shorter repeat models have shown a consistent pattern of eye toxicity. Severely degenerated eyes are seen with PR and GR at repeats up to 100 repeats[137,163,193].

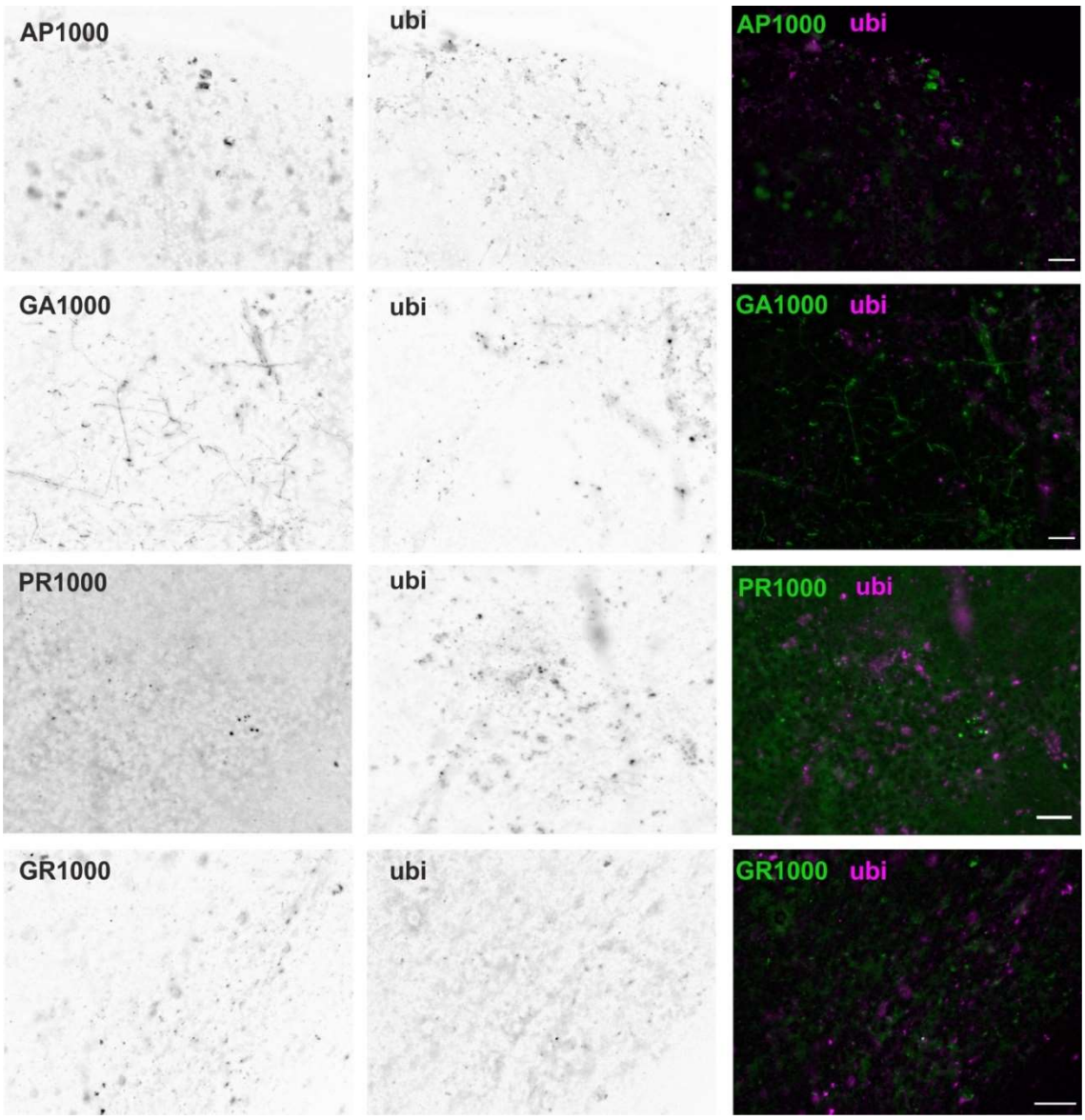

Figure 3.7 Ubiquitin localisation in adult DPR fly brains.

Ubiquitin does not colocalise with pan-neuronally (*nSyb-Gal4* III) expressed 1000 repeat DPRs in the fly brain. Brains were dissected from flies expressing DPRs under the control of *nSyb-Gal4* (III) at 28 days post-eclosion, and images show equivalent sections of the mid-brain. Ubiquitinylated proteins (ubi, magenta) were stained with anti- mono- and polyubiquitinylated conjugates. DPRs are EGFP-tagged (green) and visualised with anti-GFP-488 conjugate. Scale bars 15 µm.

Common phenotypes observed in degenerated eyes include fusion of ommatidia creating a “glazed” eye, disruption to the interommatidial bristles, colour defects, a change in overall eye shape, and the most severe often have necrotic patches (see Figure 2.4)[223]. To tease out any subtle differences and normalise comparisons between genotypes, a points-based system can be used to classify severity. For this investigation, a modified version of an 8 point classification system previously described by Pandey et al. (2007), Ritson et al., (2010) [198,199] was used (see section 2.5).

In contrast to the shorter DPRs, no 1000 repeat DPRs caused any disruption to eye morphology when expressed using *GMR-Gal4* and raised at 25 °C (Figure 3.8 A). To see if an increased DPR expression would induce a phenotype, flies were raised at 29 °C to increase *Gal4* activity[225]. A slight but significant disruption of eye morphology was observed at 29°C with GA1000, PR1000 and GR1000 but not AP1000 (Figure 3.8 A). As ectotherms, temperature strongly affects the fly's physiology; in addition to increasing the gene expression, an increasing temperature is known to influence metabolsim[226] and development[227]. Therefore, two copies of each DPR were expressed together and flies raised at 25 °C as an alternative method to increase expression without altering any other physiological processes. It is important to note, however, that two copies of the transgene increase the chance of genomic background effects. Double DPR expression resulted in a significantly more perturbed eye phenotype in all DPRs apart from GA, compared to the DPR co-expressed with GFP as a *Gal4* titration control ($p < 0.001$) (Figure 3.8 B). PR1000/PR1000 was the most toxic, with over 75 % of the flies dying before they could eclose, and those that did survive had severely degenerated eyes (Figure 3.8 C). GR1000/GR1000 and AP1000/AP1000 were not significantly from each other different in terms of their phenotype scores, but the phenotypes did look markedly different. Whilst a double AP1000 caused a "glazed" eye, indicating fused ommatidia and abnormal bristles, double GR1000 caused shape and colour defects, in addition to irregular ommatidia (Figure 3.8 C).

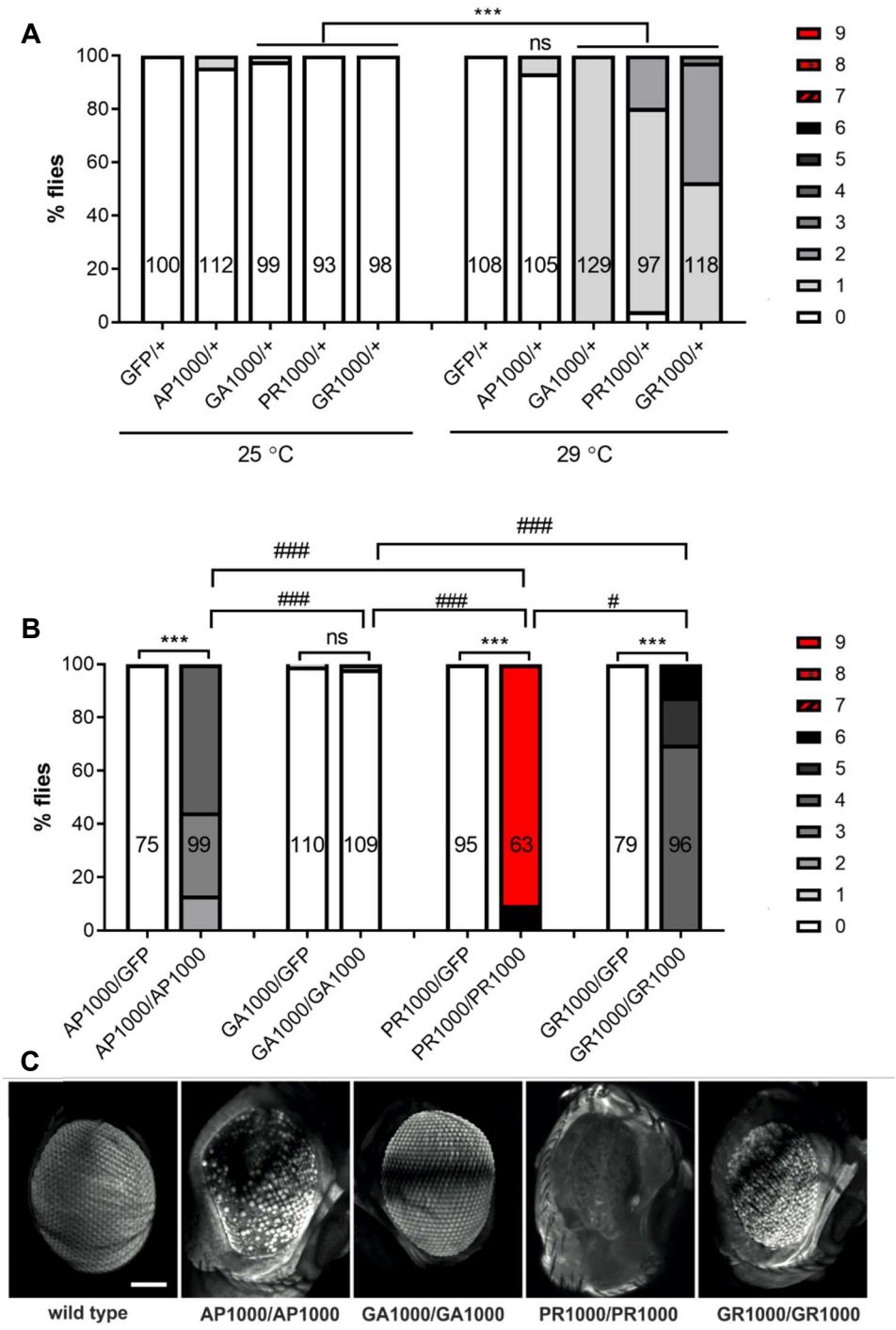

Figure 3. Dose-dependent toxicity of DPRs in the *Drosophila* eye.

All flies in this experiment are expressing DPRs under the control of a single copy of the eye specific driver *GMR-Gal4* (*GMR-Gal4*/+). Quantification of the eye phenotypes in flies expressing **A** one copy of each DPR at 25 °C and 29 °C and **B** one or two copies of each DPR reveals a dose-dependent increase in DPR toxicity (Kruskall-Wallis with Dunn's multiple comparisons test between all groups ***/### $p < 0.001$ **/## $p < 0.01$ */# $p < 0.05$). Co-expression of mCD8-GFP acts as a titration control for *GMR-Gal4*. One point is scored for each eye defect (see 2.5 for full classification). The number of flies scored is shown inside each bar. Each genotype was scored from a minimum of 3 independent crosses. **C** Representative Lightsheet micrographs showing the eye of flies expressing two copies of each DPR. Scale bar 100 µm

3.3 Discussion

3.3.1 1000 repeat DPRs are stable in the *Drosophila* genome

This chapter details the development of the first animal models expressing stable DPRs of repeat lengths comparable to those observed in people with the expansion. Regular Southern blots have demonstrated that 1000 repeats are stable in the *Drosophila* genome for over three years, and are also stable when combined with other genetic elements, such as when double balanced. This is in contrast to a previous study that attempted to generate 1000 repeat DPR mice; they reported that although the insert integrated into the genome, the 1000 repeat DPRs shrunk and subsequently dropped out completely over two generations[197]. Tandem repeat sequences are known to be inherently unstable in plasmid vectors[219,228] and in mice, at least, alternative codon sequences do not protect against excision or truncation from the genome. This raises the question as to why the repeats are stable in this *Drosophila* DPR model.

Repetitive sequences, such as ribosomal DNA (rDNA), telomeres and transposable elements, are common in most genomes and comprise over 70% of the human genome[229]. Without protective mechanisms in place, they pose a major threat to genome stability, driving chromosome rearrangements and disease. Therefore, cells have evolved mechanisms to maintain stability at endogenous repetitive DNA loci, such as assembly into silent chromatin, regulating localisation within the nucleus to prevent uncontrolled recombination[230], and adopting various non-standard DNA conformations[231]. It is possible that one or more of these mechanisms explains the stability of the DPR repeats, but it does not explain why the transgenes are stable in *Drosophila* and not mice.

Another explanation comes from the location of the transgenic insertion in our model. It is flanked by long non-coding RNAs (lncRNA) (Figure 3.1 A). LncRNA is a common modulator of genomic instability via interactions with chromatin loops and stability regulating factors and is known to direct DNA methylation for stable repression of genes[232]. In fact, lncRNA-directed methylation has been implicated in rDNA repeat stability[233]. It could be the case that the genomic location of the insert has provided protection from contraction or excision of repeats seen in the long DPR mouse model[197].

Furthermore, a study looking to determine the molecular basis for CAG repeat instability in spinocerebellar ataxia type 7 using *Drosophila* found that despite modulation of genomic context and deletion of genes which may destabilise the repeat, the repeats were perfectly preserved[234]. The authors postulated that because expanded CAG repeats are lethal in *Drosophila*, it may have evolved under selective pressure to develop robust and redundant mechanisms to keep these CAG repeats stable. However, an

expanded FMR1 CGG repeat sequence display moderate repeat instability in flies, with one large contraction and numerous small contractions reported[235], suggesting that this effect may be CAG-specific.

Whilst the exact mechanisms underpinning stability of these models is unclear, a *Drosophila* model of 1000 repeat DPRs has been generated and appears to be stable for over 3 years, equivalent to over 100 generations. In addition to the importance of these models to the field, these observations highlight this insertion site as a potentially suitable site to insert other repeat models, such as pure GGGGCC repeats.

3.3.2 1000 repeat DPR-mediated effects on longevity and viability are mild compared to shorter DPR fly models

Studies using *Drosophila* models expressing 36 and 100 repeats of PR and GR have shown that toxicity increases with length. GR36 and PR36 exhibited rough eyes when expressed using *GMR-Gal4*, and when increased to 100 repeats they had impaired viability and severely degenerated eyes[137,163]. When expressed in the nervous system post-eclosion using an inducible driver (*elav-GeneSwitch*), GR100 and PR100 die within 10 days after induction, and GA100 has a slight reduction in lifespan compared to AP100 and controls. If this length-dependent increase in toxicity was extrapolated to 1000 repeats, one would expect expression of GR1000 and PR1000 to be lethal. In contrast, pan-neuronal expression of the 1000 repeat DPRs in *Drosophila* was viable and differences between DPRs were only observed after around 40 days when GR1000 expressing flies began to die (Figure 3.4). AP1000 and to a lesser extent GA1000 actually enhance longevity. A possible reason for this is that DPR expression exerts a low level of oxidative stress, which is known to increase lifespan[236]. Crucially, expression of 1000 repeats was not induced post-eclosion and expression throughout development was not lethal, even with GR1000 and PR1000.

This raises the question as to why the 1000 repeat DPRs in our model show different levels of toxicity than the shorter repeats in other models, when it has been shown in multiple studies that length increases toxicity[126,137,153,163,216]. A reasonable explanation is that the 1000 repeat DPRs are expressed at lower levels which reduces their toxicity, but we showed in West et al. (2020) that this is not the case. Comparison of transcript expression levels of DPR constructs in larval brains and adult heads using real-time qRT-PCR showed that previously published 36, 50, and 100 repeats[137,171] were not more strongly expressed than the 1000 repeat DPRs[207]. It is not, however, possible to ascertain whether the expression levels in any of these models are equivalent to those observed in patients. Despite this, the 1000 repeat model is arguably more

representative of human disease, where patients carry the mutation throughout their lifetime and show no significant developmental phenotypes. This is reflected in the ages at which they die, relative to their total lifespan – GR1000, the most toxic, causes death around 40 days into a 60-90 day lifespan.

An alternative explanation for the lower toxicity of our 1000 repeat models is the length itself. Although studies have shown that more repeats equate to more toxicity, this is only looking at between 36 and 100 repeats. It is possible that 1000 repeat DPRs behave in a completely different manner to short repeats. There is evidence to support this idea, as studies looking at the effect of 1000 repeat DPRs SH-SY5Y cells show that electrophysiological defects only appear when DPRs are extended to 1000 repeats in length[153]. It is also likely that different repeat lengths also affect the rate of de-novo DPR synthesis. The rate limiting step of translation is the elongation phase, whereby amino acids are added to the growing peptide in a cyclic process[237]. Therefore, the length of the DNA sequence is directly correlated to the time it takes to synthesise one peptide[238]. In eukaryotes, the average speed of translation elongation is 6–9 amino acid residues per second[238], but this can vary up to ~20-fold, based on factors such as the availability of respective tRNAs and ribosome occupancy[239,240]. This suggests that 1000 repeat DPRs could be produced at a rate 10-fold slower than 100 repeat DPRs, given the amino acid composition is the same and only the length differs. However, at present quantifying DPR abundance remains an obstacle in the field. Standard quantification via western blotting is not possible due to the longer repeat providing more viable epitope regions for antibody detection. This means that there is the capacity for more than one antibody molecule to bind to one DPR molecule, and so accurate quantification of protein levels based on band intensity is not possible. Recently, a promising method utilising Meso Scale Discovery to detect GP in yeast has been developed[241], and it is hoped that this can be adapted for other DPRs in other systems.

Another possible explanation for disparities between shorter and longer DPRs is that the secondary and tertiary structures adopted by the DPRs change as the length increases, and as such they preferentially interact with different cellular proteins. Indeed, length has been shown to be an important factor in PR's ability to disrupt nucleolar organization via disruption of phase separation behaviour and sequestration of nucleolar proteins[165]. Although this study only looked at the behaviour of shorter repeats (up to 23 repeats), it indicates that increasing length has a profound impact on the interactome of DPRs, and could be responsible for the disparities in toxicity between shorter and longer *Drosophila* DPR models. Co-immunoprecipitation of DPRs of different lengths from *Drosophila* brains and subsequent mass spectrometry analysis would reveal whether different length DPRs exhibit distinct interactomes.

3.3.3 DPR1000 expression does not cause developmental toxicity to the same degree as shorter DPR models

It has been demonstrated by multiple studies that expression of the arginine-rich DPRs, PR and GR, in the eye, at lengths up to 100 repeats, is highly toxic[137,163]. Eye phenotypes are primarily associated with developmental defects[242], suggesting that PR and GR at shorter repeat lengths confer developmental toxicity. This is supported by their reduced egg-to-adult viability and the necessity to induce pan-neuronal expression to avoid developmental lethality[137]. In contrast, the models developed in this investigation do not cause developmental lethality when expressed in the eye or pan-neuronally (Figure 3.4, 3.6). However, homozygous expression of PR1000, GR1000, and AP1000 does produce an eye phenotype, and global expression of PR1000 and AP1000, and to a lesser extent GR1000, is lethal. Taken together, this implies that the 1000 repeat DPRs do not confer the same level of developmental toxicity as the shorter models, and that they only show visible developmental defects when expressed at an increased dose (homozygous expression) or in all the cells of the fly. Therefore, modelling DPR toxicity using 1000 repeat DPRs is arguably more physiologically representative of disease progression in *C9orf72* carriers, where the mutation is present from birth but disease onset is age dependent.

In addition, although not physiologically relevant in itself, the different lethal stages observed with *tubulin-Gal4* – expressed PR1000, GR1000, and AP1000, highlighted that there may be differences in how the DPRs confer toxicity. PR1000 and GR1000 caused second instar lethality whereas AP1000 caused pharate lethality, indicating that different stages of development may be more or less susceptible to different DPRs. Although developmental phenotypes caused by global expression are not relevant to disease, where toxicity is age-dependent and neuronal, these differences suggest that different mechanisms underly the toxicity caused by each DPR.

3.3.4 1000 repeat DPRs form intracellular structures reminiscent of inclusions observed in *C9orf72* carriers

Each DPR displayed a distinct localisation and morphology when expressed pan-neuronally. They resembled DPR inclusions in patient tissues, with GA1000 forming cytoplasmic fern-like inclusions, AP1000 diffuse in the cytoplasm, and PR1000 and GR1000 observed in both the nucleus and cytoplasm[99,147] (Figure 3.5 A, B). The localisation of pan-neuronally expressed DPRs in the 100 repeat flies has not been reported, but in HeLa cells DPR morphology changes with increasing length[153], with the characteristic fern structures reminiscent of the stellate DPR inclusions in patients seen

only in GA1000 expressing cells. This suggests the difference in structure and intracellular localisation between DPRs could be responsible for the differences in toxicity between fly models of different lengths. However, PR and GR of various sizes, including a 1000 repeat HeLa cell model[153], have been found capable of penetrating the nucleolus and accumulating there[140,152,153,169,243] (Figure 3.5 C), a phenomenon not observed in patients, at least at end-stage. Nucleolar localisation was not observed in our *Drosophila* model. There is a lack of data from other *Drosophila* DPR models as to the localisation of DPRs *in vivo*. Nevertheless, these data suggest that the system, as well as the length of the DPRs, is important for their intracellular morphology.

A number of *in vitro* studies have used techniques such as circular dichroism and infrared spectroscopy to determine the biochemical properties of DPRs. GA3, GA34 and GA50 peptides readily assembled into amyloid-like fibrils and aggregated[156,244,245]. Tentative links have been made between the biochemical properties of the DPRs and their length, and these seem to suggest that longer DPRs would be more aggregation prone and therefore more toxic[244]. This is not corroborated by the findings of this investigation, where the longer DPRs appear less toxic than shorter DPRs. The potential reasons for this are discussed in 3.3.2.

Evidence from the behaviour of short peptides *in vitro* suggests that they are capable of spreading between cells[156], and this is further supported by a *Drosophila* model expressing 100 and 200 repeat GA which showed that GA is capable of spreading between cells in an age- and length- dependent manner in the fly brain[216]. This is another aspect of DPR morphology that could be affected by the extension of DPRs to 1000 repeats and will be explored in Chapter 4.

3.3.5 DPR1000 expression in different tissues reveals AP1000 has the potential to be toxic, contrary to evidence from shorter repeat models

In addition to milder toxicity, another notable difference between these new DPR models and the previous shorter models is the phenotypes associated with AP. Generally considered non-toxic, AP is the least studied of the DPRs, excluding GP. However, in this study, AP1000 showed a similar degree of toxicity to GR1000 when homozygously expressed in the eye. This is in contrast to GA1000 which conferred no toxicity. The consensus is that GR and PR are the toxic species, and AP and GA of lengths up to 100 repeats do not confer toxicity when expressed using *GMR-Gal4*[137,163]. This has led to most studies focusing on mechanisms underlying PR- and GR- mediated toxicity. The discovery that AP1000 has the capacity to be toxic highlights the importance of

considering all DPRs in future investigations, rather than focusing solely on the arginine-rich DPRs.

Furthermore, when expressed globally using *tubulin-Gal4*, AP1000 was lethal. Taken in isolation, global expression is not physiologically representative of DPR expression in patients, where DPRs are detected only in the CNS and skeletal muscle[100,142]. However, global expression of GA1000 is 100% viable, suggesting that AP1000's lethality is specific. One possible explanation is that AP1000 is more abundant, despite no differences in RNA expression[207] and so the sheer amount of AP1000 overwhelms the cell and ultimately causes cell death. Indeed, AP1000 appears much more abundant in the brains when pan-neuronally expressed (Figure 3.5). The reason for this is unclear, but we can speculate that it could be due to increased synthesis or reduced degradation. If this is the case, AP1000 may be more toxic for this reason alone. Given the lack of research into AP-mediated toxicity, there is little evidence to explain why AP1000 appears more abundant. However, it is possible that AP is inhibiting proteasomal degradation and thus aiding its accumulation. There is a precedent for this, as it is well established that aggregating proteins implicated in other neurodegenerative diseases inhibit proteasomal function[246-248]. Alternatively, it has been shown that PR and GR inhibit translation[74,167-169,249], which would explain the greater signal observed with AP1000 compared to PR1000 and GR1000. Ideally, quantitative western blots would confirm whether this was the case, and hopefully in future this will be possible, perhaps using a similar ELISA and Meso Scale Discovery based method as mentioned previously[241].

3.3.6 1000 repeat *Drosophila* DPR models recapitulate some, but not all, of the pathological features observed in *C9orf72*-FTD/ALS patient tissue

TDP-43 mislocalisation and aggregation is a hallmark of *C9orf72*-related FTD/ALS pathology[1]. The *Drosophila* TDP-43 homologue TBPH has been shown to accumulate in the cytoplasm in salivary glands of *Drosophila* expressing 64 repeats of GA and GR[213]. Additionally, GA64 colocalises with cytoplasmic TBPH aggregates, whilst GR64 causes a diffuse cytoplasmic mislocalisation of TBPH and does not colocalise[213]. In West et al. 2020 we demonstrated that repeating this experiment using the 1000 repeat DPRs yields both similarities and some contrasting results[250]: AP1000 expression caused no perturbations to TBPH localisation nor increased inclusion formation; expression of GR1000 and to a less extent PR1000 resulted in a significant increase in mislocalisation of TBPH to the cytoplasm; GA1000 expression increased the number of cells with TBPH inclusions but did not cause a significant mislocalisation of TBPH to the cytoplasm[207]. This is contrary to the aforementioned study where both GR64 and GA64 expression

results in mislocalisation of TBPH to the cytoplasm[213]. However, the two studies concur that only GA colocalised with TBPH. In the 1000 repeat *Drosophila* model, over half of the TBPH inclusions contained GA1000, and 18% of GA aggregates contained TBPH. Colocalisation was not seen with any of the other DPRs[207]. Whilst they offer a large cell with giant polytene chromosomes, a limitation of salivary glands is they can only be aged to a point – at 25 °C *Drosophila* are larvae for only ~ 3 days prior to pupation. Perhaps they have not experienced enough ageing to see perturbations of TDP-43. However, looking in the fly brain has proven technically challenging and inconclusive using TBPH antibodies. Furthermore, expression of tagged TDP-43/TBPH in the fly brain is lethal, limiting the use of co-expression of tagged TDP43.

Human post-mortem studies suggest that DPR aggregation may precede TDP-43 accumulation and this is complemented by studies using SH-SY5Y cells. In patient neurons, GA aggregates were found surrounded by accumulated TDP-43[147], and in cultured SH-SY5Y cells the formation of GA aggregates induced intracellular aggregation of endogenous and exogenous TDP-43, and this was dependent on GA being over 50 repeats[251]. Furthermore, a recent study showed that GA was capable of promoting cytoplasmic mislocalisation and aggregation of TDP-43 in a non-cell-autonomous manner[252]. In contrast, *C9orf72* iPSC models have struggled to recapitulate TDP-43 pathology seen in patients, with no change in subcellular localisation observed[253]. Taken together, despite inconsistencies between models in terms of TDP-43 pathology, GA appears to be most likely to aggregate with TDP-43 whilst not necessarily capable of driving TDP-43 pathology in its own right.

In addition to pathological TDP-43 inclusions, a major pathological hallmark of *C9orf72*-FTD/ALS is ubiquitin-positive DPR inclusions[96,145,147]. In these models, there was no colocalisation between any of the DPRs and ubiquitin (Figure 3.7), which is in contrast to what is seen in patients. One explanation for this discrepancy is that these models express each DPR individually, and it is possible that interactions and associations between DPRs are required to recruit ubiquitin to inclusions, as it is well documented that multiple DPRs are present in the same cells in patients[142,143,146]. However, immunofluorescence staining of cortex from GA50-transduced mice showed GA inclusions were ubiquitin-positive[155]. Similarly, GA50 formed cytoplasmic inclusions which colocalised with both p62 and ubiquitin in HEK293 cells[157]. These results concur with data from patient tissue which show that GA co-aggregates with components of the UPS, such as ubiquillin and p62[142,145,147]. These observations do imply that GA is prone to aggregating with ubiquitin, even when expressed in isolation. However, the DPR models cited above are only 50 repeats in length, and the importance of repeat length in determining DPR morphology and behaviour is well documented[153,160,216].

A HeLa cell model expressing GA at a physiologically relevant repeat length (over 1000 repeats) showed colocalisation with only p62 and ubiquillin-2[153]. Unpublished data using the same model showed that in HeLa cells, whilst GA1000 strongly colocalised with p62 and ubiquillin-2, it did not colocalise with ubiquitin[153,254]. Similarly, in HEK293 cells, GA175 was found in aggregates with p62, strongly suggesting that it was forming ubiquitinated aggregates, but its association with ubiquitin was not shown[158]. Currently there is no data from other *Drosophila* DPR models as to whether GA, or any other DPR, colocalises with ubiquitin. Therefore, there remains a lack of conclusive evidence as to whether GA of a physiologically relevant repeat length is capable of forming ubiquitinated aggregates *in vivo*, similar to those seen in post-mortem patient brains. However, it could be argued that the aggregates seen in post-mortem brain tissue are only representative of end-stage disease, and do not show what is happening to cells that are dying as a result of DPR toxicity. Given the DPR inclusions observed in our fly model are reminiscent of those observed in patient tissue and cell models (Figure 3.5), the question remains as to the pathological significance of the lack of ubiquitinated aggregates. Future work may want to focus on determining whether other components of the UPS co-aggregate with any of the DPRs in this model, as was observed in HeLa cells expressing 1000 repeats[153], or whether there is evidence of ubiquitinated protein accumulation independent of co-aggregation, as has been reported in in various *in vitro* and *in vivo* GA models[157-159].

3.3.7 Summary

In this chapter, the first *Drosophila* model of *C9orf72*-related DPRs expressing over 1000 repeats was established and initially characterised based on their morphology and commonly used readouts of toxicity. Crucially, 1000 repeats remain stable in the genome for over 3 years, and when expressed in the nervous system the DPRs appear to form structures reminiscent of the DPR inclusions we see in patients. We have found that, in contrast to shorter DPR fly models, pan-neuronal expression is not acutely toxic and flies expressing the DPRs have subtle differences in lifespan, with only GR1000 causing a reduction in longevity. Expression in the eye, a commonly used tool to assess toxicity in fly, proved toxic in a dose-dependent manner in AP1000, PR1000 and GR1000, but not GA1000, expressing flies. This is in contrast to the severe phenotypes observed in shorter PR and GR models, and the lack of toxicity in previous AP models. It is clear that there are differences between our model and previously characterised DPR fly models, which is likely due, in part, to the difference in repeat length. The next chapter will explore the effect of pan-neuronal DPR expression on disease-relevant phenotypes, such as

motor function, electrophysiological activity, and neurodegeneration, in an attempt to tease apart the role of each DPR in FTD/ALS.

4 Characterisation of Novel *Drosophila* models of *C9orf72* DPRs

4.1 Introduction

Having developed stable *Drosophila* models of 1000 repeat DPRs and confirmed that pan-neuronal expression of these constructs was viable and that ageing was possible, the next logical step was to explore how each DPR affected physiology and behaviours classically associated with neurodegeneration and FTD/ALS spectrum disorders. Due to the relatively short lifespan of *Drosophila*, questions relating to the function and health of the nervous system can be addressed more rapidly than in mammalian models. There are a number of established phenotypes known to be readouts for neurodegeneration in flies, such as brain vacuolisation, neuromuscular junction abnormalities, electrophysiological defects, and motor defects[186,187]. It is important to note, however, that whilst flies are capable of displaying complex behaviours including learning and memory, flies are not “mini-humans” and as such are not necessarily the best models for certain aspects of cognitive decline in FTD/ALS, such as lack of insight or personality.

Despite the plethora of options for investigating neurodegeneration in flies, the acute toxicity of short DPRs has been a barrier to such studies. There is limited data on the electrophysiological impact of DPRs *in vivo*, nor any histological studies to look at neurodegeneration in the brains of flies expressing DPRs. Motor problems are a key feature of *C9orf72*-related FTD/ALS and yet the effect of each DPR on locomotion in flies is inconsistent. When expressed in motor neurons, GR36 and PR36 have significantly reduced climbing ability compared to AP36 and controls[220]. Another study using different G_4C_2 repeats to produce different levels of the DPRs in neurons found that high levels of GA and GP together (36 and 64 repeats) caused late onset climbing difficulties, in contrast to the combination of GR, GA and GP (38 repeats) which appeared to cause rapid onset severe motor problems[213]. This strongly implicates GR as the cause of the acute toxicity, but does not rule out the contribution of other DPRs.

Motor defects are a defining feature of ALS and *Drosophila* climbing assays provide a robust and physiologically relevant readout of motor function. Characterising climbing ability and other neurodegenerative phenotypes in the new 1000 repeat DPR fly models is important to provide a baseline for future mechanistic studies, as well as to gain insight into the role of each DPR in neurotoxicity. Evidence thus far suggests that PR and GR are the main toxic species, but we know that when extended to 1000 repeats *in vitro* AP causes electrophysiological defects[153]. Therefore, it is important to examine all DPRs in

the same detail and not make assumptions based on previous data. The aim of this chapter is to produce a robust and thorough characterisation of each 1000 repeat DPR model, establishing a foundation for future mechanistic interrogations. In addition, it will provide a range of readouts for genetic and drug screening to look at specific pathways and therapeutic targets.

4.2 Results

4.2.1 Pan-Neuronal Expression of 1000 Repeat DPRs affects motor function in a DPR- and age-dependent manner

The most commonly used assays to test motor function in *Drosophila* are larval crawling and adult climbing. Both are complex and highly regulated but reflect activity in different neuronal circuits. Larval crawling requires bilaterally synchronised peristaltic muscle contractions coordinated through feedback between central and peripheral synapses, and provides a robust measure of physiological output relating to NMJ activity[255,256]. The startle-induced negative geotaxis (SING) response of adults is different to spontaneous locomotion and is the innate fast-climbing response initiated by a gentle mechanical shock. SING performance declines with age, but spontaneous locomotor activity does not[257,258].

In our DPR models, larval crawling speed was significantly reduced with pan-neuronal expression of each DPR (one-way ANOVA, $p < 0.001$) compared to controls (Figure 4.1). This suggests that DPR expression is interfering with normal neuronal function. However, a limitation of the larval model is the limited opportunity to explore the role of ageing, given that *Drosophila* remain as larvae for only ~3-5 days at 25 °C. In contrast, adult flies have a lifespan of 60-90 days and thus provide a better model to examine age-related motor function. Given that age is a key risk factor for FTD/ALS, with symptoms developing in mid-life or later, it is important to allow the effect of physiological ageing on DPR toxicity to be examined.

There are different methods of measuring climbing ability but the most commonly used is the proportion of flies that reach a given height in a given time. However, this has disadvantages and often requires a large number of flies because of the variability between individuals. The binary scoring system is likely to play a part in this variability. It also misses more nuanced aspects of movement, such as speed. The median speed of the fly is more representative of its motor function than whether it can reach a given height. The aforementioned assay does not take into account whether flies get to the top and climb back down, for example. Therefore, a different approach was employed for

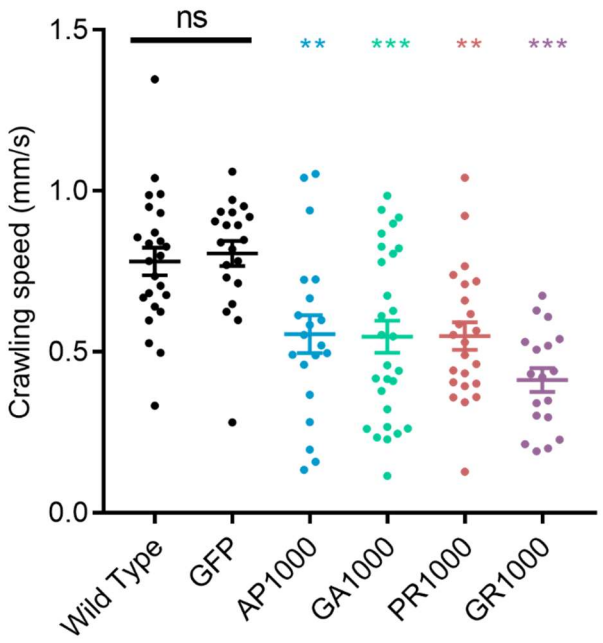

Figure 4.1 Larval crawling speed is significantly reduced with pan-neuronal DPR expression.

Median speed of third instar wandering larvae pan-neuronally (*nSyb-Gal4* III) expressing DPRs measured over a 3 minute period. GFP control is mCD8-GFP. Canton S flies outcrossed to w^{1118} were used as wild type controls. One-way ANOVA with Dunnett's multiple comparisons test to wild type controls *** $p < 0.001$ ** $p < 0.01$. Error bars = SEM.

this study using a bespoke ImageJ plugin. Each fly had its own individual tube so that the presence of other flies would not interfere or influence their climbing and their startle response was filmed. Tracking the movement of the flies via the MTrack2 plugin allowed the position of the fly in each frame of the video to be recorded as a series of coordinates that were the used to calculate the median speed. It is important to note that the variability in the "tapping down" phase of the experiment is common to all manual SING assays.

Comparisons between the median speeds of flies expressing DPRs and controls revealed striking differences that varied between DPRs and across the lifespan (Figure 4.2). Figure 4.2 A shows the average median speed for each DPR expressed in the nervous system and how this changed throughout the lifetime. Wild type and GFP flies exhibit a physiological age-dependent decline in climbing speed as expected, but this is not significant compared to GFP controls. In contrast, AP1000 flies display a significant reduction in speed, compared to wild type and GFP controls, from 1 day post-eclosion. However this remains constant throughout the lifespan, with no further age-related decline. GA1000 follows a similar pattern but with a less marked deficit. GR1000 flies begin life with a wild type climbing speed, but this declines steeply at around 14 days post-eclosion. PR1000 appears to start showing a decline at 28 days post-eclosion, but there is a large variance and as such it is not significant compared to the decline of

control flies. If the assay was extended to 56 days post-eclosion, the trend suggests that PR1000 could become significant. If we look at Figure 4.2 B, it is clear that there is a difference between alanine- and arginine- positive DPRs. AP1000 and GA1000 exhibit a significantly reduced climbing speed ($p < 0.001$ and $p < 0.05$ respectively) at 7 days post-eclosion, however this does not decline further with age. In contrast, GR1000 has a normal climbing speed at 7 days post-eclosion, but by 28 days post-eclosion it is significantly ($p < 0.001$) reduced. Similarly, PR1000, although not significantly different to controls at either 7 or 28 days post-eclosion, does exhibit a significant decline between the two ages that is not seen in wild type. This suggests that alanine- and arginine-positive DPRs may be acting through different mechanisms to cause neuronal dysfunction leading to motor problems. Additionally, once again AP1000 has a relatively severe phenotype, which contradicts previous studies suggesting it has no pathogenicity and supporting the idea that its properties change when it is extended to 1000 repeats. Since GR1000 flies have a shortened lifespan (see Figure 3.3 E), it is perhaps unsurprising that its climbing is impaired at later ages, as it nears death.

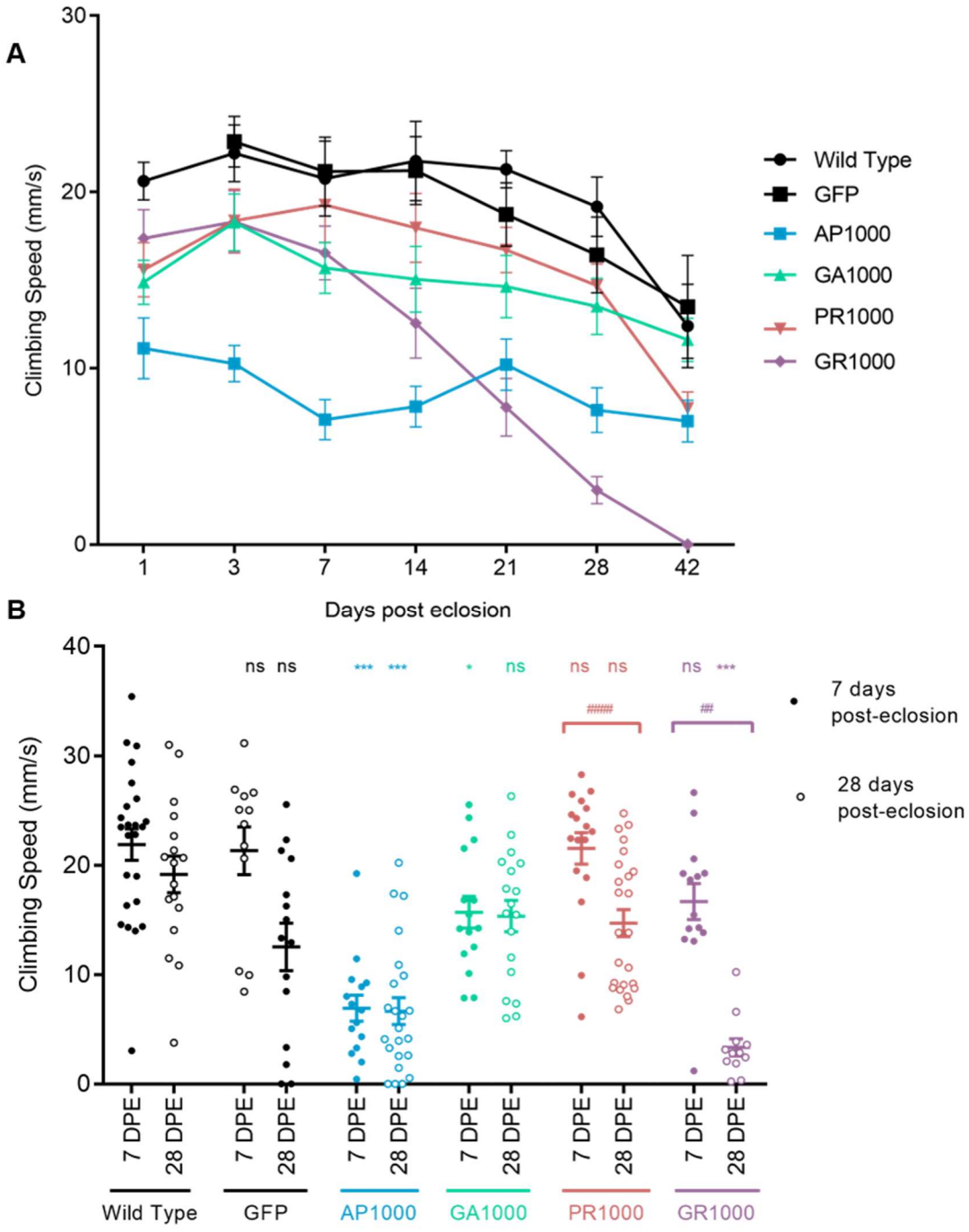

Figure 4.2 Age-related motor impairment in *Drosophila* pan-neuronally expressing DPRs. Median speed of pan-neuronally driven (*nSyb-Gal4* III) DPRs at different ages. Startle-induced negative geotaxis was assayed at 1, 3, 7, 14, 21, 28 and 42 days post-eclosion. **A** The average climbing speed across the lifespan. At day 3 a minimum of 10 flies per genotype were assayed. The minimum number of flies at any time point was 7 (GR1000 at 42 DPE), resulting from lethality at later ages. Error bars = SEM. **B** Comparison of median climbing speed between young (7 DPE) and old (28 DPE) flies. Each point represents the median speed of one fly. PR1000 and GR1000 have a significant decline with age, whereas AP1000 and GA1000 have a consistent speed across lifespan. AP1000 has a significantly slow speed that doesn't change with age, GR1000 has a significantly slow speed at 28 DPE but not 7 DPE, and PR1000 is not significantly slower

than wild type at either time point. GA1000 has a slight but significant reduction in speed at 7 DPE but not 28 DPE. One-way ANOVA with Dunnett's multiple comparisons test between DPRs and wild type control (*** $p < 0.001$ ** $p < 0.01$ * $p < 0.05$) and Tukey's multiple comparisons between time-points (### $p < 0.001$ ## $p < 0.01$) Error bars = SEM.

4.2.2 AP1000 and GR1000 cause vacuolisation indicative of neurodegeneration

Vacuolisation is a hallmark of neurodegeneration in *Drosophila* models. In addition to classical neurodegeneration mutants such as *Swiss cheese*[259], *spongecake*, and *egg roll*[260], vacuolisation is observed in fly models of AD[261], PD[262] and ALS[263]. Therefore, we looked to see if 1000 repeat DPR expression would result in age-related vacuolisation. Histological analysis of DPR-expressing *Drosophila* brains at 28 days post-eclosion revealed a DPR-specific effect (Figure 4.3 A). Based on reports of what size constitutes a neurodegenerative vacuole (> 5 µm diameter), and what is described as a "large" vacuole (>10 µm diameter)[208-210], the number of holes in a defined area and over multiple sections was quantified (Figure 4.3 B, C). Significant vacuolisation was observed in AP1000 expressing flies and to a lesser extent GR1000 expressing flies (Figure 4.3). Marked vacuolar regions were observed in AP1000 brains, and this was reflected when the number of holes larger than 10 µm in diameter. GR100 expression also resulted in more numerous holes than wild type controls, GA1000 and PR1000, but not to the same extent as AP1000 (Figure 4.3 C). This suggests that AP1000 and to a lesser extent GR1000 cause severe neurodegeneration when expressed pan-neuronally, whereas PR1000 and GA1000 do not, at least at this time point.

4.2.3 DPRs cause specific aberrations to neuronal structure and function

Drosophila neurons are similar to mammalian neurons in terms of electrophysiological properties, firing Na/K based action potentials, using conserved mechanisms for synaptic vesicle release and conserved neurotransmitters[264]. The larval NMJ is glutamatergic, the same as vertebrate central synapses (but not mammalian NMJs, which are cholinergic)[265], and has been well-characterised for the study of synaptic transmission[211,266]. Therefore, larval NMJs are widely used as a model synapse to characterise neuronal dysfunction in fly models of neurodegeneration.

Morphological analysis of NMJs from larvae expressing DPRs of 1000 repeats revealed a significant reduction in NMJ length in AP1000 expressing flies compared to wild type controls ($p < 0.001$, Figure 4.4 B), coupled with a reduction in the number of bruchpilot/nc82-positive active zones ($p < 0.05$, Figure 4.4 E). Neither PR1000, GA1000,

nor GR1000 had any effect on NMJ length, but PR1000 did cause a significant increase in the number of active zones ($p < 0.01$, Figure 4.4 E). In contrast, whilst AP1000, PR1000 nor GA1000 expression did not affect muscle size, GR1000 caused a significant reduction ($p < .01$, Figure 4.4 D). None of the DPRs affected bouton number (Figure 4.4 D). Taken together, these results suggest that whilst GA1000 expression has no effect on neuronal structure in this model synapse, PR1000, AP1000, and GR1000 act through different mechanisms to cause different neuronal defects.

Having observed these morphological defects, we assessed the electrophysiological function of DPR expressing larvae. Electrophysiological analysis of the larval NMJ (performed by Anna Munro) showed that AP1000 caused a significant ($p < 0.01$) reduction in excitatory junction potential (EJP) amplitude (Figure 4.5 A). This is consistent with the reduction in active zones. AP1000 expression was also associated with a significantly ($p < 0.05$) reduced input resistance (Ri), indicative of reduced excitability, channels but no variance in the other parameters tested (mini-evoked junction potential (mEJP) amplitude, mEJP frequency and quantal content). The other DPRs resulted in no significant variance in electrophysiological profiles compared to controls or each other (Figure 4.5).

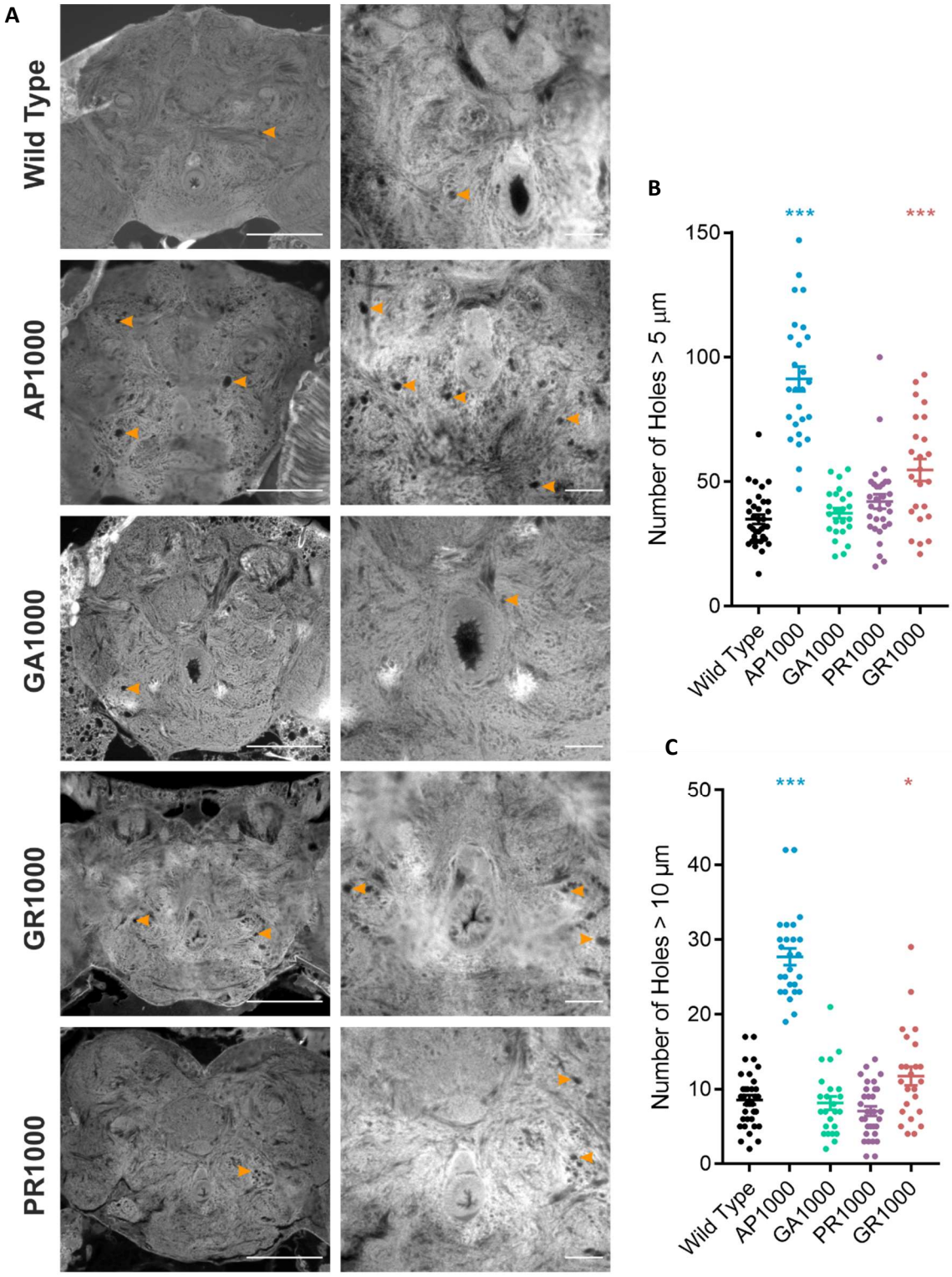

Figure 4.3 Histological analysis of *Drosophila* adult brains pan-neuronally expressing DPRs. **A** Representative images of histological sections of adult *Drosophila* brains at 28 days post-eclosion. Vacuolar holes (examples labelled with arrows) are characteristic of neurodegeneration in the *Drosophila* central nervous system. Scale bars 100 µm. **B**, **C** Quantification of the number of vacuoles > 5 µm (**B**) and > 10 µm (**C**) per defined area per histological section reveals a significant increase in the number of vacuoles in flies 28 days post-eclosion pan-neuronally expressing (*nSyb-Gal4* III) AP1000 and GR1000, compared to age-matched controls (ANOVA with post hoc Dunnett's multiple comparison to wild type controls *** $p < .001$ * $p < .05$). 3 brains (N = 3) per genotype were analysed. Error bars = SEM.

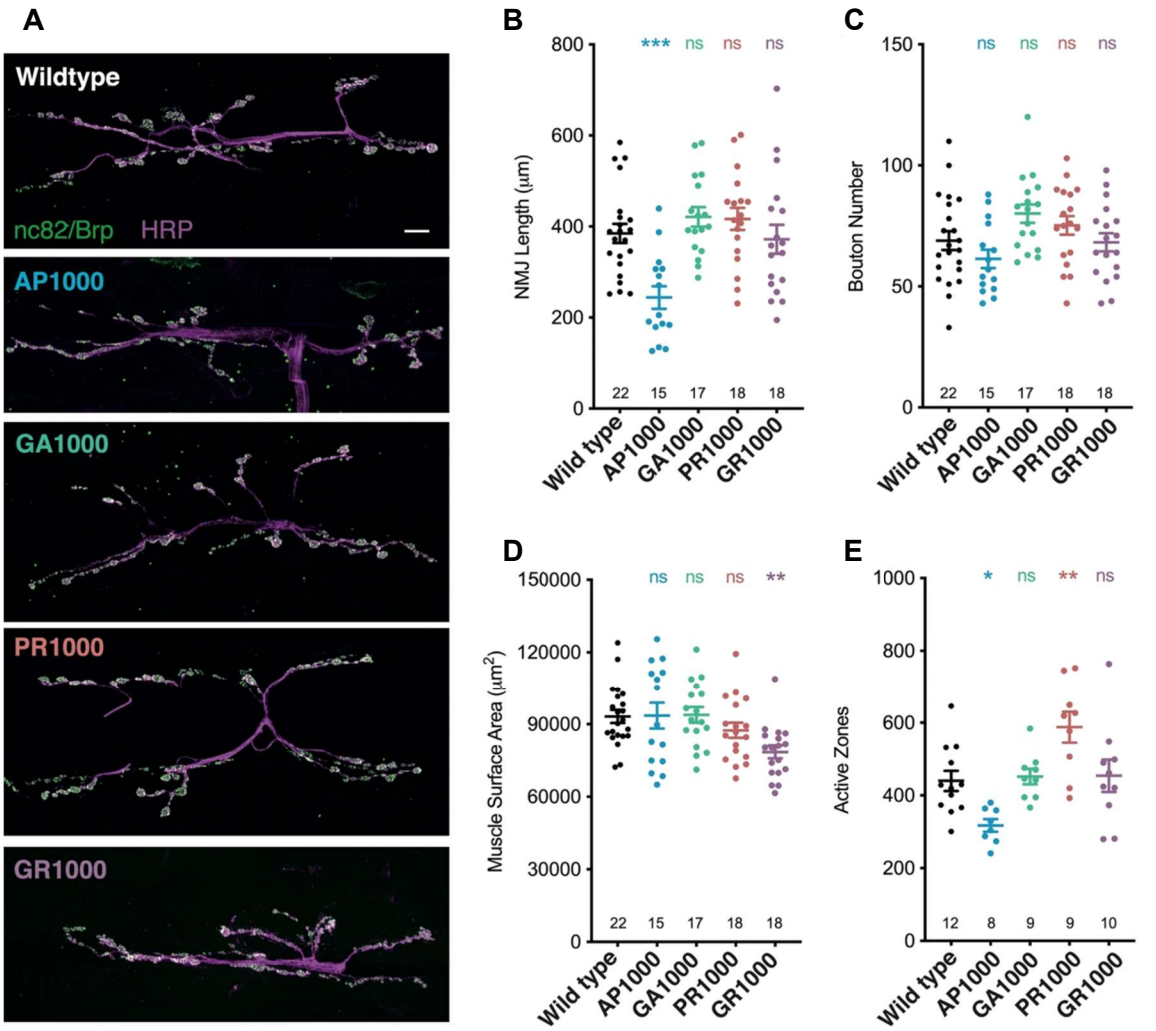

Figure 4.4 Morphological analysis of the Drosophila larval neuromuscular junction.

A Micrographs showing the neuromuscular junction (NMJ) (muscle 6/7 hemi-segment A3) of third instar larvae pan-neuronally expressing (*nSyb-Gal4* III) DPRs. Anti-HRP labels the nervous system (magenta) and anti-bruchpilot (Brp/nc82) active zones (green). Scale bars 10 µm. Quantification of **B** NMJ length, **C** muscle surface area, **D** bouton number and **E** active zone number. ANOVA with post hoc Dunnett's multiple comparison to wild type controls *** $p < .001$ ** $p < .01$ * $p < .05$. The number of NMJ's analysed are shown on each graph. NMJs were quantified from at least 8 animals (N = 8) taken from at least 3 independent crosses per genotype. Error bars = SEM.

4.2.4 DPR spreading within the *Drosophila* adult brain

Prion-like spreading of pathological proteins is a common mechanism in neurodegenerative disease, and has been posited to occur in *C9orf72*-related FTD/ALS, particularly with GA[156,267]. More recently, a *Drosophila* model expressing GA36 and GA100 in a well-defined neuronal subset showed that GA was capable of spreading within the fly brain in a length-dependent manner[216]. Therefore, the propensity for our 1000 repeat DPRs to spread in the fly brain was tested, to see if these findings were

reproducible in our model. However, due to logistical/time constraints, only AP and GA were tested. In order to assess the capacity for either GA1000 or AP1000 to spread in the fly brain, a membrane-RFP (mCD8-RFP) was co-expressed along with the DPR in a well-defined subset of olfactory projection neurons using *GH146-Gal4.* This Gal4 drives expression in a subset of relay interneurons (RI), elements usually projecting from the antennal lobes to the calyx and the lateral protocerebrum (LPR)[268]. The expression pattern of *GH146-Gal4* is shown in Figure 4.6 A. The DPR constructs are GFP-tagged, and so the pattern of RFP and GFP in flies expressing both the DPR and mCD8-RFP under the control of *GH146-Gal4* can be compared, to indicate whether there was a possibility that the DPRs had spread out of the cells in which they were expressed. To ensure that the expression pattern of each DPR was DPR-specific, and check the observed expression pattern against the documented expression pattern, a membrane-associated GFP was expressed using *GH146-Gal4* (Figure 4.6 B). The expression pattern of GFP alone resembled the pattern reported in the literature[268], but the fluorescence was comparatively weak in the calyx and pedunculus (PD) (Figure 4.6 A, B).

When expressed using the same driver, AP1000 had a distinct distribution pattern (Figure 4.7). It did not appear to be present in any of the neuronal cell bodies in the antennal lobes, but there were several AP inclusions which appeared to be in cell bodies around the calyx and LPR (Figure 4.7). In particular, there were AP inclusions which resembled cell bodies where there was no RFP visible (highlighted in two different brains in Figure 4.7). This pattern was not visible with GFP only (Figure 4.6 B). However, the pattern of expression documented in the literature suggests that the visible mCD8-RFP is not fully representative of the expression driven by *GH146-Gal4*. In Figure 4.6 A, there is clear expression clustering around the calyx. This is only faintly visible in the mCD8-GFP expressing brain, and in the mCD8-RFP channel in Figure 4.7. It is possible that where the AP inclusions appear to be isolated may, in fact, be *GH146-Gal4* expressing cells, but the RFP is not detectable.

Whilst AP appeared to form similar cytoplasmic aggregates to those seen when it is expressed in the nervous system (Figure 3.4), GA1000 looked markedly different when expressed using *GH146-Gal4*. There were very few of the characteristic stellate structures; instead, there were many small GA puncta (Figure 4.7). There were rare larger GA structures and these were mostly observed in the antennal lobes, colocalising with RFP signal (Figure 4.8, region b). The smaller GFP puncta were observed throughout the brain and outside areas of RFP expression, suggesting that smaller aggregates of GA1000 may have spread. This pattern of GFP speckling was exclusive to GA, not appearing in AP or GFP expressing brains, where the same microscope

settings were used (Figure 4.6 B, 4.7, 4.8). However, more validation to confirm that these GFP specks are in fact GA is needed.

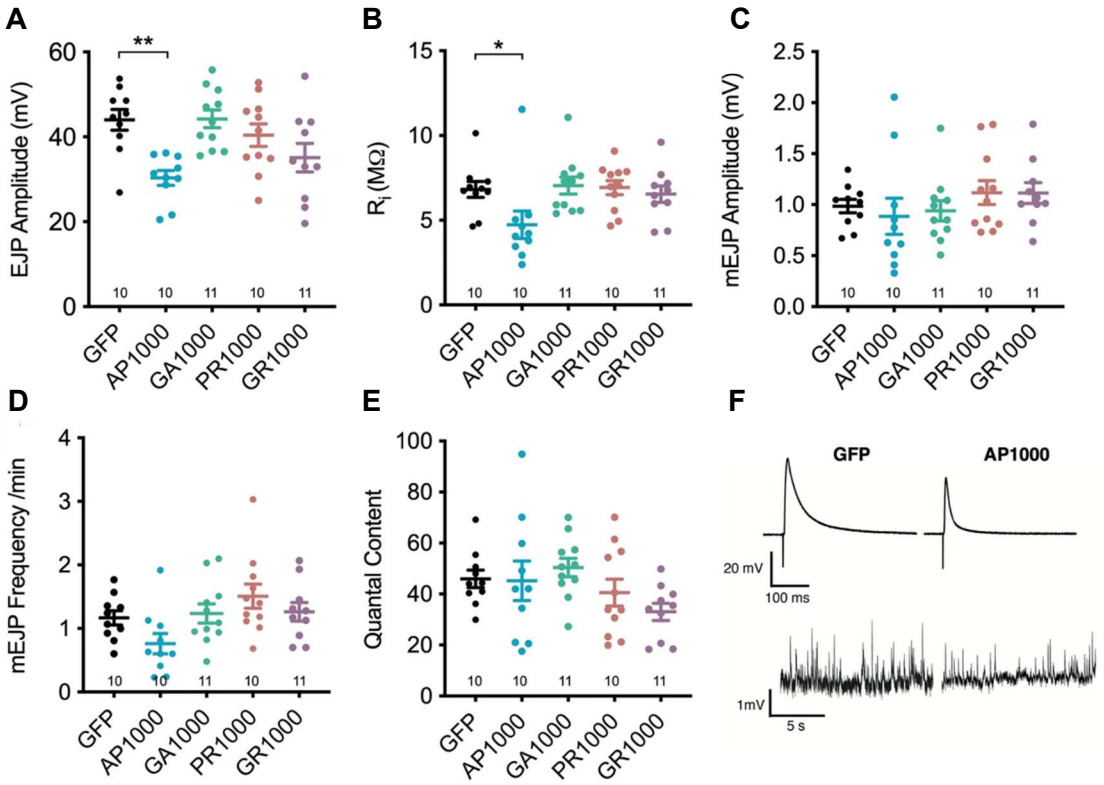

Figure 4.5 Electrophysiological analysis of larvae pan-neuronally (*nSyb-Gal4*) expressing DPRs.

A Excitatory junction potential (EJP) amplitude, **B** input resistance (Ri), **C** mini-EJP (mEJP) amplitutde**, D** mEJP frequency and **E** Quantal Content measured at muscle 6 (hemi-segment A3/4) of third instar wandering larvae pan-neuronally expressing DPRs or an mCD8-GFP control. (ANOVA with Dunnett's multiple comparisons to control; ** $p < 0.01$ * $p < 0.05$) **F** Representative traces showing evoked EJP (top traces) and spontaneous (mEJP) (bottom traces) responses in control (mCD8-GFP) and AP1000 larvae. Number of larvae tested shown on graphs. Error bars = SEM. Recordings were made from at least 5 animals (N = 5) taken from at least 3 independent crosses per genotype. Recordings and analysis performed by Anna Munro.

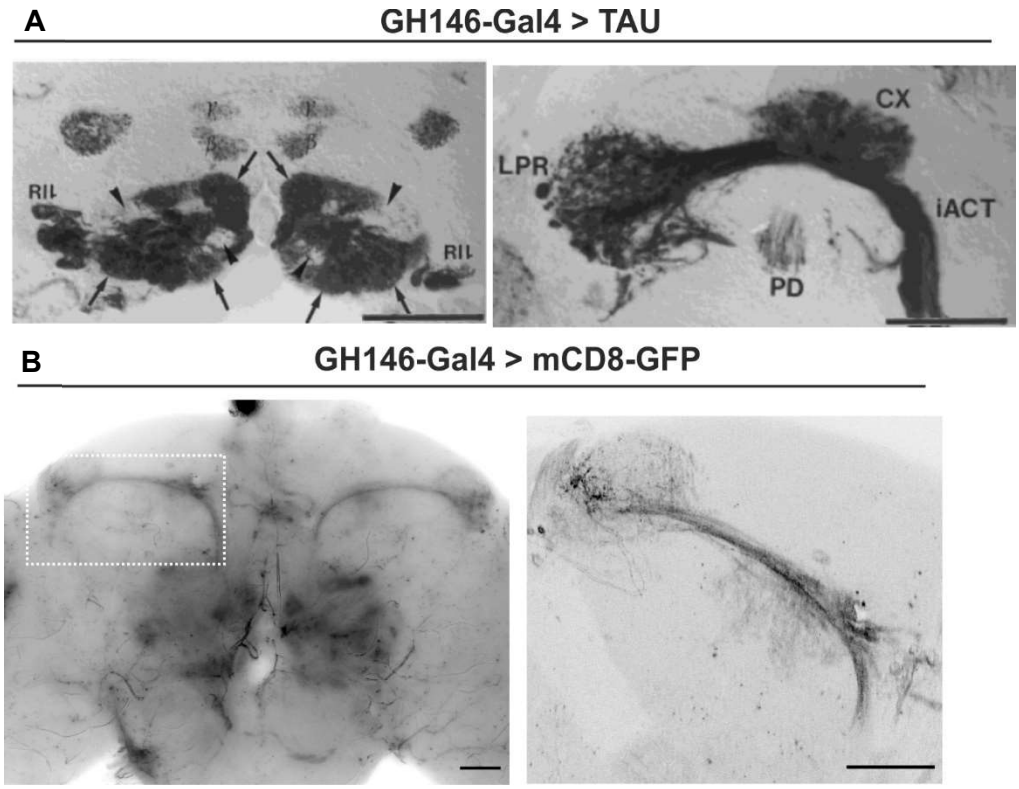

Figure 4.6 Expression pattern of *GH146-Gal4*.

A Images from Stoker et al. 1996. 10 µm cryosection of adult *Drosophila* brain expressing tau under the control of *GH146-Gal4* and microtubules labelled with anti-tau. Left panel shows expression in relay interneurons (RI) cell bodies in the antennal lobe. These project via the inner antennocerebral tract (iACT) (right panel), towards the lateral protocerebrum (LPR) and the calyx where they formed profuse terminal arborizations and tightly clustered dorsal collaterals respectively. Additionally, tau was also expressed in the pedunculus (PD). **B** Fluorescence micrographs of mCD8-GFP expressed under the control of *GH146-Gal4*. Left panel shows GFP expression in the whole brain; right panel zoom (with rotation) of highlighted area, showing the projections from RI to LPR and calyx. Scale bars 50 µm.

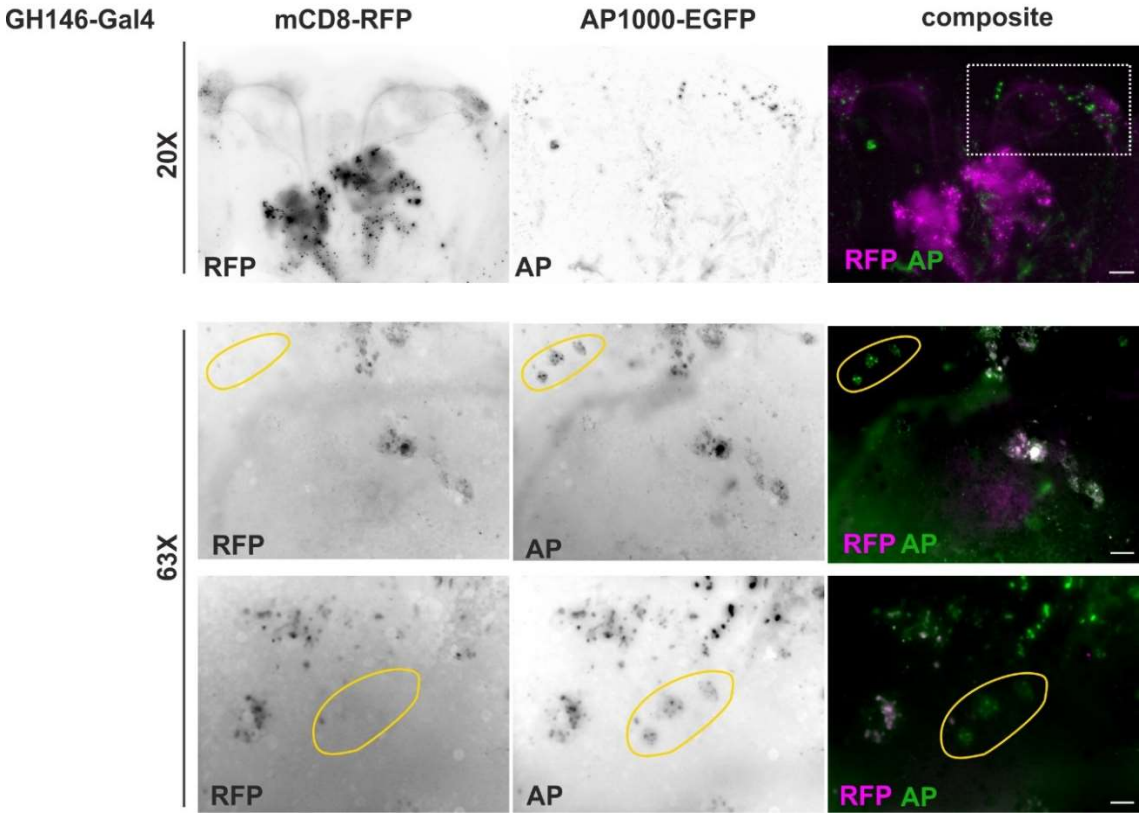

Figure 4.7 Co-expression of AP1000 and mCD8-RFP under the control of *GH146-Gal4*. Top panel shows the mid-brain with the highlighted area indicating the region of interest for below panels. Bottom two panels are images from two different brains taken at 63X of the same region. The yellow highlighted region indicates a site of possible spread of AP1000 into cells where there is no RFP signal. Scale bars: top panel 50 µm, zoom 15 µm. Representative images N=5.

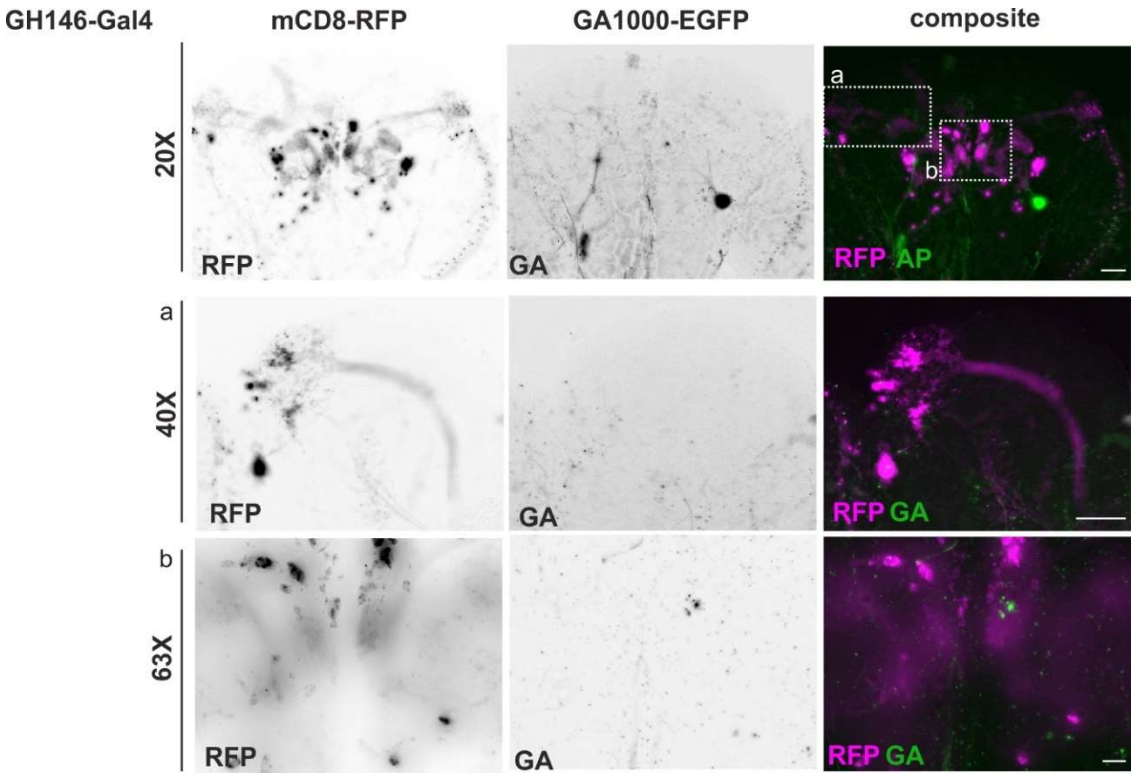

Figure 4.8 Co-expression of GA1000 and mCD8-RFP under the control of *GH146-Gal4*.
Top panel shows the mid-brain with the highlighted area indicating the regions of interest (a and b) for below panels. Bottom two panels are fluorescence micrographs of regions of interest a and b at 40x and 63x respectively. Scale bars: 20x, 40x 50 µm; 63x 15 µm. Representative images N=5.

4.3 Discussion

4.3.1 DPR1000 expression causes specific and distinct electrophysiological defects in the larval NMJ

Synaptic defects, including changes to neuronal morphology and membrane excitability have been observed in *C9orf72*-related FTD/ALS and have been proposed as a common mechanism between sporadic and familial cases[269-271]. Significant synapse loss independent of cortical atrophy was observed in the prefrontal cortex of sporadic ALS cases and correlated with the severity of cognitive impairment[272]. Morphological changes to neurons have also been reported in various models of *C9orf72*-related FTD/ALS. Decreased dendritic arborization has been reported in response to GA149 expression in mouse cortical neurons, and in rat spinal cord neurons expressing short 48 repeats of G4C2[158,191]. Excitotoxicity, whereby increased or prolonged activation of glutamate receptors results in a sustained influx of calcium into neurons and leads to several deleterious downstream consequences, ultimately resulting in neuronal loss, is heavily implicated in multiple neurodegenerative diseases[273]. There is a plethora of mechanisms that can trigger excitotoxicity such as mitochondrial dysfunction, malfunctioning glutamate receptors, and oxidative stress[273]. It has been suggested that excitotoxicity could be an early event in *C9orf72* pathogenesis, leading to synapse and axon degeneration with ageing[220]. There is some evidence to suggest that the *C9orf72* mutation enhances vulnerability of neurons to excitotoxicity. Pure repeats expressed in mutant iPSC-derived motor neurons caused increased GluA1 AMPA receptor expression, leading to enhanced vulnerability to excitotoxicity[274]. In contrast, a recent study using iPSC-derived cortical neurons found that the *C9orf72* mutation caused altered network function and impaired pre-synaptic function, but no change in AMPA receptor properties or expression levels[275]. Instead, transcriptomic analysis pointed towards defects in pathways contributing to synaptic vesicle dynamics[275]. Taken together, these studies highlight the potential for different neuronal subtypes to be differentially affected by the *C9orf72* repeat: motor neurons display an intrinsic excitability, whereas cortical neurons display functional synaptic defects which impact upon excitability in a more complex manner.

Drosophila models of the G4C2 repeat have provided consistent evidence for neuronal morphological changes in *C9orf72*-related FTD/ALS. The larval NMJ is a model synapse, both for morphological and electrophysiological analysis[211,255,256,265,266,276]. Additionally, larval crawling provides a robust measure of physiological output of the NMJ. Freibaum et al. (2015) expressed the G4C2 repeat at different lengths up to 58 repeat units in motor neurons using *OK371-Gal4* and observed a dosage and length dependent

locomotion defects and NMJ abnormalities. They found that muscle size, crawling distance and bouton number were reduced in larvae expressing 2 copies of 58 pure repeats but not 8 repeats[163]. In addition, one 48 repeat pure repeat fly model utilised the highly branched class IV epidermal sensory dendritic arborization as a model neuron to show dendritic branching defects[191]. However, which aspect of gain of function toxicity, DPR or RNA, was driving this toxicity was not explored.

The role of DPRs in synaptic defects has not been fully elucidated but data from *Drosophila* models have strongly implicated DPRs, and not repeat RNA, as the toxic species. One study investigating axonal transport as a possible toxic mechanism in *C9orf72*-FTD/ALS demonstrated that PR36 but not RNA-only and pure repeats of 36 repeat units caused a modest but significant reduction in locomotor capacity when expressed in motor neurons (*D42-Gal4*)[139]. This is consistent with our findings that DPRs are capable of causing locomotion defects when expressed in larval neurons (Figure 4.1). However, which DPRs are responsible, and precisely how they affect the larval NMJ, remains unclear. One study showed that motor neuronal (*OK6-Gal4*) expression of GR36 and GR100, but not GA of the same lengths, caused reductions in synaptic bouton number without a reduction in muscle size, indicating a specific NMJ defect rather than non-specific toxicity observed with pure repeats[277]. Additionally, GR100 produced a reduction in presynaptic vesicle markers, Synapsin and Synaptotagmin and fewer active zones. This is inconsistent with our findings where GR1000 expression led to a reduced muscle size but no other observable differences in NMJ morphology (Figure 4.4). The authors also found that overexpression of GR100 caused synaptic retraction, whereby NMJs expanded during development, but later degenerated, evidenced by a significant number of synaptic “footprints”, defined as post synaptic markers with no opposing presynaptic terminal[277]. Different results were also produced in a study by Xu et al. (2018), where they found that expression of GR36 and PR36 in glutamatergic neurons (*vGlut-Gal4*) led to an increase in the number of synaptic boutons and active zones. This was accompanied by increased extracellular glutamate and intracellular calcium levels in larval and adult brains[220]. The authors postulated that their findings were consistent with moderate toxicity conferred by low expression levels or short repeats, in contrast to the greater general toxicity observed in other models. Pan-neuronal expression of the 1000 repeat DPRs in this study revealed contrasting results with the aforementioned studies. Neither AP1000, GA1000, GR1000, or PR1000 had any effect on bouton number; AP1000 expression resulted in a reduced number of active zones but a normal muscle size; PR1000 expression caused an increase in the number of active zones; GR1000 expression resulted in a reduced muscle size (Figure 4.4). These DPR-specific phenotypes suggest that each DPR may act through a distinct mechanism to cause the locomotion defects observed. However, GA1000 expression

had no effect on the morphology of the NMJ but did have a reduced crawling speed (Figure 4.1), suggesting that GA1000 is causing neuronal defects through another mechanism.

Electrophysiological recordings from the larval NMJ are useful in determining what mechanisms might underpin synaptic dysfunction. A significant reduction in spontaneous mini excitatory post-synaptic potential (mEPSP) frequency was observed in GR100 expressing larvae. This is consistent with reduced active zone number[277]. However, it is important to consider that repeat lengths in patients are typically over 1000 repeat units and it has been shown that length can affect the toxicity of the DPRs, in particular AP, which was shown to cause electrophysiological defects at 1000 repeat lengths in differentiated SH-SY5Y cells[153]. Consistent with our findings that AP1000 expression caused a reduction in the number of active zones, AP1000 larvae showed a reduced EJP amplitude (Figure 4.5). However, despite increased numbers of active zones in PR1000 expressing larvae, no change in electrophysiological profile was observed.

The effect of AP expression is often ignored in favour of focusing on the arginine-rich species, but these results highlight the importance of including AP in future studies into the mechanisms underpinning *C9orf72*-FTD/ALS and the importance of using physiologically relevant repeat lengths. Furthermore, it is clear that there are discrepancies between models in terms of which DPRs cause aberrations to the NMJ, and the nature of these aberrations. This further emphasises the need for a consistent approach to studying DPR toxicity in *Drosophila* and other models.

4.3.2 Each DPR is associated with a distinct motor phenotype that changes across lifespan

Whilst *Drosophila* larvae are useful for studying NMJ structure and function, they are limited in their capacity to show age-related phenotypes. *Drosophila* are larvae for only ~3-5 days at 25 °C, compared to adult flies which live for ~60-90 days. Ageing is a key aspect of neurodegenerative diseases and we know that *C9orf72* patients have an average age of onset of 57 years[278,279] and so a model that can be aged provides a more relevant system in which to study *C9orf72*-FTD/ALS. Loss of motor function as a result of neuronal loss is the main symptom of ALS. Therefore, to build up a more detailed picture of the effect of each DPR on motor function, we examined the climbing speed of our *Drosophila* models. Despite the relatively short lifespan of *Drosophila*, there are relatively few studies looking at the motor function of flies expressing DPRs throughout the lifespan of the fly. One study investigated the impact of repeat RNA on climbing ability across lifespan, and found no significant drop compared to controls[190], but there remains

a lack of data for DPR models, likely due to their extreme toxicity and short lifespan[137]. Expression of PR36, but not AP36, in motor neurons (*D42-Gal4*) caused a reduction in climbing ability, given by the height a fly reached in 5 seconds[220]. These flies were aged to 7 days post-eclosion which is still fairly early in the lifetime of a fly. A model using different G4C2 repeat constructs to produce different levels of each DPR pan-neuronally (*elav-Gal4*) tested negative geotaxis of young (Day 5), mid-aged (Day 20) and older (Day 40) flies. Flies expressing high levels of arginine-rich DPRs, GR and PR of 36 repeats had severely reduced climbing ability by 5 days post-eclosion, which progressed to an inability to climb by 20 days post-eclosion[213]. In contrast, neither GA nor GP caused any motor deficits compared to controls until day 40, when they displayed a subtle reduction in performance[213]. Finally, GR80 and PR80, but not GA80 expressed in motor neurons using *OK371-Gal4* showed a significantly reduced climbing distance in 10 s at 3 days post-eclosion[193].

In this investigation, the effect of pan-neuronal expression of each DPR at a physiological repeat length was assessed at different ages. We found that each DPR was associated with a distinct phenotypic profile and in particular, there was a pattern with arginine- vs. alanine-positive DPRs. Whilst AP1000 and GA1000 were associated with a reduced climbing speed at 7 days post-eclosion that did not decline with age, PR1000 and GR1000 were associated with a significant decline with age (Figure 4.2). This implies that the alanine-positive DPRs cause a basal level of dysfunction that is not exacerbated by ageing, whereas the toxicity conferred by the arginine-rich DPRs is more directly linked to the ageing process. In fact, PR1000 expression, although declining significantly with age, did not show a reduction in climbing speed when compared to age matched controls, at any age (Figure 4.2 B). An important finding was that, in contrast to previous studies that suggest AP is not toxic[137], AP1000 expression resulted in a significantly reduced climbing speed throughout lifespan. There is almost no literature available as to the effect of pan-neuronal AP expression *in vitro* or *in vivo* and this emphasises the importance of studying all the DPRs, not just PR and GR, in a model that allows ageing.

Dopaminergic neurons are the predominant neuronal subset involved in the SING response[280]. Therefore, it would be interesting to look in more detail at which neurons the DPRs preferentially aggregate in, or whether neurodegeneration is neuron specific. This could be a future avenue for investigation using this model.

4.3.3 Vacuolisation indicative of neurodegeneration is DPR-specific

Significant vacuolisation was observed in flies expressing AP1000 and GR1000 at 28 days post-eclosion. Whilst a degree of neurodegeneration is expected due to normal

physiological ageing, and healthy aged *Drosophila* have been shown to display increased vacuolisation compared to young flies[281], an increase in number and/or size of these vacuoles indicates accelerated neurodegeneration and thus disease. Classical neurodegenerative mutants such as *spongecake* and *eggroll*[260] display distinctive vacuolisation patterns, similar to those seen in human diseases. When observed using electron microscopy, *spongecake* mutants display spongiform degenerations akin to those in Creutzfeldt-Jakob disease, and *eggroll* mutants show multilamellar structures similar to those observed in lipid storage diseases such as Tay-Sachs[260]. Furthermore, a *Drosophila* model of ALS caused by *VAPB* mutations showed vacuolisation in the optic lobe and central lobe at 12 days post-eclosion[263]. Taken together, this suggests that vacuolisation is a relevant and robust indication of neurodegeneration that is observed across neurodegenerative disease models, including ALS. However, prior to this study, vacuolisation in DPR fly models has not been investigated. Solomon et al. (2018) looked at neurodegeneration by expressing different G4C2 repeats under the control of a Rhdopsin1 promotor (*Rh1-Gal4*), using photoceptor loss as a readout for neurodegeneration[213]. Each G4C2 repeat was associated with a different level of expression of GP and GA, or GR. Flies were aged to 35 days and a significant increase in neuron loss was observed with high levels of GR expression compared to GA and GP. However, this is a less reliable method of looking at each DPR because it relies on accurate quantification of DPR levels and so cannot rule out the presence of other DPRs in this model. Furthermore, the fly retina is a less pathologically relevant tissue in which to study neurodegeneration than the brain.

To date, most studies into DPR toxicity have found PR and GR to be the most toxic, and AP and GA to have little to no toxic effects. However, previous studies have not looked at the brains for evidence of neurodegeneration. Therefore, it is unclear whether there is a link between the extreme toxicity and cellular disruption observed in PR and GR models, and age-related neurodegeneration in the central brain. The data from this study is conflicting. On the one hand, the neurodegeneration observed in GR1000 expressing flies is consistent with their reduced climbing speed at the same time point, and their reduced lifespan. In contrast, AP1000 expression caused the most significant vacuolisation but this did not negatively impact their lifespan (Figure 3.4). In fact, AP1000 expressing flies lived longer than controls. The disconnect between observed neurodegeneration and lifespan is not easily explained, but it is likely that AP1000 and GR1000 are acting through disparate mechanisms. Oxidative stress is a well-established cause of synaptic loss and has been shown to correlate with neurodegeneration in a fly model of AD[282]. Additionally, low levels of oxidative stress has been shown to increase lifespan[236]. One could speculate that in AP1000 expressing flies, oxidative stress could be the culprit behind extensive neurodegeneration and also their increased lifespan. It is

also possible that AP1000 and GR1000 may be causing the death of different cell types; we may see different patterns in the thoracic ganglion which is more similar to upper motor neurons, and also in motor neurons projecting from the thoracic ganglion to the legs.

Further information as to the nature of the neurodegeneration observed in AP1000 and GR1000 expressing flies could be gained using transmission electron microscopy, as in *spongecake* mutants where it revealed distinct membrane-bound vacuoles, swollen axons and relatively spared glia and neuronal cell bodies. It could be interesting to repeat the experiment and stain with antibodies for glia, and different neuronal subsets, to get a picture of which cells were dying and driving vacuolisation.

4.3.4 Potential for DPRs to spread requires further investigation

Seeding and spreading of pathological proteins is believed to underpin progressive nature of neurodegenerative diseases, including TDP-43 in ALS. TDP-43 oligomers are postulated to be capable of release from cells and subsequently seed for new aggregates in recipient cells[283]. DPRs are known to form insoluble aggregates in patient tissue and *in vitro*, a hallmark of disease-related proteins with the propensity to spread[284]. The propensity for all DPRs to spread between cells has been hinted by multiple *in vitro* studies[140,285] and GP has been detected in patients' cerebrospinal fluid, suggesting it has been secreted[286]. Furthermore, the pattern of aggregation found in post-mortem brains is highly suggestive of spreading, as DPRs are found in high-density clusters and isolated cells[143]. One mechanism of DPR spreading is that DPR deposits left by dying cells can persist and be phagocytosed by neighbouring cells[140]. Another proposed mechanism centres around exosomes, vesicles released by most mammalian and *Drosophila* cells that contain an assortment of mRNA, proteins and other bioactive molecules[287,288].

Recently, Morón-Oset et al. (2019) used a *Drosophila* model expressing 36, 100 and 200 repeats in a well-defined neuronal subset to show that GA, but not PR or GR, was capable of spreading within the fly brain in a length-dependent manner[216]. Spreading was greater in aged flies, suggesting that ageing-associated factors, such as impaired proteostasis[159], promote GA spread. A similar experiment was designed as part of this study, to test whether extending GA to a pathologically relevant repeat length would affect its spreading capability. In addition to testing GA1000, and unlike the aforementioned study, the propensity of AP1000 to spread was also investigated. To test this, a membrane-associated RFP was co-expressed with the DPR using an olfactory projection neuronal driver. The idea was to recapitulate experiments by Morón-Oset et

al. by examining whether the GFP-tagged DPRs would appear where the membrane-associated mCD8-RFP was not, thus implying that they had spread out of the cell in which they were expressed. However, the results were inconclusive. AP1000 appeared in bright cytoplasmic inclusions that resembled cell bodies just lateral to the iACT where no RFP signal was detected (Figure 4.7). However, the known expression pattern of *GH146-Gal4* suggests that there should be expression in this area (Figure 4.6), and so this observation could be explained by relative brightness and abundance of AP1000-GFP compared to RFP in these cells. Indeed, the pattern of *GH146-Gal4* expression described in the literature was replicated in the experiment but signal from both mCD8-RFP and mCD8-GFP was much weaker in some brain areas (Figure 4.6). Similar problems were encountered with GA1000. Whilst GFP puncta did appear in areas without RFP signal, it was difficult to define the cell borders based on RFP signal alone. Thus, although the results were intriguing, further validation is needed to be confident that the DPRs had indeed spread. Co-staining the brains with an antibody specific to this neuronal subset could help with defining neurons. However, the difficulties of distinguishing between individual neurons in a whole brain is one disadvantage of working in this system as opposed to cell culture. Nevertheless, co-culture systems cannot truly recapitulate the complexity of the brain. A combinatorial approach testing this theory in primary *Drosophila* neuronal culture as well as adult brains could prove useful.

Despite the lack of conclusive evidence in this model for DPR spreading, the morphology of GA1000 was unusual. There were few of the characteristic fern-like structures observed in adult brains expressing GA1000 in all neurons (Figure 3.5 A, B), and many smaller inclusions (Figure 4.8). This could be because GA was unable to form the larger aggregates in this particular set of neurons, or because it had spread out from the olfactory neurons as smaller oligomers. This would match the pattern seen in patient tissue[143].

4.3.5 Age-related phenotypes in *C9orf72* models

It is well established that age plays a key role in the pathogenesis of neurodegenerative diseases. The average age of onset of disease in *C9orf72* expansion carriers is 57 years of age[278]. Therefore, taking into account the physiological effects of ageing on cells and tissues is important when modelling *C9orf72*-FTD/ALS. Physiologically, ageing has a range of effects on the body that ultimately lead to increased vulnerability to death. The hallmarks of ageing include mitochondrial dysfunction, telomere attrition, genomic instability, epigenetic alterations and impaired proteostasis[289]. The brain and CNS are

particularly vulnerable to age-related defects due to their long lived and post-mitotic nature[49]. Whilst physiological ageing causes neuronal loss, neurodegenerative diseases accelerate these processes in specific neuronal populations, leading to specific symptoms[290]. Common themes between healthy ageing and neurodegenerative disease include oxidative stress caused by an elevation in reactive oxygen species, and impaired proteostasis[289,290]. Therefore, subtle age-related phenotypes caused by the long-term accumulation of DPRs may be missed in models that don't allow ageing.

Whilst cellular models are not ideal for studying ageing in a whole organism context, *C9orf72* patient iPSC-derived motor neurons do show an age-dependent increase in oxidative stress and DNA damage from 2 weeks to 4 months[170]. Furthermore, *C9orf72* astrocytes downregulated antioxidant secretions which increased oxidative stress in wild type motor neurons. Crucially this toxicity positively correlated with length of astrocyte propagation in culture[291], implicating astrocytes in age-related neurodegeneration in *C9orf72*-related FTD/ALS. Mouse models of *C9orf72* have variable age-related pathological or clinical phenotypes. An increase in number and size of GA and reduction in GP solubility in transgenic BAC mice with 450 pure repeats has been reported, but this did not correlate with any functional deficits[129,292]. Similarly, a GA149 mouse model showed an increase in the abundance of GA inclusions in neurons of the spinal cord between 1 month and 6 months of age[178]. However, this did correlate with loss of motor function.

Drosophila is an ideal model in which to study age-related diseases due to its short lifespan. However, there are few studies that age DPR-expressing flies to the relevant age. Most studies focus on larval phenotypes, eye phenotypes or adult phenotypes recorded at <10 days post-eclosion. Solomon et al. (2018) aged flies expressing different G4C2 repeats to produce different levels of DPRs to up to 40 days post-eclosion[213]. By this age, flies expressing high levels of GR at 38 repeats were dead. This corroborates our data where GR1000-expressing flies had a shortened lifespan (see 3.3). However, these GR flies had severe climbing deficits from day 5, suggesting that the toxicity was not age-related. However, a late-onset climbing defect was observed in other G4C2 repeat expressing flies, expressing higher levels of GA and GP of 32 and 64 repeats[213]. The discrepancies between models point to a necessity to use consistent pathologically relevant systems to study the mechanisms underpinning toxicity in *C9orf72*-related FTD/ALS. Age is a vital aspect of designing a good model. This is in addition to considering the impact of length, and, as will be discussed in the next chapter, looking at the interactions between DPRs.

4.3.6 Summary

This chapter focused on characterising disease-relevant phenotypes associated with pan-neuronal expression of 1000 repeat DPRs. Whilst previous *Drosophila* models have demonstrated the acute toxicity of arginine-rich DPRs, PR and GR, the short lifespan associated with their expression has thus far precluded a more detailed examination of age-related neurodegeneration in these models. This chapter has elucidated clear DPR-specific age-related phenotypes, including a full characteristic of motor phenotypes, arguably the most important phenotype in an ALS model, throughout the lifespan.

Furthermore, differences between the effects of each DPR on motor function, neuronal structure and function and neurodegeneration are consistent with the idea that each DPR acts through a different pathway. In particular, the difference in age-related decline in motor function between arginine-rich DPRs, PR and GR, and alanine-positive DPRs, AP and GA, corroborates previous studies that suggest the importance of the arginine residue in PR and GR interactions. This chapter has also highlighted the importance of studying all DPRs, rather than only focusing on PR and/or GR. It is important to examine all DPRs in each system to gain a better understanding of how each DPR may contribute to neurodegeneration in *C9orf72*-related FTD/ALS. By ignoring AP, we may be missing key phenotypes and mechanisms for therapeutic intervention.

5 Co-expression of DPRs in the nervous system reveals novel seizure phenotypes

5.1 Introduction

In *C9orf72* expansion carriers, repeat RNA and all 5 DPRs have the potential to be present in the same cell. In what proportion of cells this actually occurs is uncertain, but studies have shown that multiple DPRs are found within the same cell[142,143,146]. While a number of studies have looked at expression of single DPRs in isolation, there remains a lack of understanding of how different DPR species interact to mediate neurodegenerative cascades. This has been compounded by disproportionate levels of toxicity observed in existing *in vivo* models, expressing much shorter repeats, preventing co-expression studies being performed. Attempts to understand how co-expression of different DPRs may affect their toxicity and localisation have suggested that GA is capable of changing the localisation and thereby alter the toxicity of other DPRs. Studies in Neuro2A cells have shown that GA and GR have a propensity to co-aggreate[293], and more recently, the interaction between GA and PR was examined in more detail[294]. PR50-associated toxicity was ameliorated by GA50 expression in mouse primary neurons, and this was posited to be due to sequestration of PR from the nucleus into cytoplasmic GA inclusions[294]. Furthermore, PR20 and GA20 peptides were shown to interact in a cell-free environment, and circular dichroism spectroscopy revealed that whilst GA20 alone formed a β-sheet structure and PR20 was highly disordered, the co-aggregates formed exclusively disordered structures. This indicated that the interaction between the two DPRs results in a loss of the β-sheet structure of GA[294]. It is hypothesised this interaction ablates PR toxicity *in vitro* because PR is buried within the disordered aggregate and unable to form toxic interactions with cellular proteins[193]. The idea that GA is capable of ameliorating arginine-positive DPR toxicity is supported by research in a *Drosophila* DPR model[193]. In this study, GA80 expression ameliorated wing defects caused by GR80 and this was attributed to sequestration of GR80 into cytoplasmic inclusions by GA80[193]. There is a historic lack of *in vivo* models looking at the effects of DPR-DPR interactions. In fact, the aforementioned fly model is the only other study prior to this investigation to examine DPR interactions *in vivo.* The mechanism by which GA is capable of ameliorating arginine-positive DPR toxicity is related to physical interactions between GA and PR and/or GR that prevent them from forming toxic interactions with cellular proteins.

Despite evidence that interactions between DPRs may be an important factor in their toxicity, few studies have probed the interactions between DPRs other than GA and

PR/GR. Evidence from *C9orf72* patient frontal cortex suggests that GP and AP may be recruited into large cytoplasmic inclusions by GA, in which GA forms a "core" surrounded by GP and AP[295]. This is supported by a study in HEK-293 cells where AP and GP of 125 repeats would only aggregate in the presence of GA125[295]. It is important investigate if these interactions are consistent when DPRs are expanded to 1000 repeats. Therefore, this chapter will address the lack of data on the effects of combining different pairs of DPRs, using the 1000 repeat DPRs and examining the effects on previously characterised phenotypes. Initially, genetic interaction screens utilising the eye as a model system will be used to examine the effect of co-expressing DPRs[224]. Then the effect of combining DPRs in the nervous system will be investigated using the previously described SING assay.

5.2 Results

5.2.1 Different combinations of DPRs confer different degrees of toxicity when expressed in the eye using *GMR-Gal4*

Using the 1000 repeat DPRs characterised in the previous chapters, we looked to examine if combining pairs of DPRs in the eye using *GMR-Gal4* would potentiate or ameliorate toxicity conferred by single DPRs. Co-expressing two transgenes with one *Gal4* driver may reduce the expression of both compared to each transgene expressed individually. Therefore, for co-expression experiments, a *UAS-mCD8-EGFP* was used as a titration control.

Previously, a dose-dependent effect of DPR expression on toxicity in the eye was observed in AP1000, GR1000 and PR1000, but not GA1000 (Figure 3.7). Co-expression of GA1000 with any of the other DPRs produced no significant phenotype, although GA1000/GR1000 did produce a small number of flies with mild perturbations to the interommatidial bristles (Figure 5.1 B). Co-expressing AP1000 with either PR1000 or GR1000 produced some flies that had similar mild phenotypes, but only AP1000/PR1000 was significant (Figure 5.1 A, $p < 0.01$). The DPR combination that produced the most severe phenotypes was PR1000/GR1000; although the majority of flies had wild-type eyes, there were a significant number that had a range of defects including perturbations to the ommatidial array, gross morphological defects, and pigmentation defects (Figure 5.1 C-E, $p < 0.001$). However, the greatest toxicity was seen in flies homozygously expressing the same DPR transgene, apart from GA1000/GA1000 in which no eye defects were seen ($p < 0.001$). This suggests that, at least when expressed in the fly eye, exacerbating the phenotype caused by one DPR by doubling the dose confers a greater toxicity than any interactions between different DPRs.

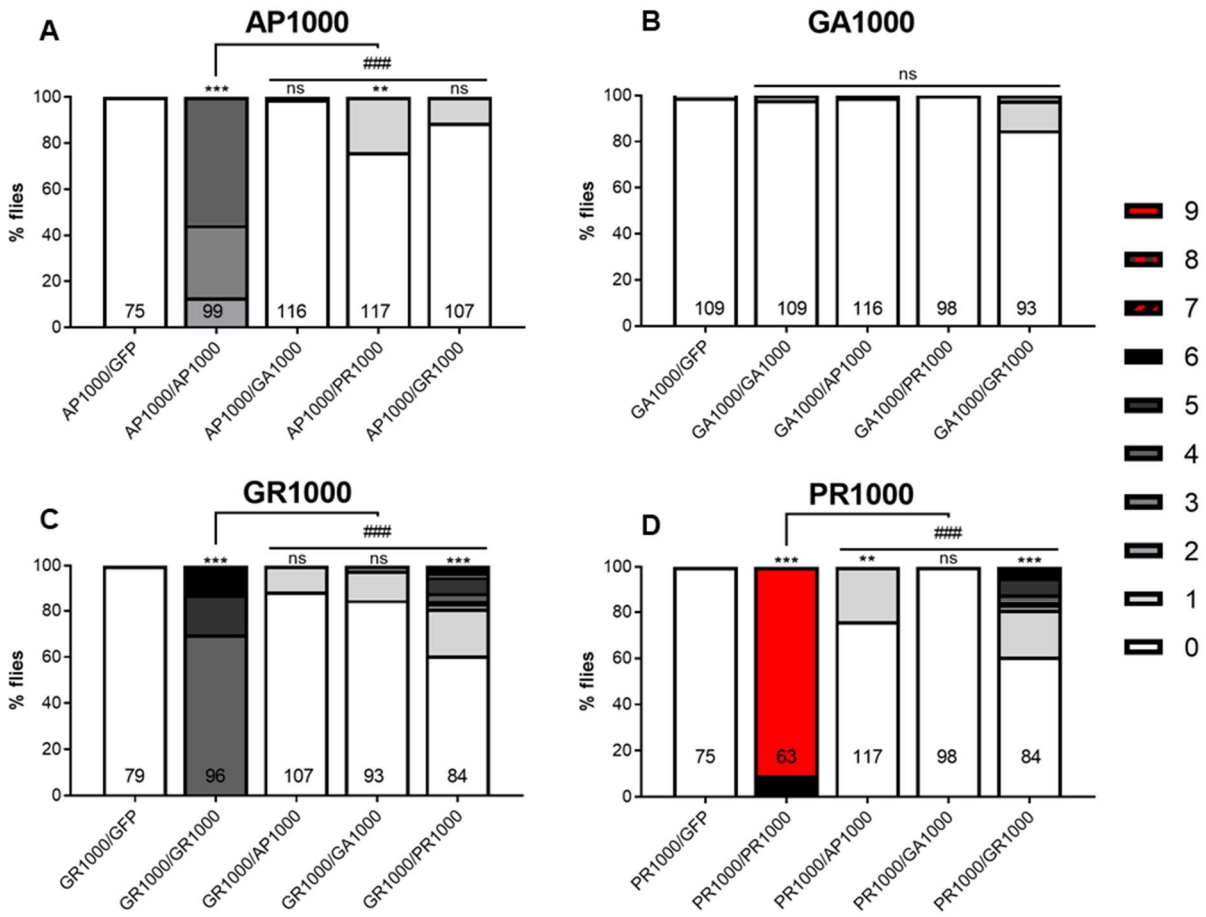

E

	+	AP1000	GA1000	PR1000	GR1000
+	0 ± 0.00	0.04 ± 0.02	0.02 ± 0.01	0.00 ± 0.00	0.00 ± 0.00
AP1000	-	3.42 ±0.08	0.01 ± 0.01	0.24 ± 0.04	0.11 ± 0.03
GA1000	-	-	0.02 ±0.00	0.00 ± 0.00	0.17 ± 0.20
PR1000	-	-	-	8.71 0.11	1.08 ± 0.09
GR1000	-	-	-	-	4.43 ± 0.07

Figure 5.1 Different combinations of DPRs modify DPR-mediated eye toxicity.
Flies expressing 1000 repeat DPRs and mCD8-EGFP (GFP) under the control of the eye specific driver GMR-Gal4 (*GMR-Gal4*/+). GFP expression acted as a titration control for *GMR-Gal4*. Quantification of eye phenotypes expressing each DPR in combination with **A** AP1000 **B** GA1000 **C** GR1000 **D** PR1000. One point is scored for each eye defect (see 2.5 for full classification). The number of flies scored is shown inside each bar. Each genotype was scored from a minimum of 3 independent crosses. AP1000/PR1000, PR1000/GR1000 showed significant toxicity compared to each DPR alone (Kruskall-Wallis with Dunn's multiple comparisons test *** $p < .001$ ** $p < 0.01$ *) Doubling the dose of AP1000, GR1000, and PR1000 caused a more severe eye phenotype than any combination of different DPRs (Kruskall-Wallis with Dunn's multiple comparisons test ### $p < .001$). **E** Mean overall classification score (± SEM) of genotypes represented in A-D.

5.2.2 Co-expression of DPRs in the nervous system results in combination specific climbing defects

While expression in the eye provides a robust model in which to investigate genetic interactions, the fly eye does not provide a functional model to explore the effect of ageing on DPR co-expression. Indeed, phenotypes observed in the eye are likely to have a largely developmental basis. In order to determine whether concomitant expression of DPRs effects motor function and whether there is an ageing component, we utilised our established SING assay. For this experiment, a different pan-neuronal driver (*nSyb-Gal4* (II)) was used to circumvent the issue of having two DPRs and a driver on the third chromosome. Therefore, any motor defects seen in this assay must be evaluated independently from the previous SING assay (Figure 4.2).

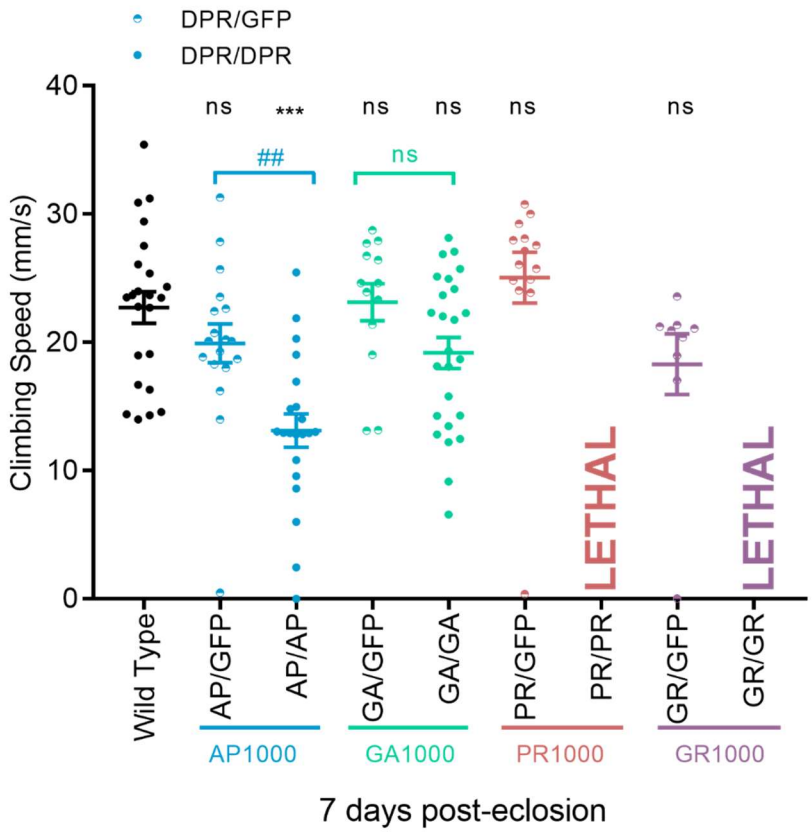

Figure 5.2 Dose-dependent effect of pan-neuronal DPR expression on climbing speed. Median climbing speed of adult *Drosophila* expressing one copy of each DPR with mCD8-EGFP, and two copies of each DPR, under the control of a single copy of the pan-neuronal driver *nSyb-Gal4* (II) (*nSyb-Gal4*/+) at 7 days post-eclosion (DPE). Error bars = SEM. ANOVA with post hoc Sidak's multiple comparison between DPR-expressing flies and wild type (*** $p < .001$), and between single and double DPRs (## $p < .01$). Each point represents an individual fly. Motor assays were performed from at least 3 independent crosses per genotype. 1000 repeat DPRs are abbreviated to e.g. AP for brevity.

Firstly, the effect of homozygous expression using *nSyb-Gal4* (II) was investigated (Figure 5.2). Pan-neuronal homozygous PR1000 or GR1000 proved lethal at an early larval stage. At 7 days post-eclosion, the climbing speed of AP1000/AP1000 expressing flies was significantly reduced compared to AP1000/GFP flies and wild type controls. Doubling the dose of GA1000 produced a slight but not significant decrease in climbing speed compared to GA1000/GFP and wild type controls. This is consistent with previous results with *nSyb-Gal4* (III) where expression of one copy of AP1000 and to a lesser extent GA1000 reduced climbing speed at 7 days post-eclosion (Figure 4.2). It also mirrors the effect of doubling the dose in the eye using *GMR-Gal4*, where GA1000 has no effect, AP1000/AP1000 has a moderately severe phenotype, and GR1000/GR1000 and PR1000/PR1000 have the most severe phenotypes (Figure 3.5 B).

Next, we examined whether there was an ageing component to the phenotypes observed with concomitant DPR expression. To do so we looked at 7 and 28 days post-eclosion. These time points were chosen based on our previous results looking at single DPR expression (Figure 4.2). All combinations of DPRs were viable, and lived to at least 7 days post-eclosion. However, AP1000/GR1000 did not survive to 28 days old (Figure 5.3). Combining the two alanine-positive DPRs (AP1000/GA1000) produced a slight but significant decrease in climbing speed at 7 and 28 days post-eclosion, but no significant decline between the ages. In fact, it was the only combination which did not exhibit a significant age-related decline in speed. All other DPR combinations contained at least one of the arginine-rich DPRs, and all showed a significant decline in climbing speed between the two ages (Figure 5.3). This pattern is most striking in Figure 5.3 C, which shows PR1000-containing combinations. Flies co-expressing PR1000 and any of the other DPRs had a speed comparable to wild type at 7 days post-eclosion, but this significantly declined with age, with all combinations having a reduced speed at 28 days post-eclosion. This is comparable to the behaviour of flies expressing PR1000 alone; whilst PR1000 expressing flies did not have a significantly slow speed compared to wild type controls, they did have a significant decrease in speed with age (Figure 4.2). In general, GR1000 appears to confer the greatest toxicity, with GR1000/GA1000 and GR1000/AP1000 flies having a significantly reduced climbing speed at 7 days post-eclosion (Figure 5.3 D).

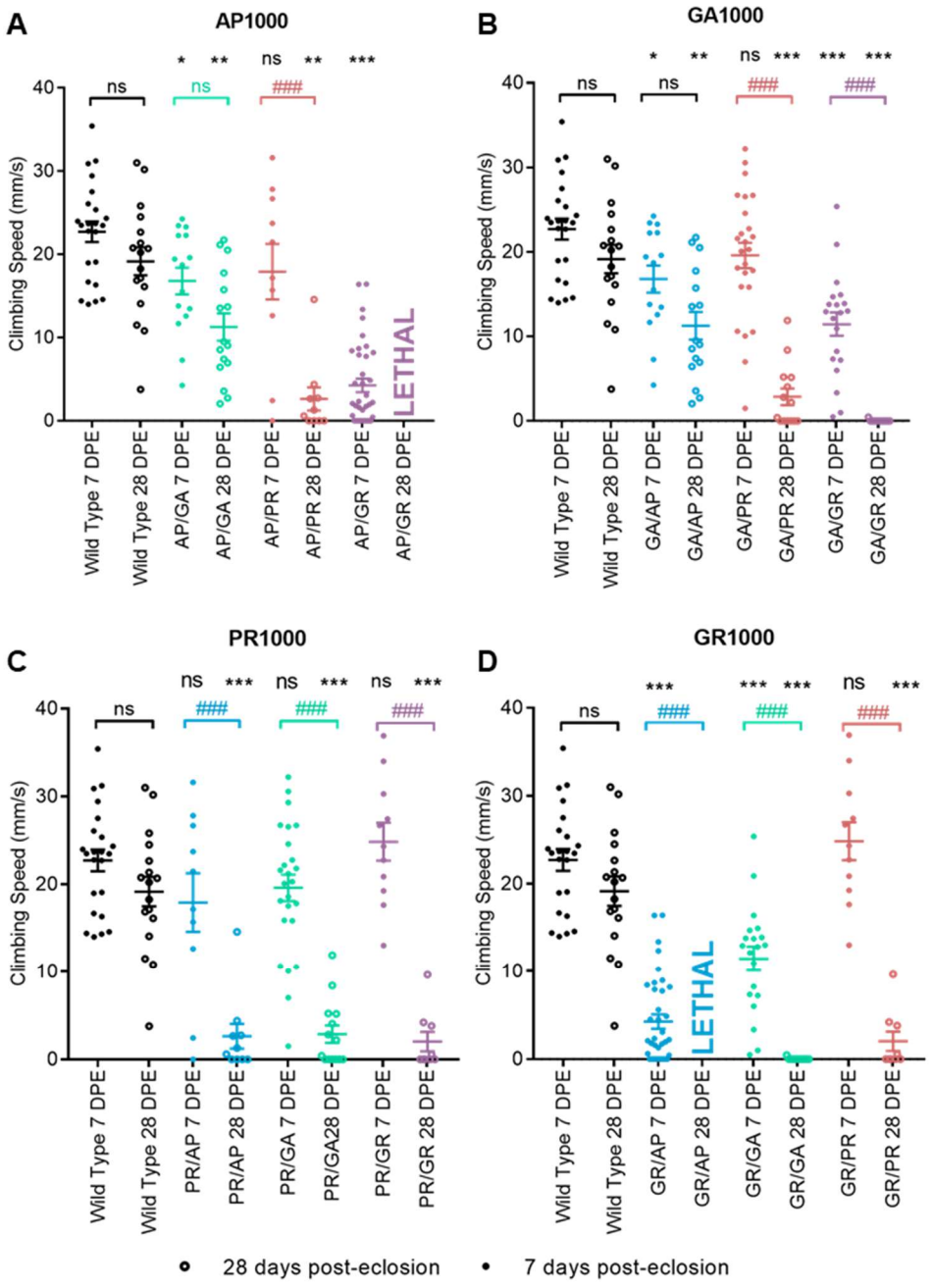

Figure 5.3 Age-related motor impairment in *Drosophila* co-expressing DPRs.
Median climbing speed of adult *Drosophila* co-expressing DPRs under the control of a single copy of the pan-neuronal driver *nSyb-Gal4* (II) (*nSyb-Gal4/+*) at 7 and 28 days post-eclosion (DPE). The data displayed in **A**, **B**, **C** and **D** is from the same data set, but displayed for each DPR for ease of comparison. Error bars = SEM. ANOVA with post hoc Sidak's multiple comparison between DPR-expressing flies and age-matched controls (*** $p < .001$; ** $p < .01$; * $p < .05$), and between ages (### $p < .001$). Each point represents an individual fly. Motor assays were performed from at least 3 independent crosses per genotype. 1000 repeat DPRs are abbreviated to e.g. AP for brevity.

5.2.3 Co-expression of DPRs in the nervous system is associated with a novel bang-sensitive seizure susceptibility

In the course of the climbing assay, where flies are "banged" to the bottom of glass boiling tubes to initiate the SING response, it was noted that some flies exhibited seizure phenotypes, characterised by high-frequency wing flapping and muscle spasms. Seizures were observed in 14-day old AP1000/GR1000 flies (33%), and 28-day old AP1000/PR1000 (40%), GA1000/PR1000 (29%), GA1000/GR1000 (100%) and GR1000/PR1000 (71%) flies. Seizures were never observed AP1000/GA1000 flies, at any age, suggesting seizure phenotypes are unique to specific DPR combinations. In order to establish whether seizure phenotypes were specifically "bang-sensitive" we asked whether pan-neuronal co-expression of DPRs resulted in temperature sensitive seizure phenotypes. Conditional temperature sensitive seizure phenotypes have previously been observed in other seizure models such as *shibire* mutants[296]. Exposing DPR flies to 38 °C for 5 mins failed to induce seizures in any model. There are a number of well-characterised *Drosophila* mutants that display bang-sensitive seizure phenotypes. The genes involved encode a variety of proteins, from sodium channels, ribosomal components, RNA-binding proteins and mitochondrial proteins[297]. Typically, in response to vortexing, bang-sensitive (BS) mutant flies show a stereotypical sequence of initial muscle spasm, paralysis, delayed spasm, and recovery to normal posture. Spasms manifest by high-frequency wing flapping, leg extension, and fully curved abdomen[298]. *Drosophila* BS mutants are often used as a model for investigating different forms of epilepsy[299] and as such, there are well-established methods to assess seizure behaviour in flies.

Seizures have not previously been observed in fly models of *C9orf72*-FTD/ALS but there is some evidence from human patients that *C9orf72* expansions may cause epileptic seizures; one study found incidences of teenage-onset myoclonic epilepsy linked to the expansions[300], and others have found evidence of epilepsy in previously diagnosed *C9orf72*-FTD patients[301,302]. Therefore, potential for DPRs to cause seizures was investigated in more detail using the well-established vortexing assay[303] to test for bang-sensitivity. Briefly, flies were transferred to empty food vials and mechanically agitated with a vortex mixer for 10 seconds. Flies were filmed and then analysed for the presence of a seizure response and time to recovery measured. Typically, this stimulus is not sufficient to initiate a seizure in wild type flies[298], therefore any seizures seen must be due to electrophysiological and neural deficits. In BS *Drosophila* mutants, the seizures become easier to trigger and the time to recovery increases, with increasing age[304]. Given the poor survival of some DPR combinations, particularly AP1000/GR10000, to later ages, the assay was undertaken at 14 days post-eclosion. Initially, due to the

preliminary observations occurring with a lesser degree of mechanical agitation (tapping), a version of the seizure assay involving tapping the flies to the bottom of their vials, in addition to the traditional vortexing assay was performed.

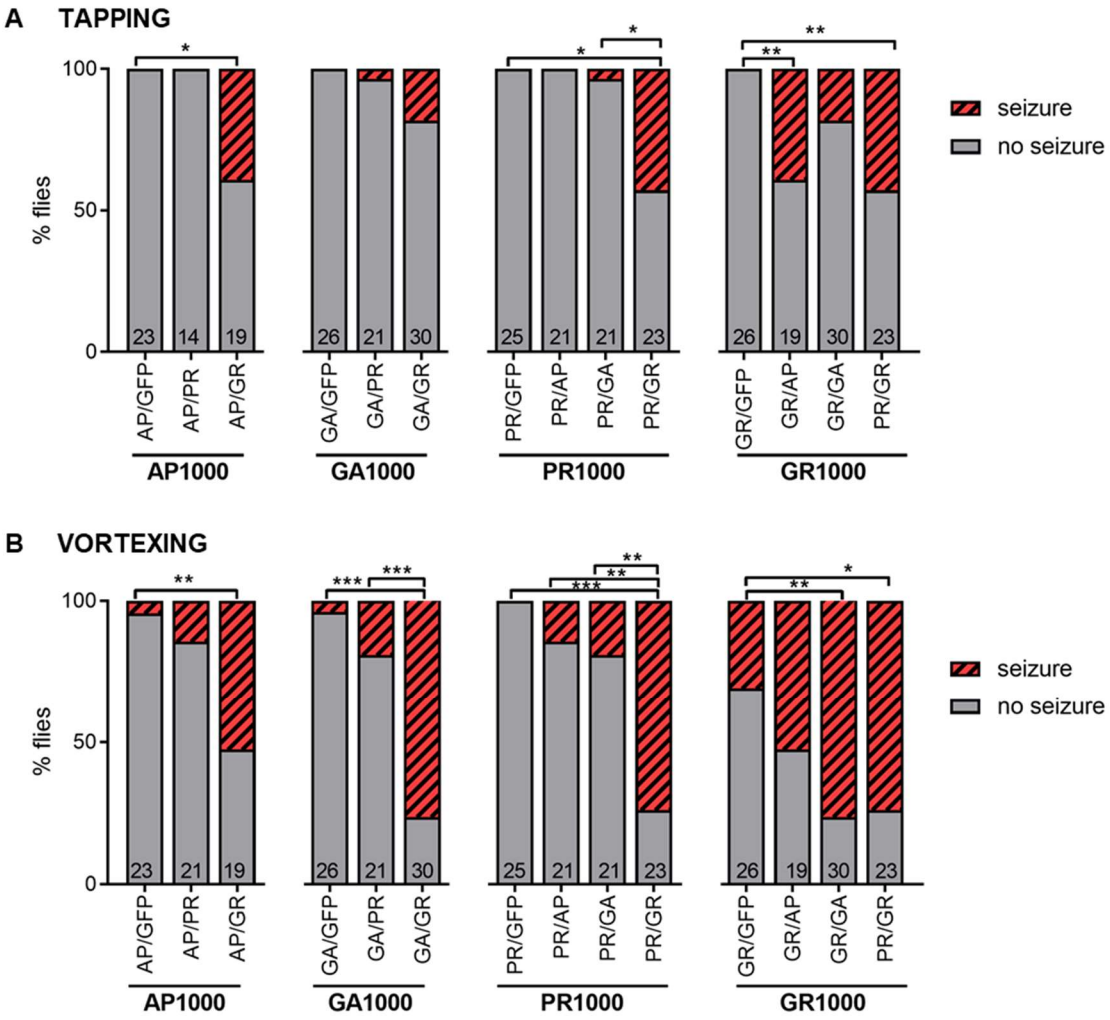

Figure 5.4 Bang sensitivity in flies co-expressing DPRs.

Bang-sensitive seizures in flies co-expressing DPRs under the control of a single copy of the pan-neuronal driver *nSyb-Gal4* (*nSyb-Gal4/+*). Flies were either **A** tapped down or **B** vortexed for 10s in an empty food vial. Flies were tested at 14 days post-eclosion. Pairwise comparisons of % bang-sensitive seizures using a post-hoc chi-square test. Bonferroni corrected *p* value for 18 comparisons: * $p < 0.05$; ** $p < 0.01$; *** $p < 0.0001$ (see Appendix 4, Appendix 5). For ease of comparison, bars are grouped by DPR, and the data for each genotype is repeated for each DPR expressed, so each bar appears twice.

The less vigorous tapping assay resulted in fewer seizures across all genotypes compared to when vortexed (Figure 5.4), suggesting that there is a threshold of mechanical agitation required to elicit a seizure. The genotypes previously observed seizing in response to the SING assay replicated the preliminary findings in the tapping assay. In addition, upon vortexing, seizures were seen in GR1000/GFP flies, and to a lesser degree AP1000/GFP and GA1000/GFP (Figure 5.4 B). It can therefore be surmised that GR1000, AP1000, and GA1000 expressing flies have a higher threshold for seizures than some of the combinations, but nonetheless have a level of neuronal dysfunction sufficient to produce seizures. The most severely affected flies were those expressing AP1000 and GR1000, GA1000 and GR1000, and PR1000 and GR1000 in combination (Figure 5.4 B). Of the flies tested, just over 50% AP1000/GR1000 flies, and around 75% PR1000/GR1000 and GA1000/GR1000 flies had seizures upon vortexing. Of all the genotypes, GA1000/GR1000 showed the biggest increase in the proportion seizing between the tapping stimulus and the vortexing stimulus; only around 20% had seizures upon tapping, compared to 75% upon vortexing. Among the other genotypes, there were some seizures observed, but only the aforementioned combinations proved significant compared to the DPR/GFP (Figure 5.4 B). Although one could argue that any seizure is significant because it is not a physiological response and is indicative of an underlying neurological problem - GFP-expressing flies do not exhibit seizure phenotypes when subjected to the same mechanical agitation (Figure 5.6).

GR1000 appears to be the biggest potentiator of seizures in these models. Whilst AP1000/GR1000 expressing flies had significantly more seizures upon vortexing than AP1000/GFP expressing flies ($p < 0.001$), this was not significant compared to GR1000/GFP, indicating that AP1000 expression did not significantly worsen the seizure response in GR1000 expressing flies (Figure 5.4 B). However, under a lesser stimulus, AP1000/GR1000 flies had a similar response to when vortexed, with around a third seizing, whereas GR1000/GFP flies had no seizures at all (Figure 5.4 A). This suggests that AP1000 may lower the threshold for seizures in GR1000 expressing flies. Combining PR1000 and the alanine-positive DPRs did elicit seizures but the proportion of flies that had seizures was not significant compared to DPRs alone (Figure 5.4 B). In fact, PR1000 was the only DPR to cause no seizures when expressed with just GFP.

In addition to scoring the flies on a “seizure” or “no seizure” basis, the time to recovery was also measure, which provides another readout for seizure susceptibility[299]. Some genotypes had very few incidences of seizures, and therefore were excluded from this analysis. The threshold for inclusion was > 20% flies with seizures. Figure 5.5 shows the time taken from seizure onset to recovery – that is, when the fly has regained control of its legs and can stand and walk. Most commonly, recovery times between 10 and 50

seconds were observed, but some longer seizures did occur, particularly in AP1000/GR1000 and GA1000/GR1000 expressing flies (Figure 5.5). However, this could be in part due to the greater number of flies that seizure and therefore a larger sample and an increased chance of observing a longer seizure. Overall, there was no significant difference in the recovery time between genotypes. As seizures are not completely penetrant, the proportion of flies that seizure seems a more robust method of scoring seizures in this context.

It is possible that the more subtle phenotypes here would become significant if the number of flies tested was greater, and that by testing relatively low numbers we are missing key differences between genotypes. However, it is clear from this data that expressing different combinations of DPRs together produces different effects compared to each DPR alone, hinting that they may interact to exacerbate existing dysfunction by acting synergistically via different mechanisms, or by acting together in the same pathway. Therefore, the logical next step was to investigate what pathways are underlying each of the DPR's toxicity in relation to seizure susceptibility, and whether this would explain the differences observed between DPRs in combination.

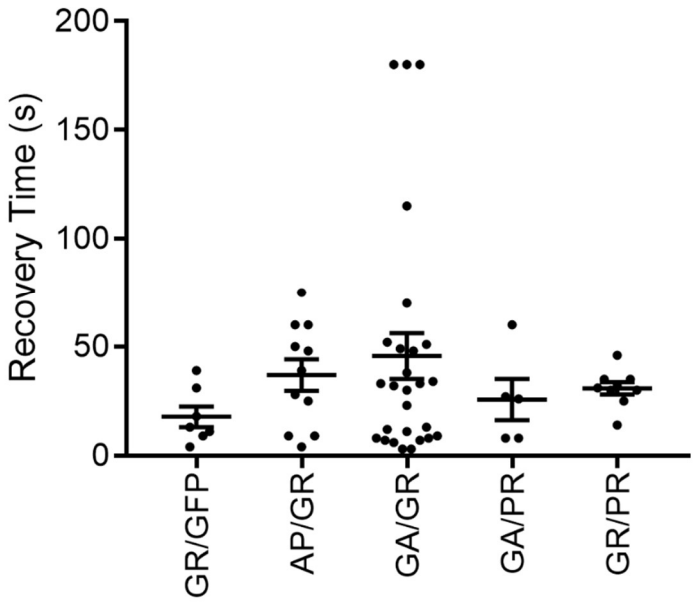

Figure 5.5 Time to recovery in BS DPR combinations.

Recovery time from bang-sensitive seizures in flies co-expressing DPRs at 14 days post-eclosion. Flies were vortexed for 10s and filmed. The time taken to recover completely, right themselves and walk, was measured. Only flies that showed seizures are included, and only genotypes were 20% or more flies had seizures. Error bars = SEM.

5.2.4 Dominant genetic modifier screen identifies potential pathways implicated in DPR-mediated seizure susceptibility

In addition to the well-characterised classical *Drosophila* BS mutants, including *bang-sensitive* (*bas*), *bang-senseless* (*bss*), *slam dance* (*sda*) and *easily shocked* (*eas*), there are a number of other mutants which have been shown to increase seizure susceptibility. The aforementioned mutants, most commonly used in epilepsy research, are dominant and completely penetrant[297]. For this investigation, the aim was to ascertain whether mutations in genes that confer increased seizure susceptibility but not elicit seizures when heterozygous could worsen, or cause, seizures in DPR expressing flies. Therefore, a fully penetrant BS mutant would not be appropriate. However, we cannot rule out the contribution of perturbations to these pathways as contributing to the observed phenotypes. Instead, mutants which exhibited seizures only when homozygous or combined with other mutant alleles were crossed into a DPR background, to see how defects in different pathways would affect seizure responses. Where possible two alleles for each gene were used, so that a total of 11 mutant alleles encompassing 7 different genes were tested. A list of the seizure mutants used and their gene products is shown in Table 5.1. These were chosen from a list of all commercially available recessive BS mutants with an orthologue in humans and links to neurodegenerative disease or neurological function.

First, a new baseline of seizure frequency was established with each DPR expressed alone (Figure 5.6). A titration control for *Gal4* expression was not required because the screen was using endogenous mutants rather than overexpression with *UAS*. However, the proportion of flies that showed seizures was similar (Figure 5.6). Expression of GR1000 caused a significant number of seizures (Chi-square, $p < 0.01$) compared to age-matched GFP controls. Next, the seizure susceptibility of flies pan-neuronally expressing each DPR alone was compared to the seizure susceptibility when mutant alleles were added into the background.

Table 5.1 Seizure mutants used in this investigation

Mutant	Gene product	Human orthologue	Pathway
Sod2^{n283} *Sod2^{KG06854}*	superoxide dismutase 2 (Mn)	superoxide dismutase 2 (Mn)	superoxide radical detoxification
kdn^{KG04873}	citrate synthase	citrate synthase	metabolism
Syn^{97}	synapsin	synapsin 3	synaptic vesicle
β4GalNAcTA$^{4.1}$	acetylglucosaminyl-transferase	β-1,4-galactosyl transferase 2	glycolipid biosynthesis, neuromuscular junction development
stai^{B200} *stai^{irdtp}*	stathmin	stathmin 3	tubulin binding protein, axon transport, synaptic growth
Sirup^{1} *Sirup^{2}*	Starvation-upregulated protein	succinate dehydrogenase complex assembly factor 4	tricarboxylic cycle, electron transport chain
kcc$^{P20-180}$ *kcc^{Ad-4}*	kazachoc	Solute Carrier Family 12 Member 4	potassium:chloride symporter

5.2.4.1 Partial loss of the K+/Cl− transporter *kazachoc* increases seizure susceptibility in PR1000 flies

The *kazachoc* (*kcc*) gene encodes the sole *Drosophila* K^+/Cl^- transporter, orthologous to mammalian SLC12A4. Reduced expression of a murine potassium chloride cotransporter has been shown to contribute to selective motor deficits and disease progression in a mouse model of ALS[305,306]. In *Drosophila,* partial loss of *kcc* causes bang-sensitive seizures, which are attributed to disruption of Cl^- gradients and signalling via the $GABA_A$ receptor. The two alleles used in this study were generated using ethyl methanesulfonate (EMS) but not molecularly mapped. The null *kcc^{Ad-4}* allele is reported to confer a greater degree of seizure susceptibility than the slightly weaker *kcc$^{P20-180}$* allele [307,308]. A threefold and 1.6 fold reduction in protein is associated with these alleles respectively[307]. In this investigation, the results did not follow the expected pattern (Figure 5.7). Heterozygous *kcc$^{P20-180}$* is not reported to produce seizures in response to

vortexing, but in the GFP controls, around 10% of flies show seizure behaviour. When combined with AP1000, neither allele increase seizure susceptibility, although the number of flies tested for AP1000 with $kcc^{P20\text{-}180}$ is low. In contrast, both alleles increased the seizure susceptibility of flies expressing GA1000; GA1000 alone produced no BS seizures, but this was increased to around 20% in a *kcc* mutant background (Figure 5.7). PR1000 expressing flies, which also do not display BS seizures, were the most strongly affected by $kcc^{Ad\text{-}4}$, but not $kcc^{P20\text{-}180}$ mutations (although again the number tested was fairly low). Over half of flies expressing PR1000 with the $kcc^{Ad\text{-}4}$ mutation had a seizure upon vortexing, and this was the only significant result in the entire screen ($p < 0.05$). As shown previously, pan-neuronal expression of GR1000 confers a degree of BS seizure susceptibility alone (Figure 5.6), and this was not significantly affected by *kcc* mutations. However, there was a slight increase in the proportion of flies seizing with the $kcc^{Ad\text{-}4}$ mutation and a decrease with $kcc^{P20\text{-}180}$, which contrasts what is seen with the GFP control. Whilst this assay is potentially underpowered, resulting in a lack of statistical significance, it identifies *kcc* as a potential modifier, elucidating pathways for further investigation. Given that kcc transporters have been implicated in ALS[305,306] and other neurodegenerative conditions such as HD[309], it is a promising avenue for future research.

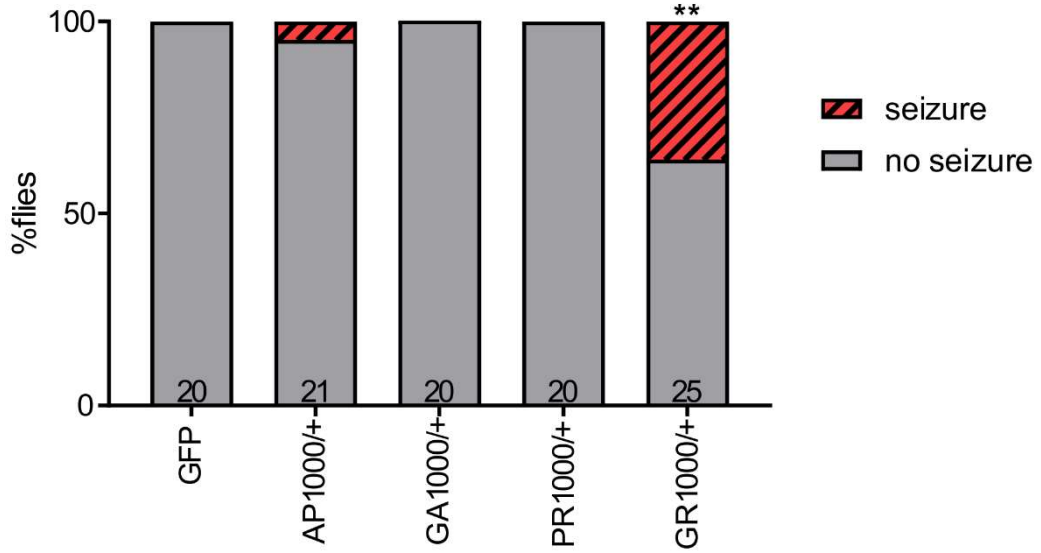

Figure 5.6 Pan-neuronal expression of GR1000 causes bang-sensitive seizures.
Flies expressing one copy of the DPR transgene under the control of *nSyb-Gal4* (II) (*nSyb-Gal4/+*) were vortexed for 10 s at 14 days post-eclosion, filmed, and scored as "seizure" or "no seizure". The percentage of flies that had seizures is shown, and the number of flies tested is show inside each bar. ** $p < 0.01$ (Chi-square, df = 1, with Bonferroni correction for 2 comparisons – see Appendix 6).

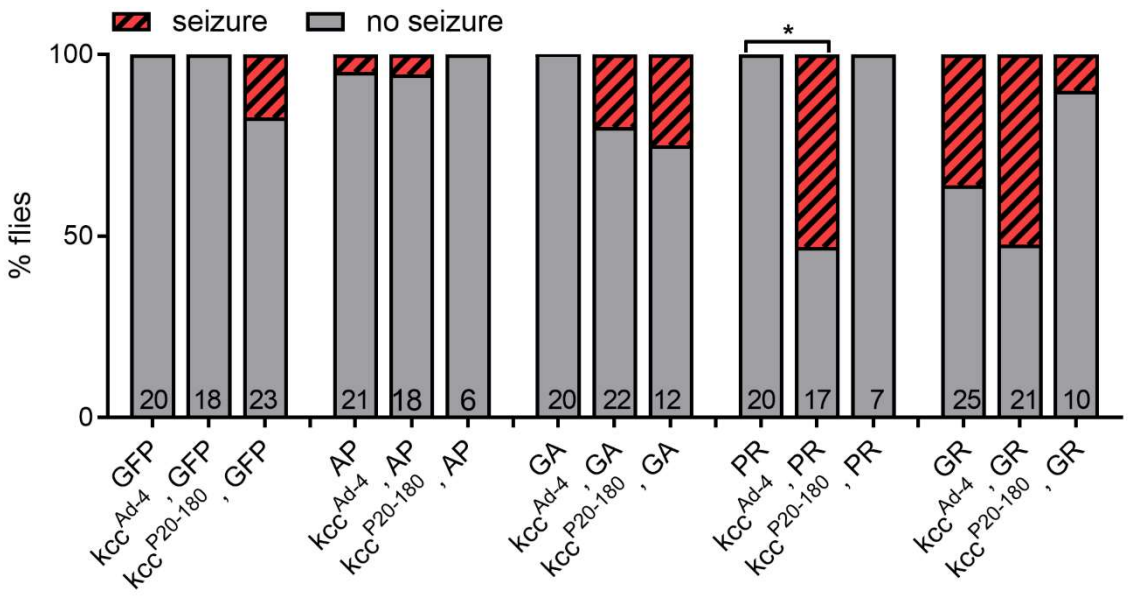

Figure 5.7 The effect of partial loss of *kcc* on seizure susceptibility in DPR flies.
Flies expressing one copy of each DPR under the control of a single copy of the pan-neuronal driver *nSyb-Gal4* (II) (*nSyb-Gal4/+*) with heterozygous *kcc* mutations ($kcc^{Ad\text{-}4}$/+, $kcc^{P20\text{-}180}$/+) were vortexed for 10 s at 14 days post-eclosion, filmed, and scored as "seizure" or "no seizure". The percentage of flies that had seizures is shown, and the number of flies tested is show inside each bar. DPR1000 abbreviated to DPR for clarity. Pairwise comparisons of % bang-sensitive seizures using a post-hoc chi-square test, Bonferroni corrected *p* value ($p = 0.0002$) for 10 comparisons: * $p < 0.05$.

5.2.4.2 Partial loss of the superoxide dismutase, *Sod2*, increases seizure susceptibility in PR1000 flies

Superoxide dismutase (Mn) 2 (Sod2) is closely related to the pathological protein found in aggregates in 2% of ALS cases, SOD1. The main difference is that SOD1 uses Cu/Zn rather than Mn for catalysing the disproportionation reaction of superoxide radicals. Mutations in *Sod2* have been shown to generate oxidative stress that results in reduced activity of critical mitochondrial enzymes. $Sod2^{n283}$ is a loss of function allele generated by the imprecise excision of a P-element (KG06854) which resides in the $Sod2^{KG06854}$ allele, sometimes referred to as $Sod2^{wk\ 310}$. Trans-heterozygous flies with both the null $Sod2^{n283}$ and the hypomorphic $Sod2^{wk}$ have been shown to exhibit increased oxidative stress and bang-sensitivity[311]. In this experiment, a very small proportion of flies with either *Sod2* allele and GFP expressed had seizures upon vortexing (Figure 5.8). Similarly, there was little effect of *Sod2* mutations on AP1000 or GA1000 expressing flies in terms of seizure susceptibility. With GR1000 expression, there is small increase in the proportion of flies with seizures when $Sod2^{wk}$ is present. $Sod2^{n283}$ mutations appear to slightly rescue GR1000 toxicity, but this was insignificant (Figure 5.8). Therefore, the

effect of *Sod2* mutations on GR1000 toxicity was inconclusive. The effect of *Sod2* mutations on PR1000 expressing flies was easier to interpret because PR1000 alone does not cause seizures in this experimental context. *Sod2*^{KG06854} mutations, and to a lesser extent *Sod2*^{n283} mutations, caused some PR1000 expressing flies to have seizures (Figure 5.8). Once again, these differences did not reach statistical significance due to the high number of groups and therefore comparisons. Despite this, 25% of flies had seizures when pan-neuronally expressing PR1000 in a *Sod2*^{KG06854} mutant background, compared to around 5% of GFP flies with *Sod2*^{KG06854} mutations. This suggests that SOD2 and oxidative stress in general could be an area for further investigation.

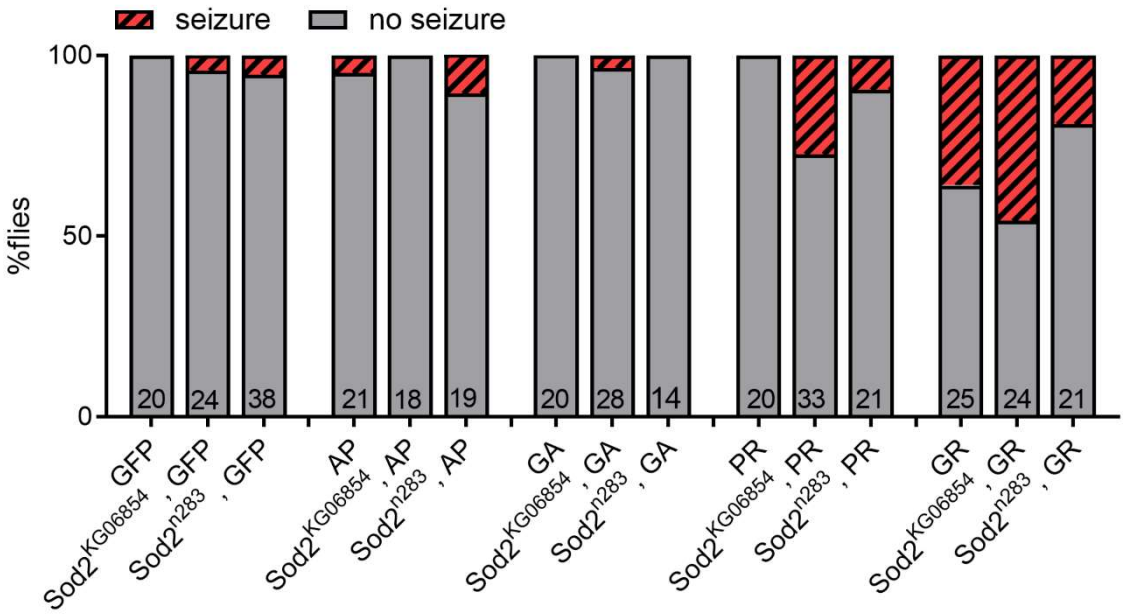

Figure 5.8 The effect of partial loss of *Sod2* on seizure susceptibility in DPR flies.
Flies expressing one copy of each DPR under the control of a single copy of the pan-neuronal driver *nSyb-Gal4* (II) (*nSyb-Gal4*/+) with heterozygous *Sod2* mutations (*Sod2*^{KG06854}/+, *Sod2*^{n283}/+) were vortexed for 10 s at 14 days post-eclosion, filmed, and scored as “seizure” or “no seizure”. The percentage of flies that had seizures is shown, and the number of flies tested is show inside each bar. DPR1000 abbreviated to DPR for clarity. The percentage of flies that had seizures is shown, and the number of flies tested is show inside each bar. Pairwise comparisons of % bang-sensitive seizures using a post-hoc chi-square test, Bonferroni corrected *p* values were not significant.

5.2.4.3 Partial loss of microtubule binding protein *Stathmin* increases seizure susceptibility of control and DPR flies, apart from PR1000

Stathmin is a microtubule-binding protein that regulates microtubule dynamics and plays an important role in axonal transport, NMJ stability, and signal integration[312]. Axonal transport defects are a common feature of ALS and have been demonstrated in different genetic *Drosophila* models[139]. Unlike in vertebrates, the Stathmin protein, which has two isoforms A and B, is encoded by a single gene, *stai,* in fly. This circumvents complications in genetic studies caused by functional compensation by other members of the *stai* family. The *stai*^{rdtp} allele used in this study was first identified from a genetic screen for recessive mutations based on a posterior paralysis of third instar larvae. Subsequently, it was characterised as a copia retrotransposon insertion, a spontaneous mutation. The *stai*^{rdtp} allele is associated with an 88% and 60% reduction in *staiA* and *staiB* transcript levels, respectively[313]. The null allele, *stai*^{B200} reduces transcripts to undetectable levels[313]. Both mutants show an age-dependent progressive bang-sensitive phenotype, with first seizures observed in homozygous *stai*^{B200} animals at 21 days post-eclosion, and heterozygous *stai*^{B200} and *stai*^{rdtp} mutants at 42 days post-eclosion[313]. In this investigation, a small number of flies pan-neuronally expressing GFP and carrying one copy of either *stai*^{B200} or *stai*^{rdtp} did display seizure behaviour, despite being aged to only 14 days post-eclosion, contrary to previous reports[313] (Figure 5.9). The most striking finding was that *stai* mutations appeared to have no effect on the seizure susceptibility of PR1000 expressing flies. Indeed, despite GFP, AP1000, GA1000, and GR1000 flies all showing a similar pattern of a greater number of flies displaying seizure behaviour when expressed in a *stai*^{B200} mutant background, no seizures were observed in *stai*^{B200} mutants expressing PR1000. The most severe combination was the pan-neuronal expression of GR1000 with a *stai*^{B200} mutation background, which resulted in ~ 65% of flies having a seizure upon vortexing (Figure 5.9).

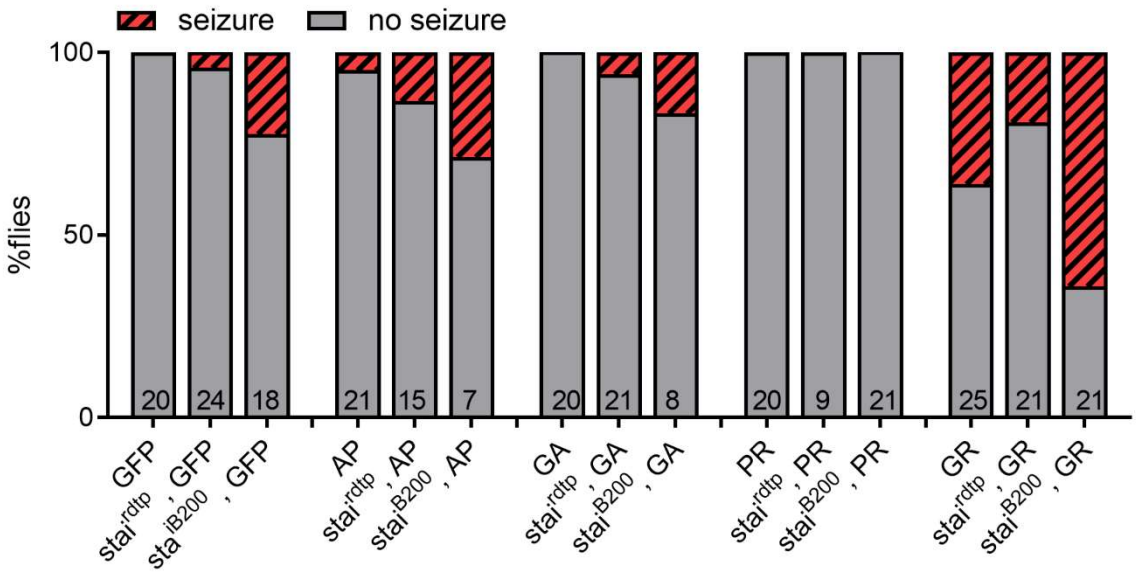

Figure 5.9 The effect of partial loss of *stai* on seizure susceptibility in DPR flies.
Flies expressing one copy of each DPR under the control of a single copy of the pan-neuronal driver *nSyb-Gal4* (II) (*nSyb-Gal4/+*) with heterozygous *stai* mutations (*stai*^{rdtp}/+, *stai*^{B200}) were vortexed for 10 s at 14 days post-eclosion, filmed, and scored as "seizure" or "no seizure". The percentage of flies that had seizures is shown, and the number of flies tested is show inside each bar. DPR1000 abbreviated to DPR for clarity. The percentage of flies that had seizures is shown, and the number of flies tested is show inside each bar. Pairwise comparisons of % bang-sensitive seizures using a post-hoc chi-square test, Bonferroni corrected *p* values were not significant.

5.2.4.4 Heterozygous mutations in succinate dehydrogenase assembly factor, *Sirup*, has no effect on seizure susceptibility of DPR flies

Sirup encodes a succinate dehydrogenase assembly factor which plays a key role in linking the electron transport chain in mitochondria with the tricarboxylic cycle[314]. Succinate dehydrogenase assembly factor 4 (SDHAF 4) has been shown to promote mitochondrial function and prevent neurodegeneration in *Drosophila* and mammalian cells[314]. The loss of function mutants, *sirup*^{1} and *sirup*^{2}, show neurodegenerative phenotypes when homozygous or trans-heterozygous and sensitivity to oxidative stress, as well as a significant bang-sensitive paralysis from 1-4 days post-eclosion[314]. *Sirup* mutations do not appear to have a large effect on the seizure susceptibility of DPR expressing flies (Figure 5.10). A small number of seizures were seen across GFP, AP1000, GA1000, and PR1000 expressing flies with *Sirup* mutations, but inconsistently between equivalent mutations. The proportion of flies expressing GR1000 with either *sirup*^{1} or *sirup*^{2} mutations that were observed to seizure varied; whilst *sirup*^{1} mutations appear to slightly reduce the frequency of seizures, *sirup*^{2} mutations seemed to increase

the frequency (Figure 5.1). However, the average of the two equivalent mutations shows negligible difference to flies expressing GR1000 alone. The relatively small number of flies tested is a key limitation of this experiment, and therefore only the biggest changes are considered noteworthy. Seizures observed in flies expressing both DPRs and carrying a mutant allele were not paralytic in nature, rather the classic muscle-spasms as observed originally in the DPR combinations, suggesting that the predominant driver of seizures in these flies was the toxicity caused by DPR expression, rather than a reduction in Sirup function.

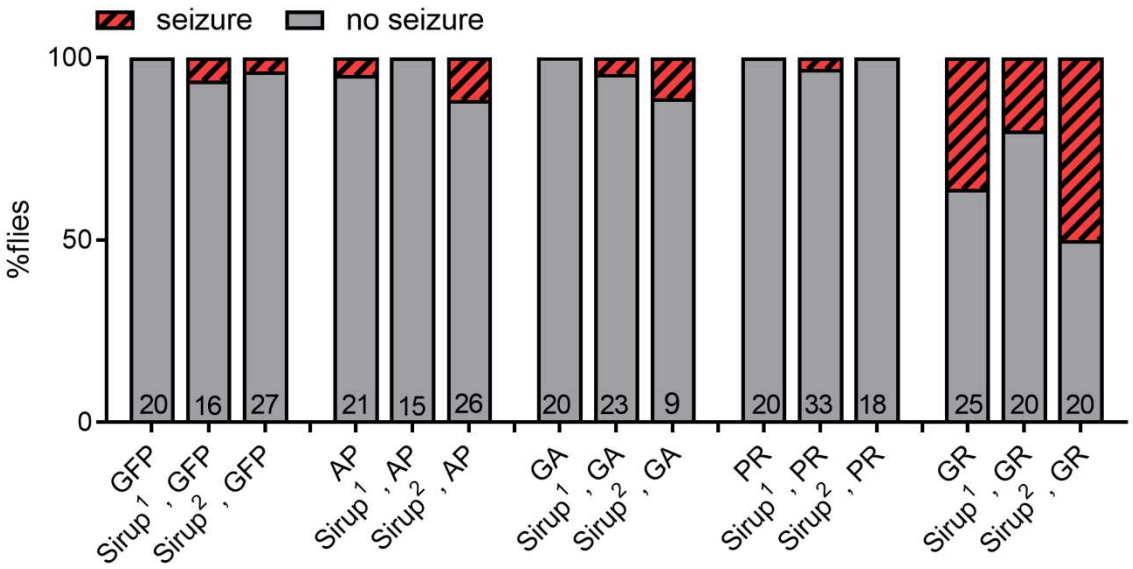

Figure 5.10 The effect of partial loss of *Sirup* on seizure susceptibility in DPR flies.
Flies expressing one copy of each DPR under the control of a single copy of the pan-neuronal driver *nSyb-Gal4* (II) (*nSyb-Gal4/+*) with heterozygous *Sirup* mutations (*Sirup^{1}/+, Sirup^{2}/+*) were vortexed for 10 s at 14 days post-eclosion, filmed, and scored as “seizure” or “no seizure”. The percentage of flies that had seizures is shown, and the number of flies tested is show inside each bar. DPR1000 abbreviated to DPR for clarity. The percentage of flies that had seizures is shown, and the number of flies tested is show inside each bar. Pairwise comparisons of % bang-sensitive seizures using a post-hoc chi-square test, Bonferroni corrected *p* values were not significant.

5.2.4.5 A reduction in *β1,4-N-acetylgalactosaminyltransferase* expression has no effect on seizure susceptibility in DPR flies or controls

β4GalNAcTA encodes a β1,4-N-acetylgalactosaminyltransferase, homologous to mammalian β1,4-galactosyltransferase. The only difference is the transfer of N-acetylgalactosamine rather than galactose[315,316]. The *β4GalNAcTA$^{4.1}$* allele contains a deletion in the *β4GalNAcTA* gene caused by imprecise excision of a P element, which renders it unable to make crucial contacts with its substrate. Therefore, it is considered a null mutant[316]. Homozygous *β4GalNAcTA$^{4.1}$* mutants show bang-sensitive

incoordination and it is postulated that this is caused by defects in synaptic vesicle dynamics resulting from loss of the *β4GalNAcTA* gene[316]. Expression of DPRs in a *β4GalNAcTA*$^{4.1}$ mutant background resulted in no change in the proportion of flies that displayed seizure behaviour compared to the DPRs expressed alone (Figure 5.11). This suggests that a reduction in β4GalNAcTA function does not exacerbate DPR-mediated toxicity. Heterozygous *β4GalNAcTA*$^{4.1}$ mutants do not display overt behavioural deficits, and there are two β1,4-N-acetylgalactosaminyltransferases in fly[20,316]. Therefore, it is likely that the reduction in function caused by one null allele is compensated for by the other. Nevertheless, this screen was designed to identify dominant modifiers, indicating an important pathway for further investigation, and the data suggest that *β4GalNAcTA* does not play a key role in DPR-mediated seizures.

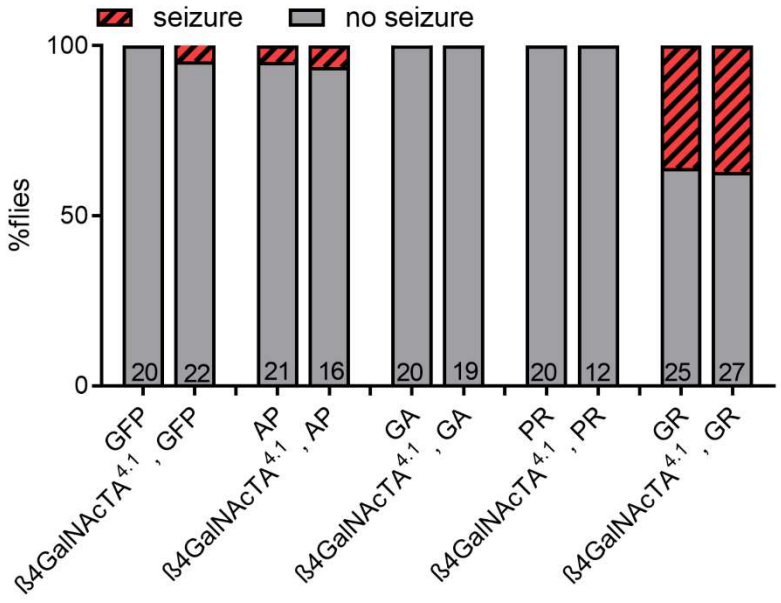

Figure 5.11 The effect of partial loss of *β4GalNAcTA* on seizure susceptibility in DPR flies.

Flies expressing one copy of each DPR under the control of a single copy of the pan-neuronal driver *nSyb-Gal4* (II) (*nSyb-Gal4/+*) with heterozygous *β4GalNAcTA*$^{4.1}$ mutation (*β4GalNAcTA*$^{4.1}$*/+*) were vortexed for 10 s at 14 days post-eclosion, filmed, and scored as "seizure" or "no seizure". The percentage of flies that had seizures is shown, and the number of flies tested is show inside each bar. DPR1000 abbreviated to DPR for clarity. The percentage of flies that had seizures is shown, and the number of flies tested is show inside each bar. Pairwise comparisons of % bang-sensitive seizures using a post-hoc chi-square test, Bonferroni corrected *p* values were not significant.

5.2.4.6 Partial loss of synaptic vesicle-associated protein *Synapsin* does not appear to increase seizure susceptibility selectively in DPR flies

Synapsin (*Syn*) encodes a phosphoprotein associated with synaptic vesicles, required for short-term learning and olfactory habituation, and important for synaptic bouton outgrowth at the larval NMJ[317]. Human *Synapsin* mutations have been linked with AD, epilepsy, and multiple sclerosis[318], and a reduction in synapsin II has been shown ina mouse model of ALS caused by *SOD1* mutations[319]. A loss of function allele, Syn^{97}, was created by the imprecise excision of a P element insertion, deleting a large region of the promoter and the first exon[320]. Homozygous Syn^{97} flies have impaired recovery from mechanical agitation by vortexing compared to wild type flies[321]. A single copy of the mutant *Syn* allele was associated with a ~ 5% increase in the number of seizures in GFP, AP1000 and GA1000 flies, and a ~ 5% reduction in seizures in GR1000 flies (Figure 5.12). In flies expressing PR1000, the *Syn* mutation is associated with a slightly larger ~ 10% increase in the number of seizures, from a baseline of 0. However, with the number of flies tested relatively low, these small changes do not point to potentiation of a specific pathological pathway, especially because GFP flies have a similar increase in seizure susceptibility (Figure 5.12).

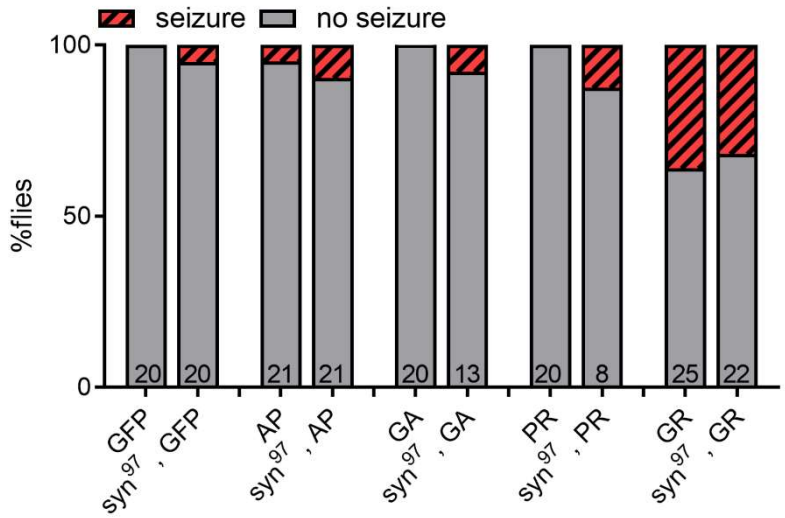

Figure 5.12 The effect of partial loss of *Syn* on seizure susceptibility in DPR flies.
Flies expressing one copy of each DPR under the control of a single copy of the pan-neuronal driver *nSyb-Gal4* (II) (*nSyb-Gal4/+*) with heterozygous Syn^{97} mutation (Syn^{97}/+) were vortexed for 10 s at 14 days post-eclosion, filmed, and scored as “seizure” or “no seizure. The percentage of flies that had seizures is shown, and the number of flies tested is show inside each bar. DPR1000 abbreviated to DPR for clarity. The percentage of flies that had seizures is shown, and the number of flies tested is show inside each bar. Pairwise comparisons of % bang-sensitive seizures using a post-hoc chi-square test, Bonferroni corrected *p* values were not significant.

5.2.4.7 Partial loss of mitochondrial citrate synthase, *knockdown*, has no effect on seizure susceptibility in DPR flies

Drosophila knockdown (*kdn*) is orthologous to mammalian citrate synthase, and plays a key role in carbohydrate metabolism and the tricarboxylic acid cycle, where it catalyses the conversion of acetyl-CoA and oxaloacetate to citrate. It is involved in regulating neuronal activity and its loss causes bang-sensitivity. Although citrate synthase specifically has not been implicated in FTD or ALS, mitochondrial dysfunction, strongly linked to citrate synthase activity, has been implicated in multiple neurodegenerative conditions, in particular PD[322]. The *kdn* gene is located on the X chromosome, and its loss is recessive lethal[323]. The $kdn^{KG04873}$ mutation is a large P element insertion, that, when homozygous, causes incompletely penetrant bang-sensitive paralysis[323]. A more severe phenotype is seen in $kdn^{KG04873}$ combined with an allele carrying a deletion in the corresponding chromosome region, suggesting that $kdn^{KG04873}$ is not a complete null[323]. In combination with pan-neuronal expression of GFP or DPRs, it has inconsistent effects (Figure 5.13). GFP flies with one copy of the mutant allele show a ~ 20% increase in seizure frequency from a baseline of 0%, whilst with PR1000 and GR1000 expression, the *kdn* mutation appears to have no effect. A slight increase in the number of seizures

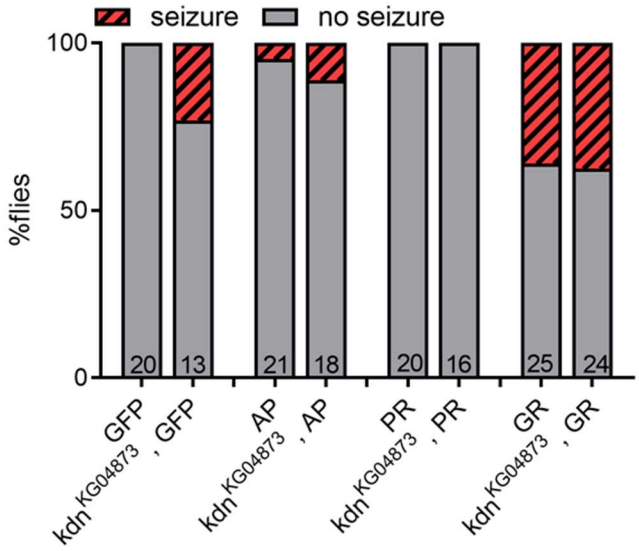

Figure 5.13 The effect of partial loss of *kdn* on seizure susceptibility in DPR flies.
Flies expressing one copy of each DPR under the control of a single copy of the pan-neuronal driver *nSyb-Gal4* (II) (*nSyb-Gal4/+*) with a heterozygous $kdn^{KG04873}$ mutation ($kdn^{KG04873}$/+) were vortexed for 10 s at 14 days post-eclosion, filmed, and scored as “seizure” or “no seizure”. The percentage of flies that had seizures is shown, and the number of flies tested is show inside each bar. DPR1000 abbreviated to DPR for clarity. The percentage of flies that had seizures is shown, and the number of flies tested is show inside each bar. Pairwise comparisons of % bang-sensitive seizures using a post-hoc chi-square test, Bonferroni corrected *p* values were not significant.

observed in AP1000 expressing flies is seen with *kdn*^{KG04873} but this is insignificant (Figure 5.13).

5.3 Discussion

5.3.1 Co-expressing DPRs in different tissues in *Drosophila* produces different patterns of toxicity

Whilst we know that in *C9orf72*-FTD/ALS patients, there is the potential for all DPRs to be present in the same cell, there is relatively little research into the interactions between the DPRs, or how multiple DPRs impact cellular health and function. Pure repeat models are useful for examining the combinatorial effect of repeat RNA and all DPRs, but given the evidence pointing to DPRs as the main toxic species, there is a lack of research into specific DPR-DPR interactions *in vivo*, likely due to the high levels of toxicity preventing more than one DPR being expressed at once. Therefore, we may be missing key phenotypes and mechanisms that only occur when DPRs are present in the same cell and able to directly or indirectly interact with each other; co-expression of two or more DPRs may alter the phenotypic profile either by physically interacting and altering their properties, or by acting through two toxic pathways in parallel.

Evidence from patient tissue and *in vitro* studies has hinted at the importance of interactions between DPRs. The main focus of previous studies has been GA and its role in sequestering the other DPR species. GA and GR have been shown to co-aggregate in Neuro2A cells[293], and GA50 ameliorated PR50-associated toxicity in mouse primary neurons[294]. Biophysical interactions between the arginine-rich DPRs and cellular components, particularly those with LCDs, have been well-documented[74,164]. However, less is known about the biophysical interactions between DPRs. One study looked at the interaction of PR20 and GA20 peptides and studied their biophysical properties using circular dichroism spectroscopy. They found that not only did PR20 interact specifically with GA20, but that the resulting aggregate was intrinsically disordered and GA's β-sheet structure was lost[294]. Taken together, this suggests that the propensity of GA to lose its rigid β-sheet structure and sequester arginine-rich DPRs could be responsible for the ameliorative effect of co-expressing GA with PR and GR. This is corroborated by the only *in vivo* study into DPR-DPR interactions before this investigation: this group used the large and easily accessible salivary glands to examine subcellular localisation of GR80 and GA80, and found that the GA80 appeared to recruit GR80 into cytoplasmic inclusions, whilst GR80 expressed alone localised in a diffuse pattern in the cytoplasm[193]. Concomitant expression of GA80 with GR80 also reduced toxicity when expressed in the wing discs using *Vg-Gal4.* In this study, the Notch pathway was implicated in GR toxicity,

as over expression of Notch partially suppresses toxicity[193]. However, the wing is not necessarily the most pathologically relevant tissue in which to study FTD/ALS and the authors urge cautious interpretation. Taken together, evidence so far suggests that there is the potential for DPR-DPR interactions to play an important role in their toxicity. Therefore, it was imperative to examine how DPRs of a pathologically relevant repeat length interact *in vivo*.

In this investigation, we made use of the robust screening potential of the eye to investigate DPR-DPR interactions. The results did not corroborate the aforementioned *Drosophila* study, but revealed some interaction between DPRs, exacerbating the phenotypes caused by expression of each DPR individually. However, by far the greatest toxicity was conferred by homozygous expression of the DPRs, apart from GA1000, which showed no phenotype (Figure 5.1 A). This implies that each DPR is affecting different downstream pathways – it is likely that the total amount of DPR would be similar in flies expressing two of the same DPR vs two different DPRs, and yet the toxicity conferred by two copies of the same DPR appears to be much greater. We can also surmise that the reason homozygous expression is more toxic than a single copy being expressed is not simply due to an increased DPR load overwhelming the proteasome or other degradation routes; if this was the case, then we would expect co-expression of two different DPRs to produce the same levels of toxicity. Whilst the majority of flies expressing combinations of the DPRs had wild type eyes, some combinations, in particular PR1000/GR1000, produced a small number of flies with severely perturbed eyes. The protective effect of GA was not seen in this experiment, but there was little toxicity to rescue in this case, as the expression of a single DPR did not cause a phenotype. This could be due to the levels of DPR produced by expression of only one copy are insufficient to cause toxicity, and so any interactions are occurring at too low a level to produce a visible phenotype. Alternatively, as the eye phenotype has a developmental basis, subtle long-term effects of DPR expression are unlikely to be detected. Therefore, expression in a functional system where the effect of concomitant DPR expression can be assessed over the lifespan is a more relevant model.

In order to assess the effect of combining DPRs in a physiologically relevant system, pairs of DPRs were expressed pan-neuronally. Firstly, the effect of dose on pan-neuronal DPR1000 expression was measured. Homozygous pan-neuronal expression of PR1000 and GR1000 were the most severe, proving lethal at an early larval stage; homozygous AP1000 expression produced a significantly reduced climbing speed compared to expression of one copy; homozygous GA1000 expression produced no difference in climbing speed compared to expression of one copy (Figure 5.2). This is consistent with results from the eye screen, and confirms a dose-dependent toxicity in GR1000,

PR1000, and AP1000. However, whilst co-expression of different DPRs in the eye did not produce dramatic phenotypes, pan-neuronal co-expression of certain combinations proved severely toxic compared to one DPR alone, and in some cases (AP1000 and GA1000) was more toxic than homozygous expression. The results revealed a pattern of toxicity distinct between alanine- and arginine-rich DPRs. For example, the exclusively alanine-positive/alanine-positive combination, AP1000/GA1000, was the only combination not to show a significant decline between 7 and 28 days post-eclosion (Figure 5.3). This corroborates the pattern from the previous climbing assay, where both GA1000 and AP1000 expressing flies had a reduced speed at 7 days post-eclosion, but this did not decline with age (Figure 4.2). The finding that GR1000 exerts the greatest toxicity across all the combinations is consistent with previous studies that have measured GR toxicity in various systems[74,137,193,213]. GA1000/GR1000 and AP1000/GR1000 expressing flies displayed a significant reduction in climbing speed compared to age matched controls (Figure 5.3), and AP1000/GR1000 expression proves lethal before 28 days post-eclosion. This is consistent with previous experiments where AP1000 confers a greater toxicity than GA1000 in terms of motor-function (Figure 4.2). Expression of both arginine-rich DPRs (PR1000/GR1000) did cause a reduction in climbing speed, but only at 28 days post-eclosion (Figure 5.3 D). This is consistent with the idea that in this model, PR1000 and GR1000 toxicity is age-dependent. However, it is not as simple as the sum of their individual toxicity because whilst PR1000 and GR1000 are lethal in homozygosity, the combination of the two is no more toxic than the combination of GR1000 with either GA1000 or AP1000. This could be due to PR1000 and GR1000 affecting different cellular pathways that do not interact to exacerbate the phenotype. Indeed, PR1000-expressing flies show the same drop off in climbing speed between 7 and 28 days post-eclosion regardless of the DPR it is paired with (Figure 5.3 C). This is in contrast to GR1000-positive combinations which have different patterns of climbing deficits (Figure 5.3 D). Accurately quantifying the levels of DPR in the fly brain has so far proved impossible, and so although we know there isn't difference between DPRs in terms of RNA expression[207], there could be different protein levels due to differential degradation which may affect how they interact. Indeed, the western blots and fluorescence levels in the brain suggest that there is less PR and GR. This could be due to a depletion in arginine within the cell. Arginine is known to be a conditionally essential amino acid, which means it can be synthesised by the cell but under conditions of stress this is unable to continue[324].

The lack of reliable DPR antibodies hindered reliable investigation of co-localisation or changes in morphology of the DPRs *in vivo*. It would be interesting to see if previous assertions that GA sequesters GR and PR held true at 1000 repeats. The results from functional interaction studies suggest that the DPRs interact differently at 1000 repeats,

but this could be due to the difference in baseline toxicity between the 1000 repeat DPRs (see chapters 3 and 4) and previously reported models. In future, generating flies expressing alternatively tagged DPR1000 constructs would allow the study of subcellular localisation and morphology of co-expressed DPRs.

5.3.2 A novel seizure phenotype in DPR models of *C9orf72*-FTD/ALS

The incompletely penetrant seizure phenotype observed in flies co-expressing different combinations of DPRs implicates DPRs in seizure susceptibility in *C9orf72*-FTD/ALS. This is the first report of seizures in a *C9orf72* model. However, reports suggest that seizures are associated with the *C9orf72* expansion[301,302,325]. Given this is the first *Drosophila* model expressing DPRs of a pathologically relevant repeat length, it is possible that the length of the DPRs is important in triggering seizures, and therefore previous models have been unable to recapitulate this particular feature.

There is a well-established link between seizures and neurodegenerative diseases. In particular, epilepsy is a relatively common comorbid condition with AD, with an incidence of between 8% and 20%[326]. A possible mechanism for this was linked to the toxic accumulation of amyloid beta in the hippocampus resulting in damage to neuronal structure triggering seizures, which caused further neuronal loss and therefore contributed to cognitive decline[327]. Furthermore, whilst most FTD patients do not have epilepsy[328], seizures have been reported in a small number of non-*C9orf72* cases, most of whom carry the heterozygous *MAPT* or homozygous *TREM2* gene mutations[329]. Studies into the relationship between epilepsy and dementias seizures have demonstrated that seizures may precede of coincide with the presentation of cognitive deficits[328]. Furthermore, riluzole, the only approved drug for ALS in the UK, is an anti-convulsant glutamate agonist which has modest clinical benefits[330].

Investigation into the frequency of seizures in *C9orf72*-FTD/ALS patients is still in its infancy, but there are several reports demonstrating a correlation between *C9orf72* expansions and cortical hyperexcitability[331]. Neuronal hyperexcitability refers to a condition in which the neuron is excessively and abnormally excitable, frequently reducing the threshold at which it will fire an action potential. The underlying cause of hyperexcitability is multifactorial, usually related to an imbalance of inhibitory and excitatory signalling at rest, often as a result of reduced inhibitory inputs from GABAergic interneurons, or altered potassium or sodium channel activity[332]. Hyperexcitability of the cortex, measured using transcranial magnetic stimulation (TMS), is present in generalised epilepsy and has been demonstrated to be an important biomarker of ALS[333]. TMS of sporadic and *C9orf72*-ALS patients has revealed a lowering of cortical

thresholds early in disease, leading to increased excitability, which generally declines as the disease progresses[334]. In contrast, in sporadic and *C9orf72*-FTD, cortical thresholds are generally normal[331,335], although cognitive impairment has been shown to correlate with cognitive impairment of ALS patients[336]. This has been suggested to be due to the specificity of TMS in detecting changes in excitability in the motor cortex, as opposed to temporal and motor areas[331]. Nevertheless, it indicated the heterogeneity in presentation of *C9orf72* expansions and suggests that, despite similarities in underlying pathology and symptoms, patterns of cortical hyperexcitability differ between *C9orf72*-related ALS and FTD.

Despite the lack of evidence pointing to cortical hyperexcitability in FTD, there are a number of reports of epileptiform seizures in *C9orf72* expansion carriers of different clinical presentations. A clinical study designed to ascertain the frequency of movement disorders in *C9orf72*-FTD/ALS patients found that seizures occurred in 4 of 17 patients[302]. Furthermore, detailed studies provide insights into individual cases. The first such report was of a 44 year old male who had experienced a generalised epileptic seizure years before he was referred to a neurological clinic for cognitive decline[325]. An abnormal electroencephalogram (EEG) recording with a slowed background pattern and photoparoxysmal response was recorded, consistent with photosensitive generalised seizures. It was subsequently discovered that he was carrying a pathogenic *C9orf72* repeat[325]. A second report included the case of a *C9orf72*-FTD/ALS with complex partial seizures concurrently with abnormal EEG recordings[301]. Another expansion carrier with bulbar-onset ALS, cognitive impairment, and abnormal EEG recordings developed tonic-clonic generalized epilepsy[301]. The correlation between *C9orf72* mutations and epilepsy is further supported by a case of teenage-onset progressive myoclonic epilepsy in an individual with the expansion[300]. The individual in question had epilepsy since the age of 15 and this progressed to multifocal myoclonus at the age of 18. Family history of epilepsy and dementia indicated an autosomal dominant inheritance pattern and this was confirmed to be due to a familial *C9orf72* repeat expansion. Post-mortem analysis confirmed the presence of p62-positive neuronal cytoplasmic inclusions[300].

Whilst the pathophysiological mechanisms underlying epilepsy in *C9orf72*-FTD/ALS remain unclear, evidence suggests it may be linked to an increase in cortical hyperexcitability. The precise mechanism through which this occurs remains unclear, but mechanisms posited to be responsible for neurodegeneration such as excitotoxicity[220,273,274] and proteasomal dysfunction[157-159] are implicated in epileptogenesis[337,338], and thus could be contributing to seizure susceptibility. Moreover, research into other causes of epilepsy such as inflammation[339], mitochondrial

dysfunction[340], and potassium channel dysfunction[341], can provide insights into what mechanisms underpin *C9orf72*-related seizures.

Drosophila is a popular model for investigating epilepsy, in particular due to its potential for high-throughput drug screening and the library of well-characterised seizure mutants[299,342]. The effect of pan-neuronal DPR co-expression on seizure susceptibility was investigated by using the proportion of flies that had seizures in response to a consistent mechanical stimulus as a readout. The results indicate that GR1000 was the main potentiator of seizures (Figure 5.4). When expressed alone, a small but not significant proportion of GR1000 flies exhibited seizure phenotypes in response to the more vigorous vortexing stimulus. This was not previously seen in any of the climbing assays because a "tapping" stimulus was not sufficient to trigger a seizure. Comparison between the "tapping" experiment and vortexing suggested that AP1000 may lower the mechanical threshold for GR1000 seizures, but it does not significantly increase seizure susceptibility. Additionally, a striking finding was that PR1000 expression did not result in seizures, but when combined with GR1000 seizures occurred at a frequency of 75% (Figure 5.4), a significant increase compared to GR1000/GFP expressing flies. Seizure susceptibility also broadly corresponds to the severity motor phenotypes. Taken together, the climbing defects and seizure frequencies associated with different DPR combinations suggest that there are significant interactions between the DPRs. In order to elucidate what these interactions could be, and which pathways are affected, a genetic modifier screen was the next step.

5.3.3 A targeted screen for dominant modifiers of seizure phenotypes in DPR1000 expressing flies

Seizure susceptibility is known to be greatly influenced by genetics. Mutations in genes that increase seizure susceptibility and those which suppress seizures have been identified in *Drosophila*[299,342]. A genetic approach using flies has identified pathways and therefore drug targets to treat previously intractable epilepsy[299]. In order to begin to elucidate pathways implicated in DPR-mediated seizure susceptibility, 7 different known BS mutants were screened against pan-neuronal expression of single DPRs. The aim was to identify potential dominant modifiers and thus pathways that might play an important role in DPR toxicity. Although the screen was potentially underpowered, it did provide an indication as to which genes and therefore pathways may potentiate DPR-elicited seizures. What these results reveal in terms of *C9orf72*-FTD/ALS pathogenesis and potential mechanisms is discussed below.

5.3.3.1 KCC – synaptic inhibition as a mechanism underlying PR1000 toxicity

Pan-neuronal expression of PR1000 in a *kcc* mutant background increased seizure susceptibility compared to expression of PR1000 alone and *kcc* mutants expressing GFP (Figure 5.6). This suggests that PR1000 is causing neuronal dysfunction via a pathway which is potentiated by reduced *kcc* expression. KCC is a K^+/Cl^- cotransporter which concomitantly extrudes potassium and chloride ions from the cell[343,344]. Its function is closely tied to inhibitory $GABA_A$ receptor signalling, the main mediator of synaptic inhibition in flies and mammals[345]. Low intracellular Cl^- levels are produced by KCC activity. This means that GABA-mediated opening of $GABA_A$ Cl^- channels produces an inward chloride ion current when there are high levels of KCC activity. The consequent hyperpolarization reduces the ability of the neuron to fire action potentials[345,346]. Therefore, when there are reduced levels of KCC and a corresponding higher level of intracellular Cl^- ions, GABA-mediated activation of $GABA_A$ channels can lead to a depolarizing outward chloride current. Thus, reduced *kcc* expression can result in aberrant synaptic excitation and hence it is implicated in epilepsy and schizophrenia[347]. Given that *kcc* mutations and PR1000 expression appear to genetically interact, this suggests that PR1000 is interfering with synaptic inhibition in some way. This is consistent with the reported cortical hyperexcitability in *C9orf72*-ALS patients[331,336]. Furthermore, there is evidence to support the contribution of other ion channels to *C9orf72* toxicity. A recent study using *Drosophila* expressing 36 pure G4C2 repeats and *C9orf72*-ALS patient-derived neurons implicated upregulated KCNN (*Drosophila* SK), a voltage-gated potassium channel, in degeneration and motor deficits[348].

There are multiple different ways that PR1000 could be interfering with synaptic inhibition. It could be directly inhibiting KCC or other ion channel activity so that a reduction in endogenous *kcc* expression pushes it far enough to result in seizures. We previously demonstrated that PR1000 expressing larvae have an increased number of active zones at the NMJ, but that this did not correspond to any electrophysiological defects (see 4.2.3). This is consistent with the lack of seizures in PR1000 expressing adult flies. However, the increase in the number of active zones could increase the susceptibility of PR1000 expressing flies to a reduction in *kcc* expression. In order to elucidate the link between KCC activity and PR1000 toxicity, further experiment to fully characterise the genetic interaction would be necessary. Future work will be discussed in more detail in 5.3.4.

There is a pharmaceutical relevance to this finding, as KCC modulation has been posited as an effective therapeutic strategy for epilepsy[349]. Augmentation of KCC function via antagonists of critical inhibitory phosphorylation sites has been suggested to facilitate

chloride ion extrusion and restore GABA inhibition[349]. However, this has been suggested for treatment of epilepsy based on the identification of mutations in human KCC in epilepsy sufferers. Therefore, it would have to be confirmed that an increase in KCC activity could ameliorate DPR-mediated toxicity and slow disease progression. It is possible that whilst there is an interaction between PR and KCC, augmenting KCC function would have no effect on overall toxicity in a system where all DPRs are present. Nevertheless, as *Drosophila* is an easily accessible and cheap tool for drug screening, treatment with KCC modulators could be considered in the future.

5.3.3.2 SOD2 – oxidative stress as a mechanism underlying PR1000 toxicity

The seizure screen highlighted the potential for *Sod2* mutations to potentiate toxicity in PR1000 expressing flies. Although not significant, PR1000 expressed in a *Sod2* mutant background did cause seizures whereas PR1000 in a wild type background did not (Figure 5.8). SOD2 is a member of the superoxide dismutase family and acts as an antioxidant. SOD enzymes play a critical role in catalysing the breakdown of highly reactive superoxide into less reactive hydrogen peroxide and oxygen. There are three distinct isoforms of SOD: copper/zinc-SOD (SOD1) is cytosolic; manganese-SOD (SOD2) is found in the mitochondria; SOD3 is extracellular[350]. Mitochondrial dysfunction and oxidative stress are intrinsically linked and their role in neurodegeneration is well-documented[351-353].

Defined as an overproduction of reactive oxygen species (ROS), oxidative stress is caused by an imbalance in redox states, either by excessive generation of ROS or inadequate removal by the antioxidant system[354]. ROS are a group of highly reactive molecules derived from incomplete reduction of oxygen. Their reactivity is conferred by unpaired electrons[355] and examples include superoxide (O_2^-), hydroxyl radical (·OH), and hydrogen peroxide (H_2O_2). Mitochondria are the main producers of ROS, and this is predominantly through enzymatic reactions occurring in the electron transport chain, where a small number of electrons “leak” and react with oxygen prematurely forming superoxide radicals[356]. The main enzyme responsible for ROS production varies between tissues or during disease. Complex I (NADH dehydrogenase) appears to produce the majority of O_2^- in the brain and is also associated with ROS production under pathological conditions, such as neurodegenerative diseases[357,358]. In excess, highly reactive ROS can react with and cause damage to cell structures, lipid membranes, proteins and DNA. Additionally, apoptotic cell death is linked to mitochondrial dysfunction via activation of caspase-3[359]. Even under normal physiological conditions, some ROS are produced and the random deleterious effects of ROS produced during metabolism

accumulate over time, giving rise to the "free radical theory of ageing"[360]. However, at low concentrations they can be beneficial, contributing to various physiological processes by functioning as cellular messenger, aiding in infection defence and even increasing lifespan[236,361]. The maintenance of "redox homeostasis" is therefore vital to prevent accelerated ageing and neurodegenerative disease. This is the role of antioxidants, of which there are a number of different types. In addition to enzymatic antioxidants such as superoxide dismutase, there are non-enzymatic antioxidants including vitamins C and E and glutathione[362]. Antioxidants react with ROS to form more stable molecules.

The brain is particularly susceptible to oxidative stress because it is a highly metabolically active tissue that relies on oxidative phosphorylation as its energy source[363]. This, in turn, results in damage to mitochondria themselves[322,353]. Mitochondrial SOD2 plays a significant in protecting neurons from the effects of ROS production, been implicated in different neurodegenerative diseases[363]. Studies in *Drosophila* have shown that reduction in *Sod2* expression is associated with increased oxidative stress, reduced longevity and neurodegeneration[310,364].

There is evidence to support the idea that mitochondrial dysfunction and oxidative stress play a role in FTD and ALS pathogenesis. Mitochondria from ALS patients show increased ROS production and associated oxidative-related damage[365], and multiple *in vitro* and *in vivo* studies have implicated aberrations in oxidative metabolism in ALS. Furthermore, mitochondrial damage has been linked to mutations in the *SOD1* gene that are known to cause ALS[35]. Several genetic and biochemical studies also provide evidence for oxidative stress in FTD[366-369]. In particular, cortical astrocytes have been implicated as having a propensity to degenerate and have a high burden of oxidative stress[367,370]. Astrocytes provide trophic support to neurons and also play a role in protecting them from oxidative stress. *MAPT* iPSC-derived astrocytes demonstrated an increased vulnerability to oxidative stress compared to controls and co-culture experiments with control neurons showed increased oxidative stress in previously healthy neurons[370]. Antioxidants have long been touted as potential treatments for ALS. However, clinical trials of vitamin E therapy proved ineffective in treating ALS[330]. Recently, the antioxidant edaravone was approved in America to treat ALS. This is only the second approved drug, after the approval of riluzole in 1995[330]. Edaravone was originally trialled for use as an antiepileptic in the early 1990s, due to its free radical scavenging properties. In Phase II and III trials, it reduced markers of oxidative stress in cerebrospinal fluid and slowed the decline in motor function of ALS patients[371]. Although antioxidants have not been universally successful in treating ALS, part of their limitation lies in when administration begins. Given symptoms present later in life, much of the

irreparable damage to neurons as already occurred before patients seek a diagnosis. Therefore, drugs given from the onset of symptoms can only halt further neurodegeneration.

There is also evidence that the *C9orf72* mutations specifically increases oxidative stress and mitochondrial dysfunction through various mechanisms. GR80 expression was shown to increase oxidative stress and cause mitochondrial dysfunction[170]. Furthermore, iPSC derived astrocytes from *C9orf72*-ALS patients showed oxidative stress and co-culture experiments showed that they were toxic to motor neurons via secreted soluble factors, including SOD2[291]. There is also evidence that *C9orf72* mediated mitochondrial dysfunction led to a shortening of axons and defective axonal transport in motor neurons, which are especially susceptible to axonal aberrations due their length[372]. This provides a causal link between two observed phenotypes in *C9orf72*-related FTD/ALS: axonal transport defects and mitochondrial dysfunction. Given that oxidative stress is a factor in many neurodegenerative diseases and there is evidence pointing to its involvement in *C9orf72*-FTD/ALS, it is perhaps unsurprising that *Sod2* mutations potentiated DPR-mediated seizure phenotypes. However, it appears that only PR1000 interacts genetically with *Sod2* mutations, which poses the question as to the role of PR vs the other DPRs in oxidative stress and provides rationale for further exploration, as detailed in 5.3.4.

5.3.3.3 Stathmin – microtubule dysfunction implicated in DPR toxicity

Partial loss of the microtubule destabilising protein Stathmin increases seizure susceptibility of control and DPR flies, apart from PR1000. Whilst the slightly weaker *stai*^{rdtp} had little effect on seizure susceptibility in any of the DPRs, the stronger *stai*^{B200} mutation appeared to increase seizure frequency in GR1000-expressing flies, although this was not significant (Figure 5.9). Flies expressing GA1000 in a *stai* mutant background also showed a number of seizures. Although only ~ 10% of flies had seizures, GA1000 expression alone did not cause seizures, suggesting that there may be an interaction even though it is not statistically significant. Studies in *Drosophila* have shown that stathmin is required for NMJ stability, likely due to loss of integrity of axonal microtubules essential for axonal transport[312,313]. *Stai* mutant flies show a reduced lifespan and a progressive age-dependent BS seizure phenotype[313]. It would therefore be interesting to see if a stronger phenotype was observed with DPR flies at a later age. There is a basis for the involvement of Stathmin proteins in FTD/ALS, not least because a common genetic cause of FTD is mutations in *MAPT,* a microtubule binding protein[51,52].

Microtubules are dynamic, large filamentous structures composed of subunits of α- and β-tubulin, and are major constituents of the cytoskeletal network. They are critical for maintaining neuronal homeostasis and do so by contributing to several aspects of neuronal structure and function. Microtubules are inherently polarised structures (α-tubulin at the "minus end" and β-tubulin at the "plus end") and thus contribute to neuronal polarity by reorganising their orientation to mark distinct axonal and dendritic domains[373]. This is vital for correct localisation of cellular cargo which is transported along the axon via microtubules[374]. Furthermore, maintenance of neuronal morphology is reliant on the stability of microtubules, which is heavily influenced by microtubule binding proteins. Both hyper-stable and unstable microtubules can result in defects such as ectopic neurite growth, loss or increase of dendritic and axonal branches. In turn, morphological defects can lead to altered synaptic plasticity[375] and other essential functions such as axon pathfinding and innervation[376]. One of the most important roles of microtubules is as the highway for cargo transport. This is particularly critical in neurons due to their long axons; cargo such as mitochondria, synaptic vesicles and associated proteins must be transported great lengths to reach their target site. With synapses major sites of neuronal energy consumption[377], trafficking of mitochondria is critical to meet the energy requirements. The microtubule motors kinesins and dynein are responsible for transporting cargos towards the plus ends and minus ends respectively[378]. Indeed, reduced microtubule stability and axonal transport defects have been observed in several neurodegenerative diseases such as AD, HD, PD as well as several tauopathies[379]. In addition, a recent study has linked arginine-rich DPRs to dynein motor dysfunction and axonal transport defects both in cultured motor neurons and *Drosophila*[380].

Microtubule binding proteins such as stathmin are vital for microtubule function. Stathmin is responsible for regulating microtubule dynamics via direct interactions with soluble tubulin and its activity is modulated by phosphorylation[381]. Whilst there is only one *stai* gene in flies, there are 4 stathmin proteins in humans, making the role of stathmin proteins in humans is more difficult to elucidate. Consistent with findings from *Drosophila* relating *stai* mutations to seizures, abnormally elevated stathmin-1 expression has been detected in patients with intractable temporal lobe epilepsy[382]. More recently, genetic studies have revealed that a variant in the *Stathmin-2* (*STMN2*) gene is a novel risk factor for ALS. Stathmin-2 promotes microtubule dynamics and neurite outgrowth, and is highly regulated by TDP-43. TDP-43 is crucial for correct splicing of *STMN2* transcript, thus when pathological aggregates of TDP-43 form in ALS or FTD, a non-functional Stathmin-2 protein is produced due to aberrant splicing[383]. This provides evidence of a conserved

mechanism between sporadic cases of FTD and ALS and functionally links loss of TDP-43 function to enhanced neuronal vulnerability via defective microtubule dynamics. Furthermore, dysregulation of stathmin was found in a *SOD1* ALS mouse model and this was associated with the Golgi complex fragmentation and collapse of microtubule networks[384]. There is also emerging evidence for dysregulated stathmin in *C9orf72* toxicity. Aberrant splicing of stathmin-2 transcripts was identified in upper and lower motor neurons across both sporadic and *C9orf72*-ALS[385]. Taken together, there is strong evidence for loss of stathmin as a key driver of motor neuron degeneration across different familial and sporadic forms of ALS. This corroborates our findings that *stai* mutations could be potentiating seizures, in particular in GR1000 expressing flies, and rationalises future investigations into this area (discussed in 5.3.4).

Targeting Stathmin has been suggested as a potential therapeutic approach, due to evidence indicating that post-translational stabilisation of aberrantly spliced *STMN2* can rescue neurite outgrowth and axon regeneration deficits induced by TDP-43 depletion[383].

5.3.3.4 Mutations in other genes – negative results does not rule out their contribution to DPR toxicity

Whilst reduction in a succinate dehydrogenase (*Sirup*), synaptic vesicle protein (*Synapsin*), β1,4-N-acetlygalactosaminyltransferase (*β4GalNAcTA*), or citrate synthase (*kdn*) did not increase seizure susceptibility in DPR flies, this does not rule out their involvement *C9orf72*-FTD/ALS. It is possible that there are subtle changes not detected by this screen, which had a relatively small sample size to accommodate the large number of genes in the time available. There is a basis for the pathways that these genes are involved in to play a role in neurodegeneration.

Sirup and *kdn* encode proteins involved in cellular metabolism, specifically the Krebs cycle[386]. Citrate synthase (*kdn*) is an enzyme involved in mitochondrial energy production, catalysing the first step of the Krebs cycle and is commonly used as a quantitative enzyme for the presence of intact mitochondria[387,388]. Whilst mitochondrial defects have been implicated in *C9orf72* pathogenesis previously[387], there is no evidence for a direct link between alterations in citrate synthase activity itself. Similarly, succinate dehydrogenase is a key component of cellular respiration, linking the Krebs cycle to the electron transport chain[386]. Mutations in proteins associated with succinate dehydrogenase, such as the assembly factor encoded by *sirup* (SDHAF4) cause a variety of diseases, including the early onset neurological Leigh syndrome[389]. In *Drosophila,* in addition to BS seizures, vacuolisation was observed in the retina of *Sirup* mutants[314]. Furthermore, overexpression of human SDHAF4 was shown to rescue this

neurodegeneration and bang sensitivity[314]. However, there is no evidence of perturbations to succinate hydrogenase activity in ALS or FTD. Nevertheless, metabolic and mitochondrial defects are well characterised in neurodegenerative diseases including *C9orf72*-FTD/ALS. The expansion has been demonstrated to alter the metabolic profiles of astrocytes, reducing the ability of astrocytes to switch between using glucose and other substrates for energy production, important for neuronal survival during times of bioenergetic stress[390]. In ALS more widely, hypermetabolism is recognised as a clinical feature[391] and there is evidence to suggest that motor neurons are selectively vulnerable to ATP depletion[377].

Synapsins are abundant on synaptic vesicles, and comprise ~1% total brain proteins[392]. They are involved in neurotransmitter release, synaptogenesis and synaptic plasticity[393,394] and are modulated via phosphorylation: upon dephosphorylation, they bind synaptic vesicles; when phosphorylated, they dissociate and mobilise[394]. In contrast to the one *Drosophila Syn* gene, there are three distinct synapsin genes in vertebrates, encoding three different isoforms, with slightly different cellular localisations – synapsin I is found only at the synapse, synapsin II is additionally found in the synapsin vesicle membrane, and synapsin III is present in cell junctions, cytoplasmic vesicles, synaptic vesicles and membrane[395]. Mutations in synapsins have been shown to cause epilepsy by triggering imbalances in synaptic vesicle release and short-term plasticity[396]. Reduced levels of synapsin II and III are associated with schizophrenia[397,398], and abnormal phosphorylation of synapsin I has been implicated in HD[399]. There is also tentative evidence pointing to a role for synapsins in ALS, with a decrease in expression of synapsin I in anterior horn of the spinal cord in ALS pateints[400]. Whilst there isn't a great deal of evidence to suggest that synapsins play a role in *C9orf72*-FTD/ALS, they are a crucial component of the synaptic machinery, and therefore it is possible that they are involved in mediating observed synaptic defects, such as excitotoxicity[331].

Finally, β*4GalNAcTA*, encoding an acetylgalactosaminyltransferase, is involved in generating glycan structures that have important functions in the neuromuscular system[316]. Mutations in β*4GalNAcTA* have been shown to reduce the NMJ size and thus alter synaptic function, reducing mEJP frequency[401]. However, there is no direct evidence implicating it in human neurodegenerative diseases.

5.3.4 Future work

In order to confirm genetic interactions suggested by the seizure screen, further genetic experiments looking to rescue impaired function are needed. Genetic rescues using human transgenes such as *SLC12A4* or human *Sod2*would provide robust evidence of

the interaction between *kcc* and/or *Sod2* and PR1000. However, PR1000 expressing flies do not show any measurable phenotypes in the climbing or seizure experiments, nor any reduction in longevity or any significant vacuolisation. A rescue experiment would therefore have to be with larval phenotypes such as crawling, which was significantly in all DPR-expressing larvae reduced compared to controls (Figure 4.1). Whilst this is less relevant because larvae cannot be aged, it would provide further evidence for the interaction between PR1000 and *kcc* or *Sod2.* Alternatively, the effect of overexpressing either *kcc* or *Sod2* in adult flies co-expressing both PR1000 and GR1000 could be measured using seizure frequency as a readout. 75% PR1000/GR1000 flies displayed a seizure phenotype upon vortexing (Figure 5.4), which was approximately double when GR1000 was expressed alone or with GFP. By overexpressing *kcc* or *Sod2* in the nervous system in a PR1000/GR1000 background, the potential for increased activity of KCC or SOD2 to rescue the phenotype could be measured. This approach could also be applied to climbing experiments where PR1000/GR1000 also showed significant motor deficits (Figure 5.3).

An alternative approach for manipulating inhibitory GABA signalling implicated in KCC–mediated seizures is by administering the convulsant drug picrotoxin (PTX). Whilst in wild type flies, PTX feeding results in an increased seizure susceptibility, in *kcc* mutant flies, it reduces seizure susceptibility[307]. This is because PTX works by inhibiting $GABA_A$, thus a reduction in $GABA_A$ activity in *kcc* mutants corresponds to a decrease in excitability and consequently decreased seizure susceptibility[307]. The effect of GABA inhibition on neuronal function could be measured using seizure susceptibility in PR1000/GR1000 adult flies or larvae.

Further investigation into the interaction between *stai* and GR1000 would be easier, as there is a phenotype to rescue in GR1000 expressing flies. However, there is currently no available *UAS-stathmin.* Given the function of stathmin is in microtubule stability, a pharmacological approach could be taken instead, as there are many drugs available that alter microtubule dynamics in various ways. For example, microtubule destabilising drugs such as colchicine could act to compensate for the loss of stathmin function[402]. However, the effects of interfering with microtubule function are multifocal. Microtubules play a role in stress granules, also implicated in *C9orf72* pathogenesis[167], by facilitating their formation and dissolution. Therefore, pharmacological approaches to target microtubules would have to be accompanied by other experiments to confirm the mechanism.

Biochemical approaches such as western blotting and qRT-PCR to ascertain protein levels and expression of the gene of interest in DPR flies would complement genetic and pharmacological studies. Furthermore, examination of the subcellular localisation of the

proteins in question by immunohistochemical analysis would hint at whether they are being sequestered by DPR aggregates, mislocalised, or have reduced levels.

5.3.5 Summary

This chapter reveals a novel seizure phenotype in DPR expressing flies and identifies potential genetic modifiers. Whilst relatively understudied, these findings support a growing body of evidence suggesting a role for *C9orf72* mutations in seizures, and relate to the general cortical hyperexcitability observed in ALS. Furthermore, this chapter highlights the importance of co-expressing DPRs in addition to using a pathologically relevant repeat length and a system which can be aged.

6 Discussion and Future Research

6.1 Introduction

The overarching aims of this research were to:

1. Generate novel *Drosophila* models expressing *C9orf72*-related DPRs of a pathologically relevant length
2. Characterise disease relevant phenotypes caused by expression of different DPRs in the nervous system across the lifespan of the fly
3. Investigate the effect of co-expressing DPRs in the *Drosophila* nervous system

This final chapter looks to address the results of this investigation in relation to the aims and objectives, and how this research fits with the current literature. It will also discuss further questions and areas for future investigation.

6.2 Novel *Drosophila* models expressing DPRs at 1000 repeat lengths

In this investigation, the first *Drosophila* models expressing 1000 repeat DPRs were generated. Despite concerns with the stability of the long DPR constructs, based on previously reported difficulties generating longer repeat DPR mice[197], the DPR constructs have remained stable in the *Drosophila* genome for over three years, equivalent to over 100 generations. A possible reason for this is that the insertion site is suited for retention of long repetitive sequences due to the presence of lncRNA[232,233], but this remains to be confirmed. Nevertheless, it has the potential to pave the way for other repeat models, such as pure repeats, to be inserted at full length into this locus. Moreover, insertion of *C9orf72* transgenes into the same genetic locus would allow better and more consistent comparisons between models. Unfortunately, these models do not include GP because of the difficulties in making a GP repeat construct. This does preclude investigations into the role that GP plays in FTD/ALS, and is a gap in the field that is important to address.

Although the expression levels in these models do not appear to differ between DPRs[207], it is possible that their relative protein levels contribute to their toxicity. Indeed, looking at their fluorescence in the fly brain, AP1000 appears much brighter and more abundant that PR1000 and GR1000, whilst GA1000 is bright but sparse throughout the brain. This could be because of the relatively low bioavailability of arginine compared to glycine or alanine, restricting the amounts of arginine-rich DPRs that can be produced. It is important to consider this when evaluating their toxicity, and comparing against previous

DPR models. It also remains unclear whether expression levels of DPRs in any models are truly representative, and how much this may be affecting the phenotypes observed. In fact, we still do not know the relative abundance of each DPR in different regions of the brain, spinal cord and muscle. In order to employ our models most effectively, as well as develop new models, it is critical that assays to accurately quantify DPRs in patient tissue are established. This is a significant challenge to the field. Despite this, the models described in this study offer an opportunity to dissect the contribution of each DPR, individually and concomitantly, to both cell autonomous and non-autonomous pathways underpinning *C9orf72*-related FTD/ALS spectrum disorders.

6.3 Each DPR presents a unique phenotypic profile

Throughout this investigation, it has become apparent that each DPR is associated with a unique set of phenotypes. Whilst many previous studies have focused on GR and PR, assuming that AP and GA show little toxicity, in this study we explored the role of all DPRs, without any preconceptions. As a result, we can now summarise and compare the phenotypes conferred by each DPR, and postulate as to what this suggests about their role in FTD/ALS. An overview of the phenotypes observed in this investigation can be found in Table 6.1.

6.3.1 AP1000

AP is generally considered to be the least toxic of the DPRs, based on multiple studies in *Drosophila* and *in vitro*[74,137,140]. However, relative to the wealth of published research on the toxic effects of PR and GR, there has been little investigation into the effects of AP. Due to the conformational restrictions conferred by the proline residue, it forms a flexible coil structure[74,162]. It is also uncharged, reducing its propensity to react with cellular components. However, the effect of length on DPR properties is well established[137,163,165,216], and *in vitro* AP only caused significant electrophysiological defects at over 1000 repeats in length[153]. Indeed, in this system we found that AP1000 did confer toxicity and was associated with a distinct set of phenotypes, including neurophysiological deficits.

Whilst other, shorter, AP models have shown no toxicity when expressed in the *Drosophila* eye[137], we found that AP1000 expression causes a dose-dependent toxicity. Homozygous expression results in a glazed eye, indicative of disorganisation of the ommatidial array. This, along with global expression of AP1000 proving lethal at the pharate stage, implied that AP1000 was capable of causing cellular dysfunction and

visible toxicity. When expressed pan-neuronally and aged, to look for disease relevant phenotypes, further aspects to AP1000-mediated toxicity were revealed. At 28 days post-eclosion, flies expressing AP1000 had numerous large vacuoles in the brain, indicative of neurodegeneration. They also had a severe climbing defect present from day 1, but this did not decline with age. In addition, AP1000 was the only DPR to cause any electrophysiological defects with a reduced EJP and Ri, consistent with a reduction in active zones. A surprising finding was that despite the aforementioned physiological defects, AP1000 expressing flies had an increased lifespan. Factors known to affect lifespan that could link the phenotypes together include oxidative stress and alterations to metabolism[403]. The link between oxidative stress and lifespan is complex. Whilst high levels of oxidative stress are implicated in numerous neurodegenerative diseases[351,352], low levels of oxidative stress are known to increase lifespan in *Drosophila* and other models[236]. In general, responses to low levels of stress have been shown to increase longevity whilst high levels are detrimental, a phenomenon known as hormesis[404,405]. Metabolic activity is intrinsically linked to oxidative stress because mitochondria, the main providers of cellular energy, produce ROS as a by-product of oxidative phosphorylation. It has been suggested that a metabolic switch to mitochondrial oxidative phosphorylation in preference to glycolysis can increase lifespan through the low level production of ROS[406]. Alternatively suppression of fatty acid oxidation has been shown to extend lifespan by conferring resistance to oxidative stress[407]. Furthermore, studies in humans, mice, and flies have shown that biological ageing is characterised by changes in metabolic profiles and accumulation of different metabolites is linked to molecular damage[408-411]. In fact, manipulating metabolic pathways has been suggested to suppress the ageing process. For example, downregulation of the tyrosine degradation pathways[403], activation of the pentose phosphate pathway[412], and suppression of purine nucleotide metabolism[413] have been linked to lifespan extension in *Drosophila.* Alterations to metabolism can therefore increase lifespan by increasing tolerance to oxidative stress directly, or indirectly by stimulating adaptation to low levels of ROS.

The fact that global expression of AP1000 is lethal, whilst pan-neuronal expression is detrimental for neurological function but increases lifespan, is consistent with the idea that low levels of stress may be responsible for AP1000's phenotypic profile. Whilst pan-neuronal expression of AP1000 reduces climbing speed and causes neurodegeneration, it could also result in adaptive responses that increase lifespan. How AP might elicit this stress is still unclear and there currently are no mechanistic studies looking at AP-mediated toxicity. Given that its biochemical properties are significantly different to the other DPRs, it is likely that it is contributing to neuronal dysfunction via different pathways and this is consistent with our findings that AP shows a distinct phenotypic profile to the other DPRs.

It is important to consider that the protein levels are unlikely to be the same between DPRs, and this could contribute to their relative toxicity. Indeed, AP1000 appears more abundant in adult brains. This idea is supported by the fact that global AP1000 expression is lethal, but pan-neuronal AP1000 expression is not, and in fact increases lifespan. This idea is discussed in more detail in chapter 3.

6.3.2 GA1000

GA is unique amongst the DPRs in that it is capable of forming beta-sheets that can aggregate into large fibrils with amyloid properties[154,156] and has been shown to spread between cells *in vitro* and in the fly brain[154,156,216]. The localisation of GA1000 was similar to that seen in patient tissue, but not the shorter repeats. When expressed in cells, GA36 forms spherical inclusions, whereas when extended to >1000 repeats it forms characteristic fern-like inclusions reminiscent of the stellate inclusions observed in patient brains[99,147,153]. This suggests that the biophysical properties do vary with length, and highlights the importance of a physiological repeat length in modelling GA toxicity.

In our model, unlike the other three DPRs, GA1000 does not cause an eye phenotype when homozygous. It is also the only DPR to be 100% viable when expressed globally using *tubulin-Gal4*. Similarly, pan-neuronal expression had minimal effects on the phenotypes examined: there was no vacuolisation in the brain, no morphological defects at the NMJ nor any electrophysiological defects. However, there was a slight decrease in climbing speed at 7 days post-eclosion compared to age-matched controls. Similar to AP1000, this was consistent across lifespan. However, the deficit was smaller than AP1000, and therefore fell back in line with wild type by 28 days post-eclosion.

Consistent with previous findings, we have also shown that the *Drosophila* TDP-43 homologue TBPH colocalises with GA1000 and GA1000 expression induces TBPH inclusion formation[207,213]. The fact that GA1000 is the only DPR to trigger TBPH inclusions and yet shows no neurodegenerative phenotypes, suggests that TDP-43 inclusions are not a primary driver of toxicity. However, GA1000 expression did not alter TBPH localisation significantly. The accumulation of cytosolic TDP-43 is postulated to drive toxicity in *C9orf72*-FTD/ALS, irrespective of inclusion formation[414]. Indeed, it appears that although GA1000 forms the characteristic fern-like inclusions and promotes aggregation of TBPH, this is insufficient to confer toxicity in our model. We can speculate that GA may play a role in DPR-mediated toxicity, but via interactions with the other DPRs. This is corroborated by the co-expression experiments that show GA1000 significantly exacerbates GR1000 mediated toxicity in the eye, climbing, and seizure

assay. This is despite not showing significant phenotypes when expressed alone. This highlights the importance of studying the DPRs in combination with each other.

6.3.3 PR1000

In our model, PR1000 expression causes distinctly different levels of toxicity depending on the dose. In fact, PR1000 shows the most dramatic dose-dependence of the DPRs, with heterozygous expression in the eye or nervous system producing few observable defects. When heterozygously expressed in the nervous system, PR1000 flies show no visible vacuolisation in the brain, nor significant climbing defects. The larval NMJ of flies heterozygously expressing PR1000 does show increased active zones, but this does not translate to detectable electrophysiological defects. In contrast homozygous expression in the nervous system is lethal and, in the eye, it is detrimental to survival, with the surviving flies having severely degenerated eyes. Global expression of PR1000 is also lethal. A significant observation made in this study was the distinct localisation patterns of 1000 repeat DPRs compared to that observed in other studies. For example, previous *in vitro* studies using both shorter and 1000 repeat DPRs have reported nucleolar PR and GR localisation[152,153,169]. In contrast, neither PR1000 nor GR1000 was observed in the nucleolus in this study. The discrepancy between 1000 repeat GR and PR when expressed in HeLa cells and *Drosophila* indicate that not only the length, but also the system in which they are expressed, can affect PR and GR localisation. Given that it has not been observed in patients, it raises the question of whether nucleolar localisation is an artefact in these models or whether it occurs early in disease progression and therefore is not observed at end-stage.

The general consensus is that PR is toxic to cells and *in vivo* but here, we show that it may be more complex than the acute toxicity shown in other, shorter models. Our PR1000 model also displays a distinct phenotypic profile compared to the other arginine-rich DPR, GR. PR and GR are often grouped together and display the same phenotypes. In 2014, Mizielinska et al. reported severely degenerated eyes that looked very similar in both PR100 and GR100, and egg-to-adult viability was also reduced to under 10% when either PR100 or GR100 were expressed in the eye, although there GR100 appears to be slightly more toxic to viability[137]. Furthermore, they also showed that when expressed pan-neuronally in the adult nervous system, both PR100 and GR100 had a similarly short lifespan, only surviving to around 10 days post-eclosion. Subsequently, research has tended to focus on PR and GR and continued to uncover similar phenotypes indicating similar pathways underpinning their toxicity. In 2015, Tao et al. found that 60 repeats of PR and GR but not GP, GA or AP suppressed ribosomal RNA

synthesis and impaired stress granule formation, leading to nucleolar stress and cell death[169]. More recently, Hayes et al. (2020) showed that PR10 and GR10 interfered with karyopherin-mediated nuclear import *in vitro* whilst equivalent length GA, GP and AP did not[415]. Another study showed that the 100-repeat arginine-rich DPRs interact with ribosomal proteins and induce translational arrest *in vivo* and in human iPSC-derived motor neurons[249].The commonalities in PR and GR's behaviour have been attributed to the arginine residue which facilitates interactions with low-complexity domain (LCD)-containing proteins[74,164,166]. LCDs are unstructured, flexible, and form multiple interactions with other proteins. This allows LCD-containing proteins to undergo liquid-liquid phase separation, a process which underpins the formation of membraneless organelles such as the nucleolus, Cajal bodies and stress granules[416]. Disruption of this vital process has been linked to PR and GR directly interacting with LCDs and lowering the critical concentration required to undergo LLPS, thus causing them to become less dynamic and altering their cellular functions[417]. If the arginine residue is responsible for these interactions and therefore GR and PR toxicity, the question remains why, in these 1000 repeat models, does PR1000 have a much lower toxicity than GR1000. One possibility is that the proline residue, which restricts the conformations that proteins can form, affects how PR can interact with LCDs only at a longer repeat length. As yet, the biophysical properties of 1000 repeat DPRs are unknown due to the difficulties in synthesising long repeat peptides. A better understanding of how repeat length affects the physical properties of DPRs would be useful for evaluating the relevance of findings from shorter models.

6.3.4 GR1000

GR1000 expression confers the greatest level of toxicity of the 1000 repeat length DPRs explored in this study, with significantly reduced lifespan, neurodegeneration, and climbing defects observed. It also causes eye-degeneration when expressed homozygously. However, in contrast to previous studies in *Drosophila* showing that GR expression affects viability and longevity, even when expressed only in the eye[137], GR1000's toxicity is more progressive and age-dependent. This is important because reduced longevity through expression solely in the eye indicates a significantly acute level of toxicity unlikely to be representative of human disease. In this GR1000 model, at 7 days post-eclosion, it has a similar climbing speed to wild type controls, but by 28 days post-eclosion climbing speed is severely reduced. At 28 days post-eclosion, GR1000-expressing flies have significant vacuolisation of the brain, indicative of neurodegeneration. They also have a significantly shortened lifespan, only living up to ~ 40 days. This suggests that GR1000 is exacerbating the effects of physiological ageing,

causing neurodegeneration and resulting in premature death. Furthermore, in salivary glands, GR1000 expression caused a significant misolcalisation of the *Drosophila* TDP-43 homologue TBPH to the cytoplasm and was the only DPR to do so[207]. GR1000 was the only DPR in this investigation to cause significant BS seizure phenotypes, suggesting that it is interfering with normal synaptic transmission in some way. Pan-neuronal GR1000 expression was lethal when homozygous, but co-expression with the other DPRs potentiated the seizure phenotype. The seizure modifier screen failed to identify any significant GR-interactors, but in future, a larger screen testing more flies may reveal subtle interactions. Nevertheless, the presence of this novel phenotype in GR1000-expressing flies indicates underlying neurological dysfunction related to synaptic excitability, hinting at a role for excitotoxicity, microtubule dysfunction, mitochondrial dysfunction, and oxidative stress.

Similar to PR, GR has a well-documented toxic effect *in vitro* and *in vivo* at shorter repeat lengths. Translational inhibiton[74,166,168,214,249,418], DNA damage[419,420], stress granule dynamics[74,421], mitochondrial dysfunction[74,170], and nucleocytoplasmic transport defects[171,415] have all been implicated in GR-mediated toxicity. The novel BS seizure phenotype uncovered in this study links to previous reports that mitochondrial function is affected by GR expression. Mutations in mitochondrial subunits are among the class of BS seizure mutants[422], and epileptiform seizures are often linked to mitochondrial disease[423,424]. Defects in mitochondrial function are also linked to axonal transport defects and oxidative stress, also posited to be involved in FTD/ALS pathogenesis[139,170,425,426]. Taken together, this provides evidence that mitochondrial dysfunction may be occurring in GR1000-expressing flies, and could be underpinning the toxicity we observe. Future investigations into the function of mitochondria in this model would support work *in vitro* that suggests mitochondrial dysfunction could be a major driver of FTD/ALS.

Table 6.1 Summary of phenotypes associated with expression of each DPR throughout the course of this study.
(PE = post-eclosion)

	Driver	Figure	AP1000	GA1000	PR1000	GR1000
Viability (global expression)	*Tubulin-Gal4*	3.4	0% (pharate lethal)	100%	0% (second instar lethal)	~ 10% (second instar lethal)
Viability (neuronal expression)	*nSyb-Gal4* (III)	3.4	100%	100%	100%	100%
Viability (glial expression)	*Repo-Gal4*	3.4	100%	100%	100%	100%
Longevity	*nSyb-Gal4* (III)	3.4	Increased (~20%)	Increased (~10%)	WT	Decreased (~25%)
Eye phenotype (homozygous expression)	*GMR-Gal4*	3.7	Glazed eye	WT	Largely lethal, remaining eyes severely degenerated	Rough shrunken eye
Motor function (larval crawling)	*nSyb-Gal4* (III)		Reduced (~30%)	Reduced (~30%)	Reduced (~30%)	Reduced (~30%)
Motor function (climbing) throughout lifespan	*nSyb-Gal4* (III)	4.2	Consistently reduced speed from 1 day PE	Consistent speed, slightly reduced (significant at 7 days PE)	No reduction in speed compared to wild type, significant decrease between 7 and 28 days PE	Age-dependent reduction in speed
Neurodegeneration	*nSyb-Gal4* (III)	4.3	Significant vacuolisation at 28 days PE	WT	WT	Significant vacuolisation at 28 days PE
NMJ morphology	*nSyb-Gal4* (III)	4.4	Reduced NMJ length, reduced active zones (muscle 6/7 hemisegment A3)	WT	Increased active zones (muscle 6/7 hemisegment A3)	Reduced muscle size (muscle 6/7 hemisegment A3)

Table 6.1 Summary of phenotypes associated with expression of each DPR throughout the course of this study.
(PE = post-eclosion)

	Driver	Figure	AP1000	GA1000	PR1000	GR1000
Electrophysiology	*nSyb-Gal4* (III)	4.5	Reduced EJP, reduced Ri	WT	WT	WT
Bang-sensitive seizure phenotype	*nSyb-Gal4* (II)	5.6	5%	WT	WT	25%

6.4 Comparisons between *C9orf72* DPR models

In order to evaluate and critique this and other data, we must take an in depth look at the differences between the models established in this project and those existing in the field. Most significantly, the length of DPRs in these models recapitulates what is predicted in patients, thus making it a more physiologically relevant model. It is well-established that length plays an important role in DPR behaviour and toxicity[122,137,153,165,216], therefore there may be important and subtle age-related phenotypes and underlying mechanisms missed in shorter models. Furthermore, age-related phenotypes can be studied using these models, where previously acute toxicity associated with PR and GR has precluded ageing past 10 days post-eclosion[137]. Given the age of onset of disease in *C9orf72* expansion carriers is around 57 years of age[278], it appears that whilst DPRs may exert toxicity across lifespan, the physiological effects of this toxicity are not apparent until mid-life or later. Therefore, it is important to take into account the physiological effects of ageing on the CNS and individual neurons when assessing DPR-toxicity. Neurons are particularly vulnerable to age-related defects due to their long lived and post-mitotic nature, and therefore are more susceptible to age-related diseases[49]. This also highlights the importance of expressing DPRs in a disease-relevant tissue. Whilst the commonly used salivary glands, eyes, and the wing are useful tool for dissecting molecular pathways, they do not respond to age in the same way as neuronal populations. Whilst the eye is a neuronal tissue, comprising mainly photoreceptor neurons and glia, it is not a brain nor does it contain motor neurons, so we must be cautious when extrapolating findings to disease.

Despite advantages to the models described in this investigation, there is still much work to be done before we are modelling *C9orf72*-related FTD/ALS in the most comprehensive and relevant way possible. Firstly, the DPRs in these models are GFP-tagged. Whilst this was useful for imaging of the DPR morphology without having to use an antibody, it presented other problems, most notably preventing investigations into the morphology and localisation of DPRs when they are co-expressed. Furthermore, many established tools for studying various mechanistic pathways in *Drosophila* involve the use of fluorescently labelled reporters. For example, to measure autophagic flux, tandem tagged mCherry-GFP-Atg8a are often used. Low lysosomal pH quenches GFP after autophagosome-lysosome fusion, and thus lysosomes and autophagosomes can be distinguished by whether they are positive for just GFP or both mCherry and GFP[427]. This system could not be used in these models because it would not be possible to distinguish between DPR-GFP and Atg8a-GFP. Generating *Drosophila* capable of expressing alternatively tagged and untagged constructs subcloned from the current pUAST-DPR1000-GFP constructs would circumvent these problems. In addition, co-

expression of an mCherry-tagged DPR with a different GFP-tagged DPR would allow colocalisation to be examined without the need for antibody staining. There are few antibodies that show reliable and consistent results, likely due in part to the nature of the DPRs and that when antibodies are raised against a limited sequence (2 amino acids repeated) they often display non-specific binding and poor affinity.

Secondly, although this remains a criticism of the field in general, at present we have only looked at the co-expression of pairs of DPRs. In contrast, all 5 DPRs can be produced from the GGGGCC repeat in patients. Therefore, we might be missing key aspects of DPR pathogenesis by expressing each DPR individually or at most, in pairs. The results of this investigation highlight the importance of co-expression. Compared to when expressed alone, DPRs show different phenotypes when expressed concomitantly with others. For example, whilst GA1000 and AP1000 do not show an age-related decline in climbing speed when expressed alone, when they are expressed with an arginine-rich DPR, they do. This suggests that toxicity conferred by arginine-rich DPRs potentiated the basal level of toxicity conferred by the alanine-rich DPRs. Furthermore, whilst a very slight mechanical shock (tapping) did not initiate seizures in single DPR-expressing flies, it was sufficient to cause seizures in flies expressing two DPRs particularly those including GR. This highlights the importance of looking at interactions between DPRs, rather than exclusively studying them in isolation. It is still unknown what the effect of co-expressing 3, 4 or 5 DPRs together does to the phenotypes observed in DPR models. Mechanisms thought to underpin the toxicity of certain DPRs may be irrelevant because they do not act through the same pathways when other DPRs are present. Currently, it is logistically difficult to express more than 2 DPRs at once in these models because they were site-landed into the same genomic location. Therefore, new models with the DPRs site-landed into a different genomic location would have to be generated in order to allow recombination, and this would affect how reliably we could compare between DPRs. There is an argument for pure repeat models in this case, as all 5 DPRs have the capacity to be produced, in addition to RNA. However, to really probe the mechanisms, it would be useful to be able to strategically manipulate the system to investigate how DPRs interact in different combinations.

Pertinent questions remain as to the relevance of looking at DPRs in isolation, as it is possible that their interacting partners will change in the presence of another DPR that could potentially disrupt these interactions, or that dysregulated pathways change when DPRs are expressed together. This is also why it is important to take data from a variety of different model systems, both loss of function and gain of function models, including pure repeat and DPR models, in order to get a full and representative picture of what pathogenic mechanisms might be driving disease progression.

6.5 Common themes implicated and how they link together

There are several mechanisms proposed to underlying DPR toxicity. In this investigation, co-expression of DPRs revealed novel seizure phenotypes. Most notably, PR1000 alone was not capable of producing seizures at the time-point tested, but when combined with GR1000 it exacerbated the seizure susceptibility of GR1000 alone, and resulted in the majority of flies showing a seizure phenotype. This suggests that the mechanisms through which GR1000 and PR1000 act are linked, thus co-expression exacerbates the dysfunction and reduces the threshold for seizures. However, it remains to be elucidated which pathways are being affected. As discussed in chapter 5, cortical hyperexcitability is a biomarker for ALS[331,336], and epileptiform seizures have been reported in *C9orf72* carriers[300,301]. There are common mechanistic themes between seizure disorders and neurodegenerative disorders, some of which are implicated in FTD/ALS. Here, the role of synaptic dysfunction, mitochondrial dysfunction, oxidative stress and axonal transport defects in FTD/ALS, and how they may link together will be explored in more detail.

6.5.1 Synaptic dysfunction

Mutations in the Cl^- / K^+ transporter transporter *kcc* were identified as a dominant modifier of PR1000 toxicity. *Kcc* mutations are reported to cause seizures in *Drosophila* via a reduction in inhibitory GABA signalling[307]. Reduced *kcc* expression was linked to BS seizure susceptibility in PR1000 expressing flies, implicating synaptic inhibition as a pathway disrupted by PR1000 expression. Furthermore, an increased number of active zones was observed at the NMJ of PR1000 expressing larvae. However, this does not correspond to significant age-related neurodegenerative phenotypes such as impaired climbing ability or vacuolisation in the brain, suggesting that PR may contribute to neurodegeneration via synaptic dysfunction in conjunction with other mechanisms associated with other DPRs.

Synaptic dysfunction refers to a broad range of defects in the morphological and biochemical properties of the synapse that result in alterations to neuronal activity[428]. The synapse is a complex structure that relies on numerous highly specialised protein complexes regulated spatially and temporally to allow synaptic plasticity. Impairment of normal synaptic function is implicated in epilepsy and neurodegeneration, as well as other neurodegenerative diseases[399,428]. There is evidence to support the idea of synaptic dysfunction as a common feature across FTD/ALS spectrum disorders. Significant synapse loss was found in the prefrontal cortex of sporadic ALS patients[272]. Furthermore, models of other genetic causes of FTD/ALS, such as *FUS* mutations,

UBQLN2, and *VCP*, displayed morphological synaptic defects including decreased dendritic spine density, reduced synapse formation, and synapse loss[429-431].

Synaptic dysfunction has been reported in *C9orf72* models: expression of GA in primary mouse cortical neurons resulted in a reduction in dendritic arborisation linked to the coaggregation of transport factor Unc119[158], and a (G4C2)48 reduced dendritic branching in rat spinal cord neurons and *Drosophila*[191]. The *Drosophila* NMJ is a well-utilised model synapse, and *C9orf72*-FTD/ALS fly models have consistently captured motor dysfunction linked to the repeat expansion. Structural abnormalities, such as change in the number synaptic boutons, active zones, increased levels of postsynaptic glutamate receptor subunits have been found in flies expressing the pure repeat and arginine rich DPRs[157,163,277]. Synaptic defects are an underlying cause of excitotoxicity, a mechanism implicated in multiple neurodegenerative diseases[273]. Briefly, excitotoxicity occurs when excess glutamate in the synaptic cleft leads to overactivation of post-synaptic glutamate receptors, which in turn triggers a molecular cascade resulting in cell death. Excitotoxicity is one of the major mechanisms proposed to contribute to motor neuron loss in ALS[432]. Indeed, hyperexcitability of the cortex has been demonstrated in almost all ALS cases[333], and it has been suggested that excitotoxicity could be an early event in *C9orf72* pathogenesis, leading to synapse and axon degeneration with ageing[220]. Hyperexcitability is also tightly linked to epileptiform seizures[433]. Changes in GABA receptor expression, K^+ channel function, voltage gated Ca^{2+} channel permeability, and AMPA receptor permeability are amongst the main mechanisms proposed to alter excitability and excitotoxicity[271]. In addition to synaptic proteins and neuronal morphology, glia play a significant role in maintaining synaptic integrity; they are responsible for mediating neurotransmitter concentrations, eliminating damaged synapses, and maintaining the myelin sheath[434]. Failure to clear glutamate from the synaptic cleft due to loss of astrocytic glutamate transporters has been proposed as a non-cell autonomous mechanism for ALS pathogenesis[435].

There is some evidence to suggest that the *C9orf72* mutation enhances vulnerability of neurons to excitotoxicity. Pure repeats expressed in mutant iPSC-derived motor neurons caused increased GluA1 AMPA receptor expression, leading to enhanced vulnerability to excitotoxicity[274]. Additionally, expression of PR36 or GR36 in *Drosophila* glutamatergic neurons led to an increase in active zones and corresponding increase in glutamate release and intracellular calcium[220]. Neurodegenerative phenotypes were observed, as well as reduced lifespan, demonstrating a mechanism of synaptic dysfunction leading to excitotoxicity and causing neurodegeneration in a non-cell autonomous manner[220].

Synaptic neuroplasticity, functional adaptations of neural circuits to changes during learning and memory, environmental changes and brain damage, is facilitated by

dendritic spine growth and synaptogenesis. Recently, a reduction in C9orf72 protein levels in mice was shown to impair long term potentiation in the brain, suggesting that *C9orf72* haploinsufficiency may contribute to loss of synaptic plasticity in *C9orf72*-related FTD/ALS[436]. Mitochondria play a vital role in this process; synaptic plasticity involves changes to mitochondrial function and expression in order to respond to changing energy requirements[437]. Mitochondria are highly abundant at axonal terminals and dendrites and play an important role in regulating calcium homeostasis, removing calcium from the cytoplasm in response to Ca^{2+} influx, and release calcium during synaptic transmission[438]. Furthermore, in response to synaptic stimulation, mitochondria relocate toward dendrites. Aggregation of mitochondria in dendrites stimulates new synapse formation and a reduction in mitochondria in dendrites has been shown to result in a loss of synapses and inhibition of dendritic growth[425,439]. Therefore, mitochondria play a vital role in maintaining synaptic function.

6.5.2 Oxidative stress and mitochondrial dysfunction

In this study, mutations in mitochondrial *Sod2* were linked to an increase in seizure susceptibility in PR1000 flies. As discussed in chapter 5, mitochondrial dysfunction and oxidative stress are intrinsically linked and their role in neurodegeneration is well-documented[351-353]. In addition, mitochondrial dysfunction has been demonstrated to cause epilepsy[340], providing a link between seizures and neurodegeneration in patients and the 1000 repeat DPR models. Emerging evidence implicates SOD2 in a protective role in neurons, whereby it reduces glutamate excitotoxicity-mediated oxidative stress[440]. This provides a link between excitotoxicity and oxidative stress. It also corroborates the idea that synaptic dysfunction and excitotoxicity may occur early in disease and act as a trigger for molecular cascades involving mitochondrial dysfunction and oxidative stress. Furthermore, it suggests that both synaptic dysfunction and mitochondrial dysfunction could increase the susceptibility of neurons to other cellular stressors, and each other. The fact that PR1000 doesn't show seizures when expressed alone, but when expressed in either a *kcc* or *sod2* mutant background, is consistent with this hypothesis.

The finding that *Sod2* mutations may increase seizure susceptibility in PR1000 flies also implicates metabolic dysfunction and mitochondrial defects more widely. Given that reduction in antioxidant capacity increases seizures in PR1000 flies, it suggests that mitochondrial ROS are in some way contributing to seizure susceptibility. This corroborates previous findings from different ALS models, which show metabolic abnormalities and oxidative stress, and clinical studies which demonstrate that mitochondria from ALS patients display oxidative damage and increased ROS

production[365,370,391]. In FTD, cortical astrocytes have been implicated as having a propensity to degenerate and have a high burden of oxidative stress[366-370]. Indeed, a particular focus of research into *C9orf72* expansions and metabolic dysfunction has been on the role of astrocytes, which provide trophic support to and protect neurons from oxidative stress. *C9orf72* astrocytes exhibit downregulated antioxidant secretions, corresponding to an increase in oxidative stress in motor neurons[291]. Additionally, the expansion has been demonstrated to alter the metabolic profiles of astrocytes, reducing their ability to cope with bioenergetic stress[390]. This is an important avenue for future work using the 1000 repeat DPR models. An *in vivo* DPR model has not yet been metabolically profiled, and thus much of our understanding of metabolic alterations in ALS come from patient tissue and *in vitro* studies. In addition, manipulation of different metabolic pathways using drugs would allow us to ascertain whether DPRs are affecting metabolic flexibility when expressed in astrocytes and neurons.

In addition to astrocytic metabolic dysfunction, GR80-mediated synaptic dysfunction has been closely linked to compromised neuronal mitochondrial function in a mouse model[441]. GR accumulated in the soma and dendrites of neurons in an age-dependent manner, and was found to bind to a mitochondrial ATP-synthase subunit[441]. Oxidative stress directly resulting from mitochondrial dysfunction led to DNA damage in GR80 mice and is corroborated by *C9orf72* iPSC-derived motor neurons[170,441]. Furthermore, GR80 expressed in fly muscle was capable of entering the mitochondria and interacting with mitochondrial components to alter mitochondrial dynamics[442]. This resulted in increased ROS production and impaired ion homeostasis and metabolism. Taken together, this strongly implicates GR in mitochondrial dysfunction.

6.5.3 Axonal transport defects

In chapter 5, mutations in the microtubule binding protein *stathmin* were identified as a potential modifier for GR1000-mediated toxicity, however further investigation is required to validate these observations. Microtubules are a major component of the cytoskeleton and are essential for efficient axonal transport and there is evidence to support the involvement of microtubule dysfunction in ALS. For example, *SOD1* ALS mouse models show deficits in motor protein activity with both dynein-mediated retrograde and kinesin-mediated anterograde transport have been shown to be impaired[443-446]. In addition, axonal transport defects have been suggested a common mechanism between different genetic forms of ALS, implicated in *TARDBP*[139,447], *FUS*[139], and *C9orf72*[139,380] ALS. The likely reason for this is the selective vulnerability of motor neurons to microtubule dysfunction. Their length (they can be up to 1 m long) and axon/dendrite polarisation

means that tight control of microtubule transport along the axon is essential to maintain neuronal function. In addition to ensuring the correct spatiotemporal distribution of cargo along the axon, axonal transport facilitates long-distance communication between the cell body and the axon via signalling endosomes[448]. This communication is vital to allow the neuron to respond to its environment.

Axonal transport is emerging as a possible contributor to *C9orf72* toxicity, which supports the idea that microtubule binding proteins such as stathmin could be involved. Data from iPSC derived *C9orf72* motor neurons revealed that motor neurons have shorter axons, corroborating findings from post-mortem *C9orf72* ALS tissue[372]. Additionally, altered mitochondrial function was implicated in impaired fast axonal transport, which relies on mitochondrial ATP[449]. PR36 expression in *Drosophila* motor neurons resulted in significant stalling of mitochondria, linked to moderate locomotion defects in larvae[139]. Moreover, a recent study using iPSC derived spinal motor neurons and *Drosophila* has strengthened the link between arginine-rich DPRs and microtubule transport defects, by showing that they interact directly with microtubules and motor proteins[380]. Loss of function *C9orf72* mice also show abnormal axonal swellings in the spinal cord and NMJs, and this was linked to the loss of association between C9orf72 and Smcr8 with dynein, causing stalling of autophagosomes on microtubules[450]. This emphasises the idea that haploinsufficiency, whilst not sufficient to cause neurodegeneration, causes cellular dysfunction which potentiates gain of function toxicity, thus contributing to pathogenesis.

Axonal transport defects are posited as an early event in ALS pathogenesis, similar to excitotoxicity and mitochondrial dysfunction, and they are intrinsically linked. Axonal transport is both itself essential for the transport of mitochondria, and also heavily reliant on mitochondrial ATP to move their cargo[449]; normal synaptic function is reliant on microtubules to maintain dendritic spines[425] and synapses are major sites of energy consumption, requiring constant supply of mitochondria[451]; glutamate toxicity interferes with mitochondria dynamics via increased ROS production, which in turn further increases oxidative stress and potentiates glutamate excitotoxicity via upregulation of glutamate receptors[426,452]. Figure 6.1 summarises how DPRs may interfere with these processes and initiate a cascade of interconnected downstream pathways, ultimately leading to neuronal death.

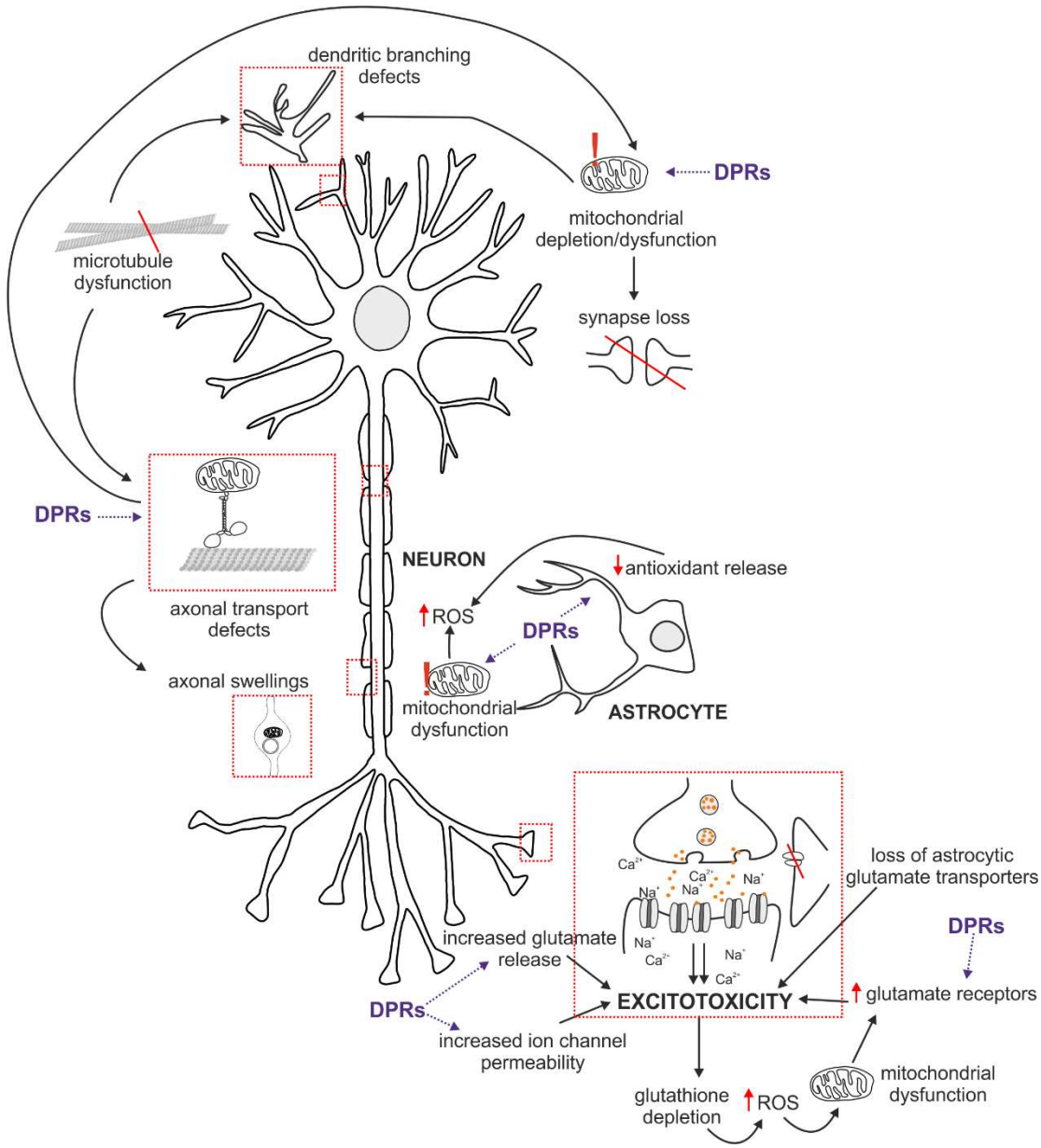

Figure 6.1 Summary of potential DPR-mediated toxic mechanisms.

DPRs may interfere with interconnected cellular processes: (1) excitotoxicity (2) axonal transport (3) mitochondrial defects, cell autonomously and non-cell autonomously and initiate a pathogenic cascade, ultimately leading to neuronal death.

6.6 Wider implications for FTD/ALS spectrum disorders and beyond

It is well established that FTD and ALS share common clinical, pathological and genetic features and are incredibly heterogeneous[147,453]. Whilst this investigation has focused on the DPRs produced from the *C9orf72* hexanucleotide expansion, it has broader implications for FTD/ALS spectrum disorders as a whole. As previously discussed, there are common mechanistic themes between genetic and sporadic forms FTD and ALS. Therefore, a robust model of *C9orf72*-related FTD/ALS will assist in elucidating in more depth the pathways involved in neurodegeneration, which will likely translate to other forms of FTD/ALS. Furthermore, throughout this study we have observed the impact of ageing in modelling DPR toxicity. This highlights the importance of age in model systems and can be applied across the FTD/ALS spectrum and to most neurodegenerative disease models. Regardless of the genetic model used, it is important to consider that important phenotypes may be missed if it cannot be aged. Additionally, despite the difficulties previously documented[197], the 1000 repeat DPR constructs have remained stable in the genome for over three years (~100 generations). We speculate that this is due to the transgene insertion site, as it is flanked by lncRNAs, which have genome stabilising properties[232,233]. This could have implications for modelling other repeat expansion disorders, or any model which involves inherently unstable DNA constructs.

6.7 Future research

In addition to the ideas for future research proposed throughout, there are key themes and unanswered questions which these DPR models are ideally placed to address. These will be discussed, along with scope for improving the relevance and utility of the model.

6.7.1 How does DPR expression affect neurophysiology?

This study used the larval NMJ as a model synapse and uncovered different neurophysiological deficits associated with each DPR (see Table 6.1). The main limitation of this was that larvae have limited capacity to show ageing, which as previously discussed, is a crucial aspect of FTD/ALS. To build on this, we could explore electrophysiology in different systems. Adult flies both *in vivo* and *ex vivo* provide the opportunity to test how neurophysiological function varies with age, and whether the same age-related decline is observed in the arginine-rich DPRs as is observed in the climbing assay. Furthermore, there is evidence that neuronal hyperexcitability is an early event in disease pathogenesis, and testing young and old adult flies would help elucidate

if DPRs play a role in this. It is possible to patch clamp individual neurons in adult flies, as described by Azevedo et al. 2020[454], and this would allow us to monitor neuronal function throughout ageing. To further explore neurophysiological function, patch clamping neurons cultured from larvae or embryos would facilitate isolation of the role of a single ion channel, although this would be limited in terms of ageing. Together, combined with the genetic tractability of *Drosophila*, we could dissect the neurophysiological impact of DPR expression, and the targets we identified in the seizure screen could be explored. In particular, *kcc*¸ which is an ion channel directly involved in synaptic function. Moreover, a multielectrode array could be used with cultured neurons to explore network properties, which have been implicated in *C9orf72* FTD/ALS previously[275].

6.7.2 How does DPR co-expression affect localisation and what is the impact for previously established mechanisms?

This study is one of only two *Drosophila* studies looking at the effect of DPR co-expression. Our findings indicate that DPRs may interact and thus produce different phenotypes than when they are expressed alone, highlighting the importance of co-expression experiments. This is a key area for further exploration using these models. The downstream consequences of DPR-DPR interactions on downstream mechanisms is poorly understood. Previous studies have suggested that GA is capable of sequestering arginine-rich DPRs, neutralising their toxicity[193,294]. This is not corroborated by the findings of this study, where GA exacerbates PR and GR toxicity. This could be because at a length of over 1000 repeats, the intermolecular interactions are considerably different and thus either GA does not sequester arginine-rich DPRs, or it does but this does not prevent PR or GR from causing downstream toxicity. Therefore, it is important to build on this work and previous studies to investigate the impacts of co-expression in more detail.

Firstly, the impact on DPR morphology and localisation must be elucidated, and this requires alternatively tagged DPRs to be generated. Building on previous work by Darling et al. (2019), who showed that PR50 and GA50 interacted to form disordered aggregates, we could investigate the effect of combining DPRs *in vivo* and investigate how morphology and colocalisation may vary with ageing. In addition, new fly lines carrying DPR transgenes inserted into a different genomic location would allow more than 2 DPRs to be expressed at once. It would also be interesting to see if expression of one DPR in a glial subset could influence the pathology of another DPR expressed in neurons. This would involve generating flies with DPR constructs under the promoter of

a different driver system, such as the *LexA* system[455]. This would also facilitate investigations into cell autonomous vs non-autonomous modes of toxicity. Whilst previous studies have indicated that *C9orf72* astrocytes are capable of disrupting the synaptic function of motor neurons in a non-cell autonomous manner[456], and that GA175 was capable of inhibiting the proteasome non-cell autonomously *in vitro*, the effect of co-expressing different DPRs in a similar system has not been explored. Alternatively, co-expression in two different cell types could be investigated *in vitro* by co-culturing embryos expressing different DPRs under the control of different *Gal4* drivers. This would circumvent the need to generate new fly lines with different driver systems.

6.7.3 Can DPRs spread between cells and how does this influence pathogenesis?

A prion-like transmission hypothesis, whereby unfolded proteins transmit between neurons via synapses, has been proposed for different neurodegenerative diseases, including *C9orf72*-FTD/ALS[457]. This hypothesis suggests that disease starts in the brain and spinal cord neurons, and spreads to distal motor neurons and extra motor areas, and is consistent with cortical hyperexcitability as an early clinical marker of FTD/ALS[336]. Although attempts were made to investigate the spreading capacity of 1000 repeat DPRs in the *Drosophila* brain, results were inconclusive (see 4.2.4). Nevertheless, there are several studies, including in *Drosophila* adult brains, that suggest DPRs, in particular GA, has the potential for cell-cell transmission[156,216,252]. It has also been suggested that GA can inhibit the proteasome non-cell autonomously by cell-to-cell transmission[252]. However, the length of GA used in these studies was much shorter than found in patients (up to 200 repeats), and so it is important to test whether GA1000 would have the same propensity to spread. In the fly brain, GA was shown to spread in a length-dependent manner up to 200 repeats, but this does not mean that spreading capacity will increase with ever increasing length. Therefore, it is important to develop a method to try and replicate these findings in our models. For this, we could use a *Gal4* driver that expressed in a very small set of neurons, or potentially just one neuron. This would be easier to mark with either a fluorescent reporter, or an antibody, to clearly define where the DPRs were expressed and if they had spread.

Westergard et al. (2016) showed that DPRs are capable of spreading between cortical neurons and astrocytes *in vitro* in both a contact dependent and independent manner. Further investigation into the mechanism of contact independent transmission revealed that GA50, and to a lesser extent AP50, GR50 and GP50 were spreading in an exosome-dependent manner[285]. Building on this, and to establish whether this is maintained at a

longer repeat length, *Drosophila* primary neurons from flies pan-neuronally expressing 1000 repeat DPRs could be cultured in transwell inserts and later placed in wells containing neurons from wild type flies. Detection of DPRs in the wild type neurons would then indicate DPR transmission. The advantages of this method are twofold: compared to co-culturing one cell type with another, *Drosophila* primary cultures have mixed cell populations which better reflects the complexity of the brain; compared to *in vivo* experiments, *Drosophila* primary cultures would facilitate single cell resolution imaging and the ability to determine if the transmission is contact independent. An alternative mechanism to exosome-mediated spread is that phagocytic glia act as obligatory intermediates, which has been observed in *Drosophila* models expressing mutant *huntingtin*[458], or that cells are dying and leaving DPRs in the cell debris, which can subsequently be "mopped up" by other cells.

6.7.4 Is the DPR interactome affected by age, repeat length or co-expression, and what are the ramifications for future mechanistic studies?

There is much we still do not fully understand about how DPRs interact with cellular components and influence gene expression. Interactome screens in different DPR models have implicated several binding partners in DPR-mediated toxicity, including splicing factors[459], nuclear transport factors[415,460], proteasomal components[158], and ribosomal proteins[74,249] and RNA binding proteins[74,461]. However, these studies use short repeat DPRs up to 150 repeat units. The interactions between 1000 repeat DPRs and cellular components may differ due to changes in their biophysical properties. Co-immunoprecipitation experiments followed by mass spectrometry analysis would reveal whether the 1000 repeat DPRs interact with the same binding partners as the shorter DPRs, which would have implications for the field in terms of which mechanistic pathways are most physiologically relevant. Furthermore, we can age these models to a physiologically relevant age, and assess their interactomes at young and old ages. It is likely physiological ageing would impact the cellular environment and therefore it is possible that DPRs may interact with different proteins at different time points. It is also important to consider that co-expression of the DPRs may affect their ability to bind certain proteins. Indeed, previous studies have suggested that GA is capable of sequestering arginine-rich DPRs and this ablates the toxicity associated with PR and GR[193,294]. This is consistent with the idea that sequestration of PR and GR alters their ability to interact with cellular proteins. Therefore, it would be useful to examine the interactome of DPRs when expressed in different combinations, as this will have implications for the field, in terms of which pathways may be more pathologically relevant.

6.7.5 How does the transcriptome associated with each DPR compare to post-mortem brain tissue and iPSC-derived motor neurons?

In addition to interactome profiling, transcriptomics would be useful to elucidate pathways that are dysregulated in response to DPR expression throughout the flies' lifespan. A previous study using patient brain tissue uncovered distinct brain transcriptome profiles associated with *C9orf72* and sporadic ALS cases and network analysis and gene ontology analysis revealed divergent pathways[462]. In particular, RNA processing defects were implicated in *C9orf72*-ALS but not sporadic cases. However, there is a question as to the relevance of RNA sequencing analysis of end stage disease because any transcriptional changes occurring earlier in disease progression are missed. Another study using iPSC-derived motor neurons found that mitochondrial calcium buffering defects were common in the transcriptomic profile of both *C9orf72* and *TARDBP* FTD/ALS[463].

There are currently no published studies that have performed RNA sequencing relating to the expression of individual DPRs. This experiment, using 1000 repeat DPRs either expressed individual or concomitantly in *Drosophila*, is a potential future experiment that would provide a wealth of information about the impact of DPR expression *in vivo*. Any pathways that are highlighted in the analysis could then be validated *in vivo* using the plethora of tools available in *Drosophila.* For example: western blotting to confirm the protein levels of proteins that are found to be down- or upregulated; immunofluorescence staining of significantly dysregulated proteins would give an insight into any changes in localisation *in vivo* and whether they are colocalising with the DPRs; genetic experiments using the *UAS/Gal4* system to pan-neuronally overexpress a gene of interest at the same time as the DPR, and seeing if this can rescue climbing or seizure defects.

6.7.6 What is the role of DPRs in different cell types?

This investigation has looked predominantly at the effects of pan-neuronal expression, but non-cell autonomous toxicity has been posited as a mechanism in *C9orf72*-related FTD/ALS pathogenesis[140,156,216,220,464]. We know from patient tissue that DPRs are found in glia and muscle[100,142], but there is less known about their toxicity in these tissues. Therefore, expressing the 1000 repeat DPRs in the relevant cell types and repeating assays such as the climbing and BS seizure assay, would give an insight into the role non-neuronal DPR expression has in neurodegeneration.

As discussed in 6.5.1, astrocytes are crucial for neuronal health and function. Indeed, astrocyte dysfunction has been shown to have a significant downstream effect on

neurodegenerative disease progression[465,466]. One of their key roles is to protect neurons from oxidative stress by secreting antioxidants, and this has been shown to be downregulated in *C9orf72* astrocytes[291]. There is also evidence to suggest that *C9orf72* mutant astrocytes cause or potentiate synaptic dysfunction in motor neurons via a non-cell autonomous mechanism not linked to DPR spreading[456]. Therefore, it would be interesting to examine the contribution of astrocytic DPR expression to the BS seizure phenotype in our *Drosophila* models, either by expressing DPRs exclusively in astrocytes or in both neurons and astrocytes. In addition, *C9orf72* expansions have been shown to reduce metabolic flexibility in astrocytes, involving defects in adenosine, fructose and glycogen metabolism[390]. This was attributed to the loss of key metabolic enzymes, but precisely how the expansion causes this remains unclear. Furthermore, the role of DPRs in metabolic defects in astrocytes has yet to be elucidated this is a valuable avenue for future research using our *Drosophila* model. The metabolic profile of *ex vivo Drosophila* brains from flies expressing DPRs in astrocytes and/or neurons at different ages could be analysed and compared to that of wild type flies to look for abnormalities. Furthermore, evidence suggests that cell stress including hypoxia may alter cellular metabolic profiles. In fact, altered hypoxia responses have been implicated in ALS[467]. Therefore, to explore whether hypoxia alters metabolic profiles and downstream neurodegeneration, we could raise DPR flies in chronic hypoxic and normoxic conditions and measure any effects on their metabolic profiles and previously characterised neurodegenerative phenotypes.

DPR inclusions, as well as phosphorylated TDP-43, p62 and ubiquitin aggregates have been identified in post-mortem skeletal muscle from *C9orf72* ALS patients[100,468]. We know that denervation of motor neurons causes muscle atrophy in ALS, but it remains unclear whether skeletal muscle-restricted expression of DPRs is sufficient to drive ALS-related phenotypes. Given muscle cells are distinctly different from neurons, in particular in their capacity to regenerate, it is likely they will be differentially affected by DPR expression. Evidence from patient tissue and fly models suggests that DPRs are directly toxic to muscle: the presence of DPRs was associated with more severe muscle atrophy[100], and a *C9orf72* fly model expressing 58 pure repeats using the muscle-specific driver *MHC-GAL4* showed age-dependent defects in indirect flight muscle resulting in permanent abnormal wing positioning[163]. However, the cellular impact of DPR expression in muscle has yet to be fully elucidated. One recent study showed that GR80 (and not any of the other DPRs of equivalent length) expressed in *Drosophila* muscle enters the mitochondria and interacts with mitochondrial components to alter mitochondrial dynamics[442]. This results in impaired ion homeostasis and metabolism, and ultimately reduces muscle integrity. This was effectively restored with nigericin feeding[442]. Nigericin acts to dissipate the change in pH across the inner mitochondrial

membrane and has been shown to reduce ROS production[469]. This could be repeated and explored further using our 1000 repeat *Drosophila* models. The first step would be to characterise any phenotypes associated with muscle-specific DPR1000 expression, such as abnormal wing posture, and altered climbing ability. We could then investigate mitochondrial function and dynamics using the plethora of tools available in *Drosophila*: quantify ROS levels with DCFH fluorescence and mito-SOX staining; examine mitochondrial morphology using fluorescent mitochondrial reporters and/or TEM; investigate whether DPRs were present inside mitochondria using western blots of mitochondria purified from fly muscle. We could also consider investigating whether nigericin feeding would ameliorate any of the established neurodegenerative phenotypes observed in DPR expressing flies.

6.8 Conclusion

In conclusion, although there remain many unanswered questions relating to the role of DPRs in *C9orf72*-related FTD/ALS, the development of these models offers a new tool to continue to unravel the mechanisms involved. This investigation has highlighted the importance of studying the contribution of all DPRs to pathogenesis, the role of age in DPR-mediated toxicity, and the necessity of considering how co-expression may affect phenotypes. The capacity for ageing and the pathologically relevant repeat length of these models, combined with the genetic tractability of *Drosophila,* offers a useful system to dissect the molecular mechanisms underpinning *C9orf72*-related FTD/ALS, and for future drug screening.

6.9 Summary of findings

The key results and conclusions of this study are summarised as follows:

1. Novel 1000 repeat DPR *Drosophila* models of *C9orf72*-FTD/ALS have been established and constructs found to be stable for over 100 generations in different genetic backgrounds.
2. Stability of the long alternative codon DPR sequence may be due to its transgenic insertion site, which is flanked by lncRNA.
3. DPRs do not affect viability when expressed in the nervous system, but have differential effects on longevity.
4. Morphology and localisation of each DPR in the nervous system is reminiscent of inclusions observed in patients.
5. Morphology and localisation appear to be dependent on both length and the system in which they are expressed.
6. DPRs show a dose dependent toxicity.
7. Distinct larval NMJ phenotypes and electrophysiological dysfunction are observed with pan-neuronal expression of DPRs.
8. Each DPR displays distinct age-dependent climbing defects when expressed pan-neuronally in adults.
9. Co-expression of DPRs confers different levels of toxicity compared to expression of an individual or homozygous DPR.
10. GR expression causes an incompletely penetrant bang-sensitive seizure phenotype which is potentiated by co-expression with the other DPRs.
11. *kcc*, *stathmin*, and *Sod2* were identified as potential modifiers of DPR-mediated seizure susceptibility but this requires further validation.

Appendices

AP1000

gaattcggatgtagaccATG[GCCCCTGCTCCTGCCCCTGCGCCGGCTCCAGCTCCAGCGCCTGCACCA
GCCCCTGCTCCTGCACCAGCACCAGCACCGGCGCCAGCTCCAGCACCAGCACCCGCTCCTGCTCCTGCT
CCCGCTCCAGCACCAGCGCCTGCTCCTGCTCCGGCCCCAGCTCCTGCTCCAGCGCCCGCGCCGGCCCCG
GCCCCAGCACCGGCCCCAGCTCCGGCCCCTGCTCCTGCCCCTGCGCCGGCTCCAGCTCCAGCGCCTGCA
CCAGCCCCTGCTCCTGCACCAGCACCAGCACCGGCGCCAGCTCCAGCACCAGCACCCGCTCCTGCTCCT
GCTCCCGCTCCAGCACCAGCGCCTGCTCCTGCTCCGGCCCCAGCTCCTGCTCCAGCGCCCGCGCCGGCC
CCGGCCCCAGCACCGGCCCCAGCTCCGGCCCCT]GTCTTCCAACGGGATCCACCGGTCGCCACCATGGT
GAGCAAGGGCGAGGAGCTGTTCACCGGGGTGGTGCCCATCCTGGTCGAGCTGGACGGCGACGTAAACGG
CCACAAGTTCAGCGTGTCCGGCGAGGGCGAGGGCGATGCCACCTACGGCAAGCTGACCCTGAAGTTCAT
CTGCACCACCGGCAAGCTGCCCGTGCCCTGGCCCACCCTCGTGACCACCCTGACCTACGGCGTGCAGTG
CTTCAGCCGCTACCCCGACCACATGAAGCAGCACGACTTCTTCAAGTCCGCCATGCCCGAAGGCTACGT
CCAGGAGCGCACCATCTTCTTCAAGGACGACGGCAACTACAAGACCCGCGCCGAGGTGAAGTTCGAGGG
CGACACCCTGGTGAACCGCATCGAGCTGAAGGGCATCGACTTCAAGGAGGACGGCAACATCCTGGGGCA
CAAGCTGGAGTACAACTACAACAGCCACAACGTCTATATCATGGCCGACAAGCAGAAGAACGGCATCAA
GGTGAACTTCAAGATCCGCCACAACATCGAGGACGGCAGCGTGCAGCTCGCCGACCACTACCAGCAGAA
CACCCCCATCGGCGACGGCCCCGTGCTGCTGCCCGACAACCACTACCTGAGCACCCAGTCCGCCCTGAG
CAAAGACCCCAACGAGAAGCGCGATCACATGGTCCTGCTGGAGTTCGTGACCGCCGCCGGGATCACTCT
CGGCATGGACGAGCTGTACAAGtaaagcggccgcgactctaga

GA1000

gaattcggatgtagaccATG[GGTGCTGGCGCGGGAGCAGGCGCTGGTGCTGGTGCAGGAGCGGGTGCG
GGAGCTGGTGCCGGCGCAGGAGCTGGAGCTGGCGCAGGAGCTGGTGCTGGGGCTGGTGCCGGTGCCGGT
GCTGGAGCTGGAGCAGGAGCAGGCGCGGGTGCAGGGGCCGGAGCGGGTGCTGGTGCTGGTGCTGGAGCG
GGAGCGGGCGCTGGAGCCGGCGCCGGTGCTGGCGCGGGAGCAGGCGCTGGTGCTGGTGCAGGAGCGGGT
GCGGGAGCTGGTGCCGGCGCAGGAGCTGGAGCTGGCGCAGGAGCTGGTGCTGGGGCTGGTGCCGGTGCC
GGTGCTGGAGCTGGAGCAGGAGCAGGCGCGGGTGCAGGGGCCGGAGCGGGTGCTGGTGCTGGTGCTGGA
GCGGGAGCGGGCGCTGGAGCCGGCGCCGGTGCT]GTCTTCCAACGGGATCCACCGGTCGCCACCATGGT
GAGCAAGGGCGAGGAGCTGTTCACCGGGGTGGTGCCCATCCTGGTCGAGCTGGACGGCGACGTAAACGG
CCACAAGTTCAGCGTGTCCGGCGAGGGCGAGGGCGATGCCACCTACGGCAAGCTGACCCTGAAGTTCAT
CTGCACCACCGGCAAGCTGCCCGTGCCCTGGCCCACCCTCGTGACCACCCTGACCTACGGCGTGCAGTG
CTTCAGCCGCTACCCCGACCACATGAAGCAGCACGACTTCTTCAAGTCCGCCATGCCCGAAGGCTACGT
CCAGGAGCGCACCATCTTCTTCAAGGACGACGGCAACTACAAGACCCGCGCCGAGGTGAAGTTCGAGGG
CGACACCCTGGTGAACCGCATCGAGCTGAAGGGCATCGACTTCAAGGAGGACGGCAACATCCTGGGGCA
CAAGCTGGAGTACAACTACAACAGCCACAACGTCTATATCATGGCCGACAAGCAGAAGAACGGCATCAA
GGTGAACTTCAAGATCCGCCACAACATCGAGGACGGCAGCGTGCAGCTCGCCGACCACTACCAGCAGAA
CACCCCCATCGGCGACGGCCCCGTGCTGCTGCCCGACAACCACTACCTGAGCACCCAGTCCGCCCTGAG

CAAAGACCCCAACGAGAAGCGCGATCACATGGTCCTGCTGGAGTTCGTGACCGCCGCCGGGATCACTCT
CGGCATGGACGAGCTGTACAAGtaaagcggccgcgactctaga

GR1000

gaattcggatgtagaccATG[GGCAGAGGACGCGGTCGGGGACGAGGAAGAGGACGGGGTAGAGGGCGA
GGTCGCGGCCGTGGTAGAGGCAGAGGTCGTGGGAGAGGCAGGGGTCGCGGACGTGGACGGGGAAGGGGA
CGAGGTAGAGGCAGGGGACGCGGACGAGGGAGAGGACGGGGCCGTGGTCGAGGGAGAGGTAGAGGCCGA
GGTCGAGGCCGAGGACGAGGACGCGGCAGAGGACGCGGTCGGGGACGAGGAAGAGGACGGGGTAGAGGG
CGAGGTCGCGGCCGTGGTAGAGGCAGAGGTCGTGGGAGAGGCAGGGGTCGCGGACGTGGACGGGGAAGG
GGACGAGGTAGAGGCAGGGGACGCGGACGAGGGAGAGGACGGGGCCGTGGTCGAGGGAGAGGTAGAGGC
CGAGGTCGAGGCCGAGGACGAGGACGCGGCA]GTCTTCCAACGGGATCCACCGGTCGCCACCATGGTGA
GCAAGGGCGAGGAGCTGTTCACCGGGGTGGTGCCCATCCTGGTCGAGCTGGACGGCGACGTAAACGGCC
ACAAGTTCAGCGTGTCCGGCGAGGGCGAGGGCGATGCCACCTACGGCAAGCTGACCCTGAAGTTCATCT
GCACCACCGGCAAGCTGCCCGTGCCCTGGCCCACCCTCGTGACCACCCTGACCTACGGCGTGCAGTGCT
TCAGCCGCTACCCCGACCACATGAAGCAGCACGACTTCTTCAAGTCCGCCATGCCCGAAGGCTACGTCC
AGGAGCGCACCATCTTCTTCAAGGACGACGGCAACTACAAGACCCGCGCCGAGGTGAAGTTCGAGGGCG
ACACCCTGGTGAACCGCATCGAGCTGAAGGGCATCGACTTCAAGGAGGACGGCAACATCCTGGGGCACA
AGCTGGAGTACAACTACAACAGCCACAACGTCTATATCATGGCCGACAAGCAGAAGAACGGCATCAAGG
TGAACTTCAAGATCCGCCACAACATCGAGGACGGCAGCGTGCAGCTCGCCGACCACTACCAGCAGAACA
CCCCCATCGGCGACGGCCCCGTGCTGCTGCCCGACAACCACTACCTGAGCACCCAGTCCGCCCTGAGCA
AAGACCCCAACGAGAAGCGCGATCACATGGTCCTGCTGGAGTTCGTGACCGCCGCCGGGATCACTCTCG
GCATGGACGAGCTGTACAAGtaaagcggccgcgactctaga

PR1000

gaattcggatgtagaccATG[GCCCCTGCTCCTGCCCCTGCGCCGGCTCCAGCTCCAGCGCCTGCACCA
GCCCCTGCTCCTGCACCAGCACCAGCACCGGCGCCAGCTCCAGCACCAGCACCCGCTCCTGCTCCTGCT
CCCGCTCCAGCACCAGCGCCTGCTCCTGCTCCGGCCCCAGCTCCTGCTCCAGCGCCCGCGCCGGCCCCG
GCCCCAGCACCGGCCCCAGCTCCGGCCCCTGCTCCTGCCCCTGCGCCGGCTCCAGCTCCAGCGCCTGCA
CCAGCCCCTGCTCCTGCACCAGCACCAGCACCGGCGCCAGCTCCAGCACCAGCACCCGCTCCTGCTCCT
GCTCCCGCTCCAGCACCAGCGCCTGCTCCTGCTCCGGCCCCAGCTCCTGCTCCAGCGCCCGCGCCGGCC
CCGGCCCCAGCACCGGCCCCAGCTCCGGCCCCT]GTCTTCCAACGGGATCCACCGGTCGCCACCATGGT
GAGCAAGGGCGAGGAGCTGTTCACCGGGGTGGTGCCCATCCTGGTCGAGCTGGACGGCGACGTAAACGG
CCACAAGTTCAGCGTGTCCGGCGAGGGCGAGGGCGATGCCACCTACGGCAAGCTGACCCTGAAGTTCAT
CTGCACCACCGGCAAGCTGCCCGTGCCCTGGCCCACCCTCGTGACCACCCTGACCTACGGCGTGCAGTG
CTTCAGCCGCTACCCCGACCACATGAAGCAGCACGACTTCTTCAAGTCCGCCATGCCCGAAGGCTACGT
CCAGGAGCGCACCATCTTCTTCAAGGACGACGGCAACTACAAGACCCGCGCCGAGGTGAAGTTCGAGGG
CGACACCCTGGTGAACCGCATCGAGCTGAAGGGCATCGACTTCAAGGAGGACGGCAACATCCTGGGGCA
CAAGCTGGAGTACAACTACAACAGCCACAACGTCTATATCATGGCCGACAAGCAGAAGAACGGCATCAA
GGTGAACTTCAAGATCCGCCACAACATCGAGGACGGCAGCGTGCAGCTCGCCGACCACTACCAGCAGAA
CACCCCCATCGGCGACGGCCCCGTGCTGCTGCCCGACAACCACTACCTGAGCACCCAGTCCGCCCTGAG

CAAAGACCCCAACGAGAAGCGCGATCACATGGTCCTGCTGGAGTTCGTGACCGCCGCCGGGATCACTCT
CGGCATGGACGAGCTGTACAAGtaaagcggccgcgactctaga

Appendix 1 DPR Sequences.

The regions within the [ ] show the DPR core sequences. These sequences are repeated up to full length (see Callister et al., 2016[153]). For practicality only the core sequence is shown. Green highlighted region shows eGFP tag.

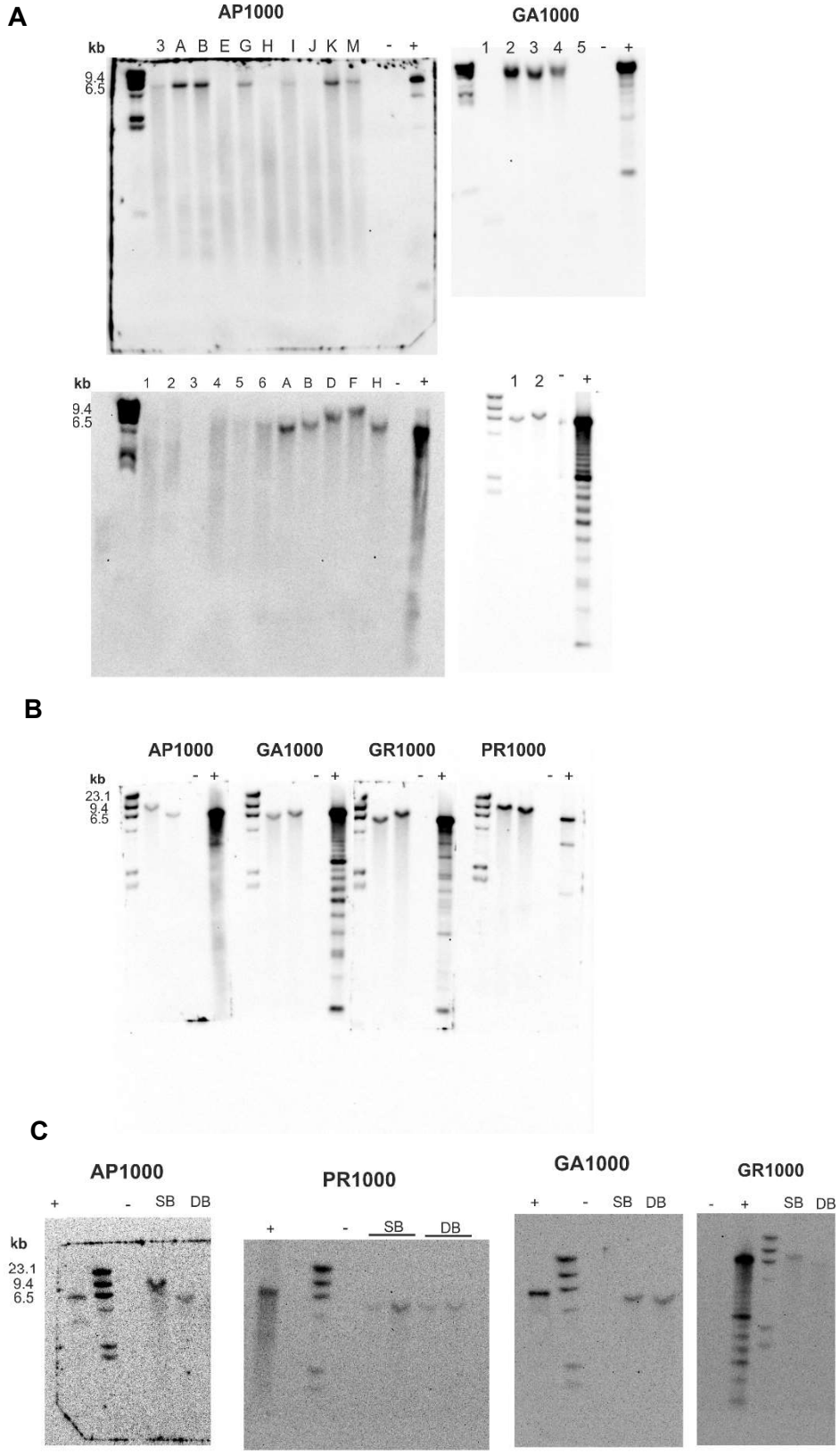

Appendix 2 Uncropped Southern blots corresponding to the blots in Figure 3.2.

Appendix 3 Pairwise comparisons associated with Figure 3.3 E.

Survival Log-Rank (Mantel-Cox) with Bonferroni correction of the *p* value : * <0.01, * **<0.001, *** <0.0002 (K=5),

	***p* value**	
Wild type vs GFP	0.3040	ns
Wild type vs AP1000	< 0.0001	***
Wild type vs GA1000	0.001	**
Wild type vs PR1000	0.0735	ns
Wild type vs GR1000	< 0.0001	***

Appendix 4 Pairwise comparisons of % bang-sensitive seizures

Flies pan-neuronally co-expressing DPRs at 14 days post-eclosion (tapping experiment – Figure 5.4 A) using a post-hoc chi-square test. Bonferroni correction of the *p* value: * < 0.00278, ** < 0.00056, *** < 0.000056 (K=18)

	***p* value**	
AP/GFP vs AP/GR	0.0017	*
AP/GFP vs AP/PR	NA	ns
AP/GR vs AP/PR	0.0071	ns
GA/GFP vs GA/PR	0.9727	ns
GA/GFP vs GA/GR	0.0218	ns
GA/PR vs GA/GR	0.0744	ns
PR/GFP vs PR/AP	NA	ns
PR/GFP vs PR/GA	0.4445	ns
PR/GFP vs PR/GR	0.0021	*
PR/AP vs PR/GA	0.4742	ns
PR/AP vs PR/GR	0.0038	ns
PR/GA vs PR/GR	0.0005	**
GR/GFP vs GR/AP	0.0005	**
GR/GFP vs GR/GA	0.0243	ns
GR/GFP vs GR/PR	0.0002	**
GR/AP vs GR/GA	0.0816	ns
GR/AP vs GR/PR	0.7879	ns
GR/PR vs GR/GA	0.0352	ns

Appendix 5 Pairwise comparisons of % bang-sensitive seizures

Flies pan-neuronally co-expressing DPRs at 14 days post-eclosion (vortexing experiment – Figure 5.4 B) using a post-hoc chi-square test. Bonferroni correction of the *p* value: * < 0.00278, ** < 0.00056, *** < 0.000056 (K=18)

	***p* value**	
AP/GFP vs AP/GR	0.00039660	**
AP/GFP vs AP/PR	0.20000000	Ns
AP/GR vs AP/PR	0.21000000	ns
GA/GFP vs GA/PR	0.09287000	ns
GA/GFP vs GA/GR	0.00000001	***
GA/PR vs GA/GR	0.00002213	***
PR/GFP vs PR/AP	0.05063000	ns
PR/GFP vs PR/GA	0.02239000	ns
PR/GFP vs PR/GR	0.00000009	***
PR/AP vs PR/GA	0.67880000	ns
PR/AP vs PR/GR	0.00007261	**
PR/GA vs PR/GR	0.00027330	**
GR/GFP vs GR/AP	0.13920000	ns
GR/GFP vs GR/GA	0.00029050	**
GR/GFP vs GR/PR	0.00257000	*
GR/AP vs GR/GA	0.06977000	ns
GR/AP vs GR/PR	0.15200000	ns
GR/PR vs GR/GA	0.83270000	ns

References

1 Mackenzie, I. R. A., Frick, P. & Neumann, M. The neuropathology associated with repeat expansions in the C9ORF72 gene. *Acta Neuropathologica* **127**, 347-357, doi:10.1007/s00401-013-1232-4 (2014).

2 Wittenberg, R., Bo, H., Barraza-Araiza, L. & Rehill, A. Projections of older people with dementia and costs of dementia care in the United Kingdom 2019–2040. (2019).

3 Livingston, G. *et al.* Dementia prevention, intervention, and care: 2020 report of the Lancet Commission. *Lancet* **396**, 413-446, doi:10.1016/s0140-6736(20)30367-6 (2020).

4 Ratnavalli, E., Brayne, C., Dawson, K. & Hodges, J. R. The prevalence of frontotemporal dementia. *Neurology* **58**, 1615-1621, doi:10.1212/wnl.58.11.1615 (2002).

5 Ringholz, G. M. *et al.* Prevalence and patterns of cognitive impairment in sporadic ALS. *Neurology* **65**, 586-590, doi:10.1212/01.wnl.0000172911.39167.b6 (2005).

6 Snowden, J. S., Neary, D. & Mann, D. M. A. Frontotemporal dementia. *British Journal of Psychiatry* **180**, 140-143, doi:10.1192/bjp.180.2.140 (2002).

7 Harvey, R. J., Skelton-Robinson, M. & Rossor, M. N. The prevalence and causes of dementia in people under the age of 65 years. *Journal of Neurology Neurosurgery and Psychiatry* **74**, 1206-1209, doi:10.1136/jnnp.74.9.1206 (2003).

8 Neary, D. *et al.* Frontotemporal lobar degeneration - A consensus on clinical diagnostic criteria. *Neurology* **51**, 1546-1554 (1998).

9 Cairns, N. J. *et al.* Neuropathologic diagnostic and nosologic criteria for frontotemporal lobar degeneration: consensus of the Consortium for Frontotemporal Lobar Degeneration. *Acta Neuropathologica* **114**, 5-22, doi:10.1007/s00401-007-0237-2 (2007).

10 McKhann, G. M. *et al.* Clinical and pathological diagnosis of Frontotemporal Dementia - Report of the work group on Frontotemporal Dementia and Pick's disease. *Archives of Neurology* **58**, 1803-1809, doi:10.1001/archneur.58.11.1803 (2001).

11 Hodges, J. R., Davies, R., Xuereb, J., Kril, J. & Halliday, G. Survival in frontotemporal dementia. *Neurology* **61**, 349-354 (2003).

12 Borroni, B. *et al.* Establishing short-term prognosis in Frontotemporal Lobar Degeneration spectrum: Role of genetic background and clinical phenotype. *Neurobiology of Aging* **31**, 270-279, doi:10.1016/j.neurobiolaging.2008.04.004 (2010).

13 Coyle-Gilchrist, I. T. S. *et al.* Prevalence, characteristics, and survival of frontotemporal lobar degeneration syndromes. *Neurology* **86**, 1736-1743 (2016).

14 Snowden, J. S. *et al.* Distinct clinical and pathological characteristics of frontotemporal dementia associated with C9ORF72 mutations. *Brain* **135**, 693-708, doi:10.1093/brain/awr355 (2012).

15 Woolley, J. D. *et al.* Frontotemporal dementia and mania. *American Journal of Psychiatry* **164**, 1811-1816, doi:10.1176/appi.ajp.2007.07061001 (2007).

16 Miller, B. L. *et al.* A study of the Lund-Manchester research criteria for frontotemporal dementia: Clinical and single-photon emission CT correlations. *Neurology* **48**, 937-942, doi:10.1212/wnl.48.4.937 (1997).

17 Miller, B. L., Boone, K., Cummings, J. L., Read, S. L. & Mishkin, F. Functional correlates of musical and visual ability in frontotemporal dementia. *British Journal of Psychiatry* **176**, 458-463, doi:10.1192/bjp.176.5.458 (2000).

18 Chio, A. *et al.* Prognostic factors in ALS: A critical review. *Amyotrophic Lateral Sclerosis* **10**, 310-323, doi:10.3109/17482960802566824 (2009).

19 Chancellor, A. M., Swingler, R. J., Fraser, H., Clarke, J. A. & Warlow, C. P. Utility Of Scottish Morbidity And Mortality Data For Epidemiologic Studies Of Motor-Neuron Disease. *Journal of Epidemiology and Community Health* **47**, 116-120, doi:10.1136/jech.47.2.116 (1993).

20 Al-Chalabi, A. & Hardiman, O. The epidemiology of ALS: a conspiracy of genes, environment and time. *Nature Reviews Neurology* **9**, 617-628, doi:10.1038/nrneurol.2013.203 (2013).

21 Foster, L. A. & Salajegheh, M. K. Motor Neuron Disease: Pathophysiology, Diagnosis, and Management. *American Journal of Medicine* **132**, 32-37, doi:10.1016/j.amjmed.2018.07.012 (2019).

22 Al-Chalabi, A. *et al.* The genetics and neuropathology of amyotrophic lateral sclerosis. *Acta Neuropathologica* **124**, 339-352, doi:10.1007/s00401-012-1022-4 (2012).

23 Hern, J. E. C. *et al.* The Scottish Motor-Neuron Disease Register - A Prospective-Study Of Adult Onset Motor-Neuron Disease In Scotland - Methodology, Demography And Clinical-Features Of Incident Cases In 1989. *Journal of Neurology Neurosurgery and Psychiatry* **55**, 536-541 (1992).

24 Shellikeri, S. *et al.* The neuropathological signature of bulbar-onset ALS: A systematic review. *Neuroscience and Biobehavioral Reviews* **75**, 378-392, doi:10.1016/j.neubiorev.2017.01.045 (2017).

25 Seelaar, H., Rohrer, J. D., Pijnenburg, Y. A. L., Fox, N. C. & van Swieten, J. C. Clinical, genetic and pathological heterogeneity of frontotemporal dementia: a review. *Journal of Neurology Neurosurgery and Psychiatry* **82**, 476-486, doi:10.1136/jnnp.2010.212225 (2011).

26 Brooks, B. R., Miller, R. G., Swash, M., Munsat, T. L. & World Federation Neurology Res, G. El Escorial revisited: Revised criteria for the diagnosis of amyotrophic lateral sclerosis. *Amyotrophic Lateral Sclerosis and Other Motor Neuron Disorders* **1**, 293-299, doi:10.1080/146608200300079536 (2000).

27 Hardiman, O. *et al.* Amyotrophic lateral sclerosis. *Nature Reviews Disease Primers* **3**, 18, doi:10.1038/nrdp.2017.71 (2017).

28 Mackenzie, I. R. A. *et al.* Nomenclature and nosology for neuropathologic subtypes of frontotemporal lobar degeneration: an update. *Acta Neuropathologica* **119**, 1-4, doi:10.1007/s00401-009-0612-2 (2010).

29 Urwin, H. *et al.* FUS pathology defines the majority of tau- and TDP-43-negative frontotemporal lobar degeneration. *Acta Neuropathologica* **120**, 33-41, doi:10.1007/s00401-010-0698-6 (2010).

30 Holm, I. E., Isaacs, A. M. & Mackenzie, I. R. A. Absence of FUS-immunoreactive pathology in frontotemporal dementia linked to chromosome 3 (FTD-3) caused by mutation in the CHMP2B gene. *Acta Neuropathologica* **118**, 719-720, doi:10.1007/s00401-009-0593-1 (2009).

31 Love, S., Saitoh, T., Quijada, S., Cole, G. M. & Terry, R. D. Alz-50, Ubiquitin And Tau-Immunoreactivity Of Neurofibrillary Tangles, Pick Bodies And Lewy Bodies. *Journal of Neuropathology and Experimental Neurology* **47**, 393-405, doi:10.1097/00005072-198807000-00001 (1988).

32 de Silva, R. *et al.* An immunohistochemical study of cases of sporadic and inherited frontotemporal lobar degeneration using 3R-and 4R-specific tau monoclonal antibodies. *Acta Neuropathologica* **111**, 329-340, doi:10.1007/s00401-006-0048-x (2006).

33 Taniguchi, S. *et al.* The neuropathology of frontotemporal lobar degeneration with respect to the cytological and biochemical characteristics of tau protein. *Neuropathology and Applied Neurobiology* **30**, 1-18, doi:10.1046/j.1365-2990.2003.0481.x (2004).

34 Shibata, N., Asayama, K., Hirano, A. & Kobayashi, M. Immunohistochemical study on superoxide dismutases in spinal cords from autopsied patients with amyotrophic lateral sclerosis. *Developmental Neuroscience* **18**, 492-498, doi:10.1159/000111445 (1996).

35 Rosen, D. R. *et al.* Mutations In Cu/Zn Superoxide-Dismutase Gene Are Associated With Familial Amyotrophic-Lateral-Sclerosis. *Nature* **362**, 59-62, doi:10.1038/362059a0 (1993).

36 Valentine, J. S. & Hart, P. J. Misfolded CuZnSOD and amyotrophic lateral sclerosis. *Proceedings of the National Academy of Sciences of the United States of America* **100**, 3617-3622, doi:10.1073/pnas.0730423100 (2003).

37 Neumann, M. *et al.* Ubiquitinated TDP-43 in frontotemporal lobar degeneration and amyotrophic lateral sclerosis. *Science* **314**, 130-133, doi:10.1126/science.1134108 (2006).

38 Winton, M. J. *et al.* Disturbance of nuclear and cytoplasmic TAR DNA-binding protein (TDP-43) induces disease-like redistribution, sequestration, and aggregate formation. *Journal of Biological Chemistry* **283**, 13302-13309, doi:10.1074/jbc.M800342200 (2008).

39 Neumann, M. *et al.* A new subtype of frontotemporal lobar degeneration with FUS pathology. *Brain* **132**, 2922-2931, doi:10.1093/brain/awp214 (2009).

40 Mackenzie, I. R. A. *et al.* A harmonized classification system for FTLD-TDP pathology. *Acta Neuropathologica* **122**, 111-113, doi:10.1007/s00401-011-0845-8 (2011).

41 Callister, J. B. & Pickering-Brown, S. M. Pathogenesis/genetics of frontotemporal dementia and how it relates to ALS. *Experimental Neurology* **262**, 84-90, doi:10.1016/j.expneurol.2014.06.001 (2014).

42 Chio, A. *et al.* Global Epidemiology of Amyotrophic Lateral Sclerosis: A Systematic Review of the Published Literature. *Neuroepidemiology* **41**, 118-130, doi:10.1159/000351153 (2013).

43 Rohrer, J. D. *et al.* The heritability and genetics of frontotemporal lobar degeneration. *Neurology* **73**, 1451-1456 (2009).

44 Rademakers, R., Neumann, M. & Mackenzie, I. R. Advances in understanding the molecular basis of frontotemporal dementia. *Nature Reviews Neurology* **8**, 423-434, doi:10.1038/nrneurol.2012.117 (2012).

45 Chow, T. W., Miller, B. L., Hayashi, V. N. & Geschwind, D. H. Inheritance of frontotemporal dementia. *Archives of Neurology* **56**, 817-822, doi:10.1001/archneur.56.7.817 (1999).

46 Wood, E. M. *et al.* Development and Validation of Pedigree Classification Criteria for Frontotemporal Lobar Degeneration. *Jama Neurology* **70**, 1411-1417, doi:10.1001/jamaneurol.2013.3956 (2013).

47 Goldman, J. S. *et al.* Comparison of family histories in FTLD subtypes and related tauopathies. *Neurology* **65**, 1817-1819, doi:10.1212/01.wnl.0000187068.92184.63 (2005).

48 Onyike, C. U. & Diehl-Schmid, J. The epidemiology of frontotemporal dementia. *International Review of Psychiatry* **25**, 130-137, doi:10.3109/09540261.2013.776523 (2013).

49 Arvanitakis, Z. Update on Frontotemporal Dementia. *Neurologist* **16**, 16-22, doi:10.1097/NRL.0b013e3181b1d5c6 (2010).

50 Snowden, J. S., Neary, D. & Mann, D. M. A. Autopsy proven sporadic frontotemporal dementia due to microvacuolar-type histology, with onset at 21 years of age. *Journal of Neurology Neurosurgery and Psychiatry* **75**, 1337-1339, doi:10.1136/jnnp.2003.028498 (2004).

51 Hutton, M. *et al.* Association of missense and 5 '-splice-site mutations in tau with the inherited dementia FTDP-17. *Nature* **393**, 702-705, doi:10.1038/31508 (1998).

52 Poorkaj, P. *et al.* Tau is a candidate gene for chromosome 17 frontotemporal dementia. *Annals of Neurology* **43**, 815-825, doi:10.1002/ana.410430617 (1998).

53 Baker, M. *et al.* Mutations in progranulin cause tau-negative frontotemporal dementia linked to chromosome 17. *Nature* **442**, 916-919, doi:10.1038/nature05016 (2006).

54 Cruts, M. *et al.* Null mutations in progranulin cause ubiquitin-positive frontotemporal dementia linked to chromosome 17q21. *Nature* **442**, 920-924, doi:10.1038/nature05017 (2006).

55 Renton, A. E. *et al.* A Hexanucleotide Repeat Expansion in C9ORF72 Is the Cause of Chromosome 9p21-Linked ALS-FTD. *Neuron* **72**, 257-268, doi:10.1016/j.neuron.2011.09.010 (2011).

56 DeJesus-Hernandez, M. *et al.* Expanded GGGGCC Hexanucleotide Repeat in Noncoding Region of C9ORF72 Causes Chromosome 9p-Linked FTD and ALS. *Neuron* **72**, 245-256, doi:10.1016/j.neuron.2011.09.011 (2011).

57 Benussi, L., Ghidoni, R. & Binetti, G. Progranulin Mutations are a Common Cause of FTLD in Northern Italy. *Alzheimer Disease & Associated Disorders* **24**, 308-309, doi:10.1097/WAD.0b013e3181d1bb13 (2010).

58 Rutherford, N. J. *et al.* Novel Mutations in TARDBP(TDP-43) in Patients with Familial Amyotrophic Lateral Sclerosis. *Plos Genetics* **4**, 8, doi:10.1371/journal.pgen.1000193 (2008).

59 Sreedharan, J. *et al.* TDP-43 mutations in familial and sporadic amyotrophic lateral sclerosis. *Science* **319**, 1668-1672, doi:10.1126/science.1154584 (2008).

60 Kwiatkowski, T. J. *et al.* Mutations in the FUS/TLS Gene on Chromosome 16 Cause Familial Amyotrophic Lateral Sclerosis. *Science* **323**, 1205-1208, doi:10.1126/science.1166066 (2009).

61 Deng, H. X. *et al.* Mutations in UBQLN2 cause dominant X-linked juvenile and adult-onset ALS and ALS/dementia. *Nature* **477**, 211-U113, doi:10.1038/nature10353 (2011).

62 Andersen, P. M. & Al-Chalabi, A. Clinical genetics of amyotrophic lateral sclerosis: what do we really know? *Nature Reviews Neurology* **7**, 603-615, doi:10.1038/nrneurol.2011.150 (2011).

63 Bruijn, L. I. *et al.* Aggregation and motor neuron toxicity of an ALS-linked SOD1 mutant independent from wild-type SOD1. *Science* **281**, 1851-1854, doi:10.1126/science.281.5384.1851 (1998).

64 Cozzolino, M. *et al.* Oligomerization of Mutant SOD1 in Mitochondria of Motoneuronal Cells Drives Mitochondrial Damage and Cell Toxicity. *Antioxidants & Redox Signaling* **11**, 1547-U1543, doi:10.1089/ars.2009.2545 (2009).

65 Kim, H. J. *et al.* Mutations in prion-like domains in hnRNPA2B1 and hnRNPA1 cause multisystem proteinopathy and ALS. *Nature* **495**, 467-+, doi:10.1038/nature11922 (2013).

66 Lin, K. P. *et al.* Mutational analysis of MATR3 in Taiwanese patients with amyotrophic lateral sclerosis. *Neurobiology of Aging* **36**, 2005-U2031, doi:10.1016/j.neurobiolaging.2015.02.008 (2015).

67 Skibinski, G. *et al.* Mutations in the endosomal ESCRTIII-complex subunit CHMP2B in frontotemporal dementia. *Nature Genetics* **37**, 806-808, doi:10.1038/ng1609 (2005).

68 Babst, M., Katzmann, D. J., Estepa-Sabal, E. J., Meerloo, T. & Emr, S. D. ESCRT-III: An endosome-associated heterooligomeric protein complex required for MVB sorting. *Developmental Cell* **3**, 271-282, doi:10.1016/s1534-5807(02)00220-4 (2002).

69 Johnson, J. O. *et al.* Exome Sequencing Reveals VCP Mutations as a Cause of Familial ALS. *Neuron* **68**, 857-864, doi:10.1016/j.neuron.2010.11.036 (2010).

70 Peters, O. M., Ghasemi, M. & Brown, R. H. Emerging mechanisms of molecular pathology in ALS. *Journal of Clinical Investigation* **125**, 1767-1779, doi:10.1172/jci71601 (2015).

71 Nishimura, A. L. *et al.* A mutation in the vesicle-trafficking protein VAPB causes late-onset spinal muscular atrophy and amyotrophic lateral sclerosis. *American Journal of Human Genetics* **75**, 822-831, doi:10.1086/425287 (2004).

72 Munch, C. *et al.* Point mutations of the p150 subunit of dynactin (DCTN1) gene in ALS. *Neurology* **63**, 724-726, doi:10.1212/01.wnl.0000134608.83927.b1 (2004).

73 Wu, C. H. *et al.* Mutations in the profilin 1 gene cause familial amyotrophic lateral sclerosis. *Nature* **488**, 499-+, doi:10.1038/nature11280 (2012).

74 Lee, K. H. *et al.* C9orf72 Dipeptide Repeats Impair the Assembly, Dynamics, and Function of Membrane-Less Organelles. *Cell* **167**, 774-+, doi:10.1016/j.cell.2016.10.002 (2016).

75 Mackenzie, I. R. *et al.* TIA1 Mutations in Amyotrophic Lateral Sclerosis and Frontotemporal Dementia Promote Phase Separation and Alter Stress Granule Dynamics. *Neuron* **95**, 808-+, doi:10.1016/j.neuron.2017.07.025 (2017).

76 Vance, C. *et al.* Familial amyotrophic lateral sclerosis with frontotemporal dementia is linked to a locus on chromosome 9p13.2-21.3. *Brain* **129**, 868-876, doi:10.1093/brain/awl030 (2006).

77 Gijselinck, I. *et al.* Identification of 2 Loci at Chromosomes 9 and 14 in a Multiplex Family With Frontotemporal Lobar Degeneration and Amyotrophic Lateral Sclerosis. *Archives of Neurology* **67**, 606-616 (2010).

78 van Es, M. A. *et al.* A Case Of ALS-FTD In A Large FALS Pedigree With A K17i ANG Mutation. *Neurology* **72**, 287-288, doi:10.1212/01.wnl.0000339487.84908.00 (2009).

79 Rollinson, S. *et al.* Frontotemporal lobar degeneration genome wide association study replication confirms a risk locus shared with amyotrophic lateral sclerosis. *Neurobiology of Aging* **32**, 7, doi:10.1016/j.neurobiolaging.2010.12.005 (2011).

80 Van Mossevelde, S., Engelborghs, S., van der Zee, J. & Van Broeckhoven, C. Genotype-phenotype links in frontotemporal lobar degeneration. *Nature Reviews Neurology* **14**, 363-378, doi:10.1038/s41582-018-0009-8 (2018).

81 Majounie, E. *et al.* Frequency of the C9orf72 hexanucleotide repeat expansion in patients with amyotrophic lateral sclerosis and frontotemporal dementia: a cross-sectional study. *Lancet Neurology* **11**, 323-330, doi:10.1016/s1474-4422(12)70043-1 (2012).

82 Oskarsson, B., Gendron, T. F. & Staff, N. P. Amyotrophic Lateral Sclerosis: An Update for 2018. *Mayo Clinic Proceedings* **93**, 1617-1628, doi:10.1016/j.mayocp.2018.04.007 (2018).

83 van der Zee, J. *et al.* A Pan-European Study of the C9orf72 Repeat Associated with FTLD: Geographic Prevalence, Genomic Instability, and Intermediate Repeats. *Human Mutation* **34**, 363-373, doi:10.1002/humu.22244 (2013).

84 Smith, B. N. *et al.* The C9ORF72 expansion mutation is a common cause of ALS+/-FTD in Europe and has a single founder. *European Journal of Human Genetics* **21**, 102-108, doi:10.1038/ejhg.2012.98 (2013).

85 McCann, E. P. *et al.* The genotype-phenotype landscape of familial amyotrophic lateral sclerosis in Australia. *Clinical Genetics* **92**, 259-266, doi:10.1111/cge.12973 (2017).

86 Nel, M. *et al.* C9orf72 repeat expansions in South Africans with amyotrophic lateral sclerosis. *Journal of the Neurological Sciences* **401**, 51-54, doi:10.1016/j.jns.2019.04.026 (2019).

87 Tsai, C. P. *et al.* A hexanucleotide repeat expansion in C9ORF72 causes familial and sporadic ALS in Taiwan. *Neurobiology of Aging* **33**, doi:10.1016/j.neurobiolaging.2012.05.002 (2012).

88 Konno, T. *et al.* Japanese amyotrophic lateral sclerosis patients with GGGGCC hexanucleotide repeat expansion in C9ORF72. *Journal of Neurology Neurosurgery and Psychiatry* **84**, 398-401, doi:10.1136/jnnp-2012-302272 (2013).

89 Ratti, A. *et al.* C9ORF72 repeat expansion in a large Italian ALS cohort: evidence of a founder effect. *Neurobiology of Aging* **33**, 8, doi:10.1016/j.neurobiolaging.2012.06.008 (2012).

90 Pliner, H. A., Mann, D. M. & Traynor, B. J. Searching for Grendel: origin and global spread of the C9ORF72 repeat expansion. *Acta Neuropathologica* **127**, 391-396, doi:10.1007/s00401-014-1250-x (2014).

91 Irwin, D. J. *et al.* Cognitive decline and reduced survival in C9orf72 expansion frontotemporal degeneration and amyotrophic lateral sclerosis. *Journal of Neurology Neurosurgery and Psychiatry* **84**, 163-169, doi:10.1136/jnnp-2012-303507 (2013).

92 Mahoney, C. J. *et al.* Longitudinal neuroimaging and neuropsychological profiles of frontotemporal dementia with C9ORF72 expansions. *Alzheimers Research & Therapy* **4**, 10, doi:10.1186/alzrt144 (2012).
93 Johnson, J. O. *et al.* Mutations in the Matrin 3 gene cause familial amyotrophic lateral sclerosis. *Nature Neuroscience* **17**, 664-+, doi:10.1038/nn.3688 (2014).
94 Cooper-Knock, J. *et al.* Clinico-pathological features in amyotrophic lateral sclerosis with expansions in C9ORF72. *Brain* **135**, 751-764, doi:10.1093/brain/awr365 (2012).
95 Hsiung, G. Y. R. *et al.* Clinical and pathological features of familial frontotemporal dementia caused by C9ORF72 mutation on chromosome 9p. *Brain* **135**, 709-722, doi:10.1093/brain/awr354 (2012).
96 Al-Sarraj, S. *et al.* p62 positive, TDP-43 negative, neuronal cytoplasmic and intranuclear inclusions in the cerebellum and hippocampus define the pathology of C9orf72-linked FTLD and MND/ALS. *Acta Neuropathologica* **122**, 691-702, doi:10.1007/s00401-011-0911-2 (2011).
97 Troakes, C. *et al.* An MND/ALS phenotype associated with C9orf72 repeat expansion: Abundant p62-positive, TDP-43-negative inclusions in cerebral cortex, hippocampus and cerebellum but without associated cognitive decline. *Neuropathology* **32**, 505-514, doi:10.1111/j.1440-1789.2011.01286.x (2012).
98 Brettschneider, J. *et al.* Pattern of ubiquilin pathology in ALS and FTLD indicates presence of C9ORF72 hexanucleotide expansion. *Acta Neuropathologica* **123**, 825-839, doi:10.1007/s00401-012-0970-z (2012).
99 Schludi, M. H. *et al.* Distribution of dipeptide repeat proteins in cellular models and C9orf72 mutation cases suggests link to transcriptional silencing. *Acta Neuropathologica* **130**, 537-555, doi:10.1007/s00401-015-1450-z (2015).
100 Cykowski, M. D. *et al.* Dipeptide repeat (DPR) pathology in the skeletal muscle of ALS patients with C9ORF72 repeat expansion. *Acta Neuropathologica* **138**, 667-670, doi:10.1007/s00401-019-02050-8 (2019).
101 Mizielinska, S. *et al.* C9orf72 frontotemporal lobar degeneration is characterised by frequent neuronal sense and antisense RNA foci. *Acta Neuropathologica* **126**, 845-857, doi:10.1007/s00401-013-1200-z (2013).
102 Lagier-Tourenne, C. *et al.* Targeted degradation of sense and antisense C9orf72 RNA foci as therapy for ALS and frontotemporal degeneration. *Proceedings of the National Academy of Sciences of the United States of America* **110**, E4530-E4539, doi:10.1073/pnas.1318835110 (2013).
103 Lee, Y. B. *et al.* Hexanucleotide Repeats in ALS/FTD Form Length-Dependent RNA Foci, Sequester RNA Binding Proteins, and Are Neurotoxic. *Cell Reports* **5**, 1178-1186, doi:10.1016/j.celrep.2013.10.049 (2013).
104 Cooper-Knock, J. *et al.* Antisense RNA foci in the motor neurons of C9ORF72-ALS patients are associated with TDP-43 proteinopathy. *Acta Neuropathologica* **130**, 63-75, doi:10.1007/s00401-015-1429-9 (2015).
105 Simon-Sanchez, J. *et al.* The clinical and pathological phenotype of C9ORF72 hexanucleotide repeat expansions. *Brain* **135**, 723-735, doi:10.1093/brain/awr353 (2012).
106 Van Mossevelde, S., van der Zee, J., Cruts, M. & Van Broeckhoven, C. Relationship between C9orf72 repeat size and clinical phenotype. *Current Opinion in Genetics & Development* **44**, 117-124, doi:10.1016/j.gde.2017.02.008 (2017).
107 Boeve, B. *et al.* Characterization of Frontotemporal Dementia +/- Amyotrophic Lateral Sclerosis Associated with the GGGGCC Repeat Expansion in C9ORF72. *Neurology* **78**, 3 (2012).
108 Gijselinck, I. *et al.* A C9orf72 promoter repeat expansion in a Flanders-Belgian cohort with disorders of the frontotemporal lobar degeneration-amyotrophic lateral sclerosis spectrum: a gene identification study. *Lancet Neurology* **11**, 54-65, doi:10.1016/s1474-4422(11)70261-7 (2012).

109 Stewart, H. *et al.* Clinical and pathological features of amyotrophic lateral sclerosis caused by mutation in the C9ORF72 gene on chromosome 9p. *Acta Neuropathologica* **123**, 409-417, doi:10.1007/s00401-011-0937-5 (2012).

110 Snowden, J. S. *et al.* Psychosis, C9ORF72 and dementia with Lewy bodies. *Journal of Neurology Neurosurgery and Psychiatry* **83**, 1031-1032, doi:10.1136/jnnp-2012-303032 (2012).

111 Majounie, E. *et al.* Repeat Expansion in C9ORF72 in Alzheimer's Disease. *New England Journal of Medicine* **366**, 283-284, doi:10.1056/NEJMc1113592 (2012).

112 Moss, D. J. H. *et al.* C9orf72 expansions are the most common genetic cause of Huntington disease phenocopies. *Neurology* **82**, 292-299, doi:10.1212/wnl.0000000000000061 (2014).

113 Lindquist, S. G. *et al.* Corticobasal and ataxia syndromes widen the spectrum of C9ORF72 hexanucleotide expansion disease. *Dementia and Geriatric Cognitive Disorders* **33**, 76-77 (2012).

114 Pati, A. R. *et al.* C9ORF72 gene expansion in a patient with intellectual disability and psychiatric disease. *Neurological Sciences* **38**, 207-208, doi:10.1007/s10072-016-2709-4 (2017).

115 Fogel, B. L. *et al.* C9ORF72 Expansion Is Not a Significant Cause of Sporadic Spinocerebellar Ataxia. *Movement Disorders* **27**, 1832-1833, doi:10.1002/mds.25245 (2012).

116 Lesage, S. *et al.* C9orf72 repeat expansions are a rare genetic cause of parkinsonism. *Brain* **136**, 385-391, doi:10.1093/brain/aws357 (2013).

117 Wilke, C. *et al.* Atypical Parkinsonism in C9orf72 expansions: A case report and systematic review of 45 cases from the literature. *Movement Disorders* **31**, S62-S62 (2016).

118 Sanders, P., Ewing, I. & Ahmad, K. C9orf72 expansion presenting as an eating disorder. *Journal of Clinical Neuroscience* **25**, 157-159, doi:10.1016/j.jocn.2015.06.019 (2016).

119 Beck, J. *et al.* Large C9orf72 Hexanucleotide Repeat Expansions Are Seen in Multiple Neurodegenerative Syndromes and Are More Frequent Than Expected in the UK Population. *American Journal of Human Genetics* **92**, 345-353, doi:10.1016/j.ajhg.2013.01.011 (2013).

120 Garcia-Redondo, A. *et al.* Analysis of the C9orf72 Gene in Patients with Amyotrophic Lateral Sclerosis in Spain and Different Populations Worldwide. *Human Mutation* **34**, 79-82, doi:10.1002/humu.22211 (2013).

121 Waite, A. J. *et al.* Reduced C9orf72 protein levels in frontal cortex of amyotrophic lateral sclerosis and frontotemporal degeneration brain with the C9ORF72 hexanucleotide repeat expansion. *Neurobiology of Aging* **35**, 9, doi:10.1016/j.neurobiolaging.2014.01.016 (2014).

122 van Blitterswijk, M. *et al.* Association between repeat sizes and clinical and pathological characteristics in carriers of C90RF72 repeat expansions (Xpansize-72): a cross-sectional cohort study. *Lancet Neurology* **12**, 978-988, doi:10.1016/s1474-4422(13)70210-2 (2013).

123 Fratta, P. *et al.* Screening a UK amyotrophic lateral sclerosis cohort provides evidence of multiple origins of the C9orf72 expansion. *Neurobiology of Aging* **36**, 7, doi:10.1016/j.neurobiolaging.2014.07.037 (2015).

124 Nordin, A. *et al.* Extensive size variability of the GGGGCC expansion in C9orf72 in both neuronal and non-neuronal tissues in 18 patients with ALS or FTD. *Human Molecular Genetics* **24**, 3133-3142, doi:10.1093/hmg/ddv064 (2015).

125 Belzil, V. V. *et al.* Reduced C9orf72 gene expression in c9FTD/ALS is caused by histone trimethylation, an epigenetic event detectable in blood. *Acta Neuropathologica* **126**, 895-905, doi:10.1007/s00401-013-1199-1 (2013).

126 Gijselinck, I. *et al.* The C9orf72 repeat size correlates with onset age of disease, DNA methylation and transcriptional downregulation of the promoter. *Molecular Psychiatry* **21**, 1112-1124, doi:10.1038/mp.2015.159 (2016).

127 Burberry, A. *et al.* Loss-of-function mutations in the C9ORF72 mouse ortholog cause fatal autoimmune disease. *Science Translational Medicine* **8**, 12, doi:10.1126/scitranslmed.aaf6038 (2016).

128 Koppers, M. *et al.* C9orf72 ablation in mice does not cause motor neuron degeneration or motor deficits. *Annals of Neurology* **78**, 426-438, doi:10.1002/ana.24453 (2015).

129 Jiang, J. *et al.* Gain of Toxicity from ALS/FTD-Linked Repeat Expansions in C9ORF72 Is Alleviated by Antisense Oligonucleotides Targeting GGGGCC-Containing RNAs. *Neuron* **90**, 535-550, doi:10.1016/j.neuron.2016.04.006 (2016).

130 Fratta, P. *et al.* C9orf72 hexanucleotide repeat associated with amyotrophic lateral sclerosis and frontotemporal dementia forms RNA G-quadruplexes. *Scientific Reports* **2**, 6, doi:10.1038/srep01016 (2012).

131 Kovanda, A., Zalar, M., Sket, P., Plavec, J. & Rogelj, B. Anti-sense DNA d(GGCCCC)(n) expansions in C9ORF72 form i-motifs and protonated hairpins. *Scientific Reports* **5**, 7, doi:10.1038/srep17944 (2015).

132 Sareen, D. *et al.* Targeting RNA Foci in iPSC-Derived Motor Neurons from ALS Patients with a C9ORF72 Repeat Expansion. *Science Translational Medicine* **5**, 13, doi:10.1126/scitranslmed.3007529 (2013).

133 Xu, Z. H. *et al.* Expanded GGGGCC repeat RNA associated with amyotrophic lateral sclerosis and frontotemporal dementia causes neurodegeneration. *Proceedings of the National Academy of Sciences of the United States of America* **110**, 7778-7783, doi:10.1073/pnas.1219643110 (2013).

134 Buratti, E. *et al.* TDP-43 binds heterogeneous nuclear ribonucleoprotein A/B through its C-terminal tail - An important region for the inhibition of cystic fibrosis transmembrane conductance regulator exon 9 splicing. *Journal of Biological Chemistry* **280**, 37572-37584, doi:10.1074/jbc.M505557200 (2005).

135 Kharel, P., Balaratnam, S., Beals, N. & Basu, S. The role of RNA G-quadruplexes in human diseases and therapeutic strategies. *Wiley Interdisciplinary Reviews-Rna* **11**, 20, doi:10.1002/wrna.1568 (2020).

136 Osborne, R. J. *et al.* Transcriptional and post-transcriptional impact of toxic RNA in myotonic dystrophy. *Human Molecular Genetics* **18**, 1471-1481, doi:10.1093/hmg/ddp058 (2009).

137 Mizielinska, S. *et al.* C9orf72 repeat expansions cause neurodegeneration in Drosophila through arginine-rich proteins. *Science* **345**, 1192-1194, doi:10.1126/science.1256800 (2014).

138 Tran, H. *et al.* Differential Toxicity of Nuclear RNA Foci versus Dipeptide Repeat Proteins in a Drosophila Model of C9ORF72 FTD/ALS. *Neuron* **87**, 1207-1214, doi:10.1016/j.neuron.2015.09.015 (2015).

139 Baldwin, K. R., Godena, V. K., Hewitt, V. L. & Whitworth, A. J. Axonal transport defects are a common phenotype in Drosophila models of ALS. *Human Molecular Genetics* **25**, 2378-2392, doi:10.1093/hmg/ddw105 (2016).

140 Wen, X. M. *et al.* Antisense Proline-Arginine RAN Dipeptides Linked to C9ORF72-ALS/FTD Form Toxic Nuclear Aggregates that Initiate In Vitro and In Vivo Neuronal Death. *Neuron* **84**, 1213-1225, doi:10.1016/j.neuron.2014.12.010 (2014).

141 Zu, T. *et al.* Non-ATG-initiated translation directed by microsatellite expansions. *Proceedings of the National Academy of Sciences of the United States of America* **108**, 260-265, doi:10.1073/pnas.1013343108 (2011).

142 Mori, K. *et al.* Bidirectional transcripts of the expanded C9orf72 hexanucleotide repeat are translated into aggregating dipeptide repeat proteins. *Acta Neuropathologica* **126**, 881-893, doi:10.1007/s00401-013-1189-3 (2013).

143 Zu, T. *et al.* RAN proteins and RNA foci from antisense transcripts in C9ORF72 ALS and frontotemporal dementia. *Proceedings of the National Academy of Sciences of the United States of America* **110**, E4968-E4977, doi:10.1073/pnas.1315438110 (2013).

144 Green, K. M. *et al.* RAN translation at C9orf72-associated repeat expansions is selectively enhanced by the integrated stress response. *Nature Communications* **8**, 13, doi:10.1038/s41467-017-02200-0 (2017).
145 Mann, D. M. A. *et al.* Dipeptide repeat proteins are present in the p62 positive inclusions in patients with frontotemporal lobar degeneration and motor neurone disease associated with expansions in C9ORF72. *Acta Neuropathologica Communications* **1**, 13, doi:10.1186/2051-5960-1-68 (2013).
146 Ash, P. E. A. *et al.* Unconventional Translation of C9ORF72 GGGGCC Expansion Generates Insoluble Polypeptides Specific to c9FTD/ALS. *Neuron* **77**, 639-646, doi:10.1016/j.neuron.2013.02.004 (2013).
147 Mackenzie, I. R. *et al.* Dipeptide repeat protein pathology in C9ORF72 mutation cases: clinico-pathological correlations. *Acta Neuropathologica* **126**, 859-879, doi:10.1007/s00401-013-1181-y (2013).
148 Mackenzie, I. R. A. *et al.* Quantitative analysis and clinico-pathological correlations of different dipeptide repeat protein pathologies in C9ORF72 mutation carriers. *Acta Neuropathologica* **130**, 845-861, doi:10.1007/s00401-015-1476-2 (2015).
149 Davidson, Y. S. *et al.* Brain distribution of dipeptide repeat proteins in frontotemporal lobar degeneration and motor neurone disease associated with expansions in C9ORF72. *Acta Neuropathologica Communications* **2**, 13, doi:10.1186/2051-5960-2-70 (2014).
150 Choi, M. L. & Gandhi, S. Crucial role of protein oligomerization in the pathogenesis of Alzheimer's and Parkinson's diseases. *Febs Journal* **285**, 3631-3644, doi:10.1111/febs.14587 (2018).
151 Quaegebeur, A., Glaria, I., Lashley, T. & Isaacs, A. M. Soluble and insoluble dipeptide repeat protein measurements in C9orf72-frontotemporal dementia brains show regional differential solubility and correlation of poly-GR with clinical severity. *Acta Neuropathologica Communications* **8**, 13, doi:10.1186/s40478-020-01036-y (2020).
152 Kwon, I. *et al.* Poly-dipeptides encoded by the C9orf72 repeats bind nucleoli, impede RNA biogenesis, and kill cells. *Science* **345**, 1139-1145, doi:10.1126/science.1254917 (2014).
153 Callister, J. B., Ryan, S., Sim, J., Rollinson, S. & Pickering-Brown, S. M. Modelling C9orf72 dipeptide repeat proteins of a physiologically relevant size. *Human Molecular Genetics* **25**, 5069-5082, doi:10.1093/hmg/ddw327 (2016).
154 Edbauer, D. & Haass, C. An amyloid-like cascade hypothesis for C9orf72 ALS/FTD. *Current Opinion in Neurobiology* **36**, 99-106, doi:10.1016/j.conb.2015.10.009 (2016).
155 Zhang, Y. J. *et al.* C9ORF72 poly(GA) aggregates sequester and impair HR23 and nucleocytoplasmic transport proteins. *Nature Neuroscience* **19**, 668-+, doi:10.1038/nn.4272 (2016).
156 Chang, Y. J., Jeng, U. S., Chiang, Y. L., Hwang, I. S. & Chen, Y. R. The Glycine-Alanine Dipeptide Repeat from C9orf72 Hexanucleotide Expansions Forms Toxic Amyloids Possessing Cell-to-Cell Transmission Properties. *Journal of Biological Chemistry* **291**, 4903-4911, doi:10.1074/jbc.M115.694273 (2016).
157 Zhang, Y. J. *et al.* Aggregation-prone c9FTD/ALS poly(GA) RAN-translated proteins cause neurotoxicity by inducing ER stress. *Acta Neuropathologica* **128**, 505-524, doi:10.1007/s00401-014-1336-5 (2014).
158 May, S. *et al.* C9orf72 FTLD/ALS-associated Gly-Ala dipeptide repeat proteins cause neuronal toxicity and Unc119 sequestration. *Acta Neuropathologica* **128**, 485-503, doi:10.1007/s00401-014-1329-4 (2014).
159 Guo, Q. *et al.* In Situ Structure of Neuronal C9orf72 Poly-GA Aggregates Reveals Proteasome Recruitment. *Cell* **172**, 696-+, doi:10.1016/j.cell.2017.12.030 (2018).
160 Zheng, S. Z., Sahimi, A., Shing, K. S. & Sahimi, M. Molecular dynamics study of structure, folding, and aggregation of poly-glycine-alanine (Poly-GA). *Journal of Chemical Physics* **150**, 12, doi:10.1063/1.5081867 (2019).

161 Doig, A. J. Frozen, but no accident - why the 20 standard amino acids were selected. *Febs Journal* **284**, 1296-1305, doi:10.1111/febs.13982 (2017).
162 Freibaum, B. D. & Taylor, J. P. The Role of Dipeptide Repeats in C9ORF72-Related ALS-FTD. *Frontiers in Molecular Neuroscience* **10**, 9, doi:10.3389/fnmol.2017.00035 (2017).
163 Freibaum, B. D. *et al.* GGGGCC repeat expansion in C9orf72 compromises nucleocytoplasmic transport. *Nature* **525**, 129-+, doi:10.1038/nature14974 (2015).
164 Lin, Y. *et al.* Toxic PR Poly-Dipeptides Encoded by the C9orf72 Repeat Expansion Target LC Domain Polymers. *Cell* **167**, 789-+, doi:10.1016/j.cell.2016.10.003 (2016).
165 White, M. R. *et al.* C9orf72 Poly(PR) Dipeptide Repeats Disturb Biomolecular Phase Separation and Disrupt Nucleolar Function. *Molecular Cell* **74**, 713-+, doi:10.1016/j.molcel.2019.03.019 (2019).
166 Boeynaems, S. *et al.* Phase Separation of C9orf72 Dipeptide Repeats Perturbs Stress Granule Dynamics. *Molecular Cell* **65**, 1044-+, doi:10.1016/j.molcel.2017.02.013 (2017).
167 Zhang, Y. J. *et al.* Poly(GR) impairs protein translation and stress granule dynamics in C9orf72-associated frontotemporal dementia and amyotrophic lateral sclerosis. *Nature Medicine* **24**, 1136-+, doi:10.1038/s41591-018-0071-1 (2018).
168 Kanekura, K. *et al.* Poly-dipeptides encoded by the C9ORF72 repeats block global protein translation. *Human Molecular Genetics* **25**, 1803-1813, doi:10.1093/hmg/ddw052 (2016).
169 Tao, Z. T. *et al.* Nucleolar stress and impaired stress granule formation contribute to C9orf72 RAN translation-induced cytotoxicity. *Human Molecular Genetics* **24**, 2426-2441, doi:10.1093/hmg/ddv005 (2015).
170 Lopez-Gonzalez, R. *et al.* Poly(GR) in C9ORF72-Related ALS/FTD Compromises Mitochondrial Function and Increases Oxidative Stress and DNA Damage in iPSC-Derived Motor Neurons. *Neuron* **92**, 383-391, doi:10.1016/j.neuron.2016.09.015 (2016).
171 Boeynaems, S. *et al.* Drosophila screen connects nuclear transport genes to DPR pathology in c9ALS/FTD. *Scientific Reports* **6**, 8, doi:10.1038/srep20877 (2016).
172 Jovicic, A. *et al.* Modifiers of C9orf72 dipeptide repeat toxicity connect nucleocytoplasmic transport defects to FTD/ALS. *Nature Neuroscience* **18**, 1226-+, doi:10.1038/nn.4085 (2015).
173 Chew, J. *et al.* C9ORF72 repeat expansions in mice cause TDP-43 pathology, neuronal loss, and behavioral deficits. *Science* **348**, 1151-1154, doi:10.1126/science.aaa9344 (2015).
174 Liu, Y. J. *et al.* C9orf72 BAC Mouse Model with Motor Deficits and Neurodegenerative Features of ALS/FTD. *Neuron* **90**, 521-534, doi:10.1016/j.neuron.2016.04.005 (2016).
175 O'Rourke, J. G. *et al.* C9orf72 BAC Transgenic Mice Display Typical Pathologic Features of ALS/FTD. *Neuron* **88**, 892-901, doi:10.1016/j.neuron.2015.10.027 (2015).
176 Peters, O. M. *et al.* Human C9ORF72 Hexanucleotide Expansion Reproduces RNA Foci and Dipeptide Repeat Proteins but Not Neurodegeneration in BAC Transgenic Mice. *Neuron* **88**, 902-909, doi:10.1016/j.neuron.2015.11.018 (2015).
177 Moens, T. G., Partridge, L. & Isaacs, A. M. Genetic models of C9orf72: what is toxic? *Current Opinion in Genetics & Development* **44**, 92-101, doi:10.1016/j.gde.2017.01.006 (2017).
178 Schludi, M. H. *et al.* Spinal poly-GA inclusions in a C9orf72 mouse model trigger motor deficits and inflammation without neuron loss. *Acta Neuropathologica* **134**, 241-254, doi:10.1007/s00401-017-1711-0 (2017).
179 Hao, Z. B. *et al.* Motor dysfunction and neurodegeneration in a C9orf72 mouse line expressing poly-PR. *Nature Communications* **10**, doi:10.1038/s41467-019-10956-w (2019).

180 LaClair, K. D. *et al.* Congenic expression of poly-GA but not poly-PR in mice triggers selective neuron loss and interferon responses found in C9orf72 ALS. *Acta Neuropathologica* **140**, 121-142, doi:10.1007/s00401-020-02176-0 (2020).
181 Chakraborty, R. *et al.* Characterization of a Drosophila Alzheimer's Disease Model: Pharmacological Rescue of Cognitive Defects. *Plos One* **6**, doi:10.1371/journal.pone.0020799 (2011).
182 Cao, W. *et al.* Identification of novel genes that modify phenotypes induced by Alzheimer's beta-amyloid overexpression in Drosophila. *Genetics* **178**, 1457-1471, doi:10.1534/genetics.107.078394 (2008).
183 Hewitt, V. L. & Whitworth, A. J. Mechanisms of Parkinson's Disease: Lessons from Drosophila. *Fly Models of Human Diseases* **121**, 173-200, doi:10.1016/bs.ctdb.2016.07.005 (2017).
184 Whitworth, A. J., Wes, P. D. & Pallanck, L. J. Drosophila models pioneer a new approach to drug discovery for Parkinson's disease. *Drug Discovery Today* **11**, 119-126, doi:10.1016/s1359-6446(05)03693-7 (2006).
185 Huang, X., Suyama, K., Buchanan, J., Zhu, A. J. & Scott, M. P. A Drosophila model of the Niemann-Pick type C lysosome storage disease: dnpc1a is required for molting and sterol homeostasis. *Development* **132**, 5115-5124, doi:10.1242/dev.02079 (2005).
186 McGurk, L., Berson, A. & Bonini, N. M. Drosophila as an In Vivo Model for Human Neurodegenerative Disease. *Genetics* **201**, 377-402, doi:10.1534/genetics.115.179457 (2015).
187 Bonini, N. M. & Fortini, M. E. Human neurodegenerative disease modeling using Drosophila. *Annual Review of Neuroscience* **26**, 627-656, doi:10.1146/annurev.neuro.26.041002.131425 (2003).
188 Gargano, J. W., Martin, I., Bhandari, P. & Grotewiel, M. S. Rapid iterative negative geotaxis (RING): a new method for assessing age-related locomotor decline in Drosophila. *Experimental Gerontology* **40**, 386-395, doi:10.1016/j.exger.2005.02.005 (2005).
189 Iliadi, K. G., Knight, D. & Boulianne, G. L. Healthy aging - insights from Drosophila. *Frontiers in Physiology* **3**, doi:10.3389/fphys.2012.00106 (2012).
190 Moens, T. G. *et al.* Sense and antisense RNA are not toxic in Drosophila models of C9orf72-associated ALS/FTD. *Acta Neuropathologica* **135**, 445-457, doi:10.1007/s00401-017-1798-3 (2018).
191 Burguete, A. S. *et al.* GGGGCC microsatellite RNA is neuritically localized, induces branching defects, and perturbs transport granule function. *Elife* **4**, 23, doi:10.7554/eLife.0881 (2015).
192 Mizielinska, S. *et al.* Bidirectional nucleolar dysfunction in C9orf72 frontotemporal lobar degeneration. *Acta Neuropathologica Communications* **5**, 11, doi:10.1186/s40478-017-0432-x (2017).
193 Yang, D. J. *et al.* FTD/ALS-associated poly(GR) protein impairs the Notch pathway and is recruited by poly(GA) into cytoplasmic inclusions. *Acta Neuropathologica* **130**, 525-535, doi:10.1007/s00401-015-1448-6 (2015).
194 Brand, A. H. & Perrimon, N. Targeted Gene-Expression as a Means Of Altering Cell Fates and Generating Dominant Phenotypes. *Development* **118**, 401-415 (1993).
195 Osterwalder, T., Yoon, K. S., White, B. H. & Keshishian, H. A conditional tissue-specific transgene expression system using inducible GAL4. *Proceedings of the National Academy of Sciences of the United States of America* **98**, 12596-12601, doi:10.1073/pnas.221303298 (2001).
196 Roote, J. & Prokop, A. How to Design a Genetic Mating Scheme: A Basic Training Package for Drosophila Genetics. *G3-Genes Genomes Genetics* **3**, 353-358, doi:10.1534/g3.112.004820 (2013).
197 Ryan, S., Hobbs, E., Rollinson, S. & Pickering-Brown, S. M. CRISPR/Cas9 does not facilitate stable expression of long C9orf72 dipeptides in mice. *Neurobiology of Aging* **84**, 8, doi:10.1016/j.neurobiolaging.2019.09.010 (2019).

198 Pandey, U. B. *et al.* HDAC6 rescues neurodegeneration and provides an essential link between autophagy and the UPS. *Nature* **447**, 859-863, doi:10.1038/nature05853 (2007).
199 Ritson, G. P. *et al.* TDP-43 Mediates Degeneration in a Novel Drosophila Model of Disease Caused by Mutations in VCP/p97. *Journal of Neuroscience* **30**, 7729-7739, doi:10.1523/jneurosci.5894-09.2010 (2010).
200 Son, W. & Choi, K. W. The Classic Lobe Eye Phenotype of Drosophila Is Caused by Transposon Insertion-Induced Misexpression of a Zinc-Finger Transcription Factor. *Genetics* **216**, 117-134, doi:10.1534/genetics.120.303486 (2020).
201 Oortveld, M. A. W. *et al.* Human Intellectual Disability Genes Form Conserved Functional Modules in Drosophila. *Plos Genetics* **9**, doi:10.1371/journal.pgen.1003911 (2013).
202 Tazelaar, G. H. P. *et al.* ATXN1 repeat expansions confer risk for amyotrophic lateral sclerosis and contribute to TDP-43 mislocalization. *Brain Communications* **2**, doi:10.1093/braincomms/fcaa064 (2020).
203 M'Angale, P. G. & Staveley, B. E. Bcl-2 homologue Debcl enhances alpha-synuclein-induced phenotypes in Drosophila. *Peerj* **4**, doi:10.7717/peerj.2461 (2016).
204 Barmchi, M. P. *et al.* A Drosophila Model of HPV E6-Induced Malignancy Reveals Essential Roles for Magi and the Insulin Receptor. *Plos Pathogens* **12**, doi:10.1371/journal.ppat.1005789 (2016).
205 Ambegaokar, S. S. & Jackson, G. R. Interaction Between Eye Pigment Genes and Tau-Induced Neurodegeneration in Drosophila melanogaster. *Genetics* **186**, 435-442, doi:10.1534/genetics.110.119545 (2010).
206 Bose, A. *et al.* Drosophila CK2 regulates lateral-inhibition during eye and bristle development. *Mechanisms of Development* **123**, 649-664, doi:10.1016/j.mod.2006.07.003 (2006).
207 West, R. J. H. *et al.* Co-expression of C9orf72 related dipeptide-repeats over 1000 repeat units reveals age- and combination-specific phenotypic profiles inDrosophila. *Acta Neuropathologica Communications* **8**, 19, doi:10.1186/s40478-020-01028-y (2020).
208 Gavin, B. A. *et al.* Accelerated accumulation of misfolded prion protein and spongiform degeneration in a Drosophila model of Gerstmann-Straussler-Scheinker syndrome. *Journal of Neuroscience* **26**, 12408-12414, doi:10.1523/jneurosci.3372-06.2006 (2006).
209 Katzenberger, R. J. *et al.* A Drosophila model of closed head traumatic brain injury. *Proceedings of the National Academy of Sciences of the United States of America* **110**, E4152-E4159, doi:10.1073/pnas.1316895110 (2013).
210 Lang, M. L. *et al.* Genetic Inhibition of Solute-Linked Carrier 39 Family Transporter 1 Ameliorates A beta Pathology in a Drosophila Model of Alzheimer's Disease. *Plos Genetics* **8**, 623-639, doi:10.1371/journal.pgen.1002683 (2012).
211 West, R. J. H., Furmston, R., Williams, C. A. C. & Elliott, C. J. H. Neurophysiology of Drosophila Models of Parkinson's Disease. *Parkinsons Disease* **2015**, doi:10.1155/2015/381281 (2015).
212 West, R. J. H., Lu, Y. B., Marie, B., Gao, F. B. & Sweeney, S. T. Rab8, POSH, and TAK1 regulate synaptic growth in a Drosophila model of frontotemporal dementia. *Journal of Cell Biology* **208**, 931-947, doi:10.1083/jcb.201404066 (2015).
213 Solomon, D. A. *et al.* A feedback loop between dipeptide-repeat protein, TDP-43 and karyopherin-alpha mediates C9orf72-re ated neurodegeneration. *Brain* **141**, 2908-2924, doi:10.1093/brain/awy241 (2018).
214 Goodman, L. D. *et al.* Toxic expanded GGGGCC repeat transcription is mediated by the PAF1 complex in C9orf72-associated FTD. *Nature Neuroscience* **22**, 863-+, doi:10.1038/s41593-019-0396-1 (2019).
215 Iacoangeli, A. *et al.* C9orf72 intermediate expansions of 24-30 repeats are associated with ALS. *Acta Neuropathologica Communications* **7**, 7, doi:10.1186/s40478-019-0724-4 (2019).

216 Moron-Oset, J. *et al.* Glycine-alanine dipeptide repeats spread rapidly in a repeat length- and age-dependent manner in the fly brain. *Acta Neuropathologica Communications* **7**, 14, doi:10.1186/s40478-019-0860-x (2019).
217 Huisinga, K. L. *et al.* Targeting of P-Element Reporters to Heterochromatic Domains by Transposable Element 1360 in Drosophila melanogaster. *Genetics* **202**, 565-+, doi:10.1534/genetics.115.183228 (2016).
218 King, T. D., Johnson, J. E. & Bateman, J. R. Position Effects Influence Transvection in Drosophila melanogaster. *Genetics* **213**, 1289-1299, doi:10.1534/genetics.119.302583 (2019).
219 Bichara, M., Wagner, J. & Lambert, I. B. Mechanisms of tandem repeat instability in bacteria. *Mutation Research-Fundamental and Molecular Mechanisms of Mutagenesis* **598**, 144-163, doi:10.1016/j.mrfmmm.2006.01.020 (2006).
220 Xu, W. C. & Xu, J. C9orf72 Dipeptide Repeats Cause Selective Neurodegeneration and Cell-Autonomous Excitotoxicity in Drosophila Glutamatergic Neurons. *Journal of Neuroscience* **38**, 7741-7752, doi:10.1523/jneurosci.0908-18.2018 (2018).
221 Mizielinska, S. & Isaacs, A. M. C9orf72 amyotrophic lateral sclerosis and frontotemporal dementia: gain or loss of function? *Current Opinion in Neurology* **27**, 515-523, doi:10.1097/wco.0000000000000130 (2014).
222 Mori, K. *et al.* The C9orf72 GGGGCC Repeat Is Translated into Aggregating Dipeptide-Repeat Proteins in FTLD/ALS. *Science* **339**, 1335-1338, doi:10.1126/science.1232927 (2013).
223 Lenz, S., Karsten, P., Schulz, J. B. & Voigt, A. Drosophila as a screening tool to study human neurodegenerative diseases. *Journal of Neurochemistry* **127**, 453-460, doi:10.1111/jnc.12446 (2013).
224 St Johnston, D. The art and design of genetic screens: Drosophila melanogaster. *Nature Reviews Genetics* **3**, 176-188, doi:10.1038/nrg751 (2002).
225 Wilder, E. L. & Perrimon, N. Dual Functions of Wingless In the Drosophila Leg Imaginal Disc. *Development* **121**, 477-488 (1995).
226 Klepsatel, P., Wildridge, D. & Galikova, M. Temperature induces changes in Drosophila energy stores. *Scientific Reports* **9**, doi:10.1038/s41598-019-41754-5 (2019).
227 Partridge, L., Barrie, B., Fowler, K. & French, V. Evolution and Development of Body-Size and Cell-Size in Drosophila melanogaster In Response to Temperature. *Evolution* **48**, 1269-1276, doi:10.2307/2410384 (1994).
228 Thapana, W., Sujiwattanarat, P., Srikulnath, K., Hirai, H. & Koga, A. Reduction in the structural instability of cloned eukaryotic tandem-repeat DNA by low-temperature culturing of host bacteria. *Genetics Research* **96**, doi:10.1017/s0016672314000172 (2014).
229 de Koning, A. P. J., Gu, W. J., Castoe, T. A., Batzer, M. A. & Pollock, D. D. Repetitive Elements May Comprise Over Two-Thirds of the Human Genome. *Plos Genetics* **7**, doi:10.1371/journal.pgen.1002384 (2011).
230 Mekhail, K., Seebacher, J., Gygi, S. P. & Moazed, D. Role for perinuclear chromosome tethering in maintenance of genome stability. *Nature* **456**, 667-U698, doi:10.1038/nature07460 (2008).
231 Stamenova, R., Maxwell, P. H., Kenny, A. E. & Curcio, M. J. Rrm3 Protects the Saccharomyces cerevisiae Genome From Instability at Nascent Sites of Retrotransposition. *Genetics* **182**, 711-723, doi:10.1534/genetics.109.104208 (2009).
232 Guo, F. F., Li, L. Y., Yang, W., Hu, J. F. & Cui, J. W. Long noncoding RNA: A resident staff of genomic instability regulation in tumorigenesis. *Cancer Letters* **503**, 103-109, doi:10.1016/j.canlet.2021.01.021 (2021).
233 Kung, J. T. Y., Colognori, D. & Lee, J. T. Long Noncoding RNAs: Past, Present, and Future. *Genetics* **193**, 651-669, doi:10.1534/genetics.112.146704 (2013).
234 Jackson, S. M. *et al.* A SCA7 CAG/CTG repeat expansion is stable in Drosophila melanogaster despite modulation of genomic context and gene dosage. *Gene* **347**, 35-41, doi:10.1016/j.gene.2004.12.008 (2005).

235 Jin, P. *et al.* RNA-mediated neurodegeneration caused by the fragile X premutation rCGG repeats in Drosophila. *Neuron* **39**, 739-747, doi:10.1016/s0896-6273(03)00533-6 (2003).
236 Ristow, M. & Schmeisser, S. Extending life span by increasing oxidative stress. *Free Radical Biology and Medicine* **51**, 327-336, doi:10.1016/j.freeradbiomed.2011.05.010 (2011).
237 Mehra, A. & Hatzimanikatis, V. An algorithmic framework for genome-wide modeling and analysis of translation networks. *Biophysical Journal* **90**, 1136-1146, doi:10.1529/biophysj.105.062521 (2006).
238 Ross, J. F. & Orlowski, M. Growth-Rate-Dependent Adjustment of Ribosome Function in Chemostat-Grown Cells of the Fungus Mucor racemosus. *Journal of Bacteriology* **149**, 650-653, doi:10.1128/jb.149.2.650-653.1982 (1982).
239 Wohlgemuth, I., Pohl, C., Mittelstaet, J., Konevega, A. L. & Rodnina, M. V. Evolutionary optimization of speed and accuracy of decoding on the ribosome. *Philosophical Transactions of the Royal Society B-Biological Sciences* **366**, 2979-2986, doi:10.1098/rstb.2011.0138 (2011).
240 Riba, A. *et al.* Protein synthesis rates and ribosome occupancies reveal determinants of translation elongation rates. *Proceedings of the National Academy of Sciences of the United States of America* **116**, 15023-15032, doi:10.1073/pnas.1817299116 (2019).
241 Yamada, S. B. *et al.* RPS25 is required for efficient RAN translation of C9orf72 and other neurodegenerative disease-associated nucleotide repeats. *Nature Neuroscience* **22**, 1383-+, doi:10.1038/s41593-019-0455-7 (2019).
242 Bonini, N. M. Surviving Drosophila eye development. *Cell Death and Differentiation* **4**, 4-11, doi:10.1038/sj.cdd.4400209 (1997).
243 Kanekura, K. *et al.* Characterization of membrane penetration and cytotoxicity of C9orf72-encoding arginine-rich dipeptides. *Scientific Reports* **8**, doi:10.1038/s41598-018-31096-z (2018).
244 Flores, B. N. *et al.* Distinct C9orf72-Associated Dipeptide Repeat Structures Correlate with Neuronal Toxicity. *Plos One* **11**, 18, doi:10.1371/journal.pone.0165084 (2016).
245 Brasseur, L., Coens, A., Waeytens, J., Melki, R. & Bousset, L. Dipeptide repeat derived from C9orf72 hexanucleotide expansions forms amyloids or natively unfolded structures in vitro. *Biochemical and Biophysical Research Communications* **526**, 410-416, doi:10.1016/j.bbrc.2020.03.108 (2020).
246 Verhoef, L., Lindsten, K., Masucci, M. G. & Dantuma, N. P. Aggregate formation inhibits proteasomal degradation of polyglutamine proteins. *Human Molecular Genetics* **11**, 2689-2700, doi:10.1093/hmg/11.22.2689 (2002).
247 Lang-Rollin, I. *et al.* A novel cell death pathway that is partially caspase dependent, but morphologically non-apoptotic, elicited by proteasomal inhibition of rat sympathetic neurons. *Journal of Neurochemistry* **105**, 653-665, doi:10.1111/j.1471-4159.2007.05165.x (2008).
248 Thibaudeau, T. A., Anderson, R. T. & Smith, D. M. A common mechanism of proteasome impairment by neurodegenerative disease-associated oligomers. *Nature Communications* **9**, doi:10.1038/s41467-018-03509-0 (2018).
249 Moens, T. G. *et al.* C9orf72 arginine-rich dipeptide proteins interact with ribosomal proteins in vivo to induce a toxic translational arrest that is rescued by eIF1A. *Acta Neuropathologica* **137**, 487-500, doi:10.1007/s00401-018-1946-4 (2019).
250 West, R. J. H., Ugbode, C., Fort-Aznar, L. & Sweeney, S. T. Neuroprotective activity of ursodeoxycholic acid in CHMP2B(Intron5) models of frontotemporal dementia. *Neurobiology of Disease* **144**, doi:10.1016/j.nbd.2020.105047 (2020).
251 Nonaka, T. *et al.* C9ORF72 dipeptide repeat poly-GA inclusions promote intracellular aggregation of phosphorylated TDP-43. *Human Molecular Genetics* **27**, 2658-2670, doi:10.1093/hmg/ddy174 (2018).
252 Khosravi, B. *et al.* Cell-to-cell transmission of C9orf72 poly-(Gly-Ala) triggers key features of ALS/FTD. *Embo Journal* **39**, doi:10.15252/embj.2019102811 (2020).

253 Almeida, S. *et al.* Modeling key pathological features of frontotemporal dementia with C9ORF72 repeat expansion in iPSC-derived human neurons. *Acta Neuropathologica* **126**, 385-399, doi:10.1007/s00401-013-1149-y (2013).
254 Ryan & Sarah. *Modelling C9orf72-linked frontotemporal dementia and amyotrophic lateral sclerosis* PhD Medicine thesis, University of Manchester, (2016).
255 Hughes, C. L. & Thomas, J. B. A sensory feedback circuit coordinates muscle activity in Drosophila. *Molecular and Cellular Neuroscience* **35**, 383-396, doi:10.1016/j.mcn.2007.04.001 (2007).
256 Gjorgjieva, J., Berni, J., Evers, J. F. & Eglen, S. J. Neural circuits for peristaltic wave propagation in crawling Drosophila larvae: analysis and modeling. *Frontiers in Computational Neuroscience* **7**, doi:10.3389/fncom.2013.00024 (2013).
257 Lebourg, E. & Lints, F. A. HYPERGRAVITY AND AGING IN DROSOPHILA-MELANOGASTER .4. CLIMBING ACTIVITY. *Gerontology* **38**, 59-64 (1992).
258 White, K. E., Humphrey, D. M. & Hirth, F. The dopaminergic system in the aging brain of Drosophila. *Frontiers in Neuroscience* **4**, doi:10.3389/fnins.2010.00205 (2010).
259 Kretzschmar, D., Hasan, G., Sharma, S., Heisenberg, M. & Benzer, S. The Swiss cheese mutant causes glial hyperwrapping and brain degeneration in Drosophila. *Journal of Neuroscience* **17**, 7425-7432 (1997).
260 Min, K. T. & Benzer, S. Spongecake and eggroll: Two hereditary diseases in Drosophila resemble patterns of human brain degeneration. *Current Biology* **7**, 885-888, doi:10.1016/s0960-9822(06)00378-2 (1997).
261 Iijima, K. *et al.* A beta 42 Mutants with Different Aggregation Profiles Induce Distinct Pathologies in Drosophila. *Plos One* **3**, doi:10.1371/journal.pone.0001703 (2008).
262 Davis, M. Y. *et al.* Glucocerebrosidase Deficiency in Drosophila Results in alpha-Synuclein-Independent Protein Aggregation and Neurodegeneration. *Plos Genetics* **12**, doi:10.1371/journal.pgen.1005944 (2016).
263 Moustaqim-Barrette, A. *et al.* The amyotrophic lateral sclerosis 8 protein, VAP, is required for ER protein quality control. *Human Molecular Genetics* **23**, 1975-1989, doi:10.1093/hmg/ddt594 (2014).
264 Fortini, M. E. & Bonini, N. M. Modeling human neurodegenerative diseases in Drosophila - on a wing and a prayer. *Trends in Genetics* **16**, 161-167, doi:10.1016/s0168-9525(99)01939-3 (2000).
265 DiAntonio, A., Petersen, S. A., Heckmann, M. & Goodman, C. S. Glutamate receptor expression regulates quantal size and quantal content at the Drosophila neuromuscular junction. *Journal of Neuroscience* **19**, 3023-3032 (1999).
266 Menon, K. P., Carrillo, R. A. & Zinn, K. Development and plasticity of the Drosophila larval neuromuscular junction. *Wiley Interdisciplinary Reviews-Developmental Biology* **2**, 647-670, doi:10.1002/wdev.108 (2013).
267 Hock, E. M. & Polymenidou, M. Prion-like propagation as a pathogenic principle in frontotemporal dementia. *Journal of Neurochemistry* **138**, 163-183, doi:10.1111/jnc.13668 (2016).
268 Stocker, R. F., Heimbeck, G., Gendre, N. & deBelle, J. S. Neuroblast ablation in Drosophila P GAL4 lines reveals origins of olfactory interneurons. *Journal of Neurobiology* **32**, 443-456, doi:10.1002/(sici)1097-4695(199705)32:5<443::aid-neu1>3.0.co;2-5 (1997).
269 King, A. E., Woodhouse, A., Kirkcaldie, M. T. K. & Vickers, J. C. Excitotoxicity in ALS: Overstimulation, or overreaction? *Experimental Neurology* **275**, 162-171, doi:10.1016/j.expneurol.2015.09.019 (2016).
270 Van den Bosch, L., Van Damme, P., Bogaert, E. & Robberecht, W. The role of excitotoxicity in the pathogenesis of amyotrophic lateral sclerosis. *Biochimica Et Biophysica Acta-Molecular Basis of Disease* **1762**, 1068-1082, doi:10.1016/j.bbadis.2006.05.002 (2006).

271 Starr, A. & Sattler, R. Synaptic dysfunction and altered excitability in C90RF72 ALS/FTD. *Brain Research* **1693**, 98-108, doi:10.1016/j.brainres.2018.02.011 (2018).
272 Henstridge, C. M. *et al.* Synapse loss in the prefrontal cortex is associated with cognitive decline in amyotrophic lateral sclerosis. *Acta Neuropathologica* **135**, 213-226, doi:10.1007/s00401-017-1797-4 (2018).
273 Armada-Moreira, A. *et al.* Going the Extra (Synaptic) Mile: Excitotoxicity as the Road Toward Neurodegenerative Diseases. *Frontiers in Cellular Neuroscience* **14**, 27, doi:10.3389/fncel.2020.00090 (2020).
274 Selvaraj, B. T. *et al.* C9ORF72 repeat expansion causes vulnerability of motor neurons to Ca2+-permeable AMPA receptor-mediated excitotoxicity. *Nature Communications* **9**, doi:10.1038/s41467-017-02729-0 (2018).
275 Perkins, E. M. *et al.* Altered network properties in C9ORF72 repeat expansion cortical neurons are due to synaptic dysfunction. *Molecular Neurodegeneration* **16**, doi:10.1186/s13024-021-00433-8 (2021).
276 Mahr, A. & Aberle, H. The expression pattern of the Drosophila vesicular glutamate transporter: A marker protein for motoneurons and glutamatergic centers in the brain. *Gene Expression Patterns* **6**, 299-309, doi:10.1016/j.modgep.2005.07.006 (2006).
277 Perry, S., Han, Y. F., Das, A. & Dickman, D. Homeostatic plasticity can be induced and expressed to restore synaptic strength at neuromuscular junctions undergoing ALS-related degeneration. *Human Molecular Genetics* **26**, 4153-4167, doi:10.1093/hmg/ddx304 (2017).
278 Murphy, N. A. *et al.* Age-related penetrance of the C9orf72 repeat expansion. *Scientific Reports* **7**, doi:10.1038/s41598-017-02364-1 (2017).
279 Chio, A. *et al.* Clinical characteristics of patients with familial amyotrophic lateral sclerosis carrying the pathogenic GGGGCC hexanucleotide repeat expansion of C9ORF72. *Brain* **135**, 784-793, doi:10.1093/brain/awr366 (2012).
280 Sun, J. *et al.* Neural Control of Startle-Induced Locomotion by the Mushroom Bodies and Associated Neurons in Drosophila. *Frontiers in Systems Neuroscience* **12**, doi:10.3389/fnsys.2018.00006 (2018).
281 Haddadi, M. *et al.* Brain aging, memory impairment and oxidative stress: A study in Drosophila melanogaster. *Behavioural Brain Research* **259**, 60-69, doi:10.1016/j.bbr.2013.10.036 (2014).
282 Dias-Santagata, D., Fulga, T. A., Duttaroy, A. & Feany, M. B. Oxidative stress mediates tau-induced neurodegeneration in Drosophila. *Journal of Clinical Investigation* **117**, 236-245, doi:10.1172/jci28769 (2007).
283 Feiler, M. S. *et al.* TDP-43 is intercellularly transmitted across axon terminals. *Journal of Cell Biology* **211**, 897-911, doi:10.1083/jcb.201504057 (2015).
284 Brettschneider, J., Del Tredici, K., Lee, V. M. Y. & Trojanowski, J. Q. Spreading of pathology in neurodegenerative diseases: a focus on human studies. *Nature Reviews Neuroscience* **16**, 109-120, doi:10.1038/nrn3887 (2015).
285 Westergard, T. *et al.* Cell-to-Cell Transmission of Dipeptide Repeat Proteins Linked to C9orf72-ALS/FTD. *Cell Reports* **17**, 645-652, doi:10.1016/j.celrep.2016.09.032 (2016).
286 Su, Z. M. *et al.* Discovery of a Biomarker and Lead Small Molecules to Target r(GGGGCC)-Associated Defects in c9FTD/ALS. *Neuron* **83**, 1043-1050, doi:10.1016/j.neuron.2014.07.041 (2014).
287 Pant, S., Hilton, H. & Burczynski, M. E. The multifaceted exosome: Biogenesis, role in normal and aberrant cellular function, and frontiers for pharmacological and biomarker opportunities. *Biochemical Pharmacology* **83**, 1484-1494, doi:10.1016/j.bcp.2011.12.037 (2012).
288 Lefebvre, F. A. *et al.* Comparative transcriptomic analysis of human and Drosophila extracellular vesicles. *Scientific Reports* **6**, doi:10.1038/srep27680 (2016).
289 Lopez-Otin, C., Blasco, M. A., Partridge, L., Serrano, M. & Kroemer, G. The Hallmarks of Aging. *Cell* **153**, 1194-1217, doi:10.1016/j.cell.2013.05.039 (2013).

290 Farooqui, T. & Farooqui, A. A. Aging: An important factor for the pathogenesis of neurodegenerative diseases. *Mechanisms of Ageing and Development* **130**, 203-215, doi:10.1016/j.mad.2008.11.006 (2009).
291 Birger, A. *et al.* Human iPSC-derived astrocytes from ALS patients with mutated C90RF72 show increased oxidative stress and neurotoxicity. *Ebiomedicine* **50**, 274-289, doi:10.1010/j.ebiom.2019.11.026 (2019).
292 Batra, R. & Lee, C. W. Mouse Models of C9orf72 Hexanucleotide Repeat Expansion in Amyotrophic Lateral Sclerosis/Frontotemporal Dementia. *Frontiers in Cellular Neuroscience* **11**, doi:10.3389/fncel.2017.00196 (2017).
293 Yamakawa, M. *et al.* Characterization of the dipeptide repeat protein in the molecular pathogenesis of c9FTD/ALS. *Human Molecular Genetics* **24**, 1630-1645, doi:10.1093/hmg/ddu576 (2015).
294 Darling, A. L. *et al.* Repeated repeat problems: Combinatorial effect of C9orf72-derived dipeptide repeat proteins. *International Journal of Biological Macromolecules* **127**, 136-145, doi:10.1016/j.ijbiomac.2019.01.035 (2019).
295 Lee, Y. B. *et al.* C9orf72 poly GA RAN-translated protein plays a key role in amyotrophic lateral sclerosis via aggregation and toxicity. *Human Molecular Genetics* **26**, 4765-4777, doi:10.1093/hmg/ddx350 (2017).
296 Vanderbliek, A. M. & Meyerowitz, E. M. Dynamin-Like Protein Encoded by the Drosophila-Shibire Gene Associated with Vesicular Traffic. *Nature* **351**, 411-414, doi:10.1038/351411a0 (1991).
297 Parker, L., Howlett, I. C., Rusan, Z. M. & Tanouye, M. A. SEIZURE AND EPILEPSY: STUDIES OF SEIZURE DISORDERS IN DROSOPHILA. *Recent Advances in the Use of Drosophila in Neurobiology and Neurodegeneration* **99**, 1-21, doi:10.1016/b978-0-12-387003-2.00001-x (2011).
298 Lee, J. & Wu, C. F. Electroconvulsive seizure behavior in Drosophila: Analysis of the physiological repertoire underlying a stereotyped action pattern in bang-sensitive mutants. *Journal of Neuroscience* **22**, 11065-11079 (2002).
299 Song, J. & Tanouye, M. A. From bench to drug: Human seizure modeling using Drosophila. *Progress in Neurobiology* **84**, 182-191, doi:10.1016/j.pneurobio.2007.10.006 (2008).
300 van den Ameele, J. *et al.* Teenage-onset progressive myoclonic epilepsy due to a familial C9orf72 repeat expansion. *Neurology* **90**, E658-E663, doi:10.1212/wnl.0000000000004999 (2018).
301 Capasso, M., Anzellotti, F., Di Giacomo, R. & Onofrj, M. Epilepsy and electroencephalographic abnormalities in C9orf72 repeat expansion. *Amyotrophic Lateral Sclerosis and Frontotemporal Degeneration* **18**, 140-141, doi:10.1080/21678421.2016.1231825 (2017).
302 Estevez-Fraga, C. *et al.* Expanding the Spectrum of Movement Disorders Associated With C9orf72 Hexanucleotide Expansions. *Neurology-Genetics* **7**, doi:10.1212/nxg.0000000000000575 (2021).
303 Ganetzky, B. & Wu, C. F. INDIRECT SUPPRESSION INVOLVING BEHAVIORAL MUTANTS WITH ALTERED NERVE EXCITABILITY IN DROSOPHILA-MELANOGASTER. *Genetics* **100**, 597-614 (1982).
304 Fergestad, T. *et al.* Neuropathology in drosophila mutants with increased seizure susceptibility. *Genetics* **178**, 947-956, doi:10.1534/genetics.107.082115 (2008).
305 Modol, L., Mancuso, R., Ale, A., Francos-Quijorna, I. & Navarro, X. Differential effects on KCC2 expression and spasticity of ALS and traumatic injuries to motoneurons. *Frontiers in Cellular Neuroscience* **8**, 7, doi:10.3389/fncel.2014.00007 (2014).
306 Fuchs, A. *et al.* Downregulation of the Potassium Chloride Cotransporter KCC2 in Vulnerable Motoneurons in the SOD1-G93A Mouse Model of Amyotrophic Lateral Sclerosis. *Journal of Neuropathology and Experimental Neurology* **69**, 1057-1070, doi:10.1097/NEN.0b013e3181f4dcef (2010).
307 Hekmat-Scafe, D. S., Lundy, M. Y., Ranga, R. & Tanouye, M. A. Mutations in the K+/Cl- cotransporter gene kazachoc (kcc) increase seizure susceptibility in

Drosophila. *Journal of Neuroscience* **26**, 8943-8954, doi:10.1523/jneurosci.4998-05.2006 (2006).

308 Wharton, K. A. *et al.* Genetic analysis of the bone morphogenetic protein-related gene, gbb, identifies multiple requirements during Drosophila development. *Genetics* **152**, 629-640 (1999).

309 Dargaei, Z. *et al.* Restoring GABAergic inhibition rescues memory deficits in a Huntington's disease mouse model. *Proceedings of the National Academy of Sciences of the United States of America* **115**, E1618-E1626, doi:10.1073/pnas.1716871115 (2018).

310 Duttaroy, A., Paul, A., Kundu, M. & Belton, A. A Sod2 null mutation confers severely reduced adult life span in Drosophila. *Genetics* **165**, 2295-2299 (2003).

311 Itsara, L. S. *et al.* Oxidative Stress Is Not a Major Contributor to Somatic Mitochondrial DNA Mutations. *Plos Genetics* **10**, doi:10.1371/journal.pgen.1003974 (2014).

312 Graf, E. R., Heerssen, H. M., Wright, C. M., Davis, G. W. & DiAntonio, A. Stathmin is Required for Stability of the Drosophila Neuromuscular Junction. *Journal of Neuroscience* **31**, 15026-15034, doi:10.1523/jneurosci.2024-11.2011 (2011).

313 Duncan, J. E., Lytle, N. K., Zuniga, A. & Goldstein, L. S. B. The Microtubule Regulatory Protein Stathmin Is Required to Maintain the Integrity of Axonal Microtubules in Drosophila. *Plos One* **8**, doi:10.1371/journal.pone.0068324 (2013).

314 Van Vranken, J. G. *et al.* SDHAF4 Promotes Mitochondrial Succinate Dehydrogenase Activity and Prevents Neurodegeneration. *Cell Metabolism* **20**, 241-252, doi:10.1016/j.cmet.2014.05.012 (2014).

315 Amado, M., Almeida, R., Schwientek, T. & Clausen, H. Identification and characterization of large galactosyltransferase gene families: galactosyltransferases for all functions. *Biochimica Et Biophysica Acta-General Subjects* **1473**, 35-53, doi:10.1016/s0304-4165(99)00168-3 (1999).

316 Haines, N. & Irvine, K. D. Functional analysis of Drosophila beta 1,4-N-acetlygalactosaminyltransferases. *Glycobiology* **15**, 335-346, doi:10.1093/glycob/cwi017 (2005).

317 Akbergenova, Y. & Bykhovskaia, M. Synapsin Regulates Vesicle Organization and Activity-Dependent Recycling at Drosophila Motor Boutons. *Neuroscience* **170**, 441-452, doi:10.1016/j.neuroscience.2010.07.021 (2010).

318 Mirza, F. J. & Zahid, S. The Role of Synapsins in Neurological Disorders. *Neuroscience Bulletin* **34**, 349-358, doi:10.1007/s12264-017-0201-7 (2018).

319 Lukas, T. J., Luo, W. W., Mao, H. H., Cole, N. & Siddique, T. Informatics-assisted protein profiling in a transgenic mouse model of amyotrophic lateral sclerosis. *Molecular & Cellular Proteomics* **5**, 1233-1244, doi:10.1074/mcp.M500431-MCP200 (2006).

320 Godenschwege, T. A., Pohar, N., Buchner, S. & Buchner, E. Inflated wings, tissue autolysis and early death in tissue inhibitor of metalloproteinases mutants of Drosophila. *European Journal of Cell Biology* **79**, 495-501, doi:10.1078/0171-9335-00072 (2000).

321 Paemka, L. *et al.* PRICKLE1 Interaction with SYNAPSIN I Reveals a Role in Autism Spectrum Disorders. *Plos One* **8**, doi:10.1371/journal.pone.0080737 (2013).

322 Filosto, M. *et al.* The role of mitochondria in neurodegenerative diseases. *Journal of Neurology* **258**, 1763-1774, doi:10.1007/s00415-011-6104-z (2011).

323 Fergestad, T., Bostwick, B. & Ganetzky, B. Metabolic disruption in Drosophila bang-sensitive seizure mutants. *Genetics* **173**, 1357-1364, doi:10.1534/genetics.106.057463 (2006).

324 Morris, C. R., Hamilton-Reeves, J., Martindale, R. G., Sarav, M. & Gautier, J. B. O. Acquired Amino Acid Deficiencies: A Focus on Arginine and Glutamine. *Nutrition in Clinical Practice* **32**, 30S-47S, doi:10.1177/0884533617691250 (2017).

325 Janssen, P., Houben, M. & Hoff, E. Photosensitivity in a patient with C9orf72 repeat expansion. *Amyotrophic Lateral Sclerosis and Frontotemporal Degeneration* **17**, 266-269, doi:10.3109/21678421.2015.1125503 (2016).
326 Amatniek, J. C. *et al.* Incidence and predictors of seizures in patients with Alzheimer's disease. *Epilepsia* **47**, 867-872, doi:10.1111/j.1528-1167.2006.00554.x (2006).
327 Noebels, J. A perfect storm: Converging paths of epilepsy and Alzheimer's dementia intersect in the hippocampal formation. *Epilepsia* **52**, 39-46, doi:10.1111/j.1528-1167.2010.02909.x (2011).
328 Sarkis, R. A., Dickerson, B. C., Cole, A. J. & Chemali, Z. N. Clinical and Neurophysiologic Characteristics of Unprovoked Seizures in Patients Diagnosed With Dementia. *Journal of Neuropsychiatry and Clinical Neurosciences* **28**, 56-61, doi:10.1176/appi.neuropsych.15060143 (2016).
329 Le Ber, I. *et al.* Homozygous TREM2 mutation in a family with atypical frontotemporal dementia. *Neurobiology of Aging* **35**, doi:10.1016/j.neurobiolaging.2014.04.010 (2014).
330 Jaiswal, M. K. Riluzole and edaravone: A tale of two amyotrophic lateral sclerosis drugs. *Medicinal Research Reviews* **39**, 733-748, doi:10.1002/med.21528 (2019).
331 Schanz, O. *et al.* Cortical Hyperexcitability in Patients with C9orf72 Mutations: Relationship to Phenotype. *Muscle & Nerve* **54**, 264-269, doi:10.1002/mus.25047 (2016).
332 Do-Ha, D., Buskila, Y. & Ooi, L. Impairments in Motor Neurons, Interneurons and Astrocytes Contribute to Hyperexcitability in ALS: Underlying Mechanisms and Paths to Therapy. *Molecular Neurobiology* **55**, 1410-1418, doi:10.1007/s12035-017-0392-y (2018).
333 Geevasinga, N., Menon, P., Ozdinler, P. H., Kiernan, M. C. & Vucic, S. Pathophysiological and diagnostic implications of cortical dysfunction in ALS. *Nature Reviews Neurology* **12**, 651-661, doi:10.1038/nrneurol.2016.140 (2016).
334 de Carvalho, M. & Swash, M. Sensitivity of Electrophysiological Tests for Upper and Lower Motor Neuron Dysfunction in ALS: a Six-Month Longitudinal Study. *Muscle & Nerve* **41**, 208-211, doi:10.1002/mus.21495 (2010).
335 Alberici, A. *et al.* The contribution of TMS to frontotemporal dementia variants. *Acta Neurologica Scandinavica* **118**, 275-280, doi:10.1111/j.1600-0404.2008.01017.x (2008).
336 Higashihara, M. *et al.* Association of Cortical Hyperexcitability and Cognitive Impairment in Patients With Amyotrophic Lateral Sclerosis. *Neurology* **96**, E2090-E2097, doi:10.1212/wnl.0000000000011798 (2021).
337 Engel, T., Lucas, J. J. & Henshall, D. C. Targeting the proteasome in epilepsy. *Oncotarget* **8**, 45042-45043, doi:10.18632/oncotarget.18418 (2017).
338 Barker-Haliski, M. & White, H. S. Glutamatergic Mechanisms Associated with Seizures and Epilepsy. *Cold Spring Harbor Perspectives in Medicine* **5**, doi:10.1101/cshperspect.a022863 (2015).
339 Vezzani, A., French, J., Bartfai, T. & Baram, T. Z. The role of inflammation in epilepsy. *Nature Reviews Neurology* **7**, 31-40, doi:10.1038/nrneurol.2010.178 (2011).
340 Kunz, W. S., Bimpong-Buta, N. Y. B., Kudin, A. P. & Elger, C. E. The role of mitochondria in epilepsy: Implications for neurodegenerative diseases. *Toxicology Mechanisms and Methods* **14**, 19-23, doi:10.1080/15376520490257374 (2004).
341 de Curtis, M., Uva, L., Gnatkovsky, V. & Librizzi, L. Potassium dynamics and seizures: Why is potassium ictogenic? *Epilepsy Research* **143**, 50-59, doi:10.1016/j.eplepsyres.2018.04.005 (2018).
342 Song, J. & Tanouye, M. A. in *Animal Models of Epilepsy: Methods and Innovations* Vol. 40 *Neuromethods* (ed S. C. Baraban) 27-43 (Humana Press Inc, 2009).

343 Mount, D. B. *et al.* The electroneutral cation-chloride cotransporters. *Journal of Experimental Biology* **201**, 2091-2102 (1998).
344 Hebert, S. C., Mount, D. B. & Gamba, G. Molecular physiology of cation-coupled Cl- cotransport: the SLC12 family. *Pflugers Archiv-European Journal of Physiology* **447**, 580-593, doi:10.1007/s00424-003-1066-3 (2004).
345 Hosie, A. M., Aronstein, K., Sattelle, D. B. & ffrenchConstant, R. H. Molecular biology of insect neuronal GABA receptors. *Trends in Neurosciences* **20**, 578-583, doi:10.1016/s0166-2236(97)01127-2 (1997).
346 Rivera, C. *et al.* The K+/Cl- co-transporter KCC2 renders GABA hyperpolarizing during neuronal maturation. *Nature* **397**, 251-255 (1999).
347 Tillman, L. & Zhang, J. W. Crossing the Chloride Channel: The Current and Potential Therapeutic Value of the Neuronal K+-Cl- Cotransporter KCC2. *Biomed Research International* **2019**, doi:10.1155/2019/8941046 (2019).
348 Castelli, L. M. *et al.* SRSF1-dependent inhibition of C9ORF72-repeat RNA nuclear export: genome-wide mechanisms for neuroprotection in amyotrophic lateral sclerosis. *Molecular Neurodegeneration* **16**, doi:10.1186/s13024-021-00475-y (2021).
349 Duy, P. Q., David, W. B. & Kahle, K. T. Identification of KCC2 Mutations in Human Epilepsy Suggests Strategies for Therapeutic Transporter Modulation. *Frontiers in Cellular Neuroscience* **13**, doi:10.3389/fncel.2019.00515 (2019).
350 Dasuri, K., Zhang, L. & Keller, J. N. Oxidative stress, neurodegeneration, and the balance of protein degradation and protein synthesis. *Free Radical Biology and Medicine* **62**, 170-185, doi:10.1016/j.freeradbiomed.2012.09.016 (2013).
351 Simonian, N. A. & Coyle, J. T. Oxidative stress in neurodegenerative diseases. *Annual Review of Pharmacology and Toxicology* **36**, 83-106, doi:10.1146/annurev.pa.36.040196.000503 (1996).
352 Chen, X. P., Guo, C. Y. & Kong, J. M. Oxidative stress in neurodegenerative diseases. *Neural Regeneration Research* **7**, 376-385, doi:10.3969/j.issn.1673-5374.2012.05.009 (2012).
353 Guo, C. Y., Sun, L., Chen, X. P. & Zhang, D. S. Oxidative stress, mitochondrial damage and neurodegenerative diseases. *Neural Regeneration Research* **8**, 2003-2014, doi:10.3969/j.issn.1673-5374.2013.21.009 (2013).
354 Kim, G. H., Kim, J. E., Rhie, S. J. & Yoon, S. The Role of Oxidative Stress in Neurodegenerative Diseases. *Experimental Neurobiology* **24**, 325-340, doi:10.5607/en.2015.24.4.325 (2015).
355 Wong, H. S., Dighe, P. A., Mezera, V., Monternier, P. A. & Brand, M. D. Production of superoxide and hydrogen peroxide from specific mitochondrial sites under different bioenergetic conditions. *Journal of Biological Chemistry* **292**, 16804-16809, doi:10.1074/jbc.R117.789271 (2017).
356 Kovacic, P., Pozos, R. S., Somanathan, R., Shangari, N. & O'Brien, P. J. Mechanism of mitochondrial uncouplers, inhibitors, and toxins: Focus on electron transfer, free radicals, and structure-activity relationships. *Current Medicinal Chemistry* **12**, 2601-2623, doi:10.2174/092986705774370646 (2005).
357 Zorov, D. B., Juhaszova, M. & Sollott, S. J. Mitochondrial ROS-induced ROS release: An update and review. *Biochimica Et Biophysica Acta-Bioenergetics* **1757**, 509-517, doi:10.1016/j.bbabio.2006.04.029 (2006).
358 Zorov, D. B., Juhaszova, M. & Sollott, S. J. Mitochondrial Reactive Oxygen Species (ROS) and ROS-Induced ROS Release. *Physiological Reviews* **94**, 909-950, doi:10.1152/physrev.00026.2013 (2014).
359 Kroemer, G. Mitochondrial control of apoptosis. *Bulletin De L Academie Nationale De Medecine* **185**, 1135-1143, doi:10.1016/s0001-4079(19)34476-0 (2001).
360 Harman, D. Aging - a Theory Based on Free-Radical and Radiation-Chemistry. *Journals of Gerontology* **11**, 298-300, doi:10.1093/geronj/11.3.298 (1956).
361 Valko, M., Rhodes, C. J., Moncol, J., Izakovic, M. & Mazur, M. Free radicals, metals and antioxidants in oxidative stress-induced cancer. *Chemico-Biological Interactions* **160**, 1-40, doi:10.1016/j.cbi.2005.12.009 (2006).

362 Valko, M. *et al.* Free radicals and antioxidants in normal physiological functions and human disease. *International Journal of Biochemistry & Cell Biology* **39**, 44-84, doi:10.1016/j.biocel.2006.07.001 (2007).
363 Flynn, J. M. & Melov, S. SOD2 in mitochondrial dysfunction and neurodegeneration. *Free Radical Biology and Medicine* **62**, 4-12, doi:10.1016/j.freeradbiomed.2013.05.027 (2013).
364 Kirby, K., Hu, J. G., Hilliker, A. J. & Phillips, J. P. RNA interference-mediated silencing of Sod2 in Drosophila leads to early adult-onset mortality and elevated endogenous oxidative stress. *Proceedings of the National Academy of Sciences of the United States of America* **99**, 16162-16167, doi:10.1073/pnas.252342899 (2002).
365 Beal, M. F. *et al.* Increased 3-nitrotyrosine in both sporadic and familial amyotrophic lateral sclerosis. *Annals of Neurology* **42**, 644-654, doi:10.1002/ana.410420416 (1997).
366 Liou, C. J., Tong, M., Vonsattel, J. P. & de la Monte, S. M. Altered Brain Expression of Insulin and Insulin-Like Growth Factors in Frontotemporal Lobar Degeneration: Another Degenerative Disease Linked to Dysregulation of Insulin Metabolic Pathways. *Asn Neuro* **11**, doi:10.1177/1759091419839515 (2019).
367 Martinez, A. *et al.* Type-Dependent Oxidative Damage in Frontotemporal Lobar Degeneration: Cortical Astrocytes Are Targets of Oxidative Damage. *Journal of Neuropathology and Experimental Neurology* **67**, 1122-1136, doi:10.1097/NEN.0b013e31818e06f3 (2008).
368 Phan, K. *et al.* Uncovering pathophysiological changes in frontotemporal dementia using serum lipids. *Scientific Reports* **10**, doi:10.1038/s41598-020-60457-w (2020).
369 Palluzzi, F. *et al.* A novel network analysis approach reveals DNA damage, oxidative stress and calcium/cAMP homeostasis-associated biomarkers in frontotemporal dementia. *Plos One* **12**, doi:10.1371/journal.pone.0185797 (2017).
370 Hallmann, A. L. *et al.* Astrocyte pathology in a human neural stem cell model of frontotemporal dementia caused by mutant TAU protein. *Scientific Reports* **7**, 1-10, doi:10.1038/srep42991 (2017).
371 Sawada, H. Clinical efficacy of edaravone for the treatment of amyotrophic lateral sclerosis. *Expert Opinion on Pharmacotherapy* **18**, 735-738, doi:10.1080/14656566.2017.1319937 (2017).
372 Mehta, A. R. *et al.* Mitochondrial bioenergetic deficits in C9orf72 amyotrophic lateral sclerosis motor neurons cause dysfunctional axonal homeostasis. *Acta Neuropathologica* **141**, 257-279, doi:10.1007/s00401-020-02252-5 (2021).
373 Dubey, J., Ratnakaran, N. & Koushika, S. P. Neurodegeneration and microtubule dynamics: death by a thousand cuts. *Frontiers in Cellular Neuroscience* **9**, doi:10.3389/fncel.2015.00343 (2015).
374 Zheng, Y. *et al.* Dynein is required for polarized dendritic transport and uniform microtubule orientation in axons. *Nature Cell Biology* **10**, 1172-1180, doi:10.1038/ncb1777 (2008).
375 Jaworski, J. *et al.* Dynamic Microtubules Regulate Dendritic Spine Morphology and Synaptic Plasticity. *Neuron* **61**, 85-100, doi:10.1016/j.neuron.2008.11.013 (2009).
376 Lewcock, J. W., Genoud, N., Lettieri, K. & Pfaff, S. L. The ubiquitin ligase phr1 regulates axon outgrowth through modulation of microtubule dynamics. *Neuron* **56**, 604-620, doi:10.1016/j.neuron.2007.09.009 (2007).
377 Le Masson, G., Przedborski, S. & Abbott, L. F. A Computational Model of Motor Neuron Degeneration. *Neuron* **83**, 975-988, doi:10.1016/j.neuron.2014.07.001 (2014).
378 Vale, R. D. *et al.* Different Axoplasmic Proteins Generate Movement in Opposite Directions Along Microtubules in vitro. *Cell* **43**, 623-632, doi:10.1016/0092-8674(85)90234-x (1985).

379 Garcia, M. L. & Cleveland, D. V. Going new places using an old MAP: tau, microtubules and human neurodegenerative disease. *Current Opinion in Cell Biology* **13**, 41-48, doi:10.1016/s0955-0674(00)00172-1 (2001).
380 Fumagalli, L. *et al.* C9orf72-derived arginine-containing dipeptide repeats associate with axonal transport machinery and impede microtubule-based motility. *Science Advances* **7**, doi:10.1126/sciadv.abg3013 (2021).
381 Curmi, P. A. *et al.* Stathmin and its phosphoprotein family: General properties, biochemical and functional interaction with tubulin. *Cell Structure and Function* **24**, 345-357 (1999).
382 Zhao, F. H. *et al.* Abnormal expression of stathmin 1 in brain tissue of patients with intractable temporal lobe epilepsy and a rat model. *Synapse* **66**, 781-791, doi:10.1002/syn.21567 (2012).
383 Klim, J. R. *et al.* ALS-implicated protein TDP-43 sustains levels of STMN2, a mediator of motor neuron growth and repair. *Nature Neuroscience* **22**, 167-+, doi:10.1038/s41593-018-0300-4 (2019).
384 Strey, C. W. *et al.* Dysregulation of stathmin, a microtubule-destabilizing protein, and up-regulation of Hsp25, Hsp27, and the antioxidant peroxiredoxin 6 in a mouse model of familial amyotrophic lateral sclerosis. *American Journal of Pathology* **165**, 1701-1718, doi:10.1016/s0002-9440(10)63426-8 (2004).
385 Melamed, Z. *et al.* Premature polyadenylation-mediated loss of stathmin-2 is a hallmark of TDP-43-dependent neurodegeneration. *Nature Neuroscience* **22**, 180-+, doi:10.1038/s41593-018-0293-z (2019).
386 Fernie, A. R., Carrari, F. & Sweetlove, L. J. Respiratory metabolism: glycolysis, the TCA cycle and mitochondrial electron transport. *Current Opinion in Plant Biology* **7**, 254-261, doi:10.1016/j.pbi.2004.03.007 (2004).
387 Onesto, E. *et al.* Gene-specific mitochondria dysfunctions in human TARDBP and C9ORF72 fibroblasts. *Acta Neuropathologica Communications* **4**, doi:10.1186/s40478-016-0316-5 (2016).
388 Wei, P., Liu, Q. H., Xue, W. & Wang, J. W. A Colorimetric Assay of Citrate Synthase Activity in Drosophila Melanogaster. *Jove-Journal of Visualized Experiments*, doi:10.3791/59454 (2020).
389 Rutter, J., Winge, D. R. & Schiffman, J. D. Succinate dehydrogenase - Assembly, regulation and role in human disease. *Mitochondrion* **10**, 393-401, doi:10.1016/j.mito.2010.03.001 (2010).
390 Allen, S. P. *et al.* C9orf72 expansion within astrocytes reduces metabolic flexibility in amyotrophic lateral sclerosis. *Brain* **142**, 3771-3790, doi:10.1093/brain/awz302 (2019).
391 Vandoorne, T., De Bock, K. & Van Den Bosch, L. Energy metabolism in ALS: an underappreciated opportunity? *Acta Neuropathologica* **135**, 489-509, doi:10.1007/s00401-018-1835-x (2018).
392 Goelz, S. E., Nestler, E. J., Chehrazi, B. & Greengard, P. Distribution of Protein-I in Mammalian Brain as Determined by a Detergent-Based Radioimmunoassay. *Proceedings of the National Academy of Sciences of the United States of America-Biological Sciences* **78**, 2130-2134, doi:10.1073/pnas.78.4.2130 (1981).
393 Hilfiker, S. *et al.* Synapsins as regulators of neurotransmitter release. *Philosophical Transactions of the Royal Society of London Series B-Biological Sciences* **354**, 269-279, doi:10.1098/rstb.1999.0378 (1999).
394 Hosaka, M., Hammer, R. E. & Sudhof, T. C. A phospho-switch controls the dynamic association of synapsins with synaptic vesicles. *Neuron* **24**, 377-387, doi:10.1016/s0896-6273(00)80851-x (1999).
395 Sudhof, T. C. *et al.* Synapsins - Mosaics of Shared and Individual Domains in a Family of Synaptic Vesicle Phosphoproteins. *Science* **245**, 1474-1480, doi:10.1126/science.2506642 (1989).
396 Lignani, G. *et al.* Epileptogenic Q555X SYN1 mutant triggers imbalances in release dynamics and short-term plasticity. *Human Molecular Genetics* **22**, 2186-2199, doi:10.1093/hmg/ddt071 (2013).

397 Porton, B. & Wetsel, W. C. Reduction of synapsin III in the prefrontal cortex of individuals with schizophrenia. *Schizophrenia Research* **94**, 366-370, doi:10.1016/j.schres.2007.04.016 (2007).
398 Vawter, M. P. *et al.* Reduction of synapsin in the hippocampus of patients with bipolar disorder and schizophrenia. *Molecular Psychiatry* **7**, 571-578, doi:10.1038/sj.mp.4001158 (2002).
399 Lievens, J. C., Woodman, B., Mahal, A. & Bates, G. P. Abnormal phosphorylation of synapsin I predicts a neuronal transmission impairment in the R6/2 Huntington's disease transgenic mice. *Molecular and Cellular Neuroscience* **20**, 638-648, doi:10.1006/mcne.2002.1152 (2002).
400 Ikemoto, A., Nakamura, S., Akiguchi, I. & Hirano, A. Differential expression between synaptic vesicle proteins and presynaptic plasma membrane proteins in the anterior horn of amyotrophic lateral sclerosis. *Acta Neuropathologica* **103**, 179-187, doi:10.1007/s004010100449 (2002).
401 Haines, N. & Stewart, B. A. Functional roles for beta 1,4-N-acetlygalactosaminyltransferase-A in Drosophila larval neurons and muscles. *Genetics* **175**, 671-679, doi:10.1534/genetics.106.065565 (2007).
402 Fanale, D. *et al.* Stabilizing versus Destabilizing the Microtubules: A Double-Edge Sword for an Effective Cancer Treatment Option? *Analytical Cellular Pathology* **2015**, 1-19, doi:10.1155/2015/690916 (2015).
403 Parkhitko, A. A. *et al.* Downregulation of the tyrosine degradation pathway extends Drosophila lifespan. *Elife* **9**, doi:10.7554/eLife.58053 (2020).
404 Rattan, S. I. S. & Demirovic, D. Hormesis as a Mechanism for the Anti-Aging Effects of Calorie Restriction. *Calorie Restriction, Aging and Longevity*, 233-245, doi:10.1007/978-90-481-8556-6_13 (2010).
405 Calabrese, E. J. & Baldwin, L. A. Defining hormesis. *Human & Experimental Toxicology* **21**, 91-97, doi:10.1191/0960327102ht217oa (2002).
406 Schulz, T. J. *et al.* Glucose restriction extends Caenorhabditis elegans life span by inducing mitochondrial respiration and increasing oxidative stress. *Cell Metabolism* **6**, 280-293, doi:10.1016/j.cmet.2007.08.011 (2007).
407 Mourikis, P., Hurlbut, G. D. & Artavanis-Tsakonas, S. Enigma, a mitochondrial protein affecting lifespan and oxidative stress response in Drosophila. *Proceedings of the National Academy of Sciences of the United States of America* **103**, 1307-1312, doi:10.1073/pnas.0510564103 (2006).
408 Yu, Z. H. *et al.* Human serum metabolic profiles are age dependent. *Aging Cell* **11**, 960-967, doi:10.1111/j.1474-9726.2012.00865.x (2012).
409 Hoffman, J. M. *et al.* Effects of age, sex, and genotype on high-sensitivity metabolomic profiles in the fruit fly, Drosophila melanogaster. *Aging Cell* **13**, 596-604, doi:10.1111/acel.12215 (2014).
410 Avanesov, A. S. *et al.* Age- and diet-associated metabolome remodeling characterizes the aging process driven by damage accumulation. *Elife* **3**, doi:10.7554/eLife.02077 (2014).
411 Tomas-Loba, A., de Jesus, B. B., Mato, J. M. & Blasco, M. A. A metabolic signature predicts biological age in mice. *Aging Cell* **12**, 93-101, doi:10.1111/acel.12025 (2013).
412 Legan, S. K. *et al.* Overexpression of Glucose-6-phosphate Dehydrogenase Extends the Life Span of Drosophila melanogaster. *Journal of Biological Chemistry* **283**, 32492-32499, doi:10.1074/jbc.M805832200 (2008).
413 Stenesen, D. *et al.* Adenosine Nucleotide Biosynthesis and AMPK Regulate Adult Life Span and Mediate the Longevity Benefit of Caloric Restriction in Flies. *Cell Metabolism* **17**, 101-112, doi:10.1016/j.cmet.2012.12.006 (2013).
414 Lee, S. M. *et al.* TDP-43 cytoplasmic inclusion formation is disrupted in C9orf72-associated amyotrophic lateral sclerosis/frontotemporal lobar degeneration. *Brain Communications* **1**, doi:10.1093/braincomms/fcz014 (2019).
415 Hayes, L. R., Duan, L., Bowen, K., Kalab, P. & Rothstein, J. D. C9orf72 arginine-rich dipeptide repeat proteins disrupt karyopherin-mediated nuclear import. *Elife* **9**, 29, doi:10.7554/eLife.51685 (2020).

416 Zaslavsky, B. Y., Ferreira, L. A. & Uversky, V. N. Driving Forces of Liquid-Liquid Phase Separation in Biological Systems. *Biomolecules* **9**, doi:10.3390/biom9090473 (2019).

417 Odeh, H. M. & Shorter, J. Arginine-rich dipeptide-repeat proteins as phase disruptors in C9-ALS/FTD. *Emerging Topics in Life Sciences* **4**, 293-305, doi:10.1042/etls20190167 (2020).

418 Hartmann, H. *et al.* Proteomics and C9orf72 neuropathology identify ribosomes as poly-GR/PR interactors driving toxicity. *Life Science Alliance* **1**, 13, doi:10.26508/lsa.201800070 (2018).

419 Andrade, N. S. *et al.* Dipeptide repeat proteins inhibit homology-directed DNA double strand break repair in C9ORF72 ALS/FTD. *Molecular Neurodegeneration* **15**, 18, doi:10.1186/s13024-020-00365-9 (2020).

420 Lopez-Gonzalez, R. *et al.* Partial inhibition of the overactivated Ku80-dependent DNA repair pathway rescues neurodegeneration in C9ORF72-ALS/FTD. *Proceedings of the National Academy of Sciences of the United States of America* **116**, 9628-9633, doi:10.1073/pnas.1901313116 (2019).

421 Bakthavachalu, B. *et al.* RNP-Granule Assembly via Ataxin-2 Disordered Domains Is Required for Long-Term Memory and Neurodegeneration. *Neuron* **98**, 754-+, doi:10.1016/j.neuron.2018.04.032 (2018).

422 Toivonen, J. M. *et al.* technical knockout, a Drosophila model of mitochondrial deafness. *Genetics* **159**, 241-254 (2001).

423 Bindoff, L. A. & Engelsen, B. A. Mitochondrial diseases and epilepsy. *Epilepsia* **53**, 92-97, doi:10.1111/j.1528-1167.2012.03618.x (2012).

424 Rahman, S. Mitochondrial disease and epilepsy. *Developmental Medicine and Child Neurology* **54**, 397-406, doi:10.1111/j.1469-8749.2011.04214.x (2012).

425 Li, Z., Okamoto, K., Hayashi, Y. & Sheng, M. The importance of dendritic mitochondria in the morphogenesis and plasticity of spines and synapses. *Cell* **119**, 873-887, doi:10.1016/j.cell.2004.11.003 (2004).

426 Nguyen, D. *et al.* A new vicious cycle involving glutamate excitotoxicity, oxidative stress and mitochondrial dynamics. *Cell Death & Disease* **2**, doi:10.1038/cddis.2011.117 (2011).

427 Lorincz, P., Mauvezin, C. & Juhasz, G. Exploring Autophagy in Drosophila. *Cells* **6**, doi:10.3390/cells6030022 (2017).

428 Torres, V. I., Vallejo, D. & Inestrosa, N. C. Emerging Synaptic Molecules as Candidates in the Etiology of Neurological Disorders. *Neural Plasticity* **2017**, doi:10.1155/2017/8081758 (2017).

429 Shiihashi, G. *et al.* Dendritic Homeostasis Disruption in a Novel Frontotemporal Dementia Mouse Model Expressing Cytoplasmic Fused in Sarcoma. *Ebiomedicine* **24**, 102-115, doi:10.1016/j.ebiom.2017.09.005 (2017).

430 Gorrie, G. H. *et al.* Dendritic spinopathy in transgenic mice expressing ALS/dementia-linked mutant UBQLN2. *Proceedings of the National Academy of Sciences of the United States of America* **111**, 14524-14529, doi:10.1073/pnas.1405741111 (2014).

431 Hall, C. E. *et al.* Progressive Motor Neuron Pathology and the Role of Astrocytes in a Human Stem Cell Model of VCP-Related ALS. *Cell Reports* **19**, 1739-1749, doi:10.1016/j.celrep.2017.05.024 (2017).

432 Taylor, J. P., Brown, R. H. & Cleveland, D. W. Decoding ALS: from genes to mechanism. *Nature* **539**, 197-206, doi:10.1038/nature20413 (2016).

433 Chang, B. S. Cortical Hyperexcitability: A New Biomarker in Generalized Epilepsy Syndromes. *Epilepsy Currents* **13**, 287-+, doi:10.5698/1535-7597-13.6.287 (2013).

434 Barres, B. A. & Barde, Y. A. Neuronal and glial cell biology. *Current Opinion in Neurobiology* **10**, 642-648, doi:10.1016/s0959-4388(00)00134-3 (2000).

435 Arbour, D., Vande Velde, C. & Robitaille, R. New perspectives on amyotrophic lateral sclerosis: the role of glial cells at the neuromuscular junction. *Journal of Physiology-London* **595**, 647-661, doi:10.1113/jp270213 (2017).

436 Ho, W. Y., Navakkode, S., Liu, F. J., Soong, T. W. & Ling, S. C. Deregulated expression of a longevity gene, Klotho, in the C9orf72 deletion mice with impaired synaptic plasticity and adult hippocampal neurogenesis. *Acta Neuropathologica Communications* **8**, doi:10.1186/s40478-020-01030-4 (2020).
437 Mattson, M. P. & Liu, D. Mitochondrial potassium channels and uncoupling proteins in synaptic plasticity and neuronal cell death. *Biochemical and Biophysical Research Communications* **304**, 539-549, doi:10.1016/s0006-291x(03)00627-2 (2003).
438 Mattson, M. P. Mitochondrial regulation of neuronal plasticity. *Neurochemical Research* **32**, 707-715, doi:10.1007/s11064-006-9170-3 (2007).
439 Cherra, S. J., Steer, E., Gusdon, A. M., Kiselyov, K. & Chu, C. T. Mutant LRRK2 Elicits Calcium Imbalance and Depletion of Dendritic Mitochondria in Neurons. *American Journal of Pathology* **182**, 474-484, doi:10.1016/j.ajpath.2012.10.027 (2013).
440 Fukui, M. & Zhu, B. T. Mitochondrial superoxide dismutase SOD2, but not cytosolic SOD1, plays a critical role in protection against glutamate-induced oxidative stress and cell death in HT22 neuronal cells. *Free Radical Biology and Medicine* **48**, 821-830, doi:10.1016/j.freeradbiomed.2009.12.024 (2010).
441 Choi, S. Y. *et al.* C9ORF72-ALS/FTD-associated poly(GR) binds Atp5a1 and compromises mitochondrial function in vivo. *Nature Neuroscience* **22**, 851-+, doi:10.1038/s41593-019-0397-0 (2019).
442 Li, S. X. *et al.* Altered MICOS Morphology and Mitochondrial Ion Homeostasis Contribute to Poly(GR) Toxicity Associated with C9-ALS/FTD. *Cell Reports* **32**, 18, doi:10.1016/j.celrep.2020.107989 (2020).
443 Zhang, B., Tu, P. H., Abtahian, F., Trojanowski, J. Q. & Lee, V. M. Y. Neurofilaments and orthograde transport are reduced in ventral root axons of transgenic mice that express human SOD1 with a G93A mutation. *Journal of Cell Biology* **139**, 1307-1315, doi:10.1083/jcb.139.5.1307 (1997).
444 Warita, H., Itoyama, Y. & Abe, K. Selective impairment of fast anterograde axonal transport in the peripheral nerves of asymptomatic transgenic mice with a G93A mutant SOD1 gene. *Brain Research* **819**, 120-131, doi:10.1016/s0006-8993(98)01351-1 (1999).
445 De Vos, K. J. *et al.* Familial amyotrophic lateral sclerosis-linked SOD1 mutants perturb fast axonal transport to reduce axonal mitochondria content. *Human Molecular Genetics* **16**, 2720-2728, doi:10.1093/hmg/ddm226 (2007).
446 Kieran, D. *et al.* A mutation in dynein rescues axonal transport defects and extends the life span of ALS mice. *Journal of Cell Biology* **169**, 561-567, doi:10.1083/jcb.200501085 (2005).
447 Wang, W. Z. *et al.* The ALS disease-associated mutant TDP-43 impairs mitochondrial dynamics and function in motor neurons. *Human Molecular Genetics* **22**, 4706-4719, doi:10.1093/hmg/ddt319 (2013).
448 De Vos, K. J. & Hafezparast, M. Neurobiology of axonal transport defects in motor neuron diseases: Opportunities for translational research? *Neurobiology of Disease* **105**, 283-299, doi:10.1016/j.nbd.2017.02.004 (2017).
449 Zala, D. *et al.* Vesicular Glycolysis Provides On-Board Energy for Fast Axonal Transport. *Cell* **152**, 479-491, doi:10.1016/j.cell.2012.12.029 (2013).
450 Liang, C. *et al.* Smcr8 deficiency disrupts axonal transport-dependent lysosomal function and promotes axonal swellings and gain of toxicity in C9ALS/FTD mouse models. *Human Molecular Genetics* **28**, 3940-3953, doi:10.1093/hmg/ddz230 (2019).
451 Ly, C. V. & Verstreken, P. Mitochondria at the synapse. *Neuroscientist* **12**, 291-299, doi:10.1177/1073858406287661 (2006).
452 Bondy, S. C. & Lebel, C. P. The Relationship Between Excitotoxicity And Oxidative Stress in the Central-Nervous-System. *Free Radical Biology and Medicine* **14**, 633-642, doi:10.1016/0891-5849(93)90144-j (1993).

453 Meloni, M. *et al.* C9ORF72 Intermediate Repeat Expansion in a Patient With Psychiatric Disorders and Progressive Cerebellar Ataxia. *Neurologist* **22**, 245-246, doi:10.1097/nrl.0000000000000147 (2017).
454 Azevedo, A. W. *et al.* A size principle for recruitment of Drosophila leg motor neurons. *Elife* **9**, doi:10.7554/eLife.56754 (2020).
455 Yagi, R., Mayer, F. & Basler, K. Refined LexA transactivators and their use in combination with the Drosophila Gal4 system. *Proceedings of the National Academy of Sciences of the United States of America* **107**, 16166-16171, doi:10.1073/pnas.1005957107 (2010).
456 Zhao, C. *et al.* Mutant C9orf72 human iPSC-derived astrocytes cause non-cell autonomous motor neuron pathophysiology. *Glia* **68**, 1046-1064, doi:10.1002/glia.23761 (2020).
457 Braak, H. *et al.* Amyotrophic lateral sclerosis-a model of corticofugal axonal spread. *Nature Reviews Neurology* **9**, 708-714, doi:10.1038/nrneurol.2013.221 (2013).
458 Donnelly, K. M. *et al.* Phagocytic glia are obligatory intermediates in transmission of mutant huntingtin aggregates across neuronal synapses. *Elife* **9**, doi:10.7554/eLife.58499 (2020).
459 Yin, S. Y. *et al.* Evidence that C9ORF72 Dipeptide Repeat Proteins Associate with U2 snRNP to Cause Mis-splicing in ALS/FTD Patients. *Cell Reports* **19**, 2244-2256, doi:10.1016/j.celrep.2017.05.056 (2017).
460 Woerner, A. C. *et al.* Cytoplasmic protein aggregates interfere with nucleocytoplasmic transport of protein and RNA. *Science* **351**, 173-176, doi:10.1126/science.aad2033 (2016).
461 Solomon, D. A., Smikle, R., Reid, M. J. & Mizielinska, S. Altered Phase Separation and Cellular Impact in C9orf72-Linked ALS/FTD. *Frontiers in Cellular Neuroscience* **15**, doi:10.3389/fncel.2021.664151 (2021).
462 Prudencio, M. *et al.* Distinct brain transcriptome profiles in C9orf72-associated and sporadic ALS. *Nature Neuroscience* **18**, 1175-+, doi:10.1038/nn.4065 (2015).
463 Dafinca, R. *et al.* Impairment of Mitochondrial Calcium Buffering Links Mutations in C9ORF72 and TARDBP in iPS-Derived Motor Neurons from Patients with ALS/FTD. *Stem Cell Reports* **14**, 892-908, doi:10.1016/j.stemcr.2020.03.023 (2020).
464 Boillee, S., Vande Velde, C. & Cleveland, D. W. ALS: A disease of motor neurons and their nonneuronal neighbors. *Neuron* **52**, 39-59, doi:10.1016/j.neuron.2006.09.018 (2006).
465 Clement, A. M. *et al.* Wild-type nonneuronal cells extend survival of SOD1 mutant motor neurons in ALS mice. *Science* **302**, 113-117, doi:10.1126/science.1086071 (2003).
466 Yamanaka, K. *et al.* Astrocytes as determinants of disease progression in inherited amyotrophic lateral sclerosis. *Nature Neuroscience* **11**, 251-253, doi:10.1038/nn2047 (2008).
467 Raman, R. *et al.* Gene expression signatures in motor neurone disease fibroblasts reveal dysregulation of metabolism, hypoxia-response and RNA processing functions. *Neuropathology and Applied Neurobiology* **41**, 201-226, doi:10.1111/nan.12147 (2015).
468 Turk, M. *et al.* C9orf72-ALS: P62-and Ubiquitin-Aggregation Pathology in Skeletal Muscle. *Muscle & Nerve* **50**, 454-455, doi:10.1002/mus.24283 (2014).
469 Kang, P. T., Chen, C. L., Lin, P., Chilian, W. M. & Chen, Y. R. Impairment of pH gradient and membrane potential mediates redox dysfunction in the mitochondria of the post-ischemic heart (vol 112, 36, 2017). *Basic Research in Cardiology* **112**, 1, doi:10.1007/s00395-017-0632-3 (2017).